Enzyme-Catalysed Siloxane Bond Formation

Thesis

Enzyme-Catalysed Siloxane Bond Formation

A thesis submitted for the degree of
Doctor of Philosophy in Chemistry

By

Kurt Friedrich Brandstadt
B.Sc., M.Sc.

November 2003

Department of Chemistry
The Open University
Walton Hall
Milton Keynes
MK7 6AA
United Kingdom

ProQuest LLC.
789 East Eisenhower Parkway
P.O. Box 1346
Ann Arbor, MI 48106 – 1346

I dedicate this to my family:
Angela, for her caring support and genuine understanding,
as well as Ben and Sarah for their encouragement.
Thank You

Submission date: 5 November 20
Award date: 19 December 20

Statement

The work embodied in this thesis was carried out by the author during the period October 1999 to November 2003 in the Department of Chemistry at the Open University and at the Dow Corning Corporation, under the supervision of Professor Alan R. Bassindale, Dr. Peter G. Taylor, and Dr. Thomas H. Lane.

Parts of the work have been communicated as listed below.

- Bassindale, A.R., Brandstadt, K.F., Lane, T.H., Taylor, P.G., "Enzyme-Catalysed Siloxane Bond Formation," Journal of Inorganic Biochemistry, **96**, 401, (2003).

- Bassindale, A.R., Brandstadt, K.F., Lane, T.H., Taylor, P.G., "Biocatalysis of Siloxane Bonds," Polymer Preprints, **44(2)**, 570, (2003).

- Bassindale, A.R., Brandstadt, K.F., Lane, T.H., Taylor, P.G., "Enzyme-catalysed siloxane bond formation," Industrial & Engineering Chemistry Poster Session, National ACS meeting, New Orleans, February 2003.

- Bassindale, A.R., Brandstadt, K.F., Lane, T.H., Taylor, P.G., "Enzyme-catalysed siloxane bond formation," Sci-Mix Poster Session, National ACS meeting, New Orleans, February 2003.

- Bassindale, A.R., Brandstadt, K.F., Lane, T.H., Taylor, P.G., "Enzyme-catalysed siloxane bond formation," Hybrid Materials Symposium, National ACS meeting, New Orleans, February 2003.

- Bassindale, A.R., Brandstadt, K.F., Lane, T.H., Taylor, P.G., "Enzyme-catalysed siloxane bond formation," Organosilicon Symposium, May 2003.

- Bassindale, A.R., Brandstadt, K.F., Lane, T.H., Taylor, P.G., "Biocatalysis of Siloxane Bonds," Biocatalysis in Polymer Science Symposium, National ACS meeting, New York, September 2003 (invited).

Acknowledgements

I express my sincere gratitude to Professor Alan R. Bassindale, Dr. Peter G. Taylor, and Dr. Thomas H. Lane for the opportunity to participate in the research degree program in the Department of Chemistry at The Open University. This was an invaluable learning experience and an extensive program in critical thinking. As advisors, their engaging manners and thoughtfulness created a dynamic environment in which to grow as a scientist. I am humbled as I reflect on my interactions with them.

I acknowledge the Dow Corning Corporation (Midland, MI) for their financial support as well as the facilities in which to conduct the research project.

I thank the professors at The Open University as well as my colleagues at the Dow Corning Corporation and Genencor International, Inc. (Palo Alto, CA) for their insightful consultations.

I appreciate the assistance of the employees at Allis Information Management (Midland, MI) in the reviewing of this manuscript.

Kurt F. Brandstadt

List of Abbreviations

Asn	asparagine
Asp	aspartic acid
BAEE	N-α-benzoyl-L-arginine ethyl ester
BBI	Bowman-Birk inhibitor
BSA	bovine serum albumin
BTEE	N-benzoyl-L-tyrosine ethyl ester
DRIFTS	diffuse reflectance infrared Fourier transform spectroscopy
DSC	differential scanning calorimetry
EDS	energy dispersive spectroscopy
ESI	electrospray ionisation
FID	flame ionisation detector
FTIR	Fourier transform infrared
GC	gas chromatography
His	histidine
HMDS	hexamethyldisiloxane
ICP-AES	inductively coupled plasma-atomic emission spectroscopy
MALDI-TOF	matrix-assisted laser desorption/ionisation time-of-flight
Me_3SiOEt	trimethylethoxysilane
Me_3SiOH	trimethylsilanol
MS	mass spectrometry
MSA	trimethylsilylacetamide
PCI	Popcorn inhibitor
RSD	relative standard deviation
SEM	scanning electron microscopy

Ser	serine
TGA	thermogravimetric analysis
TGME	tetraethylene glycol monomethyl ether
THF	tetrahydrofuran
TLCK	N-α-p-tosyl-L-lysine-chloromethyl ketone hydrochloride
TPCK	N-tosyl-L-phenylalanine chloromethyl ketone
Tris	tris(hydroxymethyl)aminomethane

Abstract

The intricate siliceous architectures of diatom species have inspired our exploration of biosilicification. Biosilicification occurs on a globally vast scale under mild conditions. Although research has progressed in the area of silica biosynthesis, the molecular mechanisms of these interactions are effectively unknown.

Previous *in vitro* studies of natural systems within the area of silica biosynthesis were complicated by other factors. These earlier mechanistic queries including biomimetic approaches often failed to recognize the chemistry of silicic acid and its analogues. In order to better understand the role of various proteins in the biosilicification process, a carefully chosen model study was performed to test the ability of homologous enzymes to catalyse the formation of molecules with a *single* siloxane bond during the *in vitro* hydrolysis and condensation of alkoxysilanes.

This model study is believed to be the first rigorous study to demonstrate biocatalysis at silicon. Our data suggests that homologous lipase and protease enzymes catalyze the formation of siloxane bonds under mild conditions. In particular, non-specific interactions with trypsin promoted the *in vitro* hydrolysis of alkoxysilanes; while, the active site was determined to selectively catalyse the condensation of silanols. Comparatively, the rate of hydrolysis was one order of magnitude faster than condensation. The rate of condensation appeared to be proportional to both the concentration of trimethylsilanol and trypsin. The trypsin-catalysed condensation of non-saturated solutions of trimethylsilanol is thought to fit the Michaelis-Menten model, where the formation of the trypsin-silanol intermediate is the rate-limiting step. This is consistent with the fact that organosilicon molecules are larger than analogous hydrocarbon tryptic substrates. Conversely, although trypsin would theoretically catalyse the hydrolysis of a siloxane bond due to the law of microscopic reversibility, the reverse reaction was not favored.

Given the selectivity and mild reaction conditions of enzymes, the opportunity to strategically use biocatalysts to synthesise novel hybrid materials with structural control and spatial order is promising.

Table of Contents

Chapter One: Introduction and Background

Chapter Two: Enzyme-Catalysed Condensation of Silanols

Chapter Three: Trypsin-Catalysed Condensation of Silanols

Chapter Four: Trypsin-Catalysed Hydrolysis and Condensation of Alkoxysilanes

Chapter One

Introduction and Background

1.0 Introduction

Silicon is often regarded as an insignificant element in our carbon-based world. Few are aware that silicon is the second most abundant element in the crust of the earth [1] or that it is essential for growth and biological function in a variety of plant, animal, and microbial systems [2, 3]. Silicate-based minerals account for more than 90% of all known terrestrial specimens [4], which are actively involved in the global silica cycle. Biosilicification occurs on a globally vast scale [5] under mild conditions (e.g. neutral pH, low temperature) [6]. In fact, minute planktonic algae (diatoms) control the marine silica cycle. These single cell plants process an estimated 200-280 teramoles or gigatons of particulate silica every year [7]. Given the complex design and diversity of the siliceous skeletons of diatoms [2], these organisms are considered paragons of nanostructural architecture (Figure 1.1) [8].

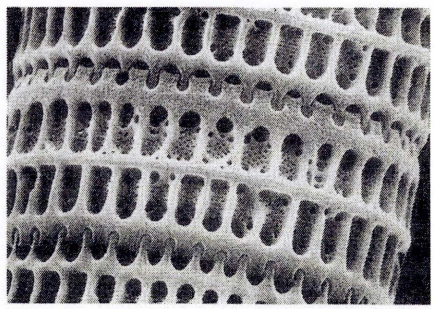

Figure 1.1: *Paralia sulcata* diatom cell wall (30μm in diameter) [9].

Although research has progressed in the area of silica biosynthesis, the molecular mechanisms of these interactions are effectively unknown [10].

The natural production of silica in the *Tethya aurantia* marine sponge [6], *Cylindrotheca fusiformis* diatom [11-14], and *Equisetum telmateia* plant [15] appear to be similar processes. The substrates, the functionality of the active amino acid residues, and the biosilica materials produced by the sponge, diatom, and plant are comparable. These

systems process silicic acid in the presence of amphiphilic nucleophiles to produce organo-biosilica composites such as spicules (sponge), cell walls (diatom), and biominerals (plant). However, *in vitro* studies of these natural systems are complicated. Additionally, these mechanistic queries often fail to recognise the chemistry of silicic acid and its analogues.

The study of the hydrolysis and condensation reactions during biosilicification is complicated due to the enhanced sensitivity of silica, silicates, and silicic acid to pH, concentration, and temperature [2]. As silicic acid precursors, tetraalkoxysilanes are easily hydrolysed and the resulting silanols are condensed during the formation of particulate silica. Silicatein (i.e. a protease isolated from the *Tethya aurantia* marine sponge) was documented [16] to catalyse the *in vitro* polycondensation of tetraethoxysilane as well as phenyl- and methyl-triethoxysilanes under mild conditions during the formation of siloxane precipitates. Based on site-directed mutagenesis results [17], the enzymatic active site of silicatein (i.e. Ser-His-Asn) was determined to catalyse the hydrolysis and/or condensation of the alkoxysilanes during the biosilicification reactions. In contrast, polypeptides isolated from the *Cylindrotheca fusiformis* diatom (i.e. silaffin) and *Equisetum telmateia* plant (i.e. biopolymer) as well as biomimetic analogues (e.g. polyamines) were reported to catalyse the *in vitro* hydrolysis [15, 18] or condensation [11-15, 18, 19] reactions during the formation of silica. Consequently, it has been shown an active site in a defined tertiary structure is not necessarily required. The data suggest that the reactions were catalysed by non-specific peptide interactions with nucleophilic, basic, and cationic amino acid residues.

In order to better understand the role of various proteins in the biosilicification process, a carefully chosen model study was performed to test the ability of homologous

enzymes to catalyse the formation of siloxane bonds during the *in vitro* hydrolysis and condensation of alkoxysilanes under mild conditions (Scheme 1.1).

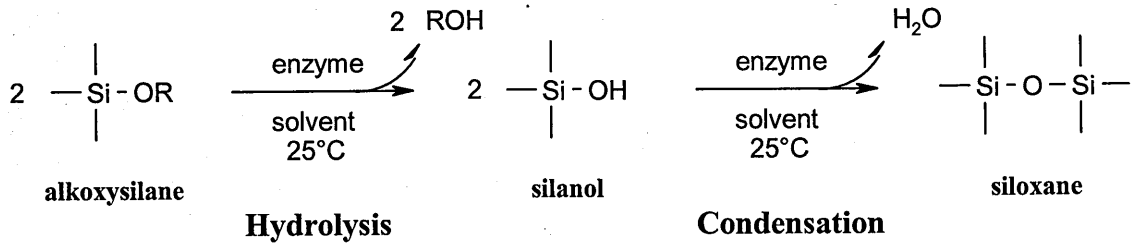

Scheme 1.1: Enzyme-catalysed siloxane bond formation.

Given the complications of silicic acid analogues [2], mono-functional silanes were chosen to focus on the formation of molecules with a *single* siloxane bond. It was understood that the *in vitro* biocatalysed reactions might not be comparable to the natural *in vivo* reactions.

1.1 Biosilicification

1.1.1 *Tethya aurantia* Marine Sponge

As part of a natural defense system, the *Tethya aurantia* marine sponge produces rod-shaped silica spicules on its surface [6, 9, 20]. The vesicle occluded spicules account for 75% of the dry weight of the organism. After harvesting the sponge, the axial filaments (> 91% protein [21]) within the silica spicules (Figure 1.2) were obtained by performing acidic digestions with H_2SO_4/HNO_3 (4:1) and HF/NH_4F [22] (pH 5). The proteinaceous solution was dialyzed nine times against 4 L of deionised (Milli-Q) water at 4°C for 4 hours prior to isolating the proteins by centrifugation.

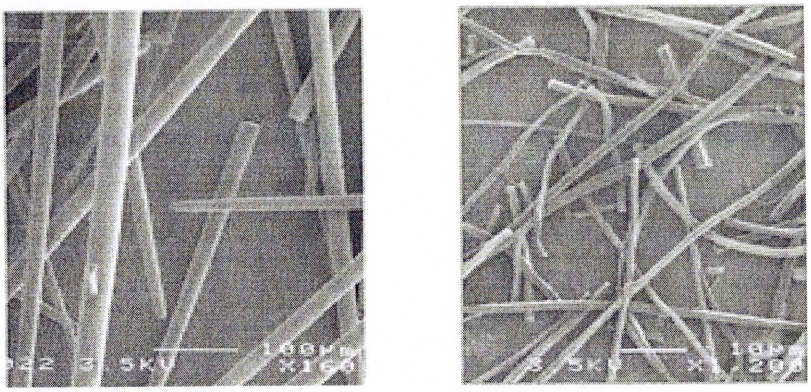

silica spicules (2 mm x 30 μm) **protein filament (2 mm x 2 μm)**

Figure 1.2: Materials isolated from *Tethya aurantia* marine sponge digestion [6].

Due to their participation in the synthesis of biosilica, the identified protein subunits were labeled silicatein α (29 kDa), β (28 kDa), and γ (27 kDa) with a relative ratio equal to 12:6:1. The subunits associate by means of nonionic, noncovalent interactions. Based on a comparative evaluation of the amino acid sequence, tertiary structure, and the presence of membrane-enclosed vesicles, silicatein was determined to be highly homologous with cathepsin L (i.e. a papain proteolytic enzyme).

Silicatein was documented [10, 16] to catalyse the *in vitro* polycondensation of tetraethoxysilane as well as phenyl- and methyl-triethoxysilanes under mild conditions during the formation of siloxane precipitates. Comparatively, the silicon-based precipitates were not observed in the absence of silicatein. Experimentally, the thermal denaturation of silicatein was observed to be irreversible. Although the velocities of the reactions were low, the kinetic properties were reported to follow the Michaelis-Menten model [20]. Based on site-directed mutagenesis results [17], the enzymatic active site of silicatein (i.e. Ser-His-Asn) was determined to catalyse the hydrolysis and/or condensation of the alkoxysilanes during the biosilicification reactions. Since the active site of silicatein is similar to the catalytic triad [23, 24] observed in select hydrolases (Figure 1.3), a general acid/base reaction mechanism (Scheme 1.2) was proposed [16] to catalyse the formation of

biosilica despite the inability of the study to differentiate between the role of silicatein in the hydrolysis and condensation reactions during biosilicification. In addition, silicatein lacked proteolytic activity as measured with synthetic chromogenic substrates [25].

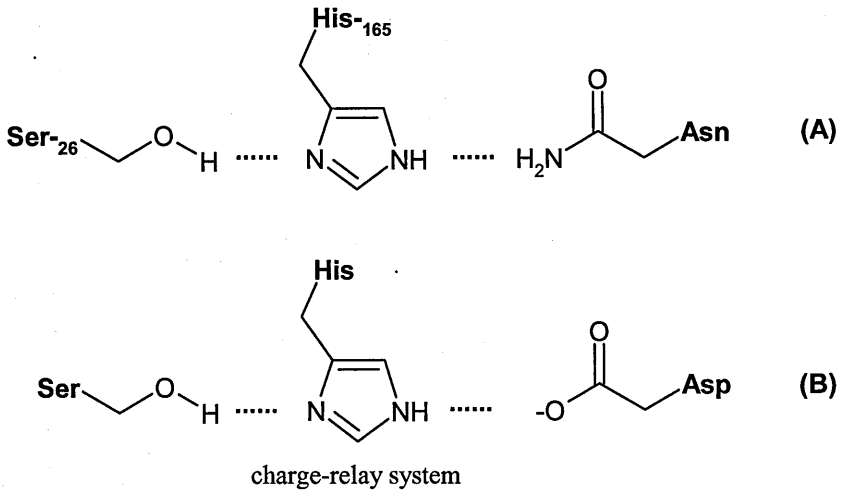

Figure 1.3: Active site residues in silicatein (A) and a serine-histidine-aspartate catalytic triad (B).

Although the natural substrates and the catalytic function of silicatein are unknown in *in vivo* biosilicification reactions [20], it has been postulated that silicatein may be used *in vitro* to control the architecture of silicon-functional materials under environmentally benign conditions [9]. It is unclear whether silicatein catalyses the complete biosilicification reaction and/or if the protein filaments function as templates in the synthesis of spicules [16, 17]. Following the nucleation of silica on silicatein filaments, long-range order was not observed [25]. Although it has been hypothesised that the high concentration of hydroxyl functionality on the silicatein protein [16] may participate in the design of the biosilica architecture [26-28], control experiments with materials (i.e. silk [29] and cellulose) known to contain high concentrations of hydroxyl groups were negative at neutral pH [16].

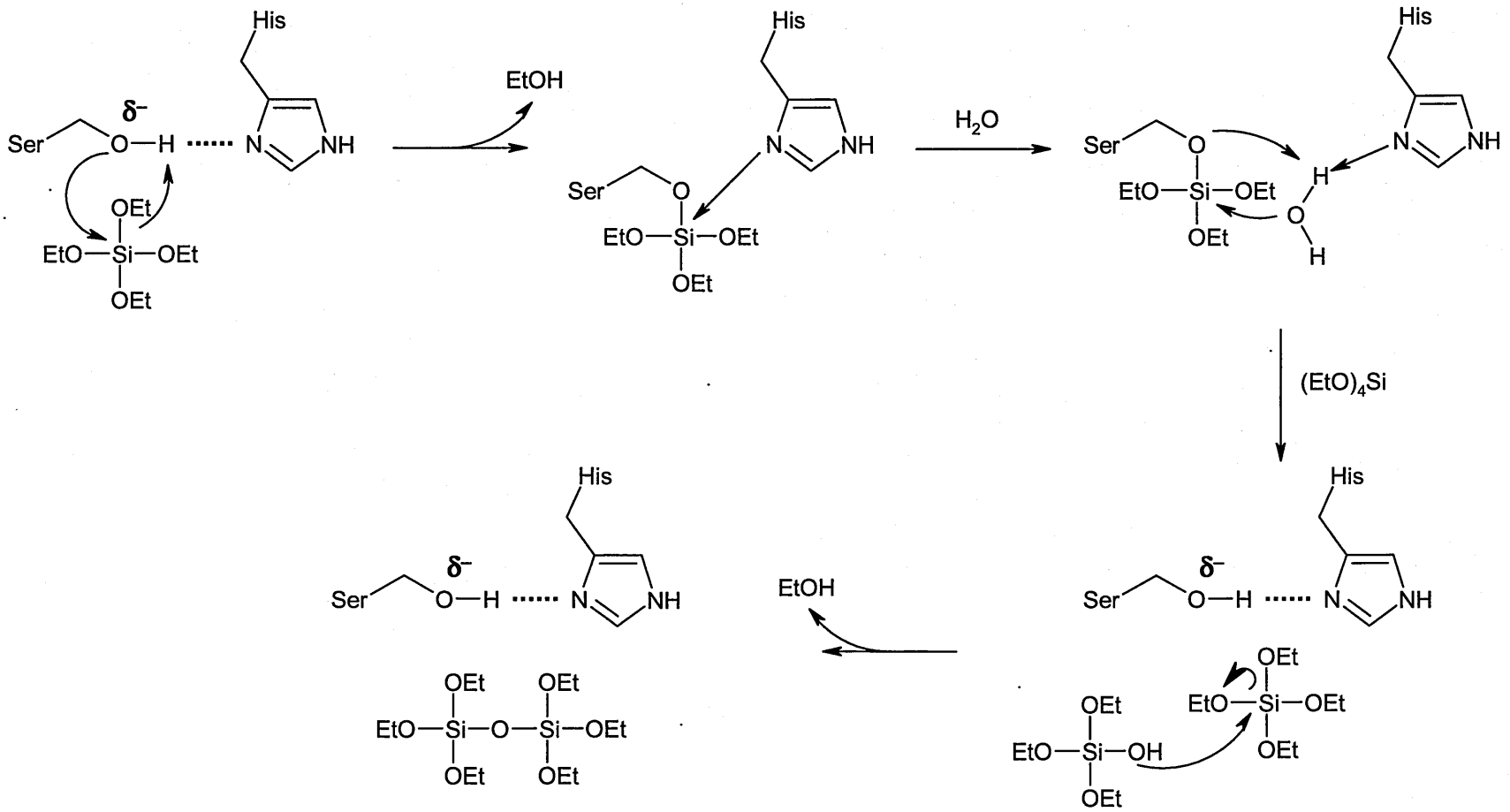

Scheme 1.2: Proposed mechanism of silicatein-catalysed polycondensation of tetraethoxysilane.

In an attempt to create a biomimetic or natural analogue to silicatein, polypeptide molecules were evaluated as silica biocatalysts [10, 18, 25]. The design of the biocatalysts was based on the nucleophilic, amine-functional active site of silicatein. Initially, select hydroxyl (e.g. serine, threonine), carboxylic acid (e.g. glutamic acid) and amine (e.g. lysine, histidine) functional homopolymers and their mixtures were observed to be catalytically unreactive; while, reduced cysteine (sulfhydryl) oligomers and amphiphilic diblock copolypeptides (e.g. cysteine-lysine, Figure 1.4) catalysed the hydrolysis and/or condensation of tetraethoxysilane (Table 1.1).

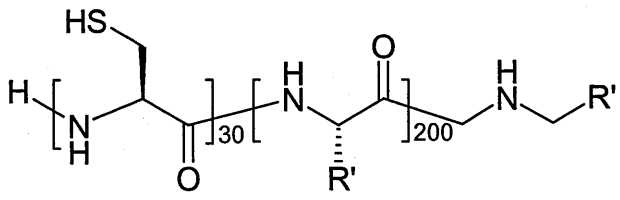

Figure 1.4: Biomimetic diblock polypeptide.
R' = $(CH_2)_4NH_3^+Br^-$.

Table 1.1: Polypeptide-catalysed polycondensation of tetraethoxysilane [18].[1]

Polypeptide	Rate (μmol silica/h)[2]
negative control[3]	0.01
poly(L-lysine$_{200}$)	0.01
poly(L-cysteine$_{30}$)	0.43, 0.08 (air)
poly(L-cysteine$_{30}$-*b*-L-lysine$_{200}$)	0.43, 0.62 (air)
poly(L-tyrosine$_{30}$-*b*-L-lysine$_{200}$)	0.30
poly(L-serine$_{30}$-*b*-L-lysine$_{200}$)	0.29
poly(L-glutamine$_{30}$-*b*-L-lysine$_{200}$)	0.22
poly(L-alanine$_{30}$-*b*-L-lysine$_{200}$)	0.09

1 The polycondensation reactions were conducted with 3.4 M tetraethoxysilane in 5-mg/mL solutions of the polypeptides in 50 mM Tris-HCl buffered (pH 6.8) media at ambient temperature under oxygen-free nitrogen atmospheres over 24 hours. Select reactions with cysteine were performed in air.

2 The silica precipitate was isolated, washed, and dissolved prior to analysis by the spectrophotometric molybdate assay.

3 The negative control reaction was performed in the absence of a polypeptide.

The amphiphilic character of the diblock polypeptides was postulated to promote the self-assembly of chains and interaction with charged substrates in an aqueous medium. The nucleophilicity of the chain segment enhanced the catalytic activity of the biomimetic catalyst (i.e. SH > C_6H_4OH > CH_2OH > $CONH_2$ > CH_3). The cysteine- and serine-functional lysine block copolypeptides were observed to control the morphology of silica. Specifically, reduced (RSH) and oxidised (RS_2R) cysteine-functional lysine copolypeptides synthesised large aggregates (~600 nm) and packed silica columns, respectively (Figure 2.2, p. 41). Comparatively, cysteine and lysine polypeptide blends catalysed the formation of amorphous silica. The opportunity to strategically use a biomimetic catalyst to synthesise a silicon-functional material with a defined architecture under benign conditions is promising.

Recently, the diblock copolypeptides were used to create multicompositional particles with structural control and spatial order over multiple length scales [30]. Specifically, the cysteine-lysine polypeptides were observed to direct the synthesis and assembly of silica- and gold-functional nanoparticles into micron-sized hollow spheres. The thermally stable porous walls were composed of distinct layers of silica on gold. The reaction sequence was determined to be critical during the assembly of the hollow spheres. Prior to silica encapsulation, the presence of inter- and intra-chain disulfide bonds in the polypeptide promoted the formation of gold-thiolate bonds. Due to their spontaneous formation, the hollow spheres did not appear to be an artifact of sample handling. The product morphology (e.g. round vs. crumpled spheres, films) was controlled by the block lengths of the cysteine-lysine polypeptide. In addition, the biomimetic process was extended to create silica coated silver hollow spheres. The ability to assemble a material with structural control and spatial order over various length scales will lead to novel three-dimensional products.

1.1.2 Diatoms

Diatoms control the marine silica cycle. These single cell plants process an estimated 200-280 teramoles of particulate silica every year [7]. Given the complex design and diversity of the siliceous skeletons of diatoms [2], the nanostructured cell walls are natural paradigms of genetically controlled architectures (Figure 1.5) [8].

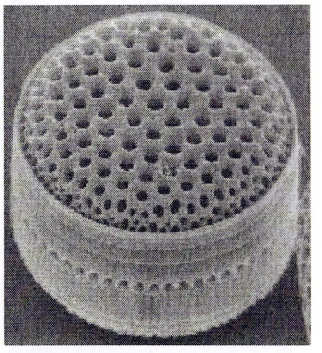

Figure 1.5: Diatomaceous skeleton (scale not cited) [31].

The unique morphologies of the "glass houses" [32] are used to classify the diatomaceous species of *Bacillariophyceae*. Ubiquitously present in water habitats, diatoms are microscopic (~1-500 μm [33]), eukaryotic, unicellular planktonic algae composed of hydrated inorganic (i.e. primarily amorphous silica, 7-1100 fmol silica/cell [34]) and organic (e.g. proteins, polysaccharides) macromolecules [35]. In addition to structural attributes, the siliceous cell walls have been postulated to function as an ultraviolet filter, cellular armour, and ballast [36]. Given a further understanding of these biosilicification mechanisms, the ability to control the morphogenesis of biosilica could create new inorganic materials with novel tertiary architectures.

Based on studies of a variety of diatoms (i.e. *Cylindrotheca fusiformis*, *Navicula pelliculosa*, *Nitzschia alba*, *Nitzschia angularis*, *Chaetoceros debilis*, *Chaetoceros didymium*, *Eucampia zodiacus*, *Phaeodactylum tricornutum*, and *Stephanopyxis turris*)

[11-14, 37-39], specific proteins and polyamines within each species were determined to promote the synthesis and formation of different cell wall structures. These proteins were obtained by digesting purified cell walls or frustules (Figure 1.6) with ethylenediaminetetraacetic acid (EDTA) to isolate intermediate protein molecules. These calcium-binding glycoproteins or isomeric frustulins (75-200 kDa) uniformly coat the outer surface of the diatoms [37, 38]. These carbohydrate-functional coatings are believed to protect the cell walls from dissolution and, possibly, bacterial degradation [26].

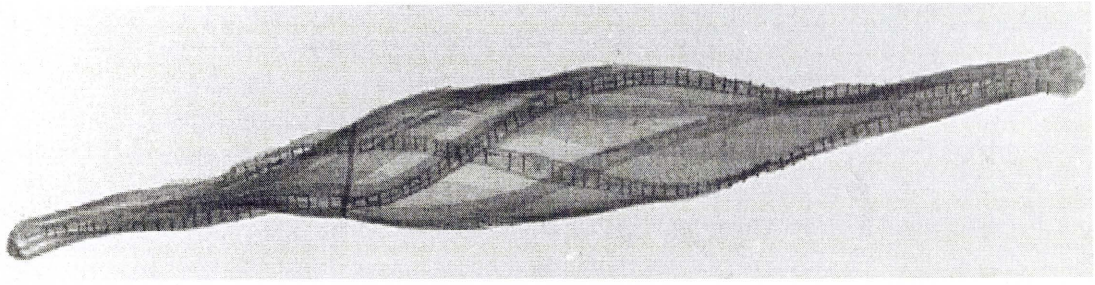

Figure 1.6: Transmission electron microscope image of a *Cylindrotheca fusiformis* diatom cell wall (36 μm in length) [11].

Subsequently, the EDTA-extract was digested with boiling sodium dodecyl sulfate (SDS) and either anhydrous hydrogen fluoride (HF) or aqueous ammonium fluoride [22] (pH 5). Following a polyacrylamide gel electrophoresis (PAGE) analysis, the extracts were observed to contain both high and low molecular weight protein fractions. In the cell walls, these fractions formed an organic-inorganic composite with silica. In *C. fusiformis*, the high molecular weight (200 kDa) HF-extractable protein (HEP) was determined to be associated with the girdle region where the two halves of a diatom are united (analogous to a petri dish) [39]. The low molecular weight proteins or silaffin molecules were composed of a distribution of similar post-translationally modified zwitterionic peptides labeled silaffin-1A (6.5 kDa [14]), -1B (8 kDa), and –2 (17 kDa) [11]. Silaffin-1A was composed of two phosphate-functional [22] isoforms, silaffin-$1A_1$ and silaffin-$1A_2$ (Figure 1.7) [13, 14].

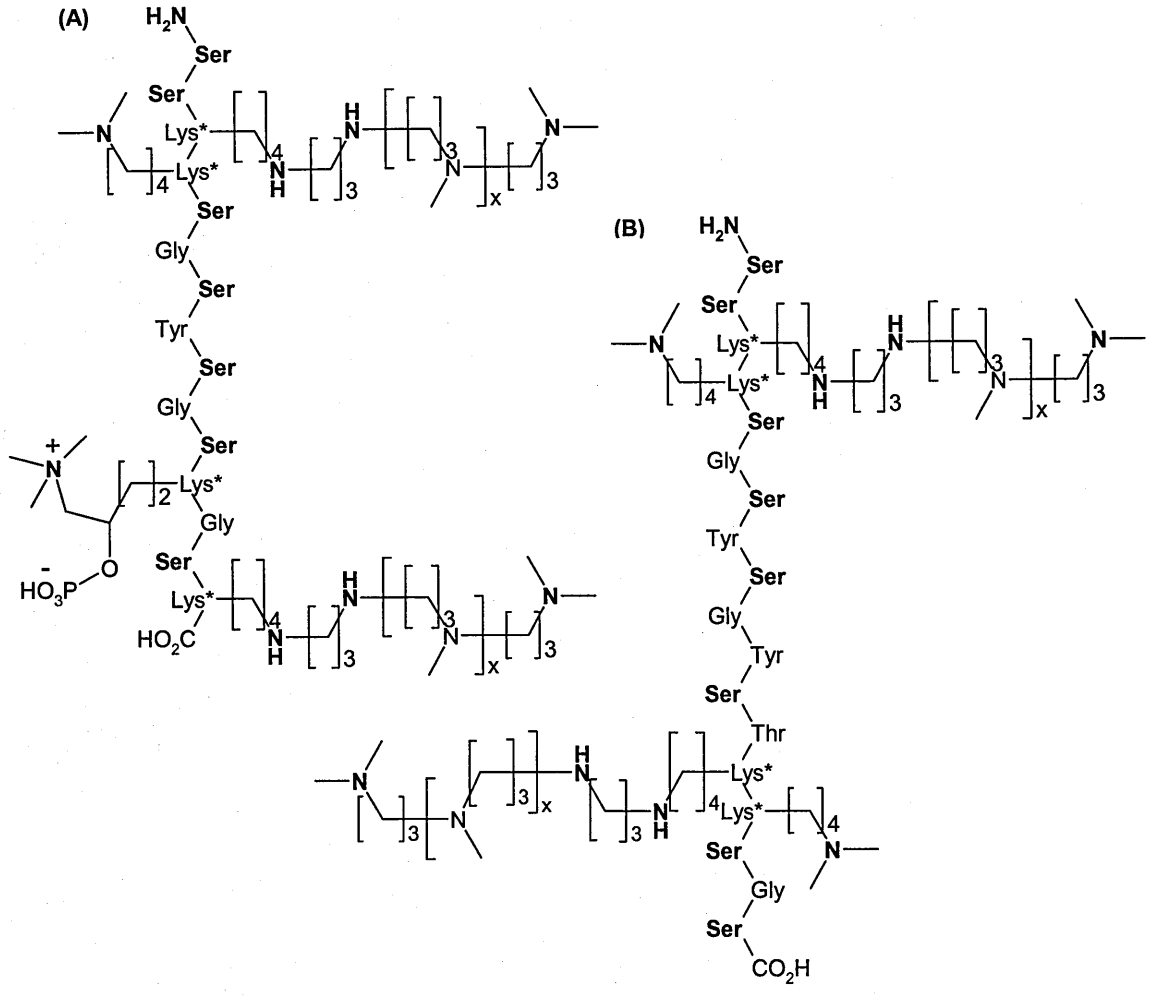

Figure 1.7: Native chemical structures of silaffin-1A$_1$ (A) and silaffin-1A$_2$ (B).
Ser = anionic phosphorylated serine (i.e. R = $CH_2OPO_3H^-$).

Silaffin-1A$_1$ was the first natural polypeptide identified to contain a quaternary amine-functional amino acid residue, phosphorylated ε-N,N,N-trimethyl-δ-hydroxylysine. A gene (sil 1) encoding a polypeptide (sil 1p) containing silaffin sequences was identified in a *C. fusiformis* genomic library with an amplified cDNA fragment of silaffin-1B [11]. Sil 1p was composed of a signal sequence, acidic functional residues, and seven repetitive (R) homologous segments containing silaffin sequences 1A$_1$ (R3-R7), 1A$_2$ (R2), and 1B (R1) [13]. Following proteolytic cleavage and post-translational modification, it appears that sil 1p may function as a selective source of silaffin peptides. In addition to the silaffins and HEP, the HF-extracts were determined to contain high concentrations of long-chain (x = 8-20) oligo-(N-methyl)propylamines attached to putrescine derivatives (Figure 1.8) [12].

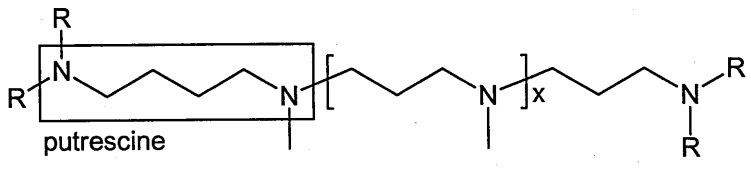

Figure 1.8: Oligo-(N-methyl)propylamine attached to putrescine derivatives.
R = H and/or CH_3.

The distribution of organic polyamine molecules was unique to each species. Given the presence of these specific molecules in the siliceous cell walls, their roles in silica biomineralisation were further investigated.

Phosphate-functional silaffins [11, 13, 14] and polyamines [12] were documented to catalyse the *in vitro* polycondensation of silicic acid within seconds and stoichiometrically precipitate with silica under mild conditions (i.e. low temperature and pressure). The zwitterionic silaffin-1A isoforms induced the precipitation of a network of nearly spherical silica particles (500-700 nm), while a mixture of the silaffin peptides resulted in the formation of small silica aggregates (< 50 nm). Since silaffin-1A did not catalyse the condensation of silicic acid in the absence of phosphate, diatoms appear to require an anionic source to promote the formation of silica. Comparatively, the polyamines promoted the formation of spherical silica particles ranging in size from 100 to 800 nm. The particle size distributions were dependent on the lengths of the polyamine molecules and the pH of the medium. In the presence of a silaffin/polyamine mixture, the morphology of the hybrid silica particles was a result of the synergistic effect of this composite material. Since the precipitation of silica appears to be controlled within acidic membrane bound cells (i.e. silica deposition vesicles, SDV), the modified amine-functional molecules would catalyse *in vivo* polycondensation under physiological conditions (i.e. pH < 7). Additionally, the silaffin and polyamine molecules [35] promoted

non-covalent interactions such as ionic and hydrogen bonding during the formation of silica [2]. Since these molecules have not been observed to control structure *in vitro*, the SDV was postulated to function as a three dimensional mold.

Consequently, a simplified phase-separation model was proposed in order to explain the formation of the intricate silica patterns formed during the morphogenesis of biosilica [40]. The model was based on a hierarchy of similar patterns (i.e. hexagonal) over several length scales due to repetitious phase separation during polycondensation. Since polyamines are stoichiometrically consumed during polycondensation, the fragmentation of these reactive interfacial surfaces resulted in the formation of the observed patterns. Although this model successfully explained the complex wall patterns observed in four species of *Coscinodiscus* diatoms, the two-dimensional model proved to be a simplification of the observed three-dimensional expansion of the SDV during biosilification.

The molecular basis of silicon transport and cellular processing in a diatom is essentially unknown. In order to further understand these mechanisms, silicon-responsive genes in the *C. fusiformis* diatom were isolated, expressed, and characterised [41]. Based on a competitive uptake study in *Xenopus laevis* oocytes, the transportation of silicic acid increased in comparison to a labeled germanium-functional analogue (i.e. germanic acid, $^{68}Ge(OH)_4$) in the presence of a cloned silicon transporter gene (SIT 1). Subsequently, a SIT gene family (SIT 1-5) was identified in a *C. fusiformis* genomic library with SIT 1 cDNA [42]. Although the SIT-encoded proteins contain different C-terminal domains, modeling data suggests that the proteins contain ten conserved transmembrane (hydrophobic) segments including their locations [34]. Based on these differences, including expression levels and patterns during the cell cycle, the homologous SIT genes

appear to direct and regulate cellular silicon transportation. Although silicon consumption may be dependent on sodium [34], diatom species have been observed to consume unionized, neutral silicic acid [10]. Given the high concentrations (saturated) of intracellular silicon, the mechanisms (e.g. ionophores, silicon transport vesicles) controlling the intracellular transportation of soluble silicon are unknown [34]. It was postulated that silicon may be solubilised by complexation with unknown organic molecules (e.g. catecholates, polysaccharides) or sequestered in unknown vesicles. Given the presence of homologous SIT genes in various marine (i.e. pinnate and centric) as well as freshwater diatoms [42], this gene family continues to provide insight into the transportation of dilute silicic acid from ocean and fresh water into and within the diatom.

After synchronizing a culture of *Navicula pelliculosa* diatoms by silicon starvation, the temporary *in vivo* formation of a hypervalent organo-silicon complex coordinated to at least one nitrogen was observed by ^{29}Si NMR [43]. For clarification, the organo-silicon complex (i.e. SiOC) did not contain a silicon-carbon bond (i.e. SiC). Following the starvation procedure, the diatoms were fed a ^{29}Si isotopically enriched potassium silicate solution to enhance the detection and identification of molecular compounds formed during the cellular processing of silicon. Given the limited time of detection, the silicon-functional complex was postulated to be a transient species. Comparatively, the transient spectral signal was reproducible in replicate studies and absent in negative control experiments without the diatoms. Based on the NMR chemical shift, the species was speculated to be an pentaoxo-azo-silicon complex. This study provided a unique *in vivo* observation of the cellular processing of a silicate molecule in a living organism.

In an attempt to extrapolate the natural activities of silaffins and polyamines in diatoms, biomimetic protein [11] and organic [12] analogues were prepared. The synthetic

molecules were based on a non-modified Sil 1p R5 peptide and a monodisperse N-methyl-propylamine oligomer, respectively. The molecules were observed to promote silicic acid polycondensation and precipitation of silica under neutral pH conditions. The use of external force was demonstrated [44] to control the morphology (e.g. arched, fibrillar) of the silica material catalysed by the biomimetic peptide. Different flow dynamics (e.g. gas bubbles, tubular shear) within the reaction mixture changed the reactive interfaces and, consequently, the directional growth and deposition of the material. Although the *in vivo* rate of silica deposition is approximately one million times faster than the abiotic reactions [11], the opportunity to explore the potential of diatoms [33] in order to gain an "understanding of the biological control of silicon chemistry is likely to be extremely beneficial [34]."

In application, the Sil 1p R5 biomimetic peptide was strategically used to create a hybrid organic/inorganic material containing an array of ordered silica nanospheres (Figure 1.9) [45].

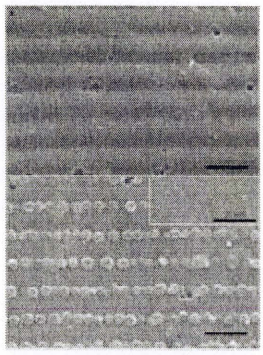

Figure 1.9: Two-dimensional array of ordered silica nanospheres [45].
Top = without peptide (scale bar is 2 μm).
Bottom = with peptide (scale bar is 2 μm, inserted scale bar is 20 μm).

Based on different cure rates (i.e. crosslink density) and the hydrophobicity of the reactants during the photopolymerisation of the material, the smaller peptide molecules were

observed to phase separate and migrate into the periodic domains of the hologram. Upon exposure to silicic acid, the peptide molecules catalysed the formation of spherically shaped silica (average diameter = 452 nm) within minutes. Comparatively, silica was not observed in the absence of the biomimetic peptides (i.e. a negative control). After evaluating this new holographic material, the diffraction efficiency and mechanical strength increased significantly when compared to the product without silica. This ability to achieve two-dimensional, nanoscale order within a material creates the opportunity to build more complex three-dimensional structures.

Based on interfacial interactions, a combinatorial phage-display library was repetitively panned to identify peptides that exhibit binding and nucleation against inorganic materials (e.g. silica, germanium) [19]. Inspired by the activity of the Sil 1p R5 biomimetic peptide, the library was composed of approximately ten billion random peptides containing twelve amino acid residues fused to the minor coat (pIII) protein of M13 phages. When compared to a control peptide with an affinity for germanium, a selection of the screened peptides was observed to preferentially bind silica. Given this recognition, a few of the peptides precipitated a network of partially fused amorphous silica spheres (250-500 nm) from a solution of silicic acid. Based on their amino acid sequences, cationic peptides with hydroxy- and imidazole-functional residues were determined to promote silica precipitation. The negative control reaction remained homogeneous for several hours prior to precipitation. The strategic use of various biomimetic peptides was postulated to control the deposition of select inorganic molecules necessary to obtain spatial order during the microfabrication of novel hybrid materials.

1.1.3 *Equisetum telmateia* Plant

Biomineralisation requires specific elements, nucleation, and regulated growth throughout the lifetime of an organism [15]. Biological organisms regulate the formation of crystalline and amorphous composite mineral phases. Biominerals are typically composed of minerals as well as organic molecules such as proteins and carbohydrates. While the presence of low levels of intercalated biopolymers effect the mechanical properties of crystalline biominerals, they have also been postulated to participate in nucleation and crystal growth. Biological mineralisation has been hypothesised to be controlled by molecular interactions achieved through spatial localization in membrane enclosed compartments and specific regions of cell walls [46]. The interactions are essentially unknown in the development of these aggregate structures. Crystalline silica has not been observed in biological sources.

In order to further understand the natural process of biosilica precipitation under mild conditions (e.g. neutral pH), protein functional biomolecules from intrasilica locations in the branches of a *Equisetum telmateia* plant were extracted with concentrated nitric, sulfuric, and hydrofluoric acid [15]. The extract contained a high concentration of serine, glutamine, glutamic acid, and glycine. In addition, select carbohydrates such as glucose and xylose as well as low molecular weight glycoproteins were identified. In the presence of the biopolymer extract, a silicon-functional catecholate complex, $K_2(Si(C_6H_4)_3)xH_2O$, partially decomposed to orthosilicic acid which condensed to form biosilica at an increased rate under mild reaction conditions. Based on transmission electron microscope images, some areas of the biosilica surface appeared to be layered, while other areas appeared to be visually similar to quartz. The siliceous materials did not form mesoporous, lamellar phases. It has been hypothesised that the prevention of crystalline phases in biosilica promotes the formation of detailed macroscopic structures.

1.2 Biotransformations

The strategic use of biological systems to conduct chemical reactions has been referred to as a "chemomimetic biological" [47] approach. Established enzymatic and microbial catalysed transformations have been documented [48, 49] under a variety of experimental conditions. Although known biocatalysts are unable to facilitate a complete range of transformations, a significant number of biotransformations may be performed. In summary, the well-established biocatalysed reactions are detailed in Table 1.2.

1.2.1 Organosilicon Biotransformations

Organosilicon molecules have begun to be explored as non-natural enzymatic substrates for novel biotransformations [50-63]. Lipase was used to study the selective synthesis of organosilicon esters under mild reaction conditions [64, 65]. Specifically, *Candida cylindracea*, *Rhizopus japonicus*, and Steapsin lipases (absorbed on Celite) were used to catalyse the enantioselective esterification of trimethylsilyl alcohols (x = 0-3) and analogous organic molecules with racemic 2-(4-chlorophenoxy)propanoic acid in water-saturated benzene at 30°C (Scheme 1.3).

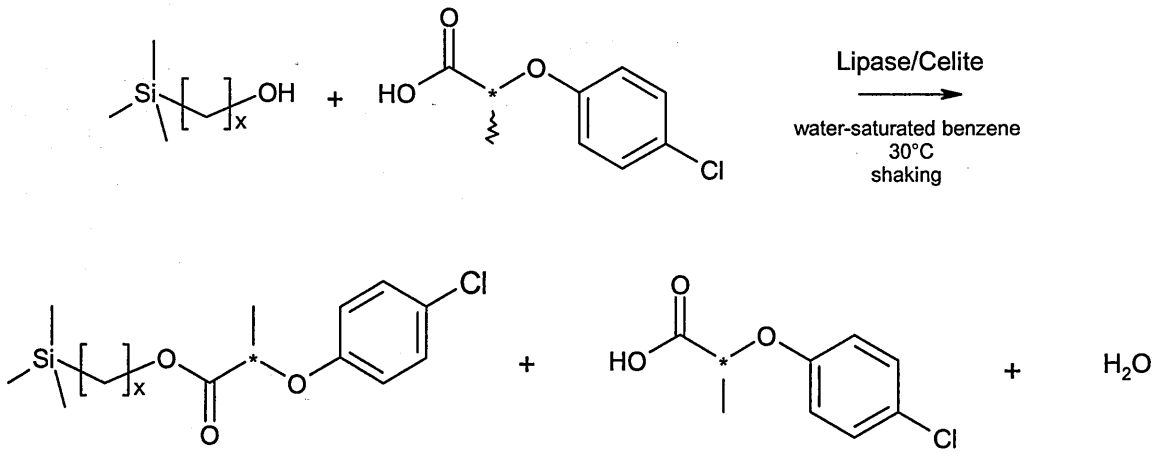

Scheme 1.3: Lipase-catalysed stereoselective esterification of racemic 2-(4-chlorophenoxy)propanoic acid with trimethylsilyl alcohols.

Table 1.2: Biotransformation matrix.

FROM	TO	acetylenes	carboxylic acids, acid halides, anhydrides	alcohols, phenols	aldehydes	alkyls, methylenes, aryls	amides	amines	esters	ethers, epoxides, peroxides	halides, sulfonates, sulfates	hydrides	ketones	nitriles	olefins	azide	phosphate
acetylenes											√		√				
carboxylic acids, acid halides, anhydrides							√		√								
alcohols, phenols				√	√				√	√			√				√
aldehydes			√	√									√	√			
alkyls, methylenes, aryls				√							√				√		
amides			√					√									
amines							√										
esters			√	√	√		√		√				√				
ethers, epoxides, peroxides				√				√					√				
halides, sulfonates, sulfates			√	√		√				√					√		
hydrides																	√
ketones				√					√					√			
nitriles			√				√	√									
olefins				√	√	√		√		√	√						
azide								√									
phosphate			√	√			√			√							√

The organosilicon molecules were observed to be acceptable enzymatic substrates. With the exception of trimethylsilanol (Scheme 1.3, x = 0) and 1,1-dimethylethanol, the trimethylsilyl alcohols (Scheme 1.3, x = 1-3) and analogous organic molecules were reported to selectively react with the D-acid. Since the rate of reaction with organic molecules is inversely related to stereoselectivity [47], the high enzymatic activity and selectivity with trimethylsilylmethanol versus the other silicon- and organo-functional alcohols was an attribute. Based on relative reaction rates, *C. cylindracea* lipase was determined to have the greatest activity.

Since β-hydroxyalkylsilanes are unstable in the presence of an acid or base, hydrolase enzymes were used to catalyse the esterification of three trimethylsilylpropanol isomers and analogous organic molecules with 5-phenylpentanoic acid under mild conditions (i.e. low temperature, neutral pH) (Scheme 1.4) [66]. Specifically, *Candida cylindracea*, *Rhizopus japonicus*, and Steapsin lipase, as well as a lipoprotein lipase and cholesterol esterase were investigated.

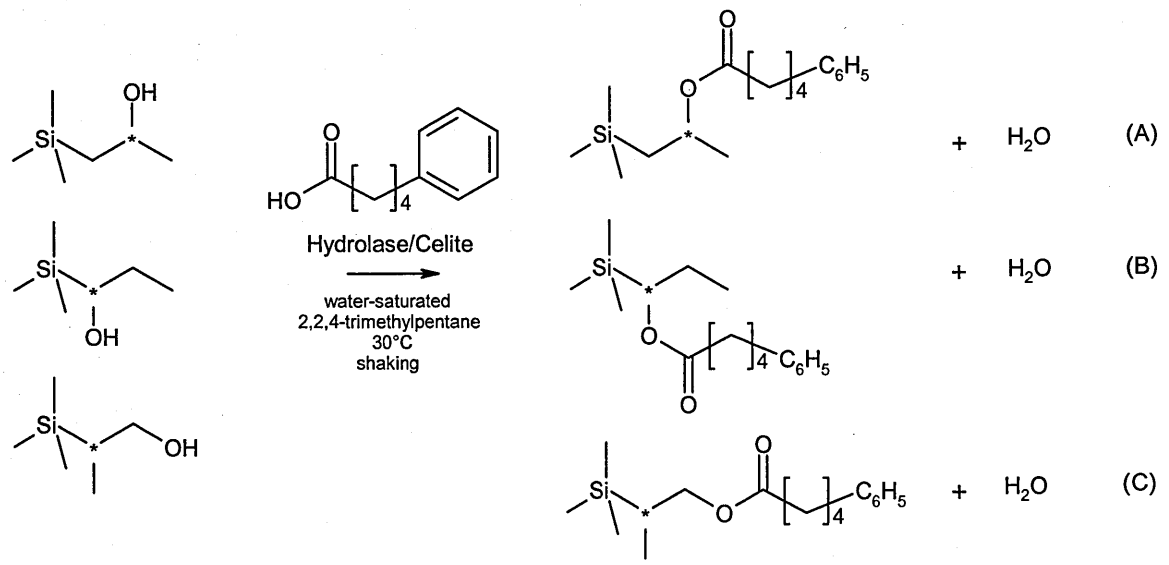

Scheme 1.4: Hydrolase-catalysed esterification of trimethylsilylpropanol isomers with 5-phenylpentanoic acid.

The hydrolases were reported to stereoselectively catalyse the esterification of the trimethylsilylpropanol isomers including the β-hydroxyalkylsilanes (Scheme 1.4, A and C) [66]. Comparatively, the hydrolase enzymes selectively catalysed the esterification of the organosilicon and organic substrates at different rates. The optical purity of the organosilicon esters appeared to increase in comparison to the organic esters.

Hydrolases have been used to catalyse the formation of organosilicon acrylate monomers, macromers, and polymers [67]. Claims have been made that pure or immobilised esterases, lipases, and proteases are preferred for catalysing the (trans)esterification of (meth)acrylates and silicone polyethers as well as carbinol-functional siloxanes at 40-70°C in 24 hours. Based on the amount of siloxane, the enzymes were typically formulated at ~1-10% (w/w). After the reaction, ~5-100% of the hydroxyl groups reacted to form acrylate esters. For example, Novozym® 435 (N435) was used to catalyse the esterification of a silicone polyether (R = $(CH_2)_3(OCH_2CH_2)_m(OCH_2CH(CH_3))_nOH$) and butyl acrylate (Scheme 1.5). N435 is a commercial source of *Candida antarctica* lipase B immobilised on acrylic resin beads.

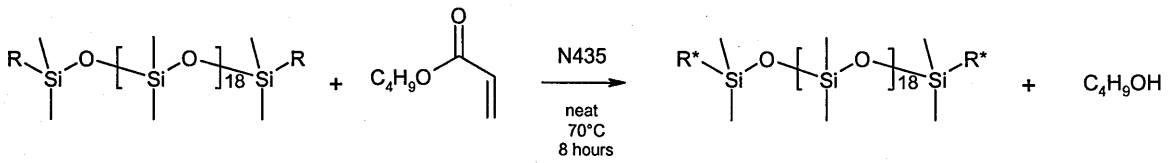

Scheme 1.5: Hydrolase-catalysed organosilicon acrylate.
R = $-(CH_2)_3(OCH_2CH_2)_m(OCH_2CH(CH_3))_nOH$.
R* = $-(CH_2)_3(OCH_2CH_2)_m(OCH_2CH(CH_3))_nO(C{=}O)CH{=}CH_2$ and/or R.

The butanol was distilled off under vacuum to promote the esterification reaction. After 8 hours, the mixture was filtered to remove the enzyme and distilled to remove residual butyl acrylate. In the product, 65% of the hydroxyl groups were reported to be acrylated. The ability to conduct this reaction under mild conditions suppressed unwanted side

reactions, eliminated undesirable colouration, and improved the safety of the workup procedure.

Given the ability to self-assemble, amphiphilic organosilicon carbohydrates were documented to have unusual properties in solution or as neat materials [68, 69]. The physical properties of the "sweet silicones [68]" are dependent on the structure of the attached carbohydrate. These polymers may be used as surfactants, adhesion promoters, or chiral templates. Traditional chemical techniques including activation and multiple protection-deprotection steps were used to synthesise polydimethylsiloxanes with pendent maltoheptaoside (Figure 1.10, n = 5) or maltoheptaonamide (Figure 1.11, n = 5) groups by hydrosilylation and/or amidation.

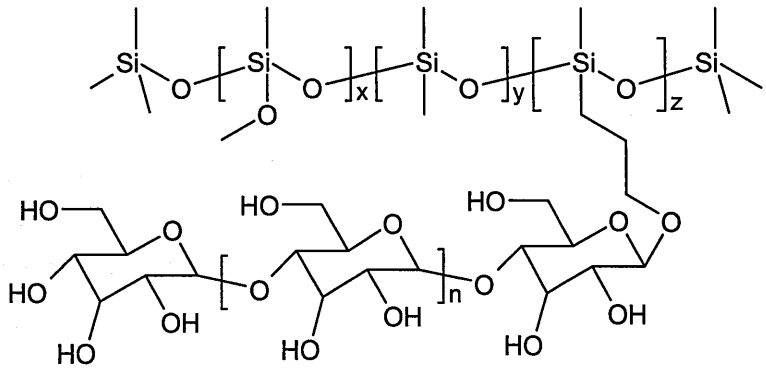

Figure 1.10: Polydimethylsiloxane with a pendent maltoheptaoside groups.

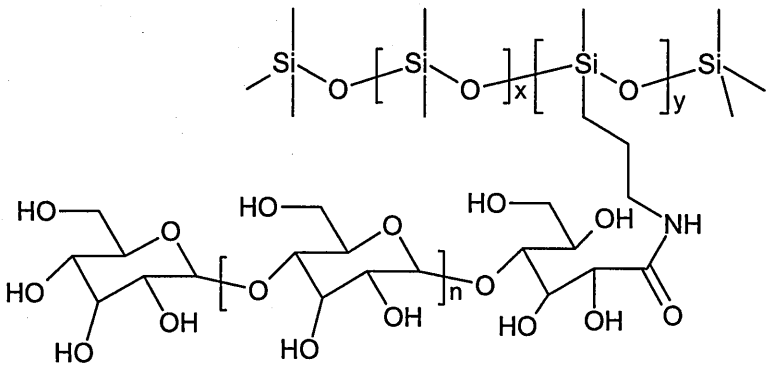

Figure 1.11: Polydimethylsiloxanes with pendent maltoheptaonamide groups.

Subsequently, potato phosphorylase was used to enzymatically catalyse the formation of poly(dimethylsiloxane-graft-(α,1→4)-D-glucopyranose (Subsequently, Figure 1.10, n = 300; Figure 1.11, n = 26) molecules with α-D-glucose-1-phosphate in a citrate buffer at 37°C. The amylose side chains were determined to have a helical structure.

Hydrolase enzymes were used to study the synthesis of organosilicon amides under mild reaction conditions. Specifically, lipases, a lipoprotein lipase, an esterase, cholesterol esterases, and proteases were used to catalyse the formation of an amide bond between octanoic acid and (aminomethyl)trimethylsilane (Scheme 1.6) as well as an analogous organic molecule (2,2-dimethylpropylamine) in wet 2,2,4-trimethylpentane at 30°C for 48 hours [70].

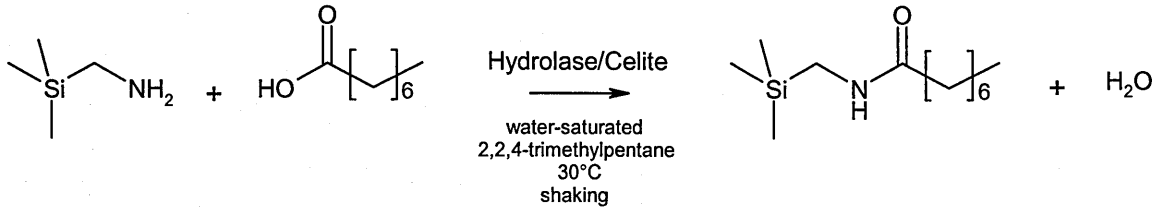

Scheme 1.6: Hydrolase-catalysed condensation of (aminomethyl)trimethylsilane and octanoic acid.

The lipoprotein lipase type A and cholesterol esterase type A from *Pseudomonas sp.* were determined to have the highest activity. In addition, *Candida antarctica* (Lipase Novo from Novo Nordisk), *Candida cylindracea*, and *Pseudomonas sp.* lipase, as well as cholesterol esterase III were reported to be active. When compared to the organic substrate, (aminomethyl)trimethylsilane was determined to be more reactive. Since silicon is less electronegative than carbon, this was postulated to be from the enhanced nucleophilicity of the nitrogen at silicon.

Optically active synthetic amino acids are used as precursors for pharmaceutical, agricultural chemical, and food products. A novel silicon-functional amino acid and peptides were synthesised to investigate the properties of these molecules [71]. Specifically, L-trimethylsilylalanine (L-TMS-Ala, > 99% ee), a leucine (Leu) analogue, was prepared by performing an acylase-I-catalysed deacetylation of racemic N-acetyl-trimethylsilylalanine [72]. Subsequently, a protease (thermolysin) was used to catalyse the formation of an amide bond between L-TMS-Ala and L-Leu in ethyl acetate with a buffer at 30°C (Scheme 1.7) [73].

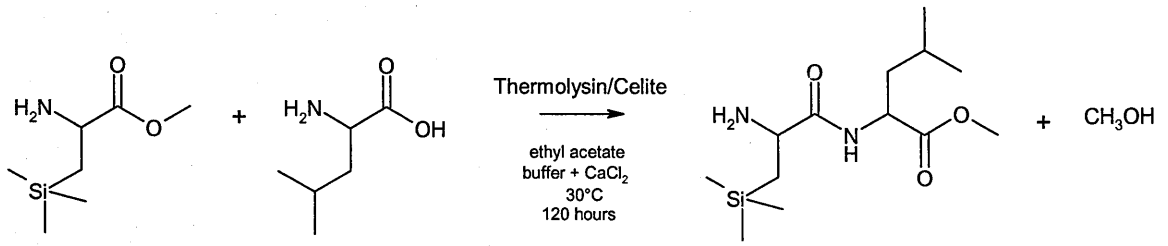

(L-TMS-Ala)-L-Leu-OMe

Scheme 1.7: Thermolysin-catalysed silicon-functional dipeptide.

Although the enzyme catalysed the formation of (L-TMS-Ala)-L-Leu-OMe, it was not possible to synthesise L-Leu-(L-TMS-Ala)-OMe or (L-TMS-Ala)-(L-TMS-Ala)-OMe. It was hypothesised that thermolysin would not accept TMS-Ala-OMe as the amine component due to steric hindrance in the region of the active site. Since Leu-Leu is known to inhibit several zinc proteases, the inhibition activity of enzymatically and chemically synthesised L-TMS-Ala- and L-Leu-functional dipeptides were investigated (Table 1.3) [71].

Table 1.3: Inhibition of a thermolysin-catalysed hydrolysis reaction.[1]

Dipeptide	Relative Inhibitory Activity[2]
L-Leu-L-Leu	100
(L-TMS-Ala)-L-Leu	8
L-Leu-(L-TMS-Ala)[3]	144
(L-TMS-Ala)-(L-TMS-Ala)[3]	24

1 Dipeptide inhibition of thermolysin-catalysed hydrolysis of N-(3-[2-furyl]acryloyl)-Gly-Leu-NH_2.
2 Inhibition activity is relative to L-Leu-L-Leu.
3 Chemically synthesized dipeptides.

Although the relative inhibitory activities of (L-TMS-Ala)-L-Leu and (L-TMS-Ala)-(L-TMS-Ala) were less than L-Leu-L-Leu, L-Leu-(L-TMS-Ala) further inhibited the thermolysin-catalysed hydrolysis of N-(3-[2-furyl]acryloyl)-Gly-Leu-NH_2.

Atsuo Tanaka (Kyoto University) wrote, "In the future, the importance may increase not only in the preparation of optically active compounds in organic syntheses but also in silicon-derived pharmaceuticals and silicon-derived agrochemicals as well as organosilicon compounds as their precursors [52]."

1.2.2 Stereoselective Organosilicon Biotransformations

Stereoselective biotransformations have been used to synthesise optically active molecules where the silicon atom is the center of chirality [50]. Alternatively, fractional crystallisation and chromatographic separations have been used to isolate similar compounds. The molecules in Figure 1.12 are optically active silanols that were isolated as nearly pure enantiomers (> 97% ee).

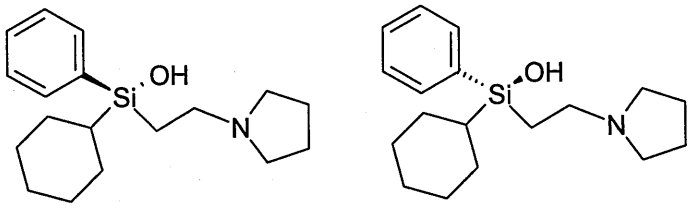

(R)-silanol **(S)-silanol**

Figure 1.12: Enantiomeric silicon compounds.

The silanol molecules form long chains through intermolecular hydrogen bonding. Based on a natural response, this was the first example of biological discrimination between enantiomeric compounds where the silicon atom was the center of chirality. Similarly, it was determined that silicon- and germanium-functional enantiomers (Figure 1.13) are bioisosteric.

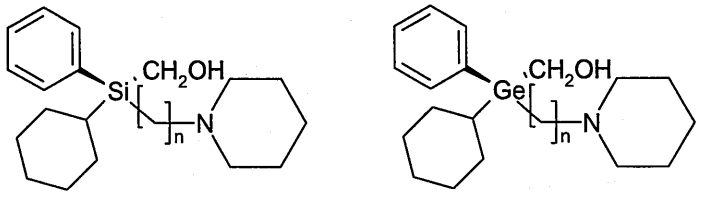

(R)-silicone **(R)-germane**

Figure 1.13: Analogous chiral silicon and germanium functional molecules.

Comparatively, the configurations of chiral silicon- and germanium-functional molecules were determined to be stable under physiological conditions. Chiral biotransformation products may be used as starting materials for the synthesis of new materials.

In general, it is difficult to prepare chiral quaternary silanes with high optical purity by a chemical route [74]. A large selection of hydrolases including lipases, a lipoprotein lipase, a cholesterol esterase, and proteases were used to catalyse the esterification between a primary alcohol with a stereogenic silicon atom, ethylmethylphenylsilylmethanol, and 5-phenylpentanoic acid (esterification) or vinyl acetate (transesterification) in wet 2,2,4-

trimethylpentane with shaking at 30°C. With the exception of the bacterial lipases (esterification) and *Bacillus sp.* proteases, the hydrolase enzymes catalysed the reactions. Although the enantioselectivity was not high in the molecules produced in the esterification (i.e. 12-61% ee) and transesterification (i.e. 0-23% ee) reactions, a moderately active protease (papain) was reported to catalyse the formation of an optically active (+)-ester (i.e. 92% ee) with the highest value obtained during transesterification (i.e. 49% ee).

1.2.3 Siloxane Biocatalysis

The hydrolysis of different silatranes was studied with an extracellular esterase [75]. The yeast, *Rhodotorula mucilaginosa* VKPM Y-706 (isolated and purified from sludge in a sewage-treatment plant [76]), expressed and secreted 90% of the hydrolase in the presence of a novel nitrogen source (i.e. 1-chloromethylsilatrane) and glucose. Based on standard assays, no phosphatase and minimal lipase activity was observed in the purified hydrolase. The esterase was observed to catalyse the complete hydrolysis of the silatranes in a tris-HCl buffer (pH 6.8) over 4 hours at 30°C (Scheme 1.8).

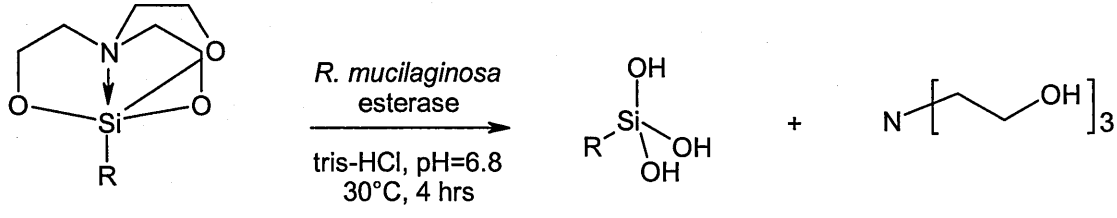

Scheme 1.8: *Rhodotorula mucilaginosa* esterase-catalysed hydrolysis of silatranes.
R = C_6H_5, $CH_2CH_2CF_3$, CH_2Cl, CH_3.

The rate of hydrolysis was dependent on the functionality of the silatrane, cyclic organosilicon tris(2-oxyalkyl)amine ester (i.e. phenyl > trifluoropropyl > chloromethyl > methyl). Subsequently, the water-soluble organosilanetriols were hypothesised to

condense in the incubated aqueous mixtures [76]. Thermal denaturation, EDTA, SDS, and $HgCl_2$ inhibited the hydrolysis reactions. Given the broad substrate specificity, the extracellular esterase was determined to be a nonspecific carboxylesterase. Comparatively, microbial esterases catalyse the hydrolysis of organophosphorus ethers in xenobiotics.

The polycondensation of diethoxydimethylsilane was studied with a lipid-coated lipase, *Rhizopus delemar* [77]. Given the amphiphilic character of the lipid, ~ 300 +/- 50 lipid molecules were determined to create a monolayer around the enzyme. In the presence of the lipid, the solubilised lipase was observed to catalyse the polycondensation of diethoxydimethylsilane over 20 hours in *iso*octane (2 wt% water) at 40°C (Scheme 1.9).

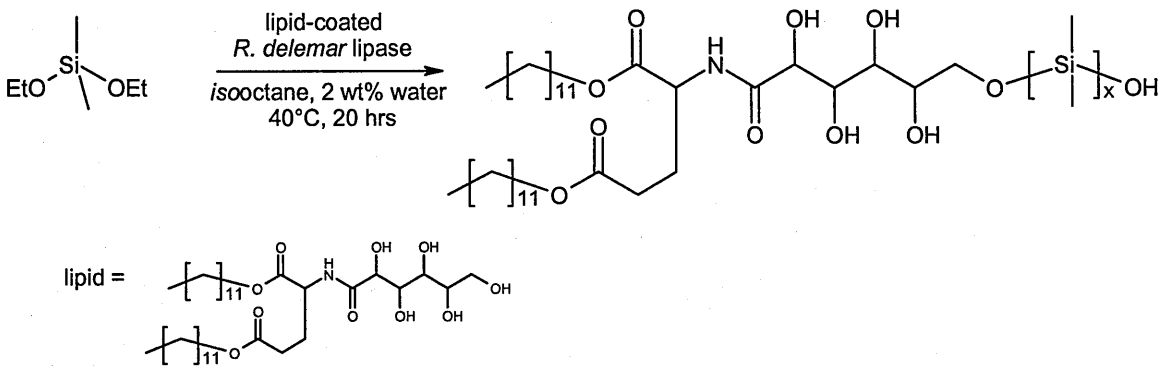

Scheme 1.9: Lipid-coated lipase-catalysed polycondensation of diethoxydimethylsilane.

The low molecular weight oligomers (Mw = 1500) were monodisperse (Mw/Mn = 1.06). Substantial condensation was not observed in the absence of the lipase, in the presence of a serine-inhibitor (phenylmethylsulfonyl fluoride), in anhydrous, aqueous and two-phase media, or blended (as opposed to treated) with the lipid. The rate of condensation was determined to follow the Michaelis-Menten model (i.e. K_m = 0.28 M) in *iso*octane at 40°C. Experimentally, the lipid was observed to participate in the reaction (80% conversion). In

addition to dissolving the enzyme in an organic medium, a single lipid molecule was observed to condense with each siloxane chain. Based on the molecular weight information, the hydroxy-functional lipid was postulated to participate in the polycondensation reactions while residing in the enzymatic cavity. Alternate lipids decreased the activity of the lipase.

1.2.4 Metabolism of Silicates: *Proteus mirabilis*

Wolfgang Heinen (The University of Nijmegen, The Netherlands) explored the potential of microorganisms to catalyse biotransformations. Specifically, Heinen studied the metabolism of silicates in bacteria [78].

Initially, *Bacillus subtilis*, *Escherichia coli*, *Serratia marcescens* and two unknown bacterial strains from 'garden soil' were evaluated [79]. It was hypothesised that a source of silicon (e.g. silicic acid) may be substituted as a natural analogue for phosphorus (e.g. phosphoric acid) in the metabolic pathways of the microorganisms. Sodium silicate, silica gel, and quartz were studied as silicon-functional alternative molecules for substitution of phosphorus-functional nutrients. The strains were cultured in standard culture solutions with different amounts of phosphorus and silicon. Based on the initial results [79], all of the bacterial strains with the exception of *Serratia marcescens* were viable in a phosphorus-free siliceous medium. The uptake of silicon-functional molecules was observed to be an active, as opposed to an adsorption process, that was dependent on experimental factors such as aeration, cell and silicate concentrations, and the pH of the culture solution. The garden soil bacterial strain (B2) was determined [79] to be the optimum strain for further investigation. Professor E. McCoy (Taxonomy Laboratory, Department of Bacteriology, The University of Wisconsin, Madison, Wisconsin) identified this bacterial strain to be *Proteus mirabilis* [80].

Since a detailed understanding of the metabolism of silicon was unknown, it was postulated that silicic acid must be solubilised, transported, deposited, and/or, potentially, consumed in a directed manner [81]. Although silicic and phosphoric acid are freely exchanged within the bacterium on different media [81], the addition of carbohydrates (e.g. glucose, sucrose), fatty acids (e.g. wheat germ oil), amino acids (e.g. cysteine, asparagine), and different ions (e.g. Na_2S, $(NH_4)_2SO_4$, KH_2PO_4, $NaNO_3$, NH_4Cl) change the mobility and distribution of silicon and phosphorus in the bacterial cell [82-84]. For example, labile organosilicon complexes such as carbohydrate silicic acid esters (i.e. Si-OX, where X = C, S, P) appear to participate in the metabolism of silicates. The maximum silicon uptake and phosphorus release from bacterial cells is obtained with silicate solutions that contain glucose or sucrose. Heinen wrote, "... the element (Si) is not only used to replace phosphorus but also gives a direct interaction with glucose or intermediates of glucose metabolism [83]."

Although the majority of the solubilised silicon-functional molecules may be transported reversibly in and out of the bacterium, a percentage of the molecules were irreversibly deposited within the cell [84, 85]. In addition to the potential formation of an insoluble polysilicate material (i.e. Si-O-Si bonds), it was hypothesised that the reduction of silicic acid could result in the formation of Si-H, Si-C, or, potentially, Si-Si bonds [84]. However, based on the mobility of the deposited silicones in the presence of carbonate, it was concluded that the immobile silicon-functional molecules could not be a polysilicate material. Heinen stated, "... silicic acid can find entry into the organic bond, possibly in place of CO_2, through, for example, the Wood-Werkman reaction, whereby a –C-Si- bond ought to be formed [84]." Based on the results [80] of an infrared spectroscopy (IR) analysis of *Proteus mirabilis* cells that had been incubated in different siliceous media including glucose, Heinen documented the observation of Si-C, Si-OC, Si-H, and Si-N

bonds. In particular, the presence of the Si-C bond was based on the observation of a "... well defined CH_3-Si band (8.2 μ) [78]." After reviewing the IR assignments published in 1965 [78], it was determined the IR band at 1205 cm^{-1} (8.2 μ) was inadvertently reported to be Si-CH_3 (1260, 870-750 cm^{-1}). In fact, a "...strong band at about 1260 cm^{-1} is always accompanied by one or more equally intense bands in the 870 to 750 cm^{-1} region from the -CH_3 rocking and the Si-C stretching vibrations [86]." However, an alternative alkyl group cannot be discounted. Although the spectral assignments for the Si-H (~ 2273 cm^{-1}) and Si-OC (~ 1100-900 cm^{-1}) bands were correct, the spectral results were ambiguous regarding the presence or absence of a Si-N bond (i.e. Si-NH_2 @ ~ 3480, 3400, and 1540 cm^{-1}, Si-NH-Si @ 3390, 1175, and 930 cm^{-1}).

In comparison to the well-established naturally occurring biomethylation processes of other elements (including germanium, mercury, tin, and arsenic) [87], the biomethylation of silicon has not been observed with the exception of the cited literature [78, 80]. Over the past 30 years, no subsequent reports have confirmed or extended the novel conclusions communicated by Heinen from 1960 to 1965. Experimental attempts to confirm Heinen's observations failed to produce convincing evidence for Si-C bond formation [88]. Heinen's microbial catalysed reduction reaction obtains significance when the large energy requirements necessary to reduce silica [89] are considered.

The inability to support Si-C bond formation seems to be in sharp contrast to the concept that the periodicity of the elements would support the potential of silicon biomethylation. The ability to bioalkylate silicon could be of significant commercial [90] value as a potential low energy route to organosilicon compounds.

1.3 Summary

Although silicon is essential for growth and biological function in a variety of plant, animal, and microbial systems [2, 3], the molecular mechanisms of these interactions are effectively unknown [10]. The *in vitro* studies [6, 11-16] of natural systems within the area of silica biosynthesis are complicated. These earlier mechanistic queries including biomimetic approaches [18, 19] often failed to recognise the chemistry of silicic acid and its analogues [2]. Based on established enzymatic and microbial catalysed transformations [48, 49], organosilicon molecules were determined to be acceptable substrates in comparison to organic materials [50-52]. In order to better understand the role of various proteins in the biosilicification process, a carefully chosen model study was performed to test the ability of homologous enzymes to catalyse the formation of siloxane bonds. Further understanding of the biotransformation strategy in the design and synthesis of structurally complex materials would be beneficial. The opportunity to strategically use biocatalysts to synthesise novel hybrid materials with structural control and spatial order is promising.

1.4 References

1. H. D. Foth, "*Fundamentals of soil science*," John Wiley & Sons, New York, (1978).

2. R. K. Iler, "*The chemistry of silica: Solubility, polymerization, colloid and surface properties, and biochemistry*," John Wiley & Sons, New York, (1979).

3. M. G. Voronkov, *in* "*Silicon in living systems*," Ellis Horwood Limited, Chichester, (1987).

4. C. C. Perry and T. Keeling-Tucker, *J. Biol. Inorg. Chem.*, **5**, 537, (2000).

5. H. A. Lowenstam, *Science*, **211**, 1126, (1981).

6. K. Shimizu, J. Cha, G. D. Stucky, and D. E. Morse, *Proc. Natl. Acad. Sci. USA*, **95**, 6234, (1998).

7. D. M. Nelson, P. Treguer, M. A. Brzezinski, A. Leynaert, and B. Queguiner, *Global Biogeochem. Cycles*, **9(3)**, 359, (1995).

8. S. Mann, *Nature*, **365**, 499, (1993).

9. D. E. Morse, *TIBTECH*, **17(6)**, 230, (1999).

10. D. E. Morse, *in* "*The chemistry of organic silicon compounds*," (eds. Z. Rappoport and Y. Apeloig), Vol. 3, John Wiley & Sons, New York, 2001.

11. N. Kroger, R. Deutzmann, and M. Sumper, *Science*, **286**, 1129, (1999).

12. N. Kroger, R. Deutzmann, C. Bergsdorf, and M. Sumper, *Proc. Natl. Acad. Sci. USA*, **97(26)**, 14133, (2000).

13. N. Kroger, R. Deutzmann, and M. Sumper, *J. Biol. Chem.*, **276(28)**, 26066, (2001).

14. N. Kroger, S. Lorenz, E. Brunner, and M. Sumper, *Science*, **298**, 584, (2002).

15. C. C. Perry and T. Keeling-Tucker, *J. Chem. Soc. Chem. Commun.*, 2587, (1998).

16. J. N. Cha, K. Shimizu, Y. Zhou, S. C. Christiansen, B. F. Chmelka, G. D. Stucky, and D. E. Morse, *Proc. Natl. Acad. Sci. USA*, **96**, 361, (1999).

17. Y. Zhou, K. Shimizu, J. N. Cha, G. D. Stucky, and D. E. Morse, *Angew. Chem. Int. Ed.*, **38(6)**, 780, (1999).

18. J. N. Cha, G. D. Stucky, D. E. Morse, and T. J. Deming, *Nature*, **403**, 289, (2000).

19. R. R. Naik, L. L. Brott, S. J. Clarson, and M. O. Stone, *J. Nanosci. Nanotech.*, **2(1)**, 95, (2002).

20. K. Shimizu and D. E. Morse, *in* "*Biomineralization*," (eds. E. Baeuerlein), Wiley-VCH, Weinheim, 2000.

21. D. E. Morse, *in "Organosilicon Chemistry IV: from Molecules to Materials,"* (eds. N. Auner and J. Weis), Wiley-VCH, New York, 1999.

22. D. M. Swift and A. P. Wheeler, *J. Phycol.*, **28**, 202, (1992).

23. L. Stryer, *"Biochemistry,"* W. H. Freeman and Company, New York, (1988).

24. G. Dodson and A. Wlodawer, *TIBS*, 347, (1998).

25. J. N. Cha, K. Shimizu, Y. Zhou, S. C. Christiansen, B. F. Chmelka, T. J. Deming, G. D. Stucky, and D. E. Morse, *Mat. Res. Soc. Symp. Proc.*, **599**, 239, (2000).

26. R. E. Hecky, K. Mopper, P. Kilham, and E. T. Degens, *Marine Biology*, **19**, 323, (1973).

27. K. D. Lobel, J. K. West, and L. L. Hench, *Journal of Materials Science Letters*, **15**, 648, (1996).

28. B. A. Hartwig and L. L. Hench, *J. Biomed. Mater. Res.*, **6**, 413, (1972).

29. K. D. Lobel, J. K. West, and L. L. Hench, *Marine Biology*, **126**, 353, (1996).

30. M. S. Wong, J. N. Cha, K. S. Choi, T. J. Deming, and G. D. Stucky, *Nano Letters*, **2(6)**, 583, (2002).

31. D. Bradley, *in "The Alchemist"*, 2002.

32. R. Wetherbee, S. Crawford, and P. Mulvaney, *in "Biomineralization,"* (eds. E. Baeuerlein), Wiley-VCH, Weinheim, 2000.

33. J. Parkinson and R. Gordon, *TIBTECH*, **17**, 190, (1999).

34. M. Hildebrand, *in "Biomineralization,"* (eds. E. Baeuerlein), Wiley-VCH, Weinheim, 2000.

35. N. Kroger and M. Sumper, *in "Biomineralization,"* (eds. E. Baeuerlein), Wiley-VCH, Weinheim, 2000.

36. A. J. Milligan and F. M. M. Morel, *Science*, **297**, 1848, (2002).

37. N. Kroger, C. Bergsdorf, and M. Sumper, *EMBO J.*, **13(19)**, 4676, (1994).

38. N. Kroger, C. Bergsdorf, and M. Sumper, *Eur. J. Biochem.*, **239**, 259, (1996).

39. N. Kroger, G. Lehmann, R. Rachel, and M. Sumper, *Eur. J. Biochem.*, **250**, 99, (1997).

40. M. Sumper, *Science*, **295**, 2430, (2002).

41. M. Hildebrand, B. E. Volcani, W. Gassmann, and J. I. Schroeder, *Nature*, **385**, 688, (1997).

42. M. Hildebrand, K. Dahlin, and B. E. Volcani, *Mol. Gen. Genet.*, **260**, 480, (1998).

43. S. D. Kinrade, A. M. E. Gillson, and C. T. G. Knight, *J. Chem. Soc., Dalton Trans.*, 307, (2002).

44. R. R. Naik, P. W. Whitlock, F. Rodriguez, L. L. Brott, D. D. Glawe, S. J. Clarson, and M. O. Stone, *J. Chem. Soc. Chem. Commun.*, 238, (2003).

45. L. L. Brott, R. R. Naik, D. J. Pikas, S. M. Kirkpatrick, D. W. Tomlin, P. W. Whitlock, S. J. Clarson, and M. O. Stone, *Nature*, **413**, 291, (2001).

46. C. C. Perry and Y. Lu, *J. Chem. Soc. Faraday Trans.*, **88**, 2915, (1992).

47. A. Tanaka, *Kagaku, Zokan*, **119**, 63, (1991).

48. K. Faber, "*Biotransformations in organic chemistry*," Springer-Verlag, New York, (2000).

49. J. B. Jones, *Tetrahedron*, **42**, 3351, (1986).

50. R. Tacke and S. A. Wagner, *in* "*The chemistry of organic silicon compounds*," (eds. Z. Rappoport and Y. Apeloig), Vol. 2(3), John Wiley & Sons, West Sussex, England, 1998.

51. T. Kawamoto and A. Tanaka, *in* "*Enzymes in nonaqueous solvents: Methods and protocols*," (eds. E. N. Vulfson, P. J. Halling, and H. L. Holland), Vol. 15, Humana Press, Inc., Totowa, NJ, 2001.

52. A. Tanaka, *Nippon Oyo Koso Kyokaishi*, **28**, 10, (1994).

53. K. Burgess and L. D. Jennings, *J. Am. Chem. Soc.*, **113**, 6129, (1991).

54. M. A. Sparks and J. S. Panek, *Tetahedron Letters*, **32**, 4085, (1991).

55. N. E. Aouf, A. H. Djerourou, and L. Blanco, *Phosphorus, Sulfur Silicon Relat. Elem.*, **88**, 207, (1994).

56. P. Davoli and F. Prati, *Heterocycles*, **53**, 2379, (2000).

57. "Preparation of optically active organic silicon compound-by reaction of a racemic mixture of silyl alcohol with carboxylic acid and organic solvent," Patent J04262794, Nitto Denko Corp., Japan, 1992.

58. S. Oiu, M. H. Zong, and R. Yao, *Gongye Weishengwu*, **27**, 16, (1997).

59. S. Oiu, M. H. Zong, R. Yao, and H. Wu, *Huanan Ligong Daxue Xuebao, Ziran Kexueban*, **25**, 51, (1997).

60. S. Oiu, R. Yao, and M. Zhong, *Guizhou Gongye Daxue Xuebao*, **27**, 91, (1998).

61. S. Oiu, M. H. Zong, and R. Yao, *Guizhou Gongye Daxue Xuebao, Ziran Kexueban*, **28**, 79, (1999).

62. M. H. Zong, Q. Cheng, and W. Du, *Gongye Weishengwu*, **28**, 17, (1998).

63. M. H. Zong, W. Du, H. Q. Li, and Y. Liu, *Huanan Ligong Daxue Xuebao, Ziran Kexueban*, **28**, 101, (2000).

64. A. Tanaka, T. Kawamoto, and K. Sonomoto, *Ann. N. Y. Acad. Sci.*, **613(Enzyme Eng. 10)**, 702, (1990).

65. T. Kawamoto, K. Sonomoto, and A. Tanaka, *Journal of Biotechnology*, **18**, 85, (1991).

66. A. Uejima, T. Fukui, E. Fukusaki, T. Omata, T. Kawamoto, K. Sonomoto, and A. Tanaka, *Appl. Microbiol. Biotechnol.*, **38**, 482, (1993).

67. B. Gruning, G. Hills, W. Josten, D. Schaefer, S. Silber, C. Weitemeyer, "Process for preparing acrylic esters and/or methacrylic esters of hydroxy-functional siloxanes and/or polyoxyalkylene-modified siloxanes and their use," U.S. Patent 6,288,129 B1, Th. Goldschmidt AG, United States, 2001.

68. V. v. Braunmuhl, G. Jonas, and R. Stadler, *Macromolecules*, **28**, 17, (1995).

69. V. v. Braunmuhl and R. Stadler, *Macromol. Symp.*, **103**, 141, (1996).

70. T. Kawamoto, R. S. So, Y. Masuda, and A. Tanaka, *Journal of Bioscience and Bioengineering*, **87(5)**, 607, (1999).

71. T. Kawamoto, H. Yamanaka, and A. Tanaka, *Applied Biochemistry and Biotechnology*, **88**, 17, (2000).

72. H. Yamanaka, T. Fukui, and T. Kawamoto, *Appl. Microbiol. Biotechnol.*, **45**, 51, (1996).

73. H. Ishikawa, H. Yamanaka, T. Kawamoto, and A. Tanaka, *Appl. Microbiol. Biotechnol.*, **51**, 470, (1999).

74. T. Fukui, T. Kawamoto, and A. Tanaka, *Tetrahedron: Asymmetry*, **5(1)**, 73, (1994).

75. A. N. Fattakhova, E. P. Chirko, and E. N. Ofitserov, *Biol. Nauki*, **4**, 100, (1992).

76. A. N. Fattakhova, E. N. Ofitserov, V. M. Diyakov, and R. P. Naumova, *FEMS Microbiology Letters*, **48**, 317, (1987).

77. H. Nishino, T. Mori, and Y. Okahata, *J. Chem. Soc. Chem. Commun.*,2684, (2002).

78. W. Heinen, *Archives of Biochemistry and Biophysics*, **110**, 137, (1965).

79. W. Heinen, *Archiv. fur Mikrobiologie*, **37**, 199, (1960).

80. W. Heinen, *Archiv. fur Mikrobiologie*, **52**, 49, (1965).

81. W. Heinen, *Archiv. fur Mikrobiologie*, **41**, 229, (1962).

82. W. Heinen, *Archiv. fur Mikrobiologie*, **45**, 148, (1963).

83. W. Heinen, *Archiv. fur Mikrobiologie*, **45**, 162, (1963).

84. W. Heinen, *Archiv. fur Mikrobiologie*, **45**, 172, (1963).

85. W. Heinen, *Archiv. fur Mikrobiologie*, **52**, 69, (1965).

86. A. L. Smith, (ed.), "*The analytical chemistry of silicones*." John Wiley & Sons, Inc., New York, 1991.

87. W. P. Ridley, L. J. Dizikes, and J. M. Wood, *Science*, **197**, 329, (1977).

88. K. F. Brandstadt, M. L. McIvor, A. M. Blancquaert, C. J. Dunning, P. C. Klykken, P. J. Oriel, and T. H. Lane. unpublished work, 2001.

89. M. A. Brook, "*Silicon in organic, organometallic, and polymer chemistry*," John Wiley & Sons, New York, (2000).

90. D. R. Weyenberg and T. H. Lane, *in* "*Silicon-based polymer science: A comprehensive resource*," (eds. J. M. Zeigler and F. W. Gordon Fearon), American Chemical Society, Washington, DC, 1990.

Chapter Two

Enzyme-Catalysed Condensation of Silanols

2.0 Introduction

The intricate siliceous architectures of diatom species (Figures 1.1 and 1.5) have inspired the exploration of silica biosynthesis. Previously, a protein isolated from the *Tethya aurantia* marine sponge (i.e. silicatein) [1, 2] as well as polypeptides isolated from a *Cylindrotheca fusiformis* diatom (i.e. silaffin) [3-6], an *Equisetum telmateia* plant (i.e. biopolymer) [7], and a phage-display library [8] were reported to catalyse the polycondensation of silicic acid analogues during the formation of particulate silica (Figure 2.1).

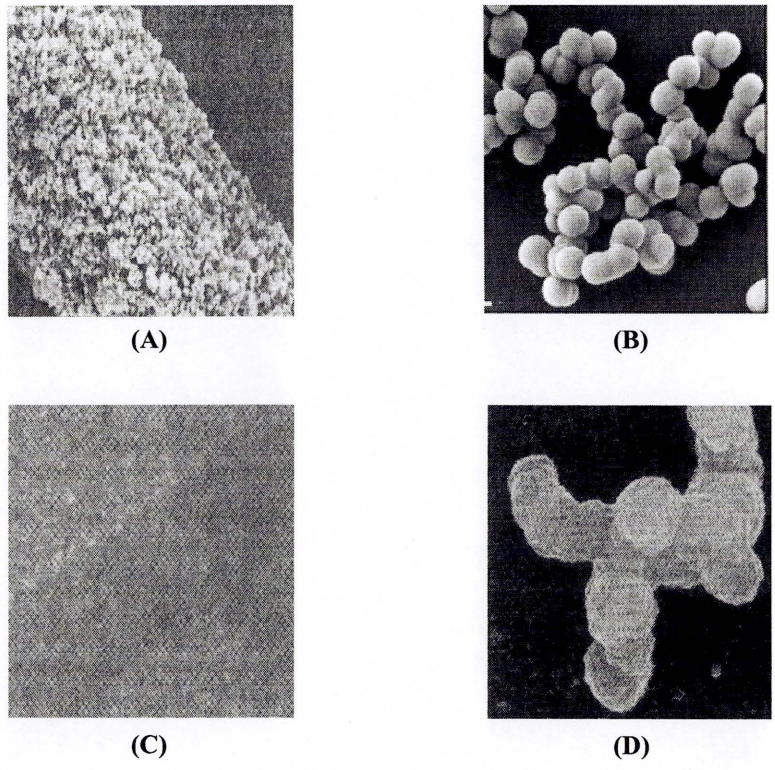

Figure 2.1: Particulate silica catalysed by silicatein (A, width is 2.4 μm) [1], silaffin (B, particle diameters are 500-700 nm) [3], biopolymer (C, image is 37 nm x 51 nm) [7], and a peptide (D, particle diameters are 200-400 nm) [8].

Despite the absence of long-range order following nucleation of silica on silicatein filaments [9], silicatein was postulated [10] to control the architecture of silicon-functional materials. In addition, silicatein-mimetic diblock polypeptides were reported [11] to control the macroscopic structure of silica (Figure 2.2).

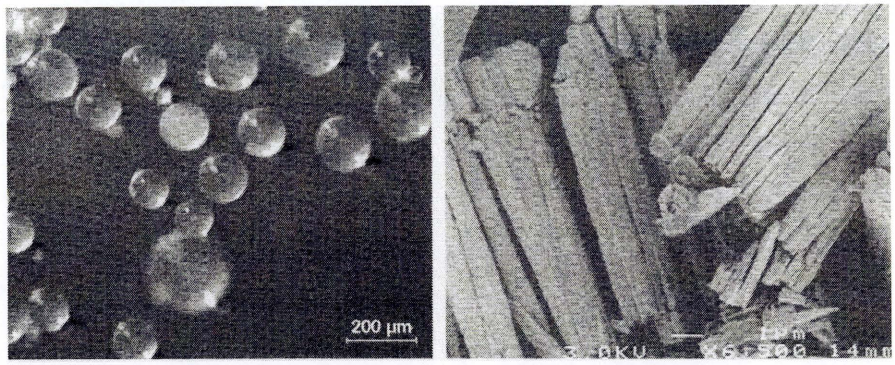

reduced **oxidised**

Figure 2.2: Silica catalysed by reduced- and oxidised- cysteine-functional lysine copolypeptides [11].

Specifically, reduced (RSH) and oxidised (RS_2R) cysteine-functional lysine copolypeptides (Figure 1.4) synthesised large aggregates (~600 nm in diameter) and packed silica columns, respectively. Comparatively, cysteine and lysine polypeptide blends catalysed amorphous silica. Based on these observations, the diblock polypeptides were documented to catalyse the polycondensation of tetraethoxysilane, while "simultaneously directing the formation of ordered silica morphologies [11]". In review, the *in vitro* studies [1, 3-7, 12] of natural systems within the area of silica biosynthesis are complicated. These earlier mechanistic queries including biomimetic approaches [8, 11] often failed to recognise the chemistry of silicic acid and its analogues [13].

The study of the hydrolysis and condensation reactions during biosilicification is complicated due to the sensitivity of silica, silicates, and silicic acid to pH, concentration, and temperature (Figure 2.3) [13]. As silicic acid precursors, tetraalkoxysilanes are easily hydrolysed and the resulting silanols are condensed during the formation of particulate silica.

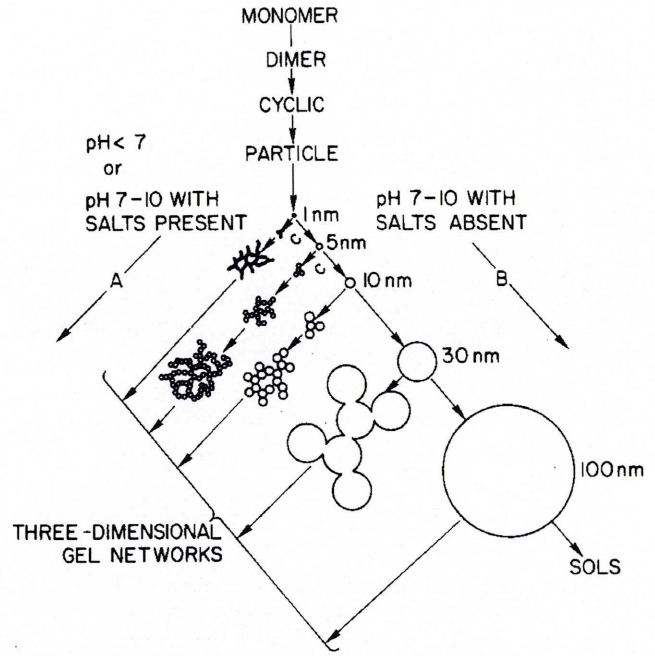

Figure 2.3: Polymerisation behavior of silica during the formation of three-dimensional aggregated- or sol-gel networks [13].[1]

[1] The circles illustrate the relative dimension (diameter) and association of the silica particles within the aggregated- or sol-gel networks.

During the formation of particulate silica, silicic acid (i.e. monomer, Figure 2.3) condenses to form low molecular weight linear and cyclic molecules, which react to form a distribution of branched and crosslinked siloxanes prior to precipitating as aggregated- or sol-gels (Scheme 2.1, Figure 2.4).

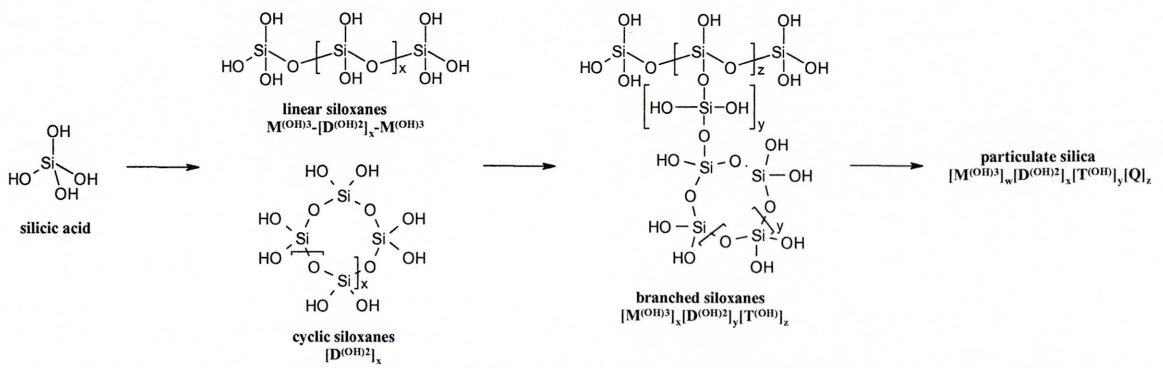

Scheme 2.1: Polycondensation of silicic acid.
$M^{(OH)3}$ = siloxane endblock, $(HO)_3SiO_{1/2}$.
$D^{(OH)2}$ = linear siloxane, $(HO)_2SiO_{2/2}$.
$T^{(OH)}$ = branched siloxane, $(HO)SiO_{3/2}$.
Q = silicon dioxide, $SiO_{4/2}$.

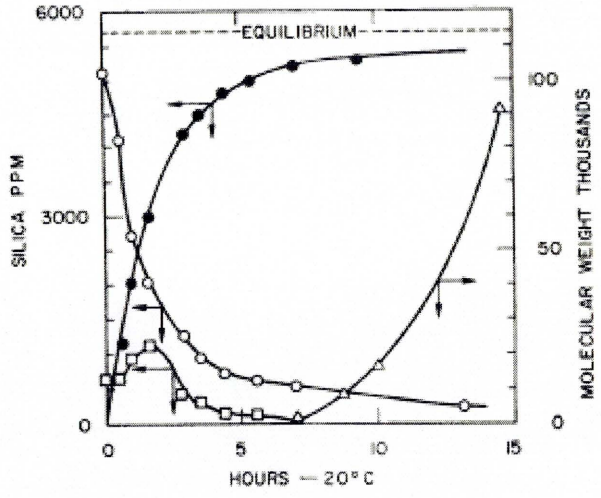

Figure 2.4: Time study of the polycondensation of silicic acid [13].
open circles = "monomer".
squares = oligomers.
solid circles = polymer.
triangles = molecular weight of silica.

As detailed in Figure 2.3, the formation of different three-dimensional gel networks is dependent on the solution and deposition of silica due to the pH of the medium as well as the presence or absence of salts. At low pH (< 7) or in the presence of salts, the collision of spherical silica particles increases due to decreased ionic charges. This promotes the formation of aggregated silica chains and gel networks. Alternatively, the particle growth of spherical silica is enhanced due to increased dissolution and deposition under basic conditions. At pH values greater than 7 in the absence of salts, the repulsion of the negatively charged particles also limits aggregation during the formation of large spherical sol-gels. The reaction mechanisms for the acid- and base-catalysed condensation of silanols are detailed in Scheme 2.2 [14].

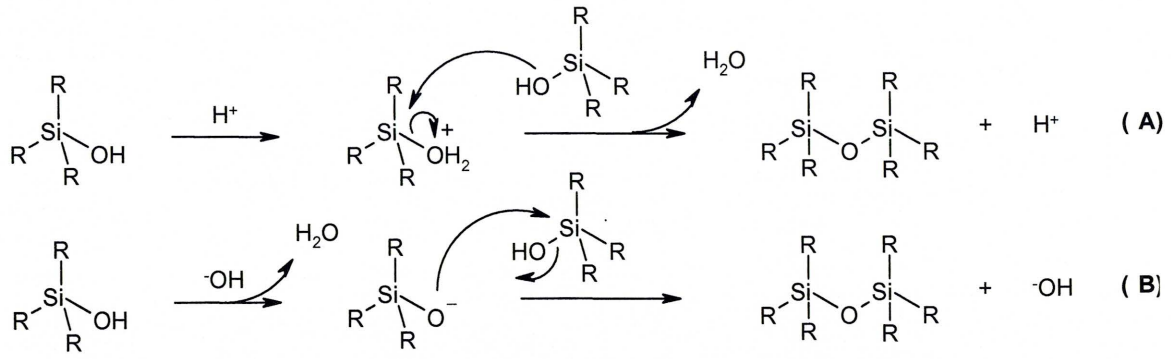

Scheme 2.2: Acid- (A) and base- (B) catalysed silanol condensation.

As illustrated in Figure 2.3, the acid-catalysed polycondensation of tetraethoxysilane, a silicic acid precursor, results in the formation of an aggregated silica gel (Figure 2.5). Comparatively, the three-dimensional structure of the aggregated silica gel was similar to the natural morphologies of the silica particles detailed in Figure 2.1.

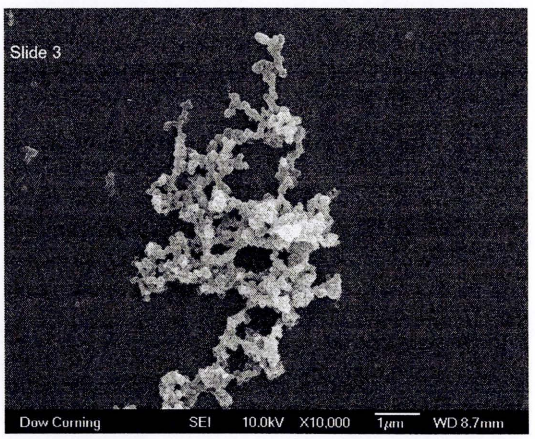

Figure 2.5: Acid-catalysed formation of an aggregated silica gel.

Furthermore, the use of external force was demonstrated [15] to control the morphology (e.g. arched, fibrillar) of a silica material catalysed by a biomimetic silaffin peptide (i.e. a non-modified Sil 1p R5 peptide). Different flow dynamics (e.g. gas bubbles, tubular shear) within the reaction mixture changed the reactive interfaces and, consequently, the directional growth and deposition of the material (Figure 2.6).

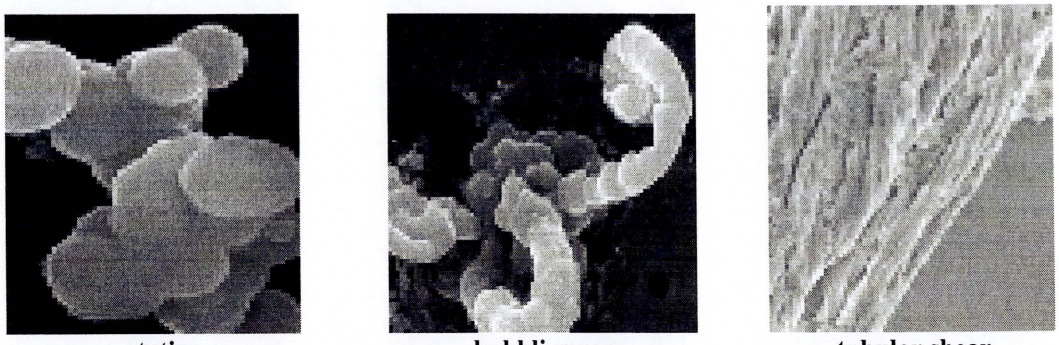

static
(image is 2.4 x 3.0 μm)

bubbling gas
(image is 4.1 x 4.1 μm)

tubular shear
(image is 9.3 x 9.6 μm)

Figure 2.6: The peptide-catalysed formation of spherical, arched, and fibrillar silica morphologies due to static, bubbling gas, and tubular shear external forces, respectively [15].

Although silicatein was determined [2] to catalyse the formation of particulate silica and silsesquioxanes, it was also shown [3-8, 11] that an active site in a defined tertiary structure was not necessarily required. This data suggests that the formation of silica is also catalysed by interactions with non-specific peptides such as nucleophilic, basic, and cationic amino acid residues. In order to better understand the role of various proteins in the biosilicification process, a series of homologous lipases and proteases were screened with a simple model compound, trimethylsilanol. Given the complications of tetra-functional silicic acid analogues [13], a mono-functional silanol was chosen to focus on the formation of a molecule, hexamethyldisiloxane, with a *single* siloxane bond during condensation (Scheme 2.3).

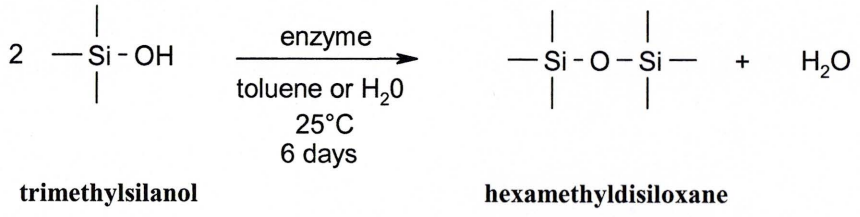

trimethylsilanol **hexamethyldisiloxane**

Scheme 2.3: Enzyme-catalysed condensation of trimethylsilanol.

In addition, trimethylsilanol was chosen as a model non-natural substrate due to its physical stability in different media in comparison to analogous organosilicon hydrides [14].

2.1 Experimental Procedure and Analysis

During the silicatein-catalysed polycondensation of tetraethoxysilane, the degree of reaction was quantified by measuring the amount of 'Polymerised Si' (nmol) via a modification of the colorimetric molybdate assay [1]. Given the amount of reactant, silicatein was documented to catalyse the formation of 214 nmol (0.005% yield) of 'Polymerised Si' in comparison to alternate proteinaceous sources such as trypsin (16 nmol, 0.0004% yield), papain (23 nmol, 0.0004% yield), and BSA (42 nmol, 0.0009% yield). In the absence of a protein, the control reaction was reported to form 10 nmol (0.0002% yield) of 'Polymerised Si.' Despite these fractional yields and insignificant conversions, the study focused on the analysis of the solid polycondensation products as opposed to a complete mass balance. In our study, since mono-functional silanes were chosen as reactants during the formation of molecules with a single siloxane bond, rigorous procedures were established to prepare glassware, as well as isolate and quantitatively analyse the reaction products by gas chromatography (GC).

Prior to reaction, the glassware was rinsed, dried, and silylated with hexamethyldisilazane in the presence of acetic acid at 25°C (Scheme 2.4, Experimental section 7.2.1). Alternatively, hexamethyldisilazane may react directly with the glassware.

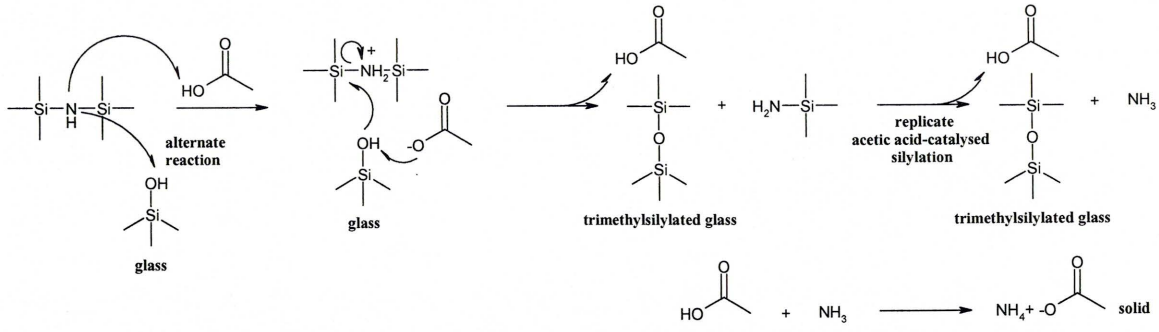

Scheme 2.4: Acid-catalysed trimethylsilylation of glassware.[1]

[1] Refer to Experimental section 7.2.1.

Subsequently, the glassware was rinsed and dried in an oven at 110°C. Since a silanol-functional glass surface could react with the alkoxysilane and silanol substrates in the model study (Scheme 2.2), the silylation procedure was performed to create an inert glass surface. The silylated glass vials were confirmed not to contaminate the reactions with trimethylsilanol or hexamethyldisiloxane (Table 7.4).

Prior to analysis, the aqueous reactions were extracted with an organic solvent, while the organic reactions were directly analysed (Experimental sections 7.2.1-7.2.3). Consequently, a study was conducted to identify a solvent that would efficiently extract reaction products from Tris-HCl buffered Milli-Q water, pH 7.0. After extracting replicate reactions twice with diethylether, tetrahydrofuran (THF), methylene chloride, and toluene, the reaction products were filtered and quantitatively analysed by GC (Figure 2.7).

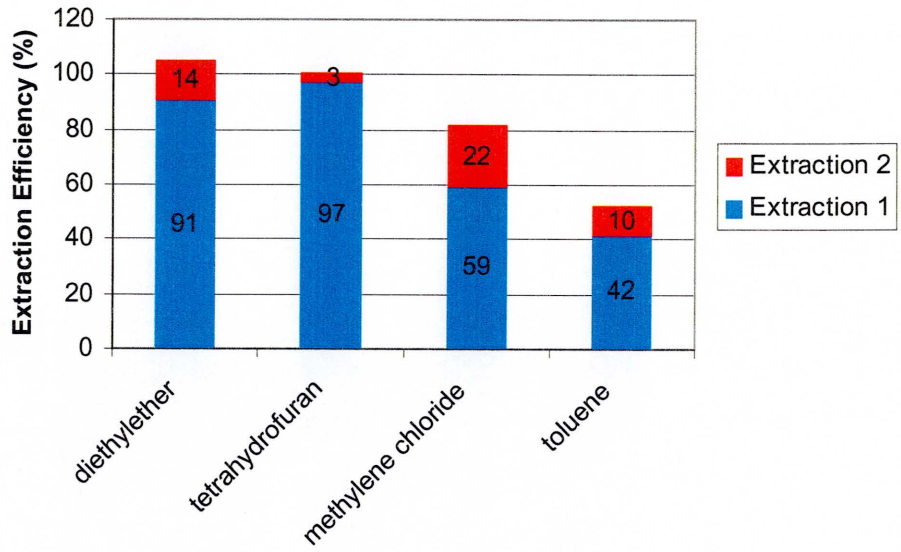

Figure 2.7: Study of the extraction efficiency of trimethylsilanol and hexamethyldisiloxane with different organic solvents.[1]

[1] Refer to Experimental section 7.2.2 and Table 7.5.

The measure of extraction efficiency was defined as the percent yield of reactants and products. The mass balances were equal to the sum total of the extraction values. Based on the chromatographic results, the extraction efficiencies varied as follows: diethylether (105%) > THF (100%) > methylene chloride (81%) > toluene (52%). Notably, the mass balance of the reaction extracted with diethylether was greater than 100%. Since this extraction was performed at 25°C, the values were calculated in error due to the evaporative loss of solvent during the extractions. Given the boiling point of diethylether (34.5°C), the extractions should have been performed on ice. Regardless, the extraction efficiency of THF was excellent. In addition, the extractions could easily be conducted at 25°C due to the increased boiling point of THF (65-67°C). Sodium chloride was used to change the ionic strength of the water-phase in order to separate the miscible THF-phase. Comparatively, the extraction efficiencies of methylene chloride and toluene were not sufficient to quantitate the mass balances of the reactions. Consequently, THF was chosen as the ideal solvent to extract organosilicon molecules from aqueous media during the

model study. Based on two extractions, mass balances greater than 98% were routinely obtained with THF (Experimental section 7.3.2). These conclusions were in agreement with a previous study [16] that detailed the preferential use of THF to extract a variety of silicones from biological matrices.

The GC analysis was performed on a Hewlett-Packard 6890 plus gas chromatograph with a flame ionisation detector (Experimental section 7.3.2). Dodecane was used as an internal standard to gravimetrically quantify the chromatographic analyses. The analytical samples were prepared at approximately 1% (w/w) product in a THF solution containing 1% (w/w) dodecane. Based on triplicate measurements, the response factors [17] for the analytes were calculated and determined to be linear as a function of concentration over three orders of magnitude (i.e. 0.1-10% (w/w), Table 7.2). Encompassing experimental and instrumental errors, the relative standard deviation of the measurements range between 0.3-10% depending on the concentration and, correspondingly, the yield of the analyte (Table 7.4). Furthermore, the alkoxysilane, silanol, and disiloxane analytes were chromatographically resolved as illustrated in Figure 2.8 and detailed in Table 7.2.

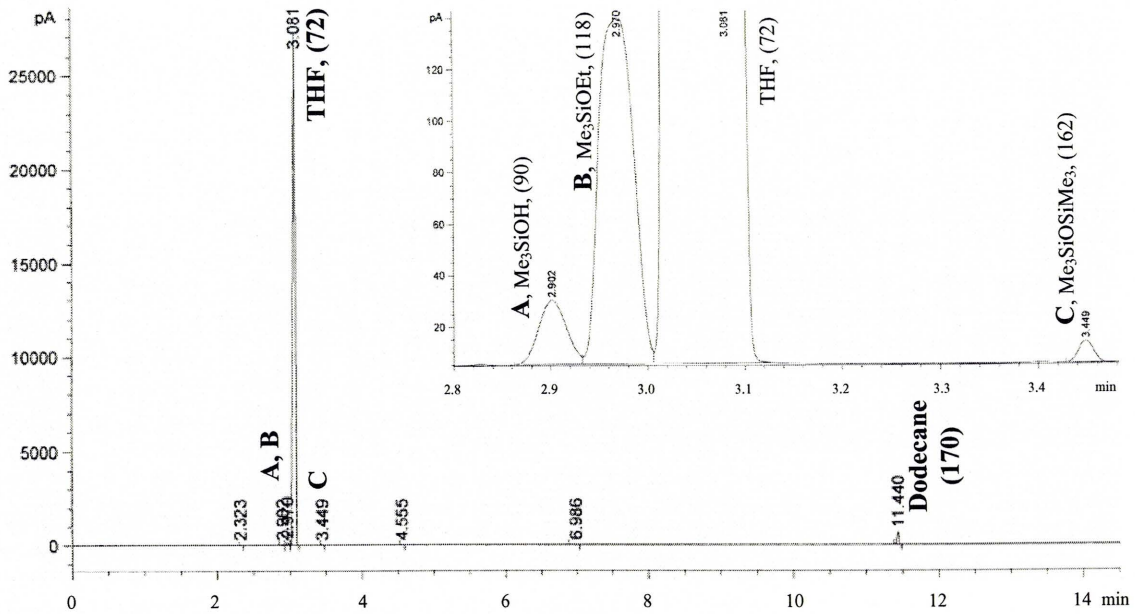

Figure 2.8: GC-FID chromatogram of a trimethylethoxysilane negative control reaction.[1]

[1] Refer to Experimental sections 7.2.3 and 7.3.2. The molecular mass of the molecules are in parenthesis.

The ability to resolve these analytes was necessary to differentiate between the role of an enzyme in the hydrolysis and condensation reactions during biosilicification. Comparatively, given the limitations of the product and resultant analyses, the *Tethya aurantia* marine sponge (i.e. silicatein) [1] and *Equisetum telmateia* plant (i.e. biopolymer) [7] studies including a silicatein-mimetic approach (i.e. diblock polypeptides) [11] were not able to differentiate between the role of the proteins or polypeptide in the hydrolysis and condensation reactions during biosilicification.

In summary, this model study is believed to be the first rigorous (quantitative) test of the ability of enzymes to catalyse the formation of siloxane bonds during the *in vitro* hydrolysis and condensation of alkoxysilanes.

2.2 Enzyme-Catalysed Condensation Study

Based on the similarities of the proteins isolated from the *Tethya aurantia* marine sponge (silicatein), *Cylindrotheca fusiformis* diatom (silaffin), and *Equisetum telmateia* plant (biopolymer extract), a series of lipases and serine-proteases were selected as homologous proteolytic enzymes. In addition to catalysing comparable reactions (i.e. the hydrolysis of amide and/or ester bonds [18, 19]), the active sites in the hydrolase enzymes are composed of similar serine-histidine-aspartate catalytic triads (Figure 1.3) [20, 21]. In comparison to control reactions, the mammalian, fungal, and bacterial lipases and proteases detailed in Table 2.1 were screened with trimethylsilanol in order to evaluate their ability to catalyse the formation of a siloxane bond. In this study, control reactions were defined as non-enzymatic reactions. Specifically, experiments conducted in the absence of a protein were defined as negative control reactions. Proteinaceous molecules such as bovine serum albumin (BSA, Figure 2.9) and porcine γ-globulins were used to study non-specific protein catalysis.

Table 2.1: Enzyme screen.

Mammalian	Fungal	Bacterial
bovine pancreatic α-chymotrypsin	*Aspergillus niger* lipase	*Pseudomonas cepacia* lipase
bovine pancreatic phospholipase A2	*Candida antarctica* lipase	*Pseudomonas fluorescens* lipase
bovine pancreatic trypsin	*Candida antarctica* lipase B[1]	
porcine pancreatic lipase	*Candida lipolytica* lipase	
	Mucor javanicus lipase	
	Penicillium roqueforti lipase	
	Rhizomucor miehei lipase	
	wheat germ lipase	

[1] *Candida antarctica* lipase B was immobilised on acrylic resin beads (Novozym® 435).

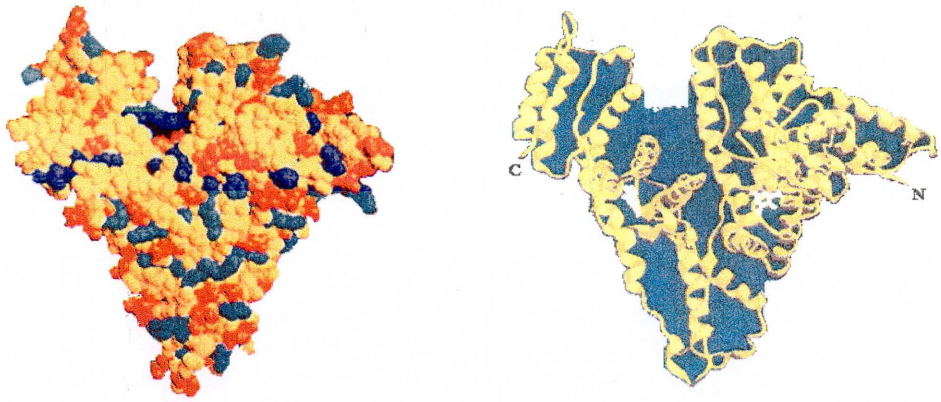

Figure 2.9: Tertiary structures of bovine serum albumin: (A) Space filling model (red = acidic residues, blue = basic residues, yellow = neutral residues), (B) Ribbon image (spirals = α-helices) [22].

Given the broad selection of enzymes, the condensation study was performed in suitable organic and aqueous media. Toluene was chosen as a hydrophobic solvent in order to potentially promote the lipase-catalysed interfacial reactions [23]. Water was selected as an alternate medium in order to evaluate the activity of solubilised enzymatic solutions. The reactions were formulated with a 5:1 trimethylsilanol to protein weight ratio (> 1000:1 silanol to enzyme mole ratio) and conducted in inert glass vials at 25°C with magnetic stirring for six days. The reaction products were isolated and quantitatively analysed by GC. The results are summarised in Table 2.2. In comparison to negative control and non-specific protein (i.e. BSA) reactions, select lipases as well as trypsin and α-chymotrypsin were observed to catalyse the condensation of trimethylsilanol during the formation of hexamethyldisiloxane under mild conditions (Tables 7.6-7.9). The enzymes highlighted or checked (√) in Table 2.2 were determined to catalyse the condensation of greater than ten times more trimethylsilanol than the negative control reactions; as well as, greater than three or ten times more trimethylsilanol than the BSA reactions in organic and aqueous media, respectively. Conversely, the ability of the unchecked enzymes in Table 2.2 to catalyse the model condensation reaction was not substantially different than the control reactions. In review, the relative rate of condensation increased in water. As opposed to lipases, proteases will only interact with water soluble substrates [24]. The estimated water solubility of trimethylsilanol is 4.2% (i.e. 42.56 mg/mL) [25].

Table 2.2: Enzyme-catalysed condensation study of trimethylsilanol after six days.[1]

Enzyme	Dry Toluene	Wet Toluene	Water	Buffered pH 7
negative control				
bovine serum albumin				
Aspergillus niger lipase				
Candida antarctica lipase			√	
Candida antarctica lipase B[2]			√	
Candida lipolytica lipase				
α-chymotrypsin	√	√	√	√
Mucor javanicus lipase				
Penicillium roqueforti lipase				
phospholipase A2				
porcine pancreatic lipase				
Pseudomonas cepacia lipase				
Pseudomonas fluorescens lipase				
Rhizomucor miehei lipase			√	
trypsin	√	√	√	√
wheat germ lipase		√	√	

[1] Refer to Experimental section 7.2.1 and Tables 7.6-7.9.

[2] *Candida antarctica* lipase B was immobilised on acrylic resin beads (Novozym® 435).

√ The checked enzymes catalysed the condensation of > 10x more trimethylsilanol than the negative control reactions; as well as > 3 or 10x more trimethylsilanol than the BSA reactions in organic and aqueous media, respectively.

Based on crystallographic studies [24], lipases are α/β proteins that contain a central, predominately parallel β-sheet structure surrounded by α-helices as illustrated in Figure 2.10.

***Candida antarctica* lipase B** [26]

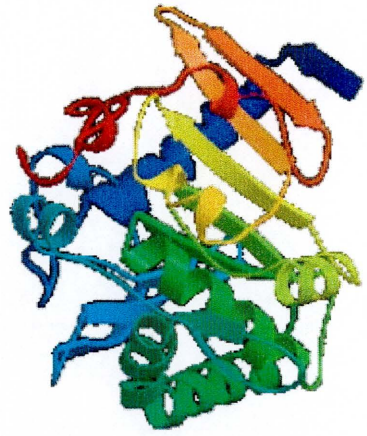

***Rhizomucor miehei* lipase** [27]

Figure 2.10: Tertiary structures of lipase.
spirals = α-helices, arrows = β-sheets.

Typically in lipases, the serine-histidine-aspartate catalytic triad [20, 21] is buried beneath a few helices referred to as the lid. Upon interaction with a substrate interface, the configuration of the enzyme changes, altering the position of the lid to expose a large hydrophobic surface resulting in interfacial activation. Notably, *Candida antarctica* lipase (identified in Table 2.2) has a small lid. Comparatively, the catalytic regions of the active serine-proteases (trypsin and α-chymotrypsin) screened in Table 2.2 are open. Within the *Rhizomucor* fungal family, the active *Candida antarctica* and *Rhizomucor miehei* lipases also contain comparable acyl binding regions. These regions are short troughs located just below the hydrophobic region beneath the lid. In the absence of a substantial lid, the model organosilicon molecule, trimethylsilanol, appears to be an acceptable non-natural substrate as highlighted in Table 2.2.

2.3 Protease-Catalysed Condensation Study

Based on the exceptional activity of trypsin and α-chymotrypsin from bovine pancreas (Table 2.2), protease enzymes were identified as target catalysts. Consequently, a series of serine-, cysteine-, aspartic-, and metallo-proteases were selected in order to

evaluate their ability to catalyse the formation of a molecule with a siloxane bond in a neutral medium (pH 7.0) (Scheme 2.5).

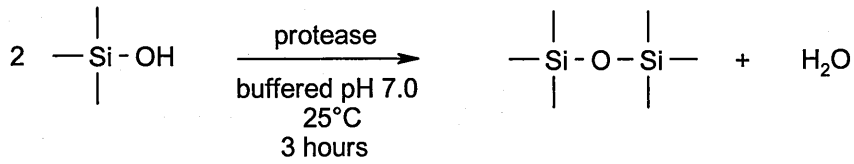

Scheme 2.5: Protease-catalysed condensation of trimethylsilanol.

Proteases are classified according to the nucleophilic amino acid residue in their catalytic centers, respectively. In nature, these proteolytic enzymes catalyse the selective hydrolysis of amide (e.g. polypeptides, Scheme 2.6) and ester (e.g. carbohydrates, lipids) bonds [19].

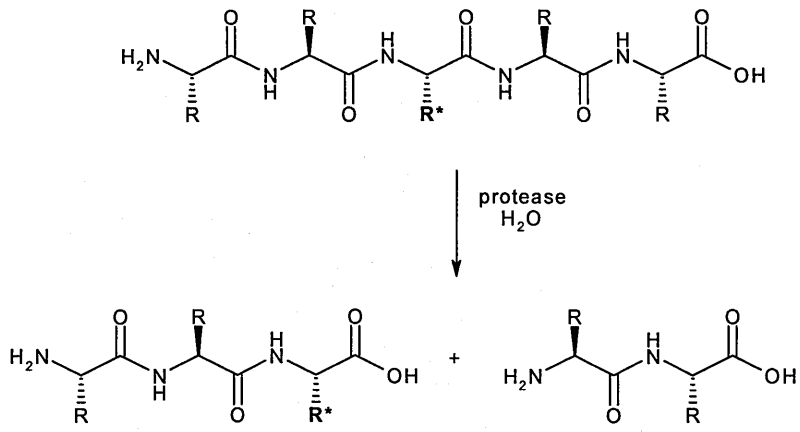

Scheme 2.6: Protease-catalysed hydrolysis of an amide bond.
* specific amino acid residues.

The function of the catalytic triad [20, 21] is based on a charge-relay system through a network of nucleophilic, basic, and acidic amino acid hydrogen bonds (Scheme 2.7). Stabilised by the illustrated [28] charge-relay systems, enzymatic nucleophilic atoms (δ^-) attack the carbonyl carbons of select amide- and ester-functional substrates.

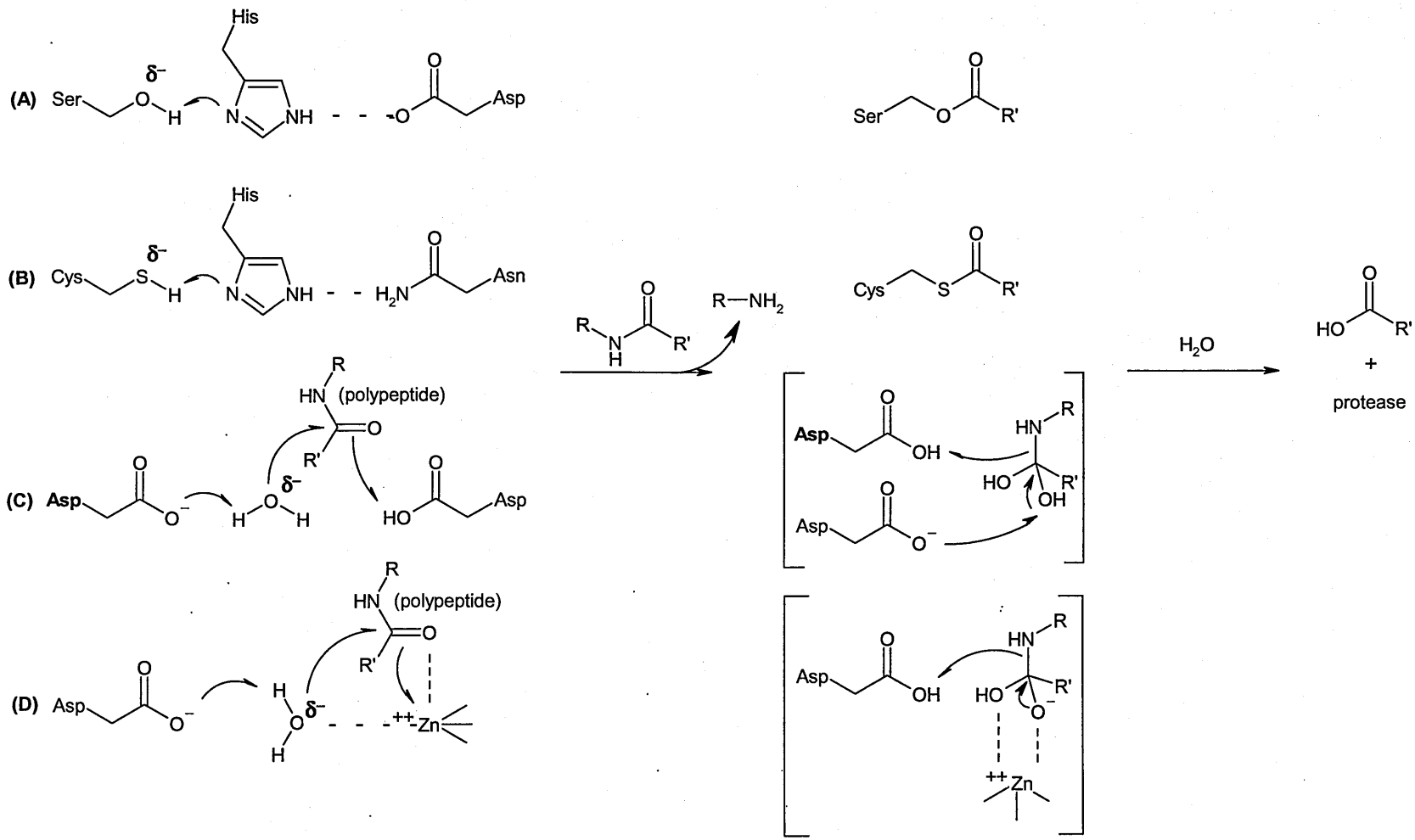

Scheme 2.7: Mechanism of serine- (A), cysteine- (B), aspartic- (C), and metallo- (D) protease reactions.

The target bonds in the tetrahedral complexes break releasing amine, alcohol, and acid by-products. Not all hydrolytic reactions proceed through a covalent intermediate, acyl-enzyme complex (Scheme 2.7, A-B). Regardless, the enzyme is recovered in the presence of water.

In comparison to control reactions, the ability of the proteases detailed in Table 2.3 to catalyse siloxane condensation was screened with trimethylsilanol. The reactions were formulated with a 4:1 trimethylsilanol to protein weight ratio (~1000:1 silanol to protease mole ratio) and conducted in Tris-HCl buffered water (pH 7.0) at 25°C for three hours. Comparatively, the original reactions conducted in the enzyme-catalysed condensation study were performed for six days (Scheme 2.3) versus three hours in this study (Scheme 2.5). Based on the estimated solubility of trimethylsilanol in water (42.56 mg/mL) [25], the concentration of trimethylsilanol (~160 mg/mL) saturated the aqueous media and created two-phase reaction mixtures. Although the pH may not be optimal for the proteases [19], a neutral pH was used to minimise acid- and base-catalysed silanol condensation [13]. The reaction products were isolated and quantitatively analysed by GC. The results are illustrated in Figure 2.11.

Table 2.3: Protease screen.

Serine-Protease	Cysteine-Protease	Aspartic-Protease	Metallo-Protease
α-chymotrypsin (bovine pancreatic)	cathepsin L (bovine kidney)	pepsin (hog stomach)	carboxypeptidase B (porcine pancreas)
elastase (porcine pancreatic)	cathepsin L (human liver)		
subtilisin Carlsberg (*B. licheniformis*)	cathepsin L (*Paramecium tetraurelia*)		
trypsin (bovine pancreatic)	papain (papaya latex)		

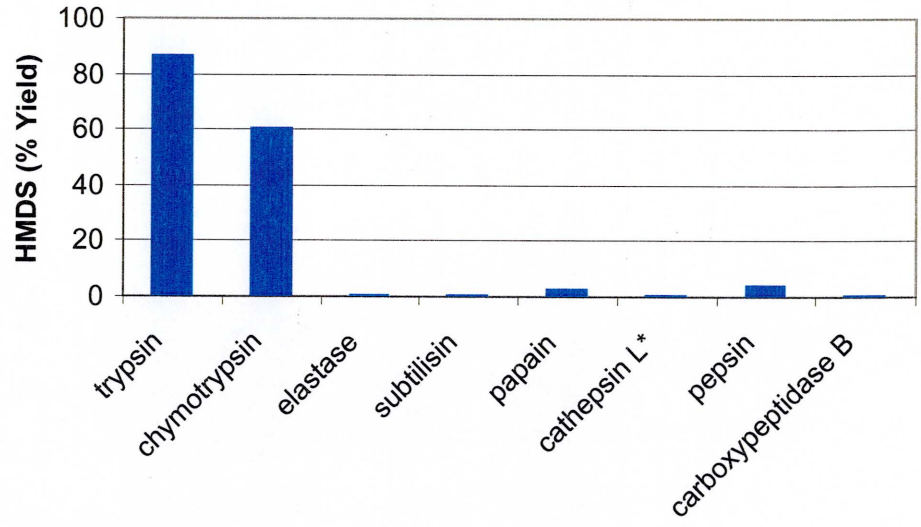

Figure 2.11: Protease-catalysed condensation study of trimethylsilanol after three hours.[1]
[1] Refer to Experimental section 7.2.2 and Table 7.10.
* representative yield from the three sources of cathepsin L detailed in Table 2.3.

In review, trypsin and α-chymotrypsin preferentially catalysed the condensation of trimethylsilanol under mild conditions. Again, a neutral medium (pH 7.0) was used to differentiate enzymatic vs. chemical catalysis. As cited [19], this criterion is not ideal for the broad selection of proteolytic enzymes. For example, the optimum pH for pepsin is pH 2 to pH 3 in gastric juice [20]. Pepsin is active when the two catalytic aspartic acid residues are both ionized and un-ionized (Scheme 2.7, C). The tertiary and secondary structures of the digestive enzymes vary according to function. Given the specificity in the catalytic regions, the proteases are substrate selective. Trimethylsilanol was chosen as a model silanol to study the role of an enzyme in the formation of molecules with a single siloxane bond. Notably, three sources of cathepsin L did not catalyse the condensation reaction. In contrast, silicatein catalysed the formation of particulate silica and silsesquioxanes. Although silicatein was documented to be highly homologous with cathepsin L (i.e. a cysteine-protease) [12], the marine protein lacked proteolytic activity as measured with synthetic chromogenic substrates [9]. In addition, the nucleophilic residue within the enzymatic active site of silicatein (i.e. Ser-His-Asn) was determined to be serine

[2] as opposed to cysteine in cathepsin L. Correspondingly, the activities of the enzymes depend upon the functionality of the non-natural organosilicon substrates.

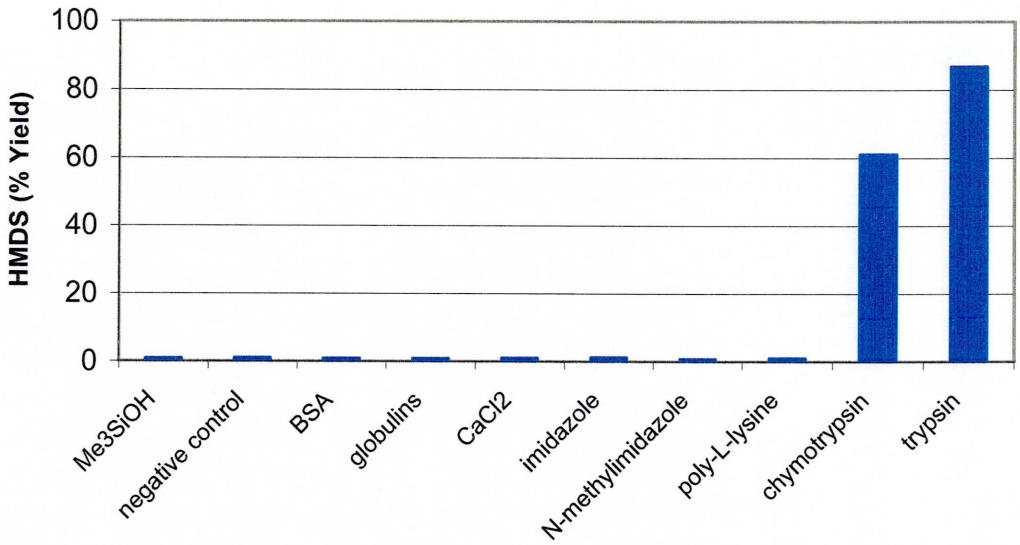

Figure 2.12: Condensation control reactions with trimethylsilanol after three hours.[1]

[1] Refer to Experimental section 7.2.2 and Table 7.11.

Substantial condensation of trimethylsilanol was not observed in the negative control, non-specific protein (i.e. BSA, γ-globulins), small molecule (i.e. $CaCl_2$, imidazole, N-methylimidazole), and polypeptide (i.e. poly-L-lysine) reactions in comparison to the raw material (Figure 2.12). In addition to the proteins, the small molecules were chosen to independently evaluate non-specific catalysis based on the functionality of catalytically active trypsin. Since calcium is required to maximise tryptic activity and stability [19, 29], trypsin may be treated with calcium chloride. Analogous to the amino-functional residues on the surface of trypsin [30], imidazole, N-methylimidazole, and poly-L-lysine were included to assess base catalysis in a neutral medium. Similarly, BSA [1] and poly-L-lysine (Table 1.1) [11] were not observed to catalyse the polycondensation of tetraethoxysilane in aqueous media (pH = 6.8).

2.4 Impurity Study

Trypsin, chymotrypsin, and elastase are the primary digestive enzymes in the pancreas [20]. These proteolytic enzymes are secreted as inactive precursors or zymogens. In response to physiological conditions, the zymogens are activated with specific proteases. Specifically, trypsinogen is activated by enteropeptidase or autolysis [19]. Subsequently, trypsin catalyses the hydrolysis and assists in the activation of all digestive enzymes. Since trypsin selectively digests chymotrypsinogen during the activation of α-chymotrypsin, Sigma-Aldrich confirmed the presence of trypsin as a substantial enzymatic impurity in the experimental source of α-chymotrypsin [31]. Comparatively, commercial sources of trypsin are typically contaminated with other pancreatic enzymes [19]. Despite similar tertiary structures (Figure 2.13) and catalytic mechanisms including the presence of serine-histidine-aspartate catalytic triads, the serine-proteases are substrate selective due to different binding sites (i.e. secondary structures, Figure 2.13) [20, 32]. Based on an analysis of the primary amino acid sequences, trypsin, α-chymotrypsin, and elastase are approximately 50% identical and extensively homologous or similar. Furthermore, the residues located in the interior (60%) as opposed to the surface (10%) are conserved. Consequently, the majority of the amino acids located on the surface including external loops account for the difference. Since these external loops contribute to the lining of the binding sites, the differences in these regions further define the criteria of an acceptable substrate. Based on these regions, trypsin has an affinity for basic residues in the substrate such as arginine and lysine due to an electrostatic attraction with an aspartate residue at the bottom of the pocket. In the absence of the aspartate residue, α-chymotrypsin preferentially binds large hydrophobic side chains such as phenylalanine, tyrosine, tryptophan, and leucine. In elastase, the presence of two bulky residues, valine and threonine, restrict the entry of large side chains at the mouth of the pocket versus glycine in trypsin and α-chymotrypsin, while binding small residues such as alanine.

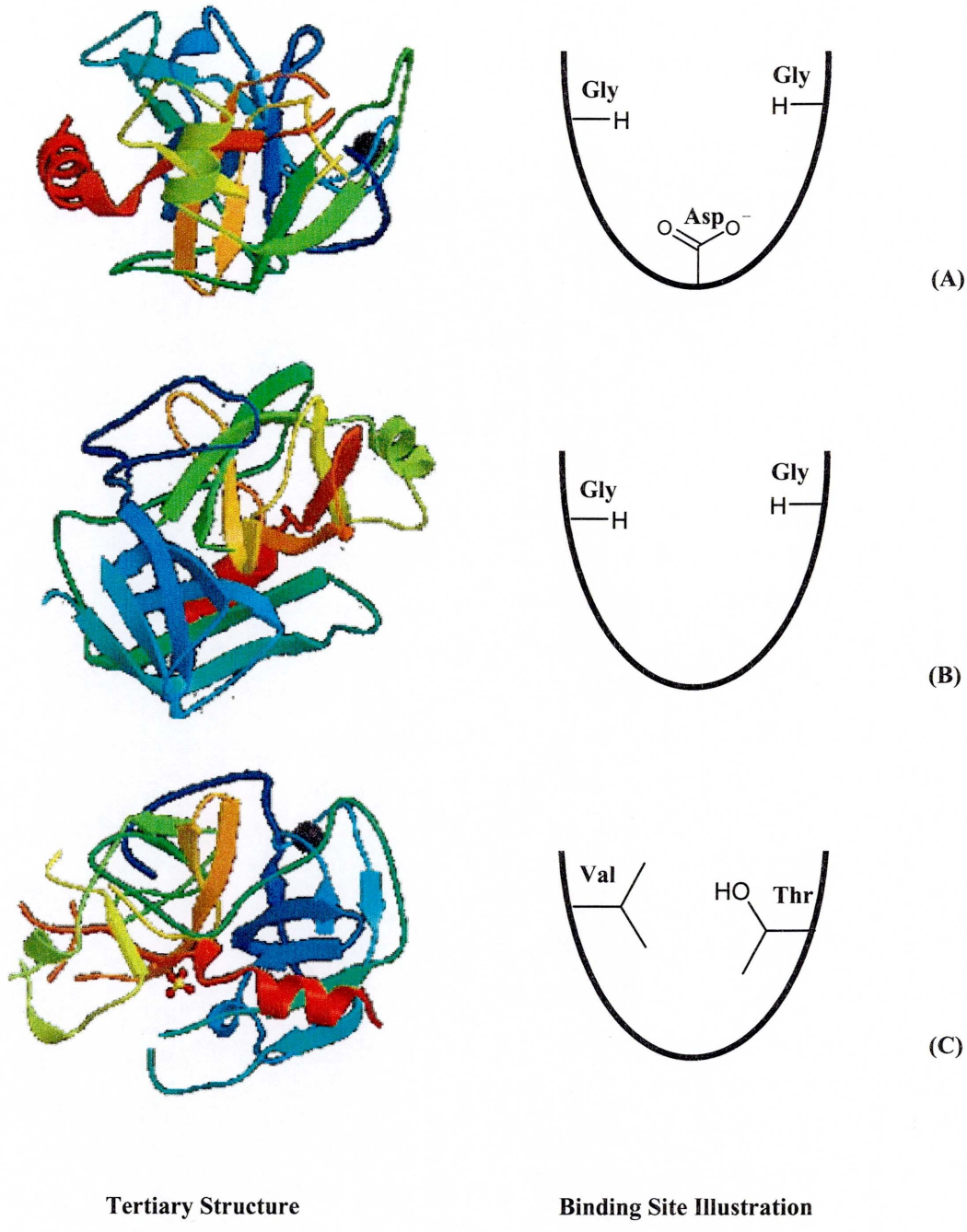

Figure 2.13: Tertiary structures [33-35] and binding site illustrations [20] of trypsin (A), α-chymotrypsin (B), and elastase (C).

Within these regions, non-covalent interactions participate in the stabilization of substrates throughout the enzymatic reactions.

Given an enhanced preference for basic residues such as arginine and lysine, N-α-*p*-tosyl-L-lysine chloromethyl ketone hydrochloride (TLCK, Figure 2.14) selectively and irreversibly inhibits trypsin activity without affecting α-chymotrypsin activity [19].

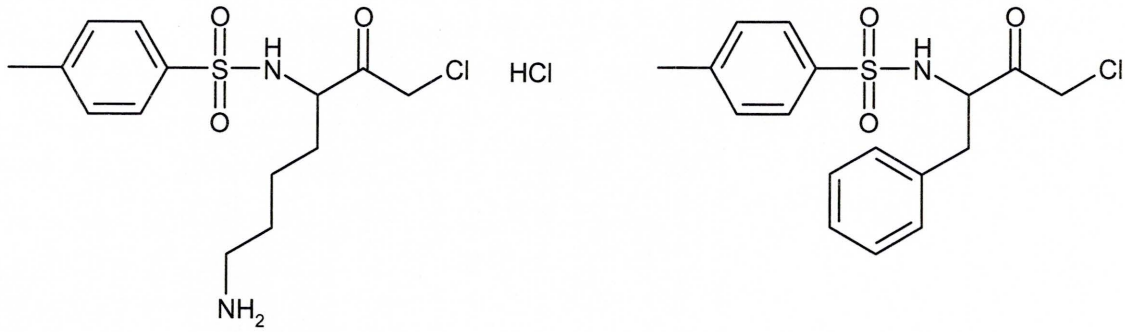

TLCK **TPCK**

Figure 2.14: N-α-*p*-tosyl-L-lysine chloromethyl ketone hydrochloride (TLCK) and N-tosyl-L-phenylalanine chloromethyl ketone (TPCK).

TLCK inhibits trypsin by alkylating the histidine residue in the catalytic triad [30]. After treating α-chymotrypsin with TLCK, the product yield significantly decreased in the replicate condensation experiment (Figure 2.15).

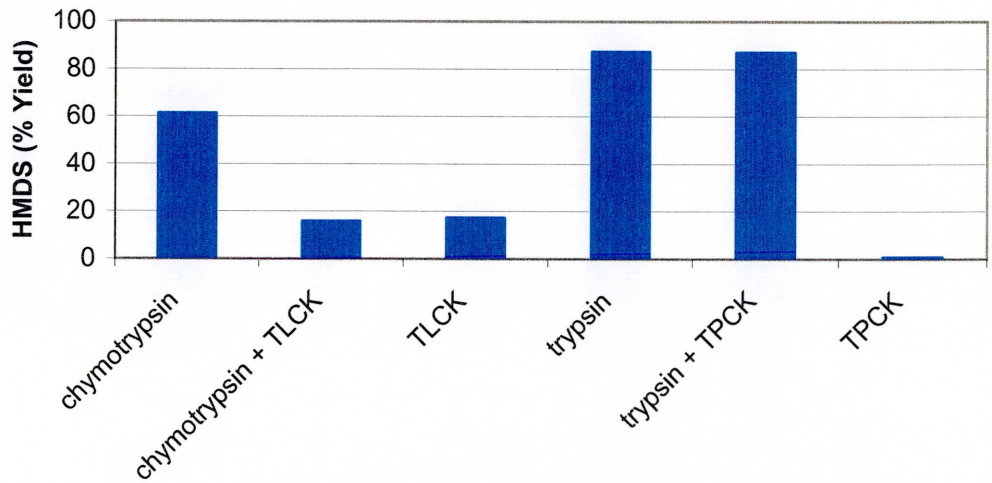

Figure 2.15: The use of N-α-*p*-tosyl-L-lysine chloromethyl ketone hydrochloride (TLCK) and N-tosyl-L-phenylalanine chloromethyl ketone (TPCK) to assess the proteolytic impurity of α-chymotrypsin and trypsin during the condensation of trimethylsilanol.[1]

[1] Refer to Experimental section 7.2.2 and Table 7.12.

Based on the product yield of the TLCK control reaction (Figure 2.15), α-chymotrypsin did not catalyse the condensation of trimethylsilanol. Alternatively, trypsin treated with N-tosyl-L-phenylalanine chloromethyl ketone (TPCK, Figure 2.14), an irreversible chymotrypsin inhibitor [19, 36], was used to complement the TLCK treated α-chymotrypsin experiment. Given the specificity of chymotrypsin to hydrophobic residues such as phenylalanine, TPCK inhibited chymotrypsin by alkylating the histidine residue in the catalytic triad. Based on the chromatographic results (Figure 2.15) and the inactivity of elastase (Figure 2.11), trypsin as opposed to α-chymotrypsin was determined to catalyse the condensation of trimethylsilanol. Furthermore, the exceptional activity of trypsin and α-chymotrypsin observed in the original enzyme-catalysed condensation study (Table 2.2) was solely due to a tryptic impurity.

2.5 Summary

The *in vitro* studies [1, 3-7, 12] of natural systems within the area of silica biosynthesis are complicated. These earlier mechanistic queries including biomimetic approaches [8, 11] often failed to recognise the chemistry of silicic acid and its analogues [13]. The study of the hydrolysis and condensation reactions during biosilicification is complicated due to the sensitivity of silica, silicates, and silicic acid to pH, concentration, and temperature [13]. As a silicic acid precursor, tetraalkoxysilanes are easily hydrolysed and the resulting silanols are condensed during the formation of particulate silica. Given these complications, a series of homologous enzymes were screened with a simple model compound, trimethylsilanol. Trimethylsilanol was chosen to focus on the formation of a molecule, hexamethyldisiloxane, with a *single* siloxane bond during condensation. The data suggests that homologous lipases and proteases catalyse the formation of siloxane bonds under mild conditions. Since the exceptional activity of trypsin and α-chymotrypsin

observed in the enzyme-catalysed condensation study was solely due to a tryptic impurity, trypsin preferentially catalysed the condensation of trimethylsilanol. Although trimethylsilanol appears to be an acceptable substrate, the activities of the enzymes are dependent on the functionality of the non-natural organosilicon substrates.

2.6 References

1. J. N. Cha, K. Shimizu, Y. Zhou, S. C. Christiansen, B. F. Chmelka, G. D. Stucky, and D. E. Morse, *Proc. Natl. Acad. Sci. USA*, **96**, 361, (1999).

2. Y. Zhou, K. Shimizu, J. N. Cha, G. D. Stucky, and D. E. Morse, *Angew. Chem. Int. Ed.*, **38(6)**, 780, (1999).

3. N. Kroger, R. Deutzmann, and M. Sumper, *Science*, **286**, 1129, (1999).

4. N. Kroger, R. Deutzmann, C. Bergsdorf, and M. Sumper, *Proc. Natl. Acad. Sci. USA*, **97(26)**, 14133, (2000).

5. N. Kroger, R. Deutzmann, and M. Sumper, *J. Biol. Chem.*, **276(28)**, 26066, (2001).

6. N. Kroger, S. Lorenz, E. Brunner, and M. Sumper, *Science*, **298**, 584, (2002).

7. C. C. Perry and T. Keeling-Tucker, *J. Chem. Soc. Chem. Commun.*, 2587, (1998).

8. R. R. Naik, L. L. Brott, S. J. Clarson, and M. O. Stone, *J. Nanosci. Nanotech.*, **2(1)**, 95, (2002).

9. J. N. Cha, K. Shimizu, Y. Zhou, S. C. Christiansen, B. F. Chmelka, T. J. Deming, G. D. Stucky, and D. E. Morse, *Mat. Res. Soc. Symp. Proc.*, **599**, 239, (2000).

10. D. E. Morse, *TIBTECH*, **17(6)**, 230, (1999).

11. J. N. Cha, G. D. Stucky, D. E. Morse, and T. J. Deming, *Nature*, **403**, 289, (2000).

12. K. Shimizu, J. Cha, G. D. Stucky, and D. E. Morse, *Proc. Natl. Acad. Sci. USA*, **95**, 6234, (1998).

13. R. K. Iler, "*The chemistry of silica: Solubility, polymerization, colloid and surface properties, and biochemistry*," John Wiley & Sons, New York, (1979).

14. C. Eaborn, "*Organosilicon compounds*," Butterworths Scientific Publications, London, (1960).

15. R. R. Naik, P. W. Whitlock, F. Rodriguez, L. L. Brott, D. D. Glawe, S. J. Clarson, and M. O. Stone, *J. Chem. Soc. Chem. Commun.*, 238, (2003).

16. S. Varaprath, K. L. Salyers, K. P. Plotzke, and S. Nanavati, *Analytical Biochemistry*, **256(1)**, 14, (1998).

17. A. L. Smith, (ed.), "*The analytical chemistry of silicones*." John Wiley & Sons, Inc., New York, 1991.

18. C. A. Burtis and E. R. Ashwood, "*Clinical chemistry*," W.B. Saunders, Philadelphia, (1994).

19. A. J. Barrett, N. D. Rawlings, and J. F. Woessner, (eds.), "*Handbook of proteolytic enzymes*." Academic Press, San Diego, 1998.

20. L. Stryer, "*Biochemistry*," W. H. Freeman and Company, New York, (1988).

21. G. Dodson and A. Wlodawer, *TIBS*, 347, (1998).

22. D. C. Carter and J. X. Ho, *Adv. Protein Chem.*, **45**, 153, (1994).

23. J. W. Lagocki, J. H. Law, and F. J. Kezdy, *J. Biol. Chem.*, **248(2)**, 580, (1973).

24. U. T. Bornscheuer and R. J. Kazlauskas, "*Hydrolases in organic synthesis*," Wiley-VCH, Weinheim, (1999).

25. EPI Suite Software version 3.11, Environmental Protection Agency, http://www.epa.gov/opptintr/exposure/docs/episuite.htm, 2000.

26. J. Uppenberg and T. A. Jones, *Structure*, **2**, 293, (1994).

27. L. Brady, A. M. Brzozowski, Z. S. Derewenda, E. J. Dodson, G. G. Dodson, S. P. Tolley, J. P. Turkenburg, L. Christiansen, B. Huge-Jensen, L. Norskov, and L. Thim, *Acta Crystallogr. B*, **48**, 307, (1992).

28. C. H. Wong and G. M. Whitesides, "*Enzymes in synthetic organic chemistry*," Elsevier Science Ltd, Kidlington, Oxford, (1994).

29. T. Sipos and J. R. Merkel, *Biochemistry*, **9(14)**, 2766, (1970).

30. B. Keil, *in* "*Hydrolysis: Peptide bonds*," (eds. P. D. Boyer), Vol. 3, Academic Press, New York, 1971.

31. Sigma-Aldrich, personal communication, 2002.

32. A. Fersht, "*Structure and mechanism in protein science: A guide to enzyme catalysis and protein folding*," W.H. Freeman and Company, New York, (1999).

33. W. Bode, H. Fehlhammer, and R. Huber, *J. Mol. Biol.*, **111**, 415, (1977).

34. S. T. Freer, J. Kraut, J. D. Robertus, H. T. Wright, and N. H. Xuong, *Biochemistry*, **9**, 1997, (1970).

35. M. Schiltz, W. Shepard, R. Fourme, T. Prange, E. DeLaFortelle, and G. Bricogne, *Acta Crystallogr. D Biol. Crystallogr.*, **53**, 78, (1997).

36. V. Kostka and F. H. Carpenter, *J. Biol. Chem.*, **239(6)**, 1799, (1964).

Chapter Three

Trypsin-Catalysed Condensation of Silanols

3.0 Introduction

Based on the results of the condensation study, *Bos taurus* or bovine pancreatic trypsin (i.e. serine-protease) was chosen to investigate the role of the enzymatic active site in the condensation of trimethylsilanol under mild conditions (Scheme 3.1).

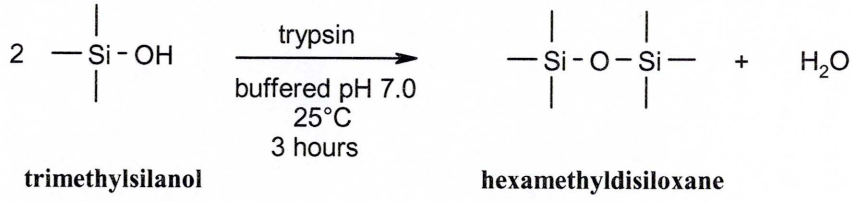

Scheme 3.1: Trypsin-catalysed condensation of trimethylsilanol.

Trypsinogen (Figures 3.1-3.3) is activated following the hydrolysis of the Lys6-Ile7 peptide bond and formation of β-trypsin (i.e. a disulfide cross-linked single polypeptide chain) [1, 2].

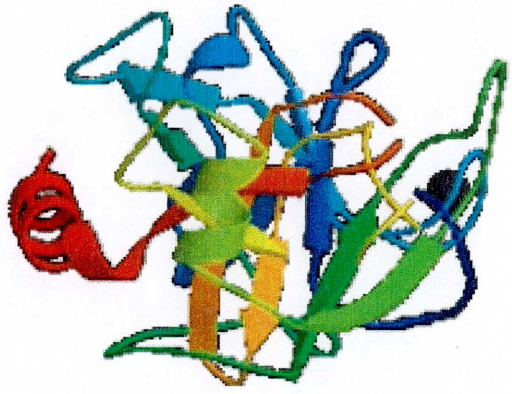

Figure 3.1: Tertiary structure of trypsinogen [3].
spirals = α-helices, arrows = β-sheets, black circle = calcium atom.

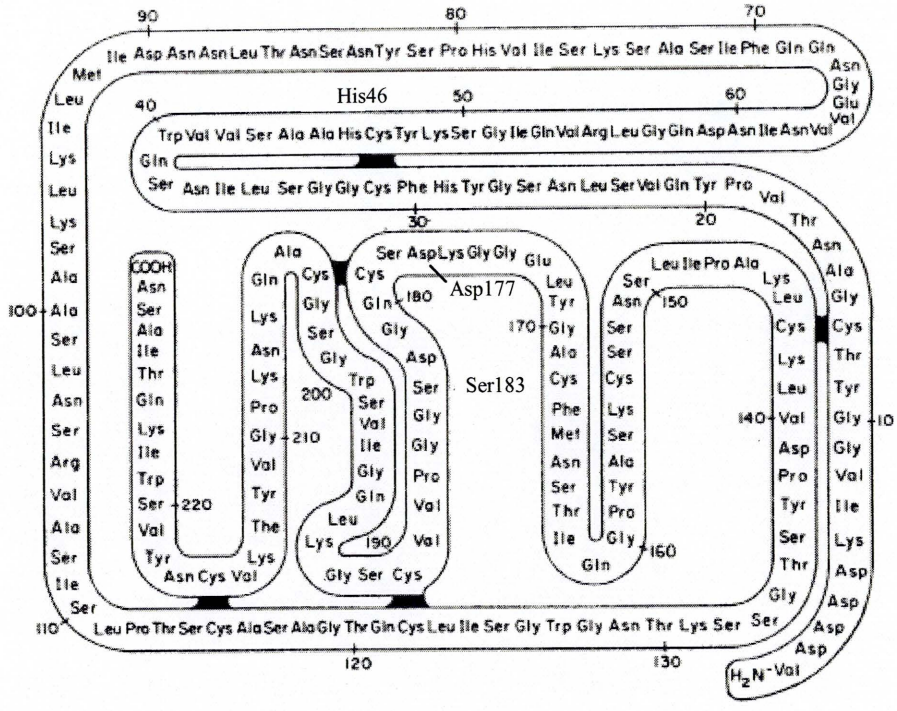

Figure 3.2: Primary structure of trypsinogen [2].

Hydrophobic interactions with the new N-terminal isoleucine residue lead to the formation of regions such as the binding domain and oxyanion hole, which are known to participate in substrate recognition. As defined by these regions, trypsin selectively hydrolyses peptide bonds adjacent to basic residues (i.e. arginine > lysine >> natural amino acids). Following activation, autolysis of the Lys131-Ser132 and Lys176-Asp177 bonds leads to the formation of α-trypsin (i.e. a cross-linked two-chain structure) and pseudotrypsin (i.e. a cross-linked three-chain structure), respectively.

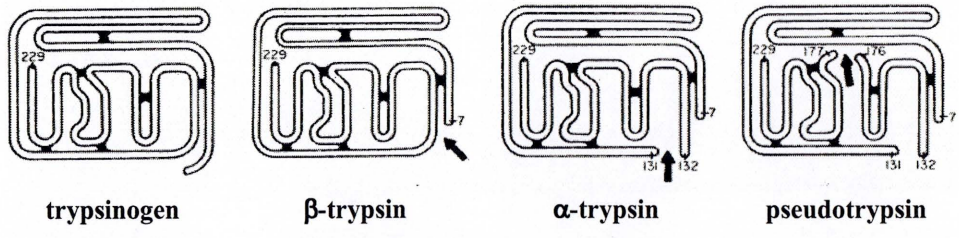

Figure 3.3: Activation of trypsinogen [2].

Notably, the activation reactions and structural changes cause negligible alterations to the region of the catalytic triad (i.e. Ser183-His46-Asp177, Figure 3.2). Ultimately, trypsin will self-deactivate due to autolysis. This process is dependent on the pH, temperature, and concentration of the protein sample. Commercial preparations of trypsin contain a mixture of predominately α- and β-trypsin as well as other digestive enzymatic contaminates [1, 2]. Optical and microscope images of the commercial source of bovine pancreatic trypsin (Experimental section 7.1.1) are detailed in Figure 3.4.

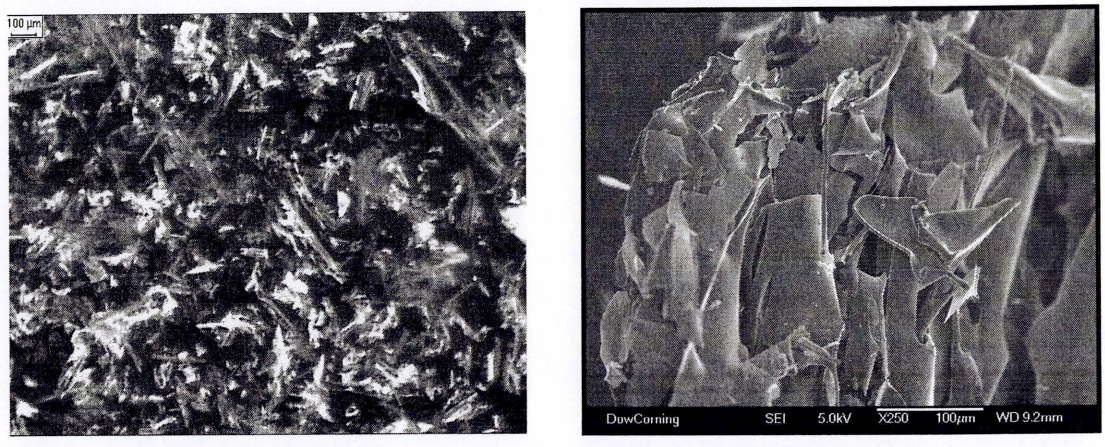

Optical Image (40x) **Scanning Electron Microscope Image (250x)**

Figure 3.4: Lyophilised trypsin.[1]

[1] Refer to Experimental section 7.3.8.

Lyophilised trypsin is a flaky white solid. Based on the primary structure, the molecular weight of trypsin is 23,305 [4]. The molecular weight of the commercial source of bovine pancreatic trypsin was determined to be 23,288 by matrix-assisted laser desorption/ionisation mass spectrometry (MALDI-TOF MS) (Figure 3.5). The difference between the theoretical and experimental average molecular weight values is within the experimental error of the mass calibration (Experimental section 7.3.6).

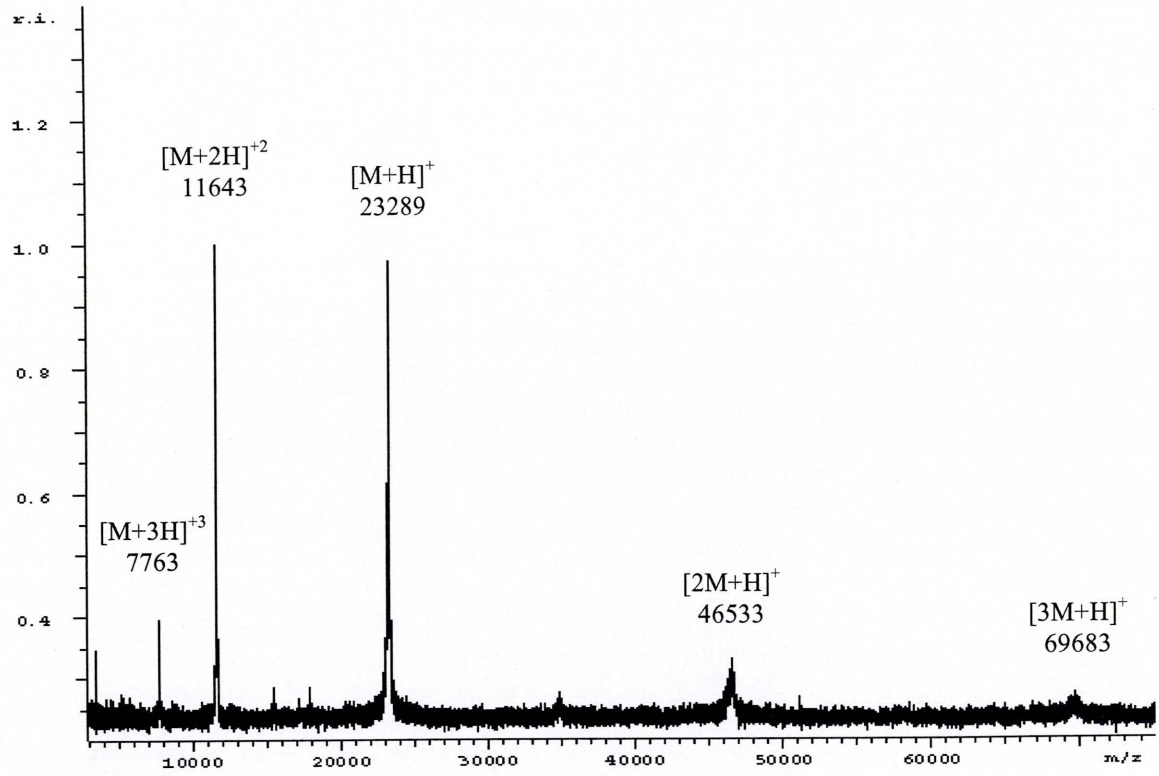

Figure 3.5: Matrix-assisted laser desorption/ionisation mass spectrum of trypsin (TPCK).[1]

[1] Refer to Experimental section 7.3.6.
M = trypsin.

3.1 Proteinaceous Inhibition Study

A proteinaceous inhibition study was conducted to investigate the role of the enzymatic active site in the model silanol condensation reaction (Scheme 3.1). Specifically, trypsin and α-chymotrypsin were inhibited with two distinctly different natural polypeptide inhibitors from soybean (Figure 3.6): a trypsin-chymotrypsin inhibitor (i.e. the Bowman-Birk Inhibitor, BBI [5]) and a trypsin inhibitor from Glycine max (i.e. the Kunitz soybean trypsin inhibitor or Popcorn inhibitor, PCI [6, 7]).

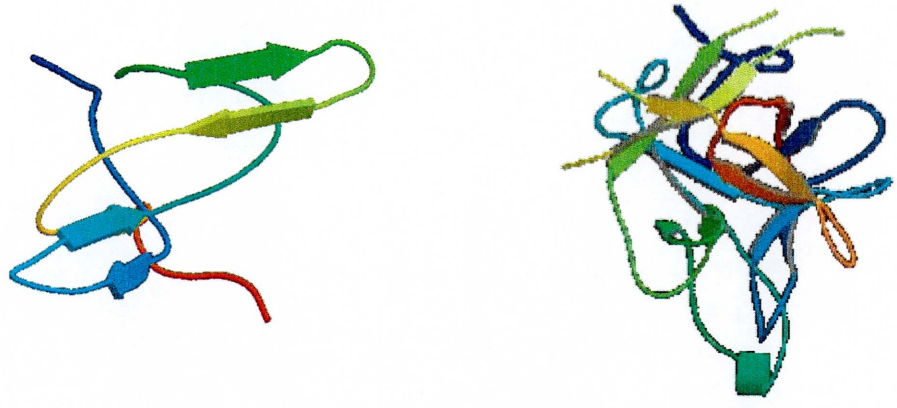

BBI [8] **PCI** [9]

Figure 3.6: Tertiary structures of the Bowman-Birk (BBI) and Popcorn (PCI) inhibitors. spirals = α-helices, arrows = β-sheets.

The soybean inhibitors are highly stable proteins with well-defined inhibitory sites. Although the proteinaceous inhibitors originate from the same source, the amino acid sequences, tertiary structures, and properties of the polypeptides are different. The BBI and PCI proteins contain 71 (MW = 7,975) and 181 (MW = 21,700) amino acids, respectively. BBI contains dual independent regions that selectively inhibit trypsin and chymotrypsin. The reactive sites within these regions are defined as Lys16-Ser17 (trypsin) and Leu43-Ser44 (chymotrypsin). The kinetics and equilibria of the inhibition reactions are independent. PCI selectively inhibits trypsin through interactions with an Arg63-Ile64 reactive site.

Prior to reaction, the enzymes were inhibited with excess inhibitor (i.e. > 1:1 (w/w) or 4:1 BBI to protease and 2:1 PCI to protease mole ratios, respectively) in stirred neutral media (pH 7.0) for two hours. Based on standard enzymatic activity assays [10], trypsin (Figure 3.7) was fully inhibited with BBI (98%) and PCI (91%), while α-chymotrypsin was partially inhibited with BBI (63%) (Table 7.38).

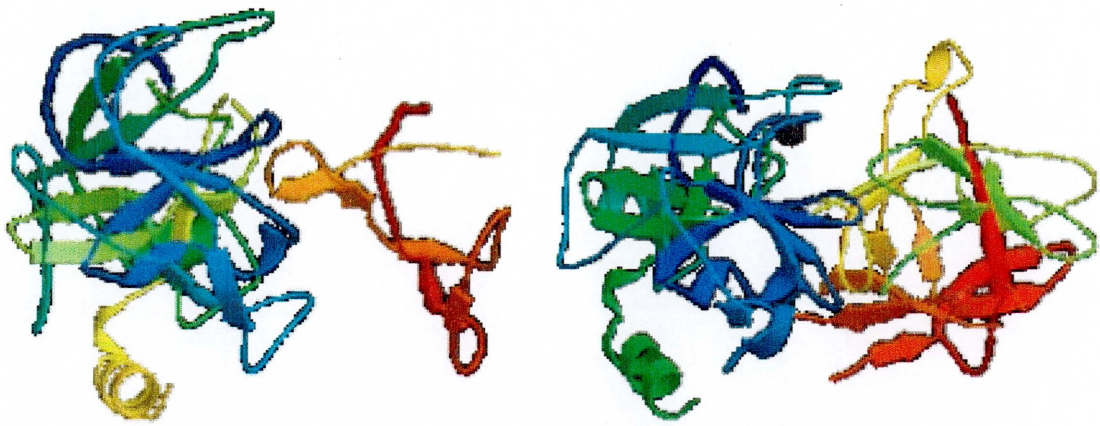

trypsin-BBI complex [11] **trypsin-PCI complex [9]**

Figure 3.7: Tertiary structures of the proteinaceous inhibition of trypsin.
spirals = α-helices, arrows = β-sheets.

The reactions were formulated with a 4:1 monomer to enzyme weight ratio (~1000:1 silanol to protease mole ratio) and conducted at 25°C for three hours. The reaction products were isolated and quantitatively analysed by GC (Figure 3.8).

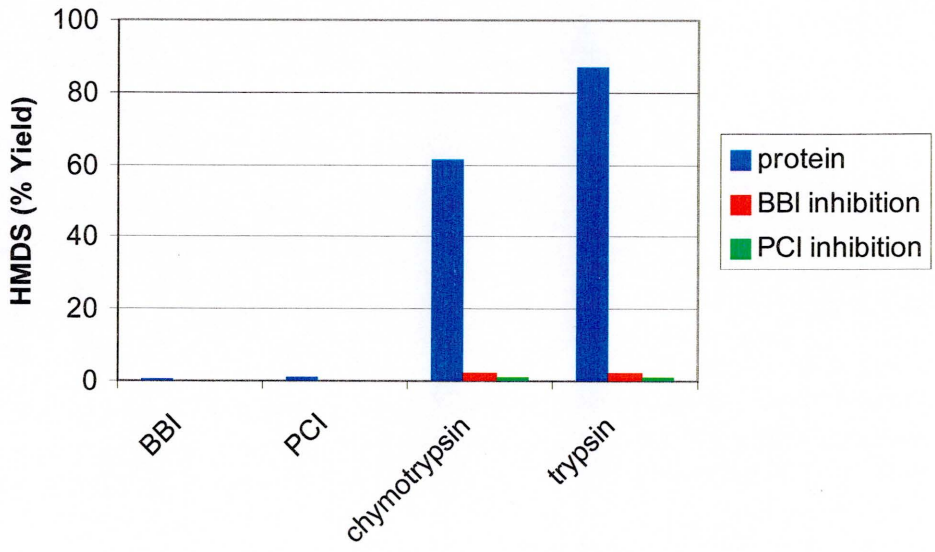

Figure 3.8: Proteinaceous inhibition of the condensation of trimethylsilanol.[1]
[1] Refer to Experimental section 7.2.2 and Table 7.13.

In comparison to the control reactions, the proteinaceous inhibitors completely inhibited the protease-catalysed condensation reactions. Since α-chymotrypsin was inhibited by PCI, the presence of trypsin in α-chymotrypsin was confirmed. In addition, condensation was not observed despite the partial inhibition of α-chymotrypsin with BBI. Consequently, it appears that the tertiary structure, functionality of the active site, and catalytic triad of trypsin are directly involved in the *in vitro* condensation of trimethylsilanol. Although trypsin and α-chymotrypsin are serine proteases, the observed substrate selectivity with trimethylsilanol may be due to the documented differences in their binding domains [1, 12].

3.2 Temperature Study

The effect of temperature on trypsin as well as the enzyme-catalysed condensation reaction was studied. Prior to reaction, buffered aqueous solutions (pH 7.0) of trypsin were stirred and equilibrated at set temperatures in a thermostated water bath (+/- 0.1°C) for 20 minutes. The reactions were formulated with a 4:1 monomer to enzyme weight ratio (~1000:1 silanol to trypsin mole ratio) and conducted at set temperatures for three hours. In the thermal denaturation experiments, trypsin was boiled for 20 minutes and three hours, independently, before performing the condensation reaction at 25°C. The reaction products were isolated and quantitatively analysed by GC (Figure 3.9).

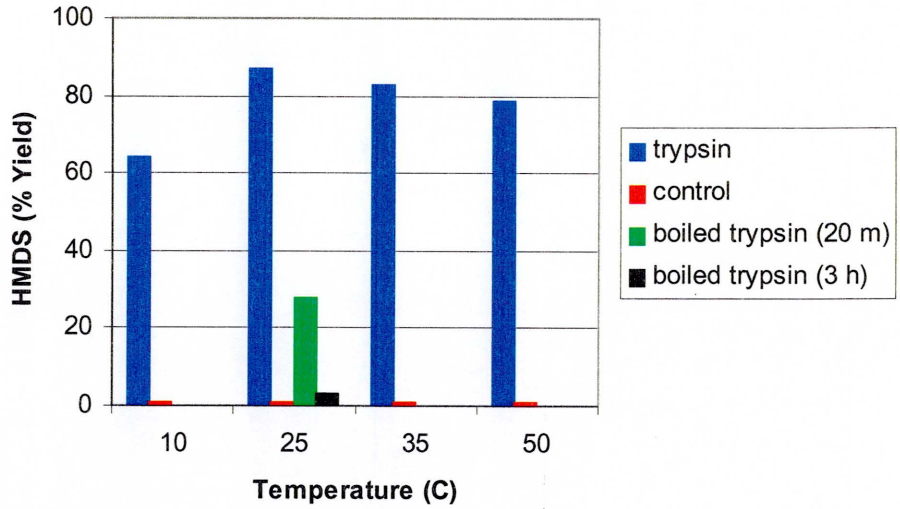

Figure 3.9: The effect of temperature on the trypsin-catalysed condensation of trimethylsilanol.

[1] Refer to Experimental section 7.2.2 and Table 7.14.

In comparison to the control reactions, trypsin appears to be catalytically active over a broad temperature range. The optimum temperature of the reaction was approximately 25°C. After boiling the solutions of trypsin (40 mg/mL) for different periods of time (i.e. 20 minutes vs. 3 hours), the rates of the trypsin-catalysed condensation reactions decreased due to the degree of thermal denaturation. Although enzymatic reaction rates may increase with temperature [13], elevated temperatures have been reported [14, 15] to reversibly unfold and irreversibly inactivate enzymes including trypsin [16] in water due to decomposition. Since the rate of reaction was dependent on the degree of thermal denaturation, a natural substrate, N-α-benzoyl-L-arginine ethyl ester (BAEE), was used to study the activity [10] of boiled tryptic solutions as a function of concentration in neutral media (pH 7.0). Different concentrations of trypsin (i.e. 2-40 mg/mL) were prepared in 0.5 mL of 50 mM Tris-HCl buffered Milli-Q water (pH 7.0). The solutions were boiled for 20 minutes before measuring the activity of the boiled trypsin by recording the change in absorbance at 253 nm due to the formation of N-α-benzoyl-L-arginine (Scheme 3.2). The spectrophotometric activity data is illustrated in Figure 3.10.

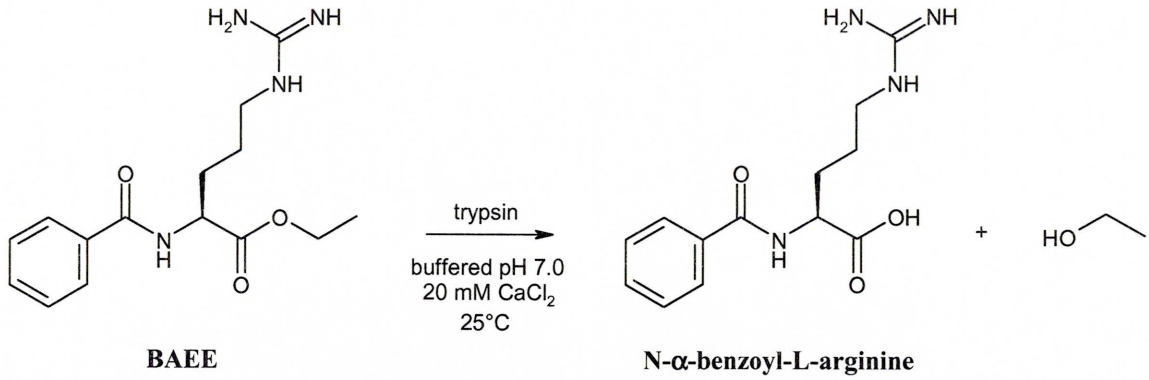

Scheme 3.2: Trypsin-catalysed hydrolysis of N-α-benzoyl-L-arginine ethyl ester (BAEE).[1]

[1] Refer to Experimental section 7.3.7.

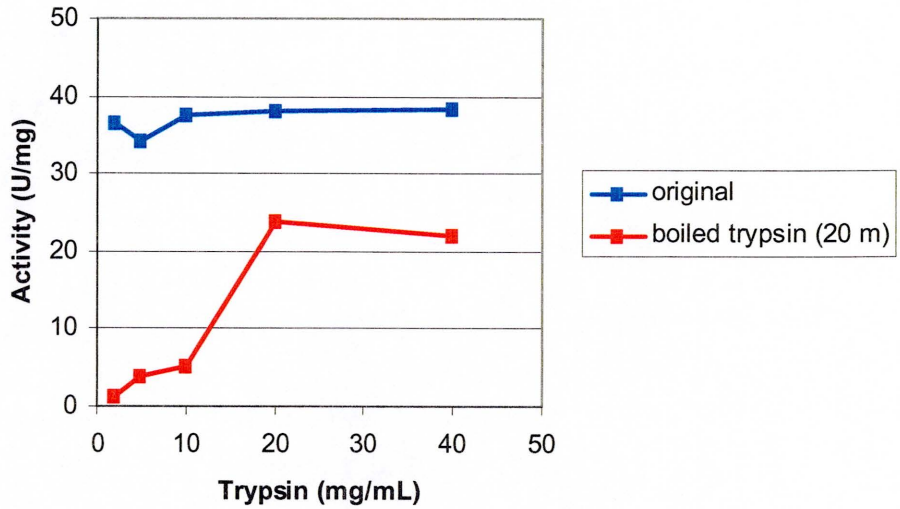

Figure 3.10: Study of the thermal denaturation of trypsin in neutral media as a function of the concentration of trypsin.[1]

[1] Refer to Experimental section 7.3.7 and Table 7.39.

As measured by the rate of hydrolysis of BAEE, the activity of the boiled tryptic solutions decreased at lower concentrations due to increased denaturation. Comparatively, the relative decrease in the rate of silanol condensation (Figure 3.9) correlated with the enhanced stability of trypsin at higher protein concentrations (Figure 3.10). Based on a thermogravimetric analysis (Figure 3.11), trypsin experienced a small mass loss (5%) from room temperature to 100°C and a critical mass loss at 225°C. The thermal profile supports

the potential loss of water prior to physical decomposition. Visually, the recovered sample was significantly charred. In a differential thermogram (Figure 3.12), an irreversible endothermic melt (Tm) was observed at 40°C due to a crystalline or ordered phase in the enzyme. It appears that trypsin was irreversibly denaturated due to the lack of a replicate endothermic melt during the second heating cycle.

3.3 Time Study

The trypsin-catalysed condensation of trimethylsilanol was studied over a 24-hour period at 25°C. Independent reactions were formulated with a 4:1 monomer to enzyme weight ratio (~1000:1 silanol to trypsin mole ratio) in a neutral medium (pH 7.0) and performed for defined periods of time over 24 hours. The reaction products were isolated and quantitatively analysed by GC (Figure 3.13). The trypsin-catalysed condensation of trimethylsilanol was nearly complete after three hours at 25°C. Based on the stoichiometry of the condensation reaction (Scheme 3.1), two moles of trimethylsilanol were consumed for each mole of hexamethyldisiloxane (HMDS) produced (mass balance, Figure 3.13). Conversely, the reversibility of the trypsin-catalysed condensation reaction was studied with hexamethyldisiloxane in a neutral medium (pH 7.0) as well as an organic solvent (toluene). Since trimethylsilanol was not observed in the chromatographic results (Table 7.16), trypsin was not observed to catalyse the hydrolysis of a siloxane bond in either medium. Although trypsin would theoretically catalyse the hydrolysis of a siloxane bond due to the law of microscopic reversibility, the reverse reaction was not favored under these conditions.

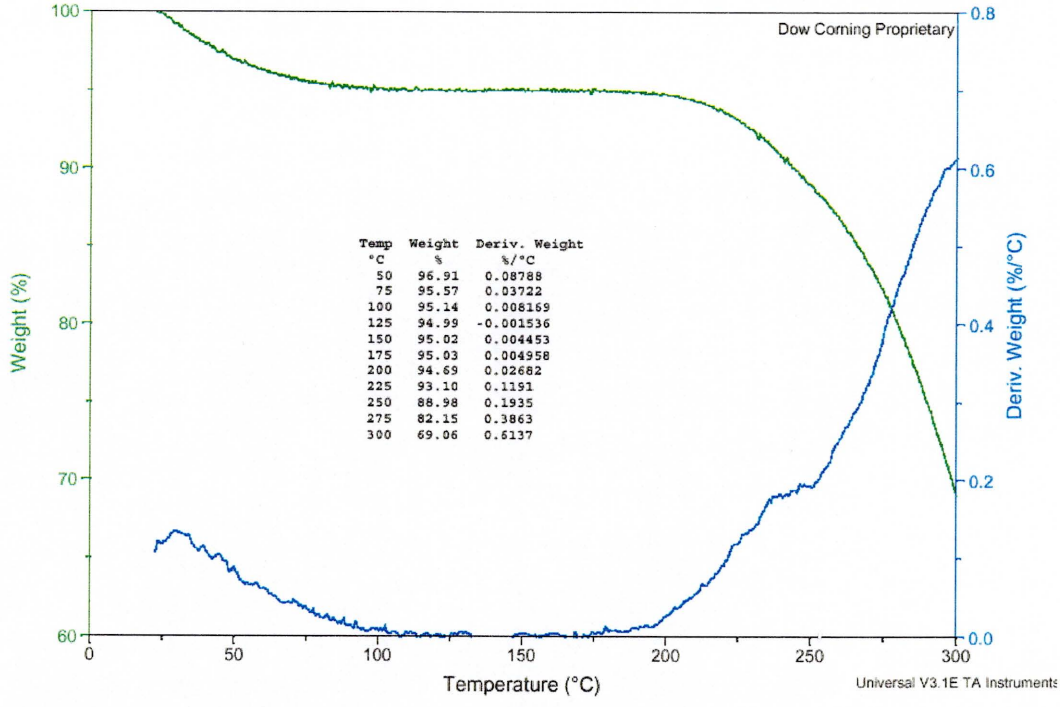

Figure 3.11: Thermogravimetric analysis of trypsin (TPCK).[1]

[1] Refer to Experimental section 7.3.9.

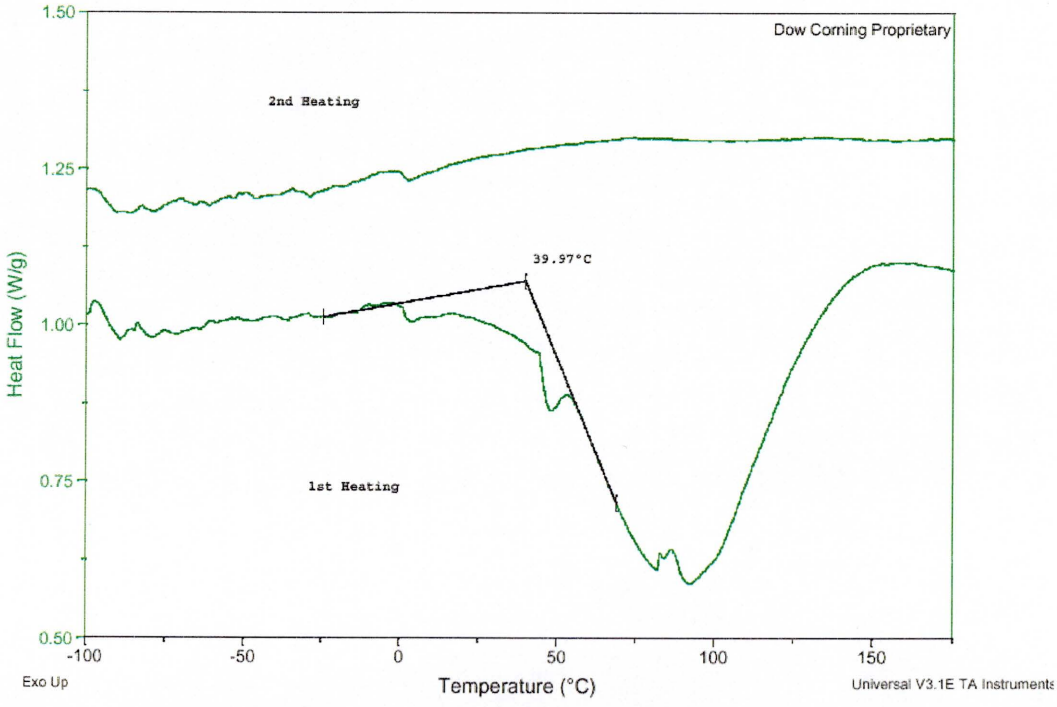

Figure 3.12: Differential scanning calorimetry thermogram of trypsin (TPCK).[1]

[1] Refer to Experimental section 7.3.9.

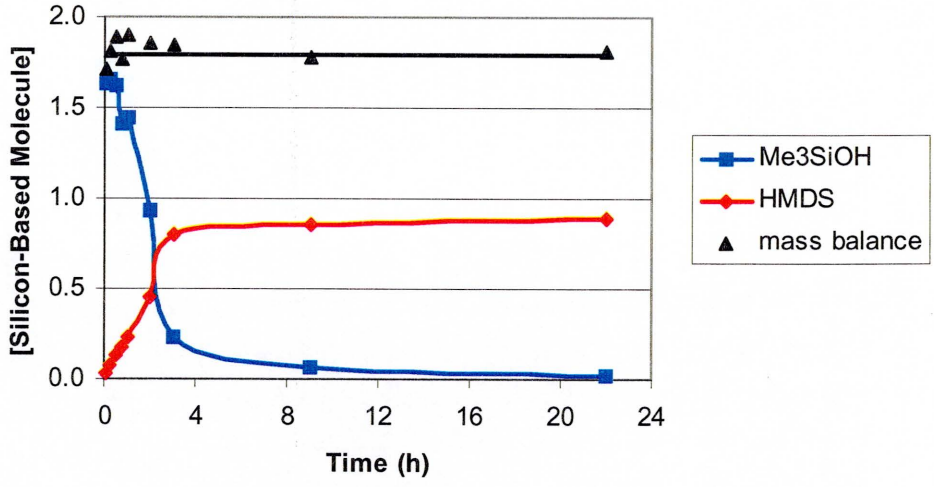

Figure 3.13: Trypsin-catalysed condensation of trimethylsilanol at 25°C.[1]
[1] Refer to Experimental section 7.2.2 and Table 7.15.

Based on the estimated solubility of trimethylsilanol in water (42.56 mg/mL) [17], the concentration of trimethylsilanol (~160 mg/mL) saturated the aqueous medium and created a two-phase reaction mixture. Since proteases will only interact with water-soluble substrates [18], the trypsin-catalysed condensation of trimethylsilanol was postulated to occur in the aqueous phase (Scheme 3.3). Although the condensation reaction was conducted in water, the enzyme-catalysed reaction was promoted by the phase separation of the product. The immiscibility of the product, hexamethyldisiloxane, changed the equilibrium [19] and promoted the condensation reaction in the presence of water. Since the aqueous medium was saturated with trimethylsilanol, the reactant would continue to enter the aqueous phase due to the dynamic equilibrium of the condensation reaction. In addition, the hydrolysis or reverse reaction would be severely hindered due to the immiscibility of the disiloxane product in the aqueous phase.

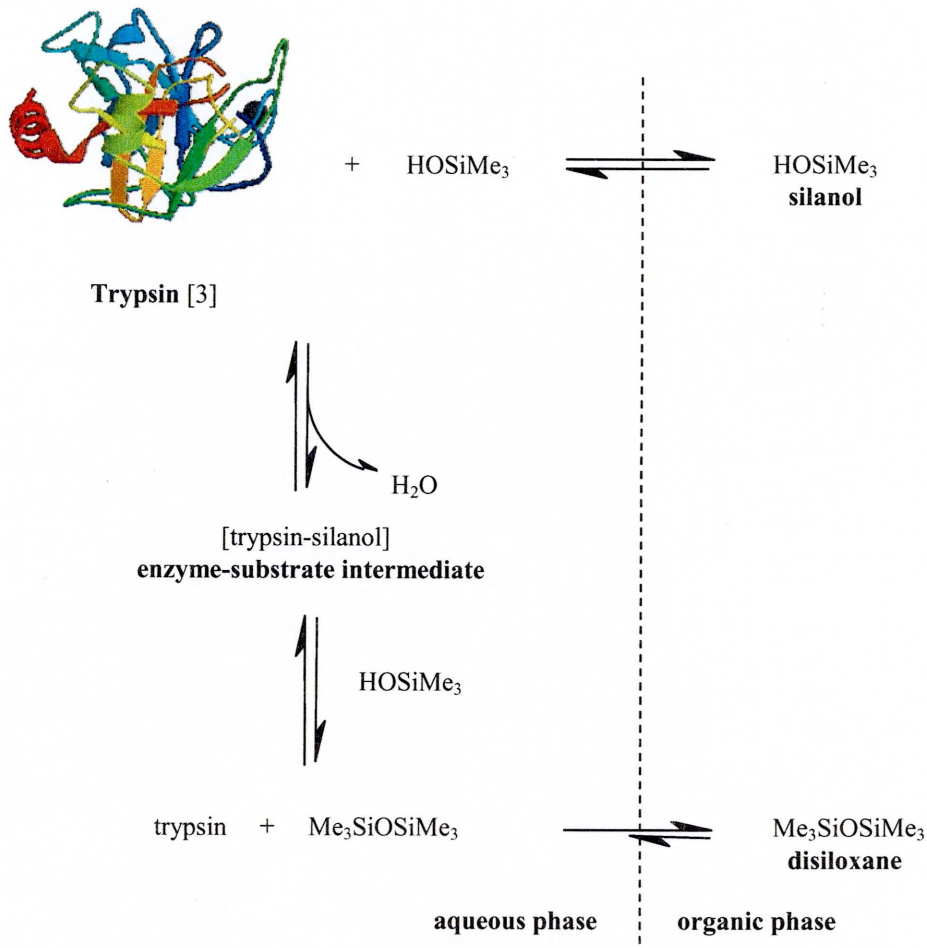

Scheme 3.3: Proposed condensation of trimethylsilanol in water.

The rate of condensation during the time study was analysed, in order to begin to study the kinetics [20] of the reaction catalysed by trypsin at 25°C. Based on the time-independent stoichiometry of the proposed reaction (Scheme 3.1), the rate (V) of condensation (Equation 3.1) and theoretical rate (Equation 3.2) equations were defined.

$$V = -0.5*(\delta[Me_3SiOH]/ \delta t) = 1*(\delta[HMDS]/ \delta t) \quad \textbf{(3.1)}$$

$$V = k_R[Me_3SiOH]^{\alpha}[trypsin]^{\beta} \quad \textbf{(3.2)}$$

In Equation 3.1, the rate of condensation was defined as the change in concentration (i.e. [Molarity] = moles/L) of the reactant or product with time (e.g. δ[HMDS]/ δt). In equation

3.2, the experimental rate constant (k_R) and the partial orders of reaction (i.e. α and β) with respect to each reactant were defined. The overall order of reaction is the sum of the partial orders (i.e. $\alpha + \beta$). Since trypsin was not consumed during the condensation reaction (i.e. a catalyst), the term was included in the rate constant (k_R') and the theoretical rate equation (Equation 3.2) was simplified as defined in Equation 3.3.

$$V = k_R'[Me_3SiOH]^{\alpha},\ k_R' = k_R[trypsin]^{\beta} \quad \textbf{(3.3)}$$

Subsequently, the general rate equation (Equation 3.4) was integrated, in order to determine if the partial order of reaction with respect to trimethylsilanol was first- ($\alpha = 1$) or second- ($\alpha = 2$) order (Equations 3.5-3.6, respectively).

$$V = -0.5*(\delta[Me_3SiOH]/\delta t) = k_R'[Me_3SiOH]^{\alpha},\ A = \text{reactant},\ \alpha = 1 \text{ or } 2 \quad \textbf{(3.4)}$$

$$\log[Me_3SiOH]_t = -(2*k_R'/2.303)t + \log[Me_3SiOH]_o \quad \textbf{(3.5)}$$

$$1/[Me_3SiOH]_t = 2*k_R't + 1/[Me_3SiOH]_o \quad \textbf{(3.6)}$$

Based on the chromatographic data set acquired during the time study (Table 7.15), the concentration of trimethylsilanol could be used in these linear (i.e. $y = mx + b$) equations to determine the order with respect to trimethylsilanol. The extent of reaction can also be determined by measuring the concentration of the product, hexamethyldisiloxane, with time (i.e. $[Me_3SiOH]_t = 2*([HMDS]_\infty - [HMDS]_t)$). Therefore, the reactant and product data can be used in Equations 3.5 and 3.6. Consequently, $\log[Me_3SiOH]_t$ vs. t and $\log([HMDS]_\infty - [HMDS]_t)$ vs. t (Equation 3.5), as well as $1/[Me_3SiOH]_t$ vs. t and $1/([HMDS]_\infty - [HMDS]_t)$ vs. t (Equation 3.6) were plotted (Figures 3.14-3.15) in order to experimentally assess the partial order of reaction with respect to trimethylsilanol.

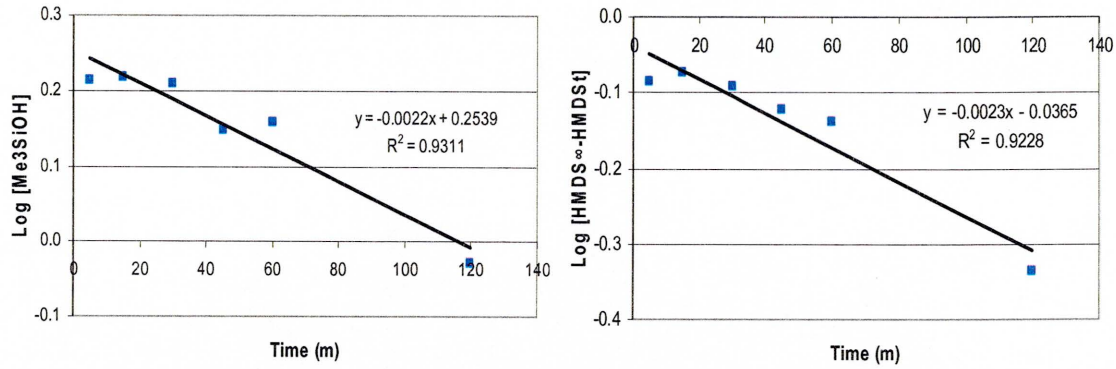

Figure 3.14: First-order evaluation of the condensation of trimethylsilanol at 25°C.[1]

[1] Refer to Table 7.15.

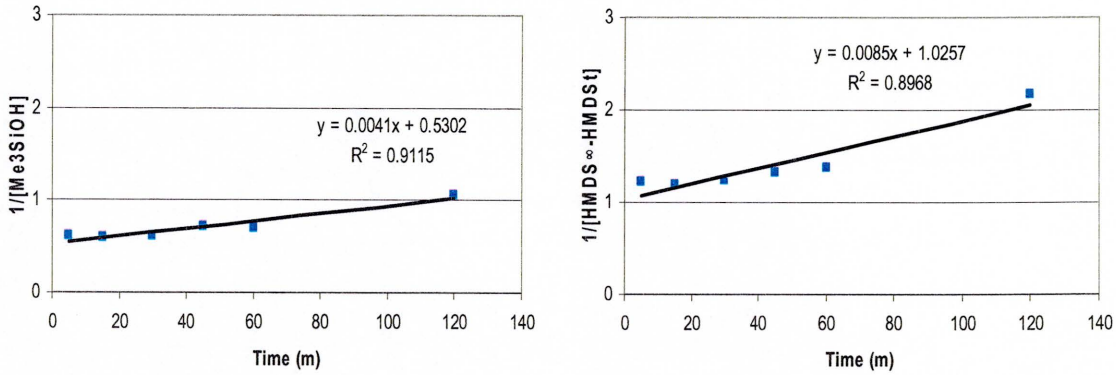

Figure 3.15: Second-order evaluation of the condensation of trimethylsilanol at 25°C.[1]

[1] Refer to Table 7.15.

The rate constants (k_R', Table 3.1) calculated with the concentration of trimethylsilanol or the extent of reaction (i.e. $[HMDS]_\infty - [HMDS]_t$) were comparable for the first- and second-order plots (Figures 3.14-3.15), respectively.

Table 3.1: Condensation rate constants (k_R') of trimethylsilanol at 25°C.[1]

		k_R'[2]
Partial order of reaction with respect to Me_3SiOH[3]	$[Me_3SiOH^3]_t$	$2*([HMDS]_\infty - [HMDS]_t)$[4]
first-order	$0.0025\ s^{-1}$	$0.0026\ s^{-1}$
second-order	$0.0021\ Lmol^{-1}s^{-1}$	$0.0021\ Lmol^{-1}s^{-1}$

1 Refer to Equations 3.5-3.6 and Figures 3.14-3.15.
2 k_R' = rate constant = $k_R[trypsin]^\beta$. Refer to Equation 3.3.
3 Me_3SiOH = trimethylsilanol.
4 $2*([HMDS]_\infty - [HMDS]_t) = [Me_3SiOH]_t$ = extent of reaction, where HMDS = hexamethyldisiloxane.

However, after reviewing the correlation coefficients (R^2) of the first- and second-order plots, the order of reaction with respect to trimethylsilanol was ill defined based on this data. In fact, the two-phase reaction mixture may have complicated this experimental assessment. Since the solution is saturated with trimethylsilanol during most of the condensation reaction, the absolute amount of trimethylsilanol may be effectively constant. Given constant concentrations of trimethylsilanol and trypsin (i.e. catalyst), these reaction conditions would lead to a zero-order theoretical rate equation (Equation 3.2). In other words, the rate of condensation would be approximately constant. Since the initial (< 3 hours) and final (> 3 hours) rates of condensation or formation of HMDS are constant or linear (Figure 3.13), the data set appears to support this assessment. Based on the concentration of trypsin (i.e. $[E_t]$ = [trypsin] = 1.7 mM) and the rate of condensation (i.e. $V = -\delta[Me_3SiOH]/\delta t = 0.0064$ M/m ~ $2\delta[HMDS]/\delta t = 0.0072$ M/m, Figure 3.16), a relative value of the turnover number (k_{cat}) or "number of substrate molecules converted into product by an enzyme molecule in a unit time when the enzyme is fully saturated with substrate [12]" was calculated to be 4.0 reactions per minute (m^{-1}) or 0.066 reactions per second (s^{-1}) at 25°C (Equation 3.7).

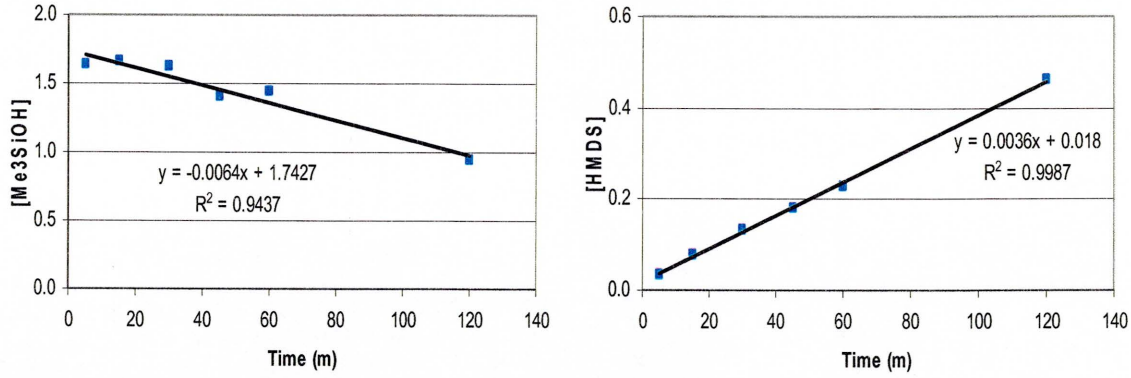

Figure 3.16: The rate of the trypsin-catalysed condensation of trimethylsilanol at 25°C.[1]

[1] Refer to Table 7.15.

$$k_{cat} = V_{max} / [Et] \qquad \textbf{(3.7)}$$

Since trypsin may not be saturated due to the limited solubility of trimethylsilanol in water, the turnover number was treated as a relative value. Given a relative turnover number equal to 0.066 s^{-1}, the time period between each condensation reaction catalysed by trypsin was calculated to be 15 s. In comparison to the maximum turnover numbers of other enzymes with their physiological substrates (Table 3.2) [12], the turnover number of the trypsin-catalysed condensation of trimethylsilanol at 25°C was several orders of magnitude (i.e. ~10-10,000,000) slower than the cited values. For example, the turnover number of the trypsin-catalysed condensation of trimethylsilanol was approximately 1500 times slower than a natural chymotrypsin-catalysed hydrolysis reaction.

Table 3.2: Turnover numbers of natural enzymatic reactions [12].

Enzyme	Turnover Number (s^{-1})
carbonic anhydrase	600,000
3-ketosteroid isomerase	280,000
acetylcholinesterase	25,000
penicillinase	2,000
lactate dehydrogenase	1,000
chymotrypsin	100
DNA polymerase I	15
tryptophan synthetase	2
lysozyme	0.5

Given the potential for autolysis as well as reactant and product inhibition, BAEE, a natural substrate, was used to study the activity [10] of trypsin during a condensation reaction with trimethylsilanol. However, since trypsin will deactivate due to autolysis, the self-hydrolysis of different concentrations of trypsin in Tris-HCl buffered Milli-Q water (pH 7.0) was first studied over a one-day period in the absence of trimethylsilanol. The spectrophotometric activity data is illustrated in Figure 3.17.

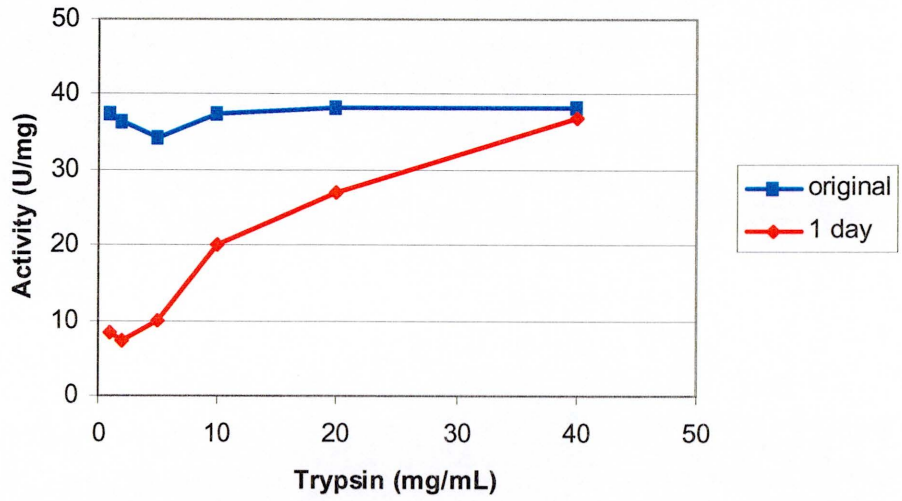

Figure 3.17: Autolysis of trypsin at 25°C.[1]

[1] Refer to Experimental section 7.3.7 and Table 7.40.

As measured by the rate of hydrolysis of BAEE, the activity of the tryptic solutions increased at high concentrations due to decreased autolysis. In other words, the self-hydrolysis of trypsin in buffered water (pH 7.0) decreased with increasing concentration. After a one-day period, autolysis was observed to decrease from 78% to 3% in 1- and 40-mg/mL solutions of trypsin, respectively (Table 7.40). Although the rate of autolysis was reduced at higher concentrations, the activity of the 40-mg/mL solution of trypsin decreased by 31% over four days (Table 7.41). The increased stability has been attributed to self-association at higher protein concentrations [1]. This observation compliments the enhanced thermal stability of trypsin at increased concentrations. After 20 minutes in boiling water, the inhibition of trypsin decreased from 96% to 43% in 2- and 40-mg/mL solutions, respectively (Table 7.39). Again, concentrated solutions of trypsin were active over a broad temperature range. Based on these measurements, a 40-mg/mL solution of trypsin was an ideal concentration to conduct the model reactions.

Since the trypsin-catalysed trimethylsilanol condensation reaction was effectively complete after three hours, reactant and product inhibition were studied by measuring the activity of trypsin with BAEE throughout the condensation reaction. The spectrophotometric activity data is illustrated in Figure 3.18. As measured by the rate of hydrolysis of BAEE, the activity of the tryptic solutions was constant with time. In comparison to a control reaction conducted without the reactant, neither trimethylsilanol nor hexamethyldisiloxane inhibition was observed in the trypsin-catalysed condensation reaction over a three-hour period in a neutral medium (pH 7.0) (Table 7.42).

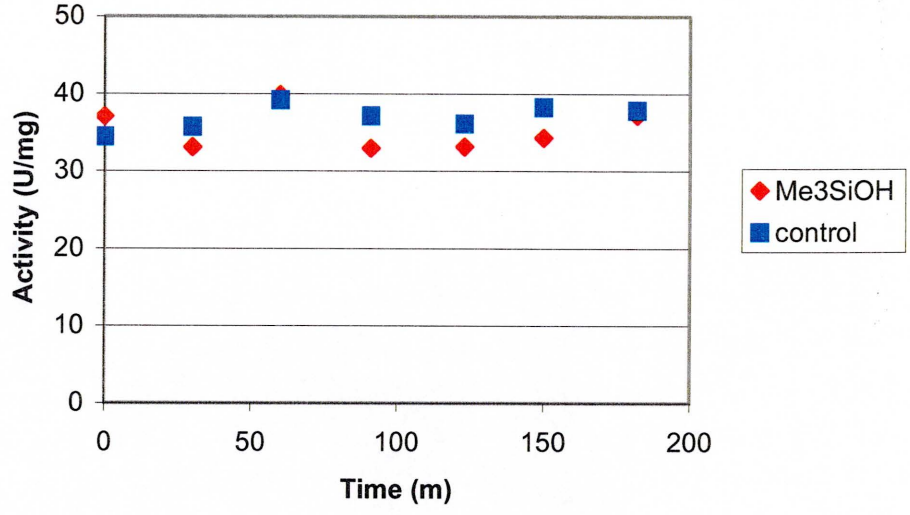

Figure 3.18: Reactant (trimethylsilanol) and product (hexamethyldisiloxane) inhibition study during the condensation of trimethylsilanol in a neutral medium (pH 7.0).[1]

[1] Refer to Experimental section 7.3.7 and Table 7.42.

In addition, a replicate condensation reaction of trimethylsilanol was conducted with a solution of trypsin, in order to further substantiate the absence of either reactant or product inhibition in a neutral medium. The initial reaction was formulated with a 4:1 monomer to enzyme weight ratio (~1000:1 silanol to trypsin mole ratio) and conducted in Tris-HCl buffered water (pH 7.0) at 25°C for three hours. Following the completion of the first three-hour reaction with trimethylsilanol, another aliquot of reactant was added to the two-phase reaction mixture for an additional three-hour reaction. After the completion of this replicate condensation reaction, the reaction products were isolated and quantitatively analysed by GC (Table 7.17). Based on the chromatographic data, the solution of trypsin was successfully recycled to catalyse an additional three-hour condensation reaction with trimethylsilanol, which further confirmed the absence of reactant and product inhibition in a neutral medium.

3.4 Evaluation of the Monomer to Enzyme Mole Ratio

The rate of trimethylsilanol condensation was studied as a function of the monomer to enzyme mole ratio. The mole ratios were formulated with a constant amount of trimethylsilanol (160 mg/mL) and a variable amount of trypsin (2-198 mg/mL) in buffered water (pH 7.0). The closed (screw capped) reactions were conducted at 25°C with magnetic stirring for three hours. The reaction products were isolated and quantitatively analysed by GC (Figure 3.19).

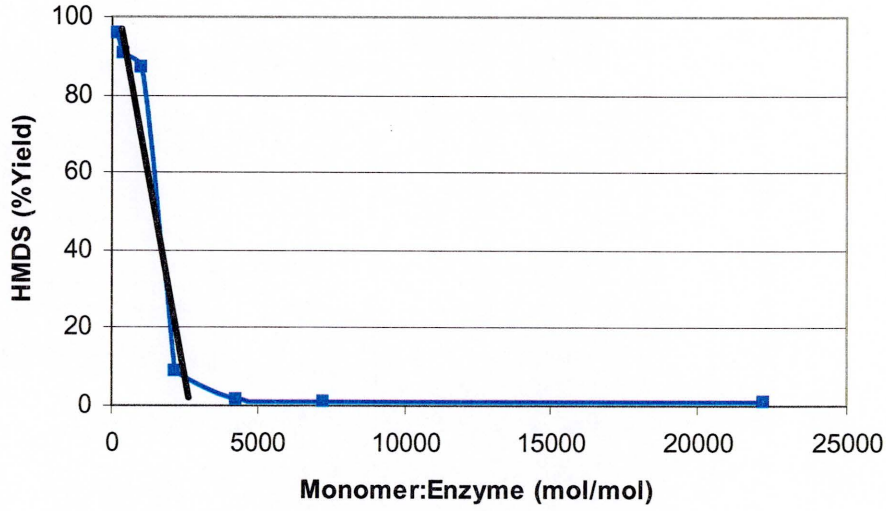

Figure 3.19: Study of the condensation of a saturated-solution of trimethylsilanol as a function of the amount of trypsin at 25°C.[1]

[1] Refer to Experimental section 7.2.2 and Table 7.18.

Based on the chromatographic results, the rate of reaction was determined to be dependent on the amount of trypsin. In addition, the interaction between these experimental variables was complicated due to the potential for autolysis at dilute concentrations of trypsin (i.e. < 20 mg/mL, Table 7.40). Given the decreased stability of dilute trypsin solutions (Figure 3.17), a 1000:1 monomer to enzyme mole ratio was formulated in a 40-mg/mL solution of trypsin throughout the condensation study.

Since the reactions were conducted with a constant concentration of trimethylsilanol, a simplified theoretical rate equation (Equation 3.8) was used to perform a preliminary assessment of the partial-order of reaction with respect to trypsin. If the partial-order of reaction with respect to trypsin was first-order ($\beta = 1$), the ratio of the rate of condensation (V) to the concentration of trypsin would be a constant value (Equation 3.9).

$$V = k_R'[\text{trypsin}]^{\beta},\ k_R' = k_R[Me_3SiOH]^{\alpha} \quad \textbf{(3.8)}$$

$$k_R' = V/[\text{trypsin}]^{1} \quad \textbf{(3.9)}$$

Since the condensation reactions were conducted for a fixed period of time (i.e. three hours), the amount of hexamethyldisiloxane (μmole) formed will be related to the rate of condensation (i.e. $V = [\text{HMDS}]_{3\ \text{hours}}$). A review of the chromatographic results (Table 3.3) showed that the calculated hexamethyldisiloxane to trypsin mole ratios were indeed approximately constant.

Table 3.3: First-order evaluation with respect to trypsin during the condensation of trimethylsilanol at 25°C.[1]

Trypsin[2]			HMDS[3]	HMDS[3]/Trypsin[2]
mg/mL	mg	μmol	μmol	(μmol/μmol)
198	99	4.2	451	106
20	10	0.4	42	98
2	1	0.04	4.7	109

1 Refer to Table 7.18.
2 Trypsin = TPCK treated trypsin.
3 HMDS = hexamethyldisiloxane.

In other words, the rate of condensation seemed to be directly proportional to the concentration of trypsin (theoretical black line, Figure 3.19 and Equation 3.10).

$$V = k_R[Me_3SiOH]^{\alpha}[trypsin]^1 \quad (3.10)$$

As observed in Table 3.3, reducing the amount of trypsin by a factor of ten decreased the product yield by a factor of ten. This experimental observation supports the role of trypsin as a catalyst in the condensation of trimethylsilanol in a neutral medium and that it proceeds via a simple enzyme-substrate intermediate.

3.5 Kinetic Study of the Trypsin-Catalysed Condensation of Non-Saturated Solutions of Trimethylsilanol

Since proteases only interact with water-soluble substrates [18], the concentration of trimethylsilanol was decreased (< 42.56 mg/mL [17]) to study the rate of condensation as a function of monomer concentration in a non-saturated medium. The amount of trimethylsilanol (~10-40 mg/mL, ~60-222 μmole) was adjusted to create homogeneous solutions in 40-mg/mL neutral (pH 7.0) solutions of trypsin. The reactions were conducted at 25°C and 15°C with magnetic stirring. After quenching the independent reactions, the reaction products were isolated and quantitatively analysed by GC every 15 minutes over one-hour periods (Tables 7.19-7.20). Based on the chromatographic data set acquired during the time studies, the integrated rate equations (Equations 3.5-3.6) were used in order to determine if the partial order of reaction with respect to trimethylsilanol was first- or second-order. However, after reviewing the correlation coefficients (R^2) of the first- and second-order plots at 25°C and 15°C, the order of reaction with respect to trimethylsilanol was not definitive as illustrated in Figures 3.20-3.21.

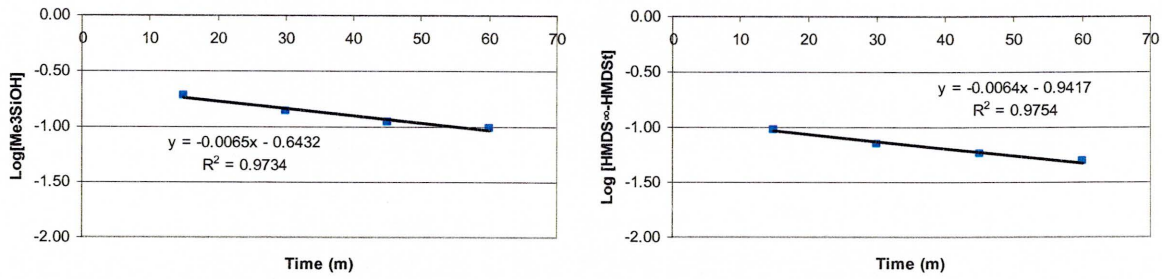

Figure 3.20: First-order evaluation of the condensation of a 20-mg/mL solution of trimethylsilanol at 25°C.[1]

[1] Refer to Table 7.19.

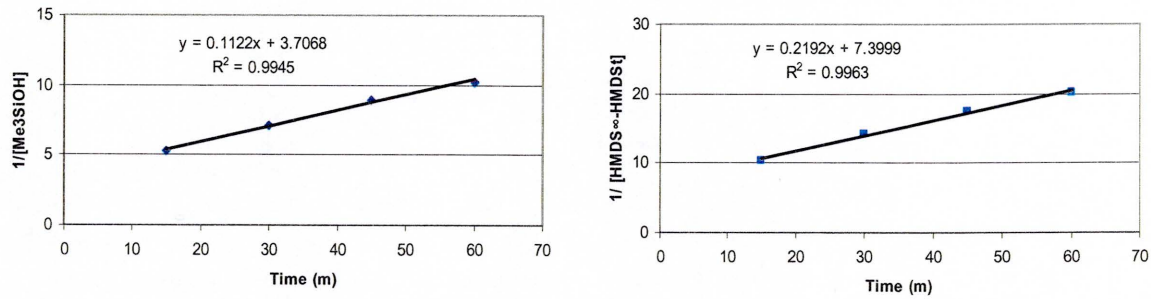

Figure 3.21: Second-order evaluation of the condensation of a 20-mg/mL solution of trimethylsilanol at 25°C.[1]

[1] Refer to Table 7.19.

Based on the extent of the non-saturated condensation reactions over one-hour periods (% yield, Tables 7.19-7.20), the initial data points were not plotted in the integrated rate equations as illustrated in Figures 3.20-3.21. Specifically, the initial rate of condensation was not measured. Given the necessity to independently conduct, quench, extract, isolate, and analyse the reactions at defined periods of time, the study of the kinetics of this model condensation reaction catalysed by trypsin was difficult. The calculated kinetic values obtained with this chromatographic data set (Tables 7.19-7.20) are estimates due to the repetitive errors of the study. Encompassing experimental and instrumental errors, the relative standard deviation of the measurements range between 0.3-10% depending on the concentration and, correspondingly, the yield of the analyte (Table 7.4).

Subsequently, a differential method was used to determine the partial order of reaction with respect to trimethylsilanol. The logarithm of the theoretical rate equation (Equation 3.3) was calculated to yield a linear equation (Equation 3.11) in which the slope (α) was equal to the partial order of reaction with respect to trimethylsilanol.

$$\text{Log}(V) = \alpha\text{Log}[Me_3SiOH] + \text{Log}(k_R') \qquad \textbf{(3.11)}$$

After plotting Log(V) vs. Log[Me_3SiOH] at 25°C ($\alpha = 0.9$, Figure 3.22) and 15°C ($\alpha = 1.0$, Figure 3.23), the partial order of reaction with respect to trimethylsilanol was estimated to be first-order.

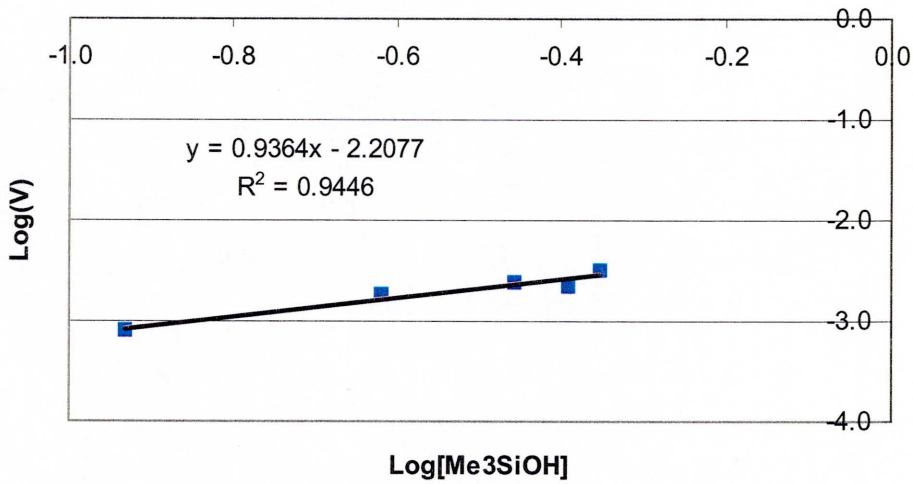

Figure 3.22: Differential rate equation plot with respect to trimethylsilanol during the trypsin-catalysed condensation reaction at 25°C.[1]

[1] Refer to Table 7.21.

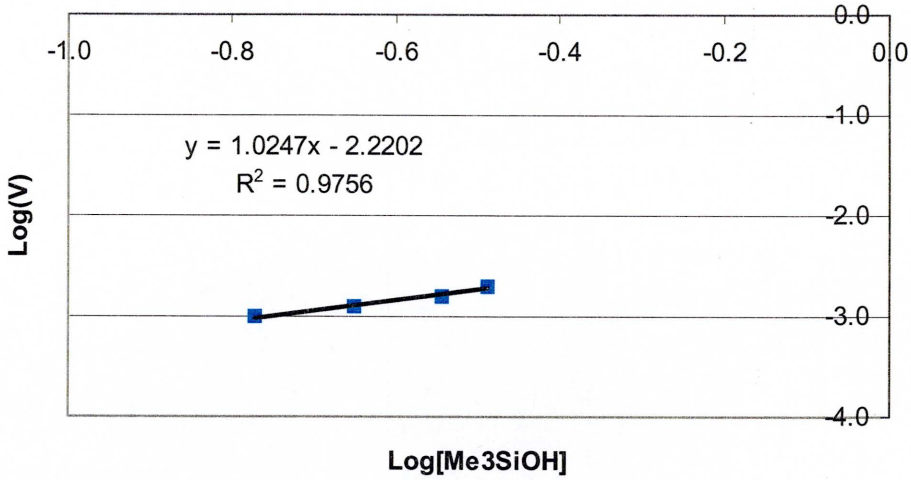

Figure 3.23: Differential rate equation plot with respect to trimethylsilanol during the trypsin-catalysed condensation reaction at 15°C.[1]

[1] Refer to Table 7.22.

The plots of the differential rate equations (Figures 3.22-3.23) with respect to trimethylsilanol were linear. The correlation coefficient (R^2) values were 94% and 98%, respectively. Since the rate of reaction was determined to be linearly dependent on the soluble amount of trimethylsilanol in the 40-mg/mL neutral (pH 7.0) solutions of trypsin, the reactions seem to be first-order with respect to trimethylsilanol. As hypothesised, the rate of condensation appears to be proportional to both the concentration of trimethylsilanol and trypsin (Equation 3.12).

$$V = k_R[Me_3SiOH]^1[trypsin]^1 \qquad \textbf{(3.12)}$$

Furthermore, the Lineweaver-Burk equation was used to study the ability of the trypsin-catalysed condensation of trimethylsilanol to fit the Michaelis-Menten kinetic model [12]. The Michaelis-Menten model is based on the hypothesis that enzymatic reactions proceed through an enzyme-substrate intermediate during catalysis (Scheme 3.4).

$$E + S \underset{k_2}{\overset{k_1}{\rightleftharpoons}} ES \xrightarrow{k_{cat}} E + P$$

Scheme 3.4: Michaelis-Menten model of an enzymatic reaction.[1]

[1] E = enzyme, S = substrate, ES = enzyme-substrate intermediate, P = product.

The Lineweaver-Burk equation (Equation 3.13) is the reciprocal of the Michaelis-Menten equation (Equation 3.14).

$$1/V = 1/V_{max} + (K_m/V_{max})*1/[S] \quad \textbf{(3.13)}$$

$$V = V_{max}*([S]/([S] + K_m)) \quad \textbf{(3.14)}$$

In Equations 3.13-3.14, V = the rate of catalysis, $V_{max} = k_{cat}*[E_t]$ = the maximum rate of catalysis, K_m = Michaelis constant = $(k_2 + k_{cat})/k_1$, and [S] = the concentration of the substrate. In review, the chromatographic data sets acquired during the time studies at 25°C and 15°C yielded linear Lineweaver-Burk plots (Figures 3.24-3.25).

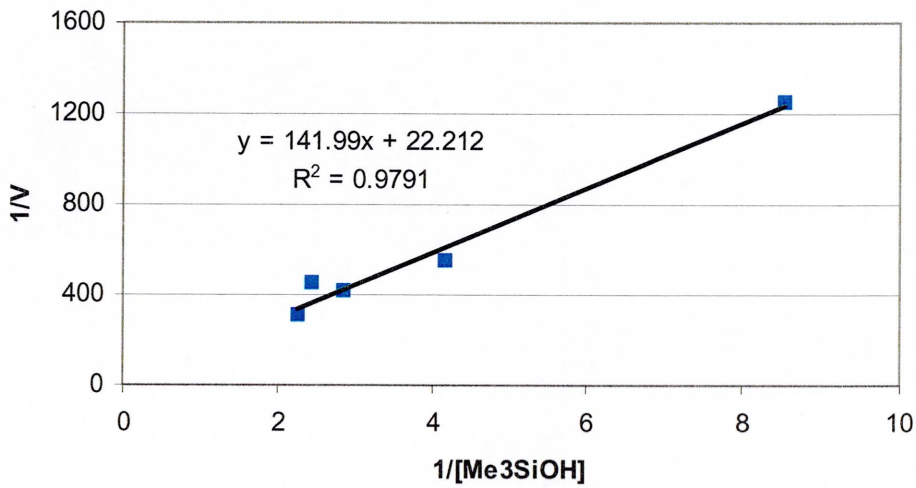

Figure 3.24: Lineweaver-Burk plot of the trypsin-catalysed condensation of trimethylsilanol at 25°C.[1]

[1] Refer to Table 7.21.

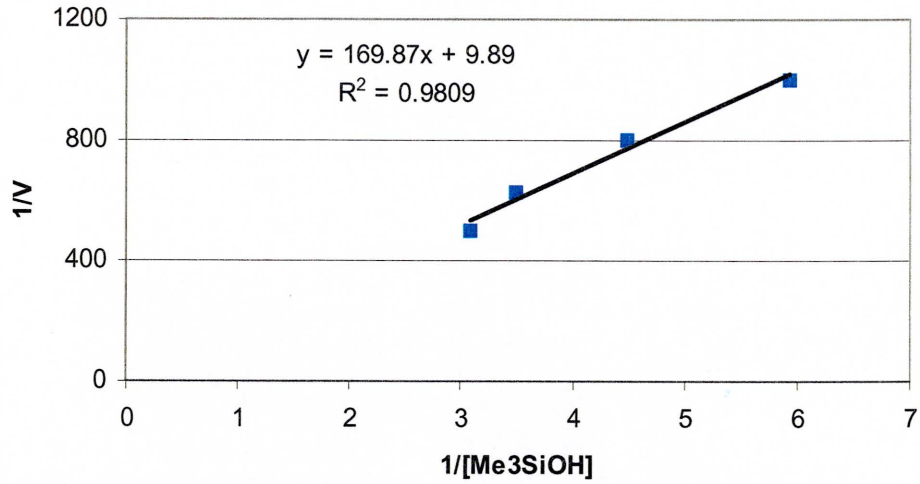

Figure 3.25: Lineweaver-Burk plot of the trypsin-catalysed condensation of trimethylsilanol at 15°C.[1]

[1] Refer to Table 7.22.

Based on the positive intercepts in the linear Lineweaver-Burk plots, the trypsin-catalysed condensation of trimethylsilanol appears to fit the Michaelis-Menten kinetic model. However, this assessment is not definitive. Due to solubility limitations in water, trypsin was not saturated with trimethylsilanol during the condensation reactions. This was evident due to the absence of a constant rate with respect to the concentration of trimethylsilanol in Figures 3.24-3.25. Given the repetitive errors of the study, this assessment was an estimate, which resulted in relative values. Based on the linear equations of the experimental Lineweaver-Burk plots, the relative Michaelis constant (K_m) and maximum rate (V_{max}) values were calculated (Table 3.4).

Table 3.4: Relative Michaelis-Menten kinetic values during the trypsin-catalysed condensation of trimethylsilanol.[1]

Reaction Temperature	K_m (μM)	V_{max} (Mm^{-1})
25°C	6,000,000	0.05
15°C	17,000,000	0.10

[1] Refer to Tables 7.21-7.22.

Although the Michaelis-Menten kinetic values are relative, the large K_m values indicate that the binding strength of the enzyme-substrate intermediate is weak. Comparatively, these K_m values are several orders of magnitude (i.e. ~1,000-25,000,000) larger than the K_m values of other enzymes (Table 3.5) [12]. For example, the relative K_m value of the trypsin-catalysed condensation of trimethylsilanol at 25°C was approximately 1200 times larger than the chymotrypsin-catalysed hydrolysis of acetyl-L-tryptophanamide.

Table 3.5: Enzymatic K_m values [12].

Enzyme	Substrate	K_m (μM)
chymotrypsin	acetyl-L-tryptophanamide	5000
lysozyme	hexa-N-acetylglucosamine	6
β-galactosidase	lactose	4000
threonine deaminase	threonine	5000
carbonic anhydrase	CO_2	8000
penicillinase	benzylpenicillin	50
pyruvate carboxylase	pyruvate	400
	HCO_3^-	1000
	ATP	60
arginine-tRNA synthetase	arginine	3
	tRNA	0.4
	ATP	300

Since the relative K_m values are large and the V_{max} values are slow, the formation of the trypsin-silanol intermediate appears to be the rate-limiting step in the condensation reaction. This is consistent with the fact that trypsin was not saturated with trimethylsilanol in aqueous media. Therefore, the rate of condensation or hydrolysis of the trypsin-silanol intermediate must be faster than the formation of the enzymatic intermediate.

Finally, the effect of temperature on the rate of the trypsin-catalysed condensation reaction was studied. Although trypsin was observed to be catalytically active over a broad temperature range (Figure 3.9), the optimum temperature of the silanol condensation reaction was approximately 25°C. Based on the results in the differential thermogram of trypsin (Figure 3.12), it appears that trypsin was irreversibly denatured at approximately 40°C. Given the thermal stability and, corresponding, activity of trypsin in neutral media, the rates of the condensation of non-saturated solutions of trimethylsilanol (~30 mg/mL, ~175 μmole) were studied between 6-25°C. Prior to reaction, 40-mg/mL buffered aqueous solutions (pH 7.0) of trypsin were stirred and equilibrated at set temperatures in a thermostated water bath (+/- 0.1°C) for 20 minutes. After quenching the independent reactions, the reaction products were isolated and quantitatively analysed by GC every 15 minutes over one-hour periods (Table 7.23). Subsequently, the natural logarithm of the Arrhenius equation (Equation 3.15) was solved (Equation 3.16) and plotted (Figure 3.25) in order to study the rate of condensation with respect to temperature.

$$k_R = A * e^{(-Ea/RT)} \quad \textbf{(3.15)}$$

$$\ln(k_R) = \ln(A) - E_a/RT \quad \textbf{(3.16)}$$

In Equations 3.15-3.16, k_R = the rate constant, A = Arrhenius A-factor, E_a = the activation energy, R = gas constant, and T = temperature (Kelvin).

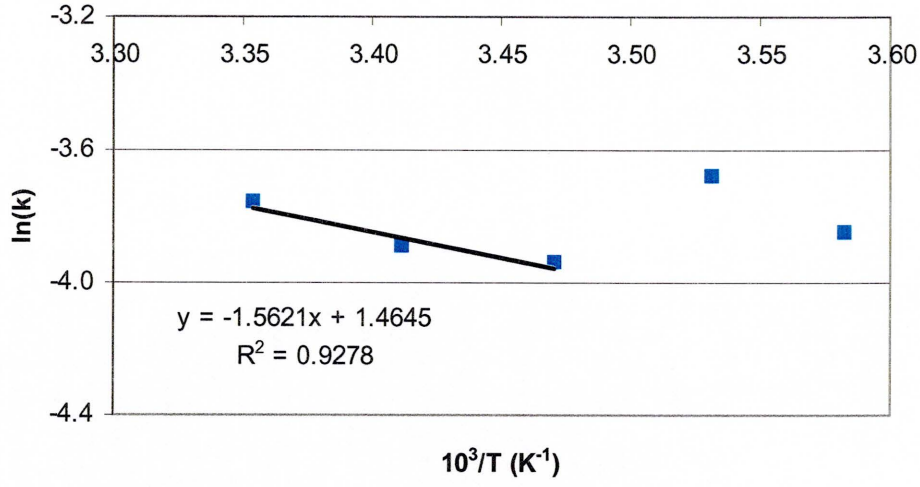

Figure 3.25: Logarithmic Arrhenius plot of the trypsin-catalysed condensation of trimethylsilanol.[1]

[1] Refer to Table 7.24.

The effect of temperature on the rate of the trypsin-catalysed condensation reaction was not definitive due to the scattered data in the logarithmic Arrhenius plot. Given the decreased thermal stability and, corresponding, activity of trypsin at elevated temperatures, the temperature range (~20°C) of the study was quite narrow. Despite these limitations, estimated Arrhenius parameters (i.e. E_a, A) were calculated with the relative trendline (black line, Figure 3.25). Based on the trendline of the select data points, the estimated activation energy (E_a) was approximately 13 kJ/mol and the A-factor was approximately 4 s^{-1}. In review, the effect of temperature on the rate of the trypsin-catalysed condensation of non-saturated solutions of trimethylsilanol was inconclusive.

Based on the stoichiometry of the silanol condensation reaction (Scheme 3.1) and the rate of condensation (Equation 3.12), the trypsin-catalysed condensation of trimethylsilanol was hypothesised to have a reaction mechanism (Scheme 3.5) similar to the proteolytic hydrolysis [1] of amide and ester bonds (Scheme 2.7). Activated and stabilized by the charge-relay system of the catalytic triad [12, 21], the nucleophilic

oxygen atom of serine was postulated to attack the electropositive silicon atom [22] of trimethylsilanol. Equivalent to the acyl-enzyme complex, a silylated trypsin intermediate would form, followed by the loss of water. In addition, the nitrogen atom of the histidine could form a stabilized pentacoordinate species [23, 24] with the silicon atom in the intermediate. Based on the rate equation (Equation 3.12) as well as the large relative K_m and slow V_{max} values, the formation of the trypsin-silanol intermediate appears to be the rate-limiting step. This is consistent with the fact that organosilicon molecules are larger than analogous hydrocarbon tryptic substrates. Although silicon and carbon are group IV elements, the elements are different as highlighted in Table 3.6.

Table 3.6: Silicon and carbon properties [25-27].

Properties	Silicon (Si)	Carbon (C)
atomic weight	28.086	12.011
electronic structure	$[Ne]3s^2 3p^2$	$[He]2s^2 2p^2$
melting point	1410°C	3652°C (sublimes)
electronegativity	1.74	2.50
atomic radius	1.06 angstrom	0.66 angstrom
atom volume	12.1 cm^3/mole	5.3 cm^3/mole
Si-C vs. C-C bond length	1.87 angstrom	1.53 angstrom
Si-O-Si vs. C-O-C bond angle	144.1°	111.5°

Subsequently, the silylated trypsin intermediate may participate in either a condensation or hydrolysis reaction with trimethylsilanol or water leading to the formation of the hexamethyldisiloxane (product) or trimethylsilanol (reactant), respectively. Since trypsin was not saturated with trimethylsilanol in aqueous media, the rate of condensation or hydrolysis of the trypsin-silanol intermediate must be faster than the formation of the enzymatic intermediate. Regardless, trypsin would be recovered at the completion of either reaction.

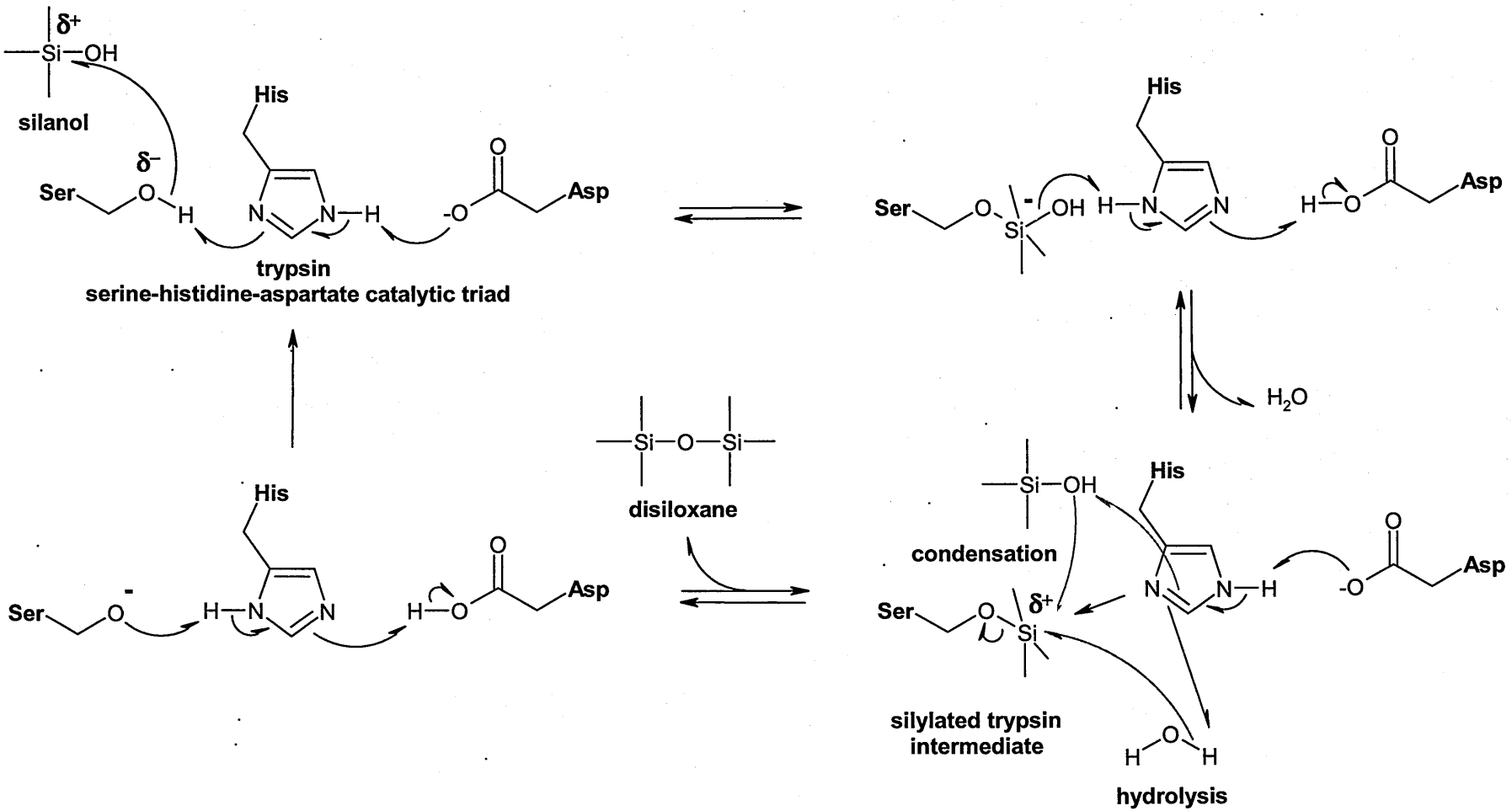

Scheme 3.5: Proposed reaction mechanism of trypsin-catalysed condensation of trimethylsilanol.

3.6 Trypsin pH Study

In nature, the optimum pH for trypsin-catalysed hydrolysis is approximately 8. However, this is species dependent [1]. As measured with a natural substrate (BAEE) [10], the activities of different sources of trypsin were studied as a function of pH (Figure 3.26).

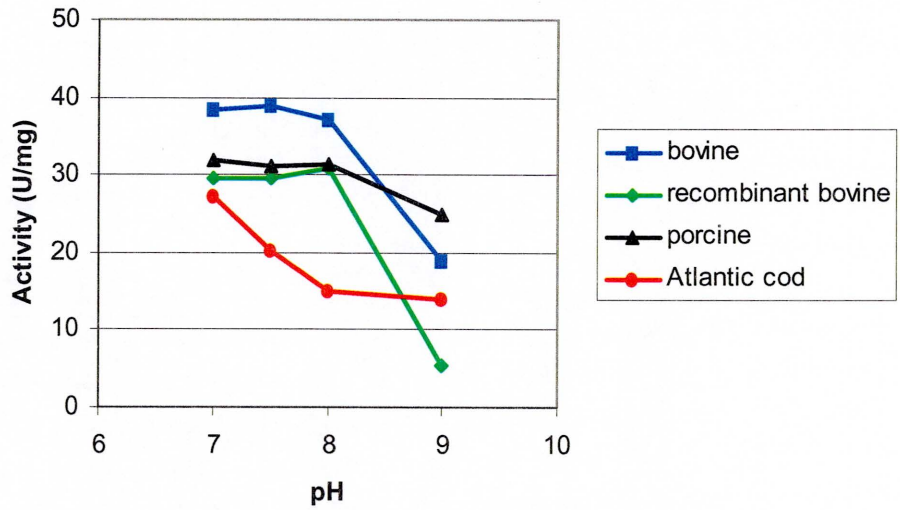

Figure 3.26: pH study of the activity of different tryptic species.
[1] Refer to Experimental section 7.3.7 and Table 7.43.

Based on the spectrophotometric data, the profiles of the mammalian tryptic activities including the recombinant enzyme as a function of pH were similar. The mammalian source of bovine trypsin was observed to have the highest activity at pH 7.0. In comparison, the optimum pH of *Gadus morhua* (i.e. Atlantic cod) trypsin appeared to be more acidic. Since calcium was required to achieve the maximum activity and stability of trypsin [1], the differences in the relative activities may be due to variable levels of calcium.

Based on an inductively coupled plasma-atomic emission spectroscopic analysis, the amount of calcium present in the commercial sources of trypsin was shown to be very different (Table 3.7).

Table 3.7: Elemental analysis of calcium in different sources of trypsin.[1]

Trypsin	Calcium (ppm)
porcine pancreas	< detection limit[2]
recombinant bovine	109
bovine pancreas	886
Atlantic cod	21343

[1] Inductively Coupled Plasma-Atomic Emission Spectroscopic (ICP-AES) analysis. Refer to Experimental section 7.3.4.

[2] detection limit = 50 ppm.

Calcium activation of trypsin induces changes in the tertiary structure of the enzyme [28]. Specifically, calcium creates a compact structure due to increased helical content or an altered β-structure. The conformational changes have been hypothesised to be responsible for the documented [28] increased enzymatic activity and thermal stability. Since the activity of trypsin is optimal in the presence of > 10 mM (ideally, 20 mM or 400 ppm) calcium [28], the decreased levels of calcium in porcine pancreas and recombinant bovine trypsin correlate with their activities in comparison with bovine pancreatic trypsin.

Subsequently, the ability of bovine pancreatic trypsin to catalyse the trimethylsilanol condensation reaction was studied as a function of pH. The reactions were formulated with a 4:1 monomer to enzyme weight ratio (~1000:1 silanol to trypsin mole ratio) in aqueous media buffered from pH 4.0 to pH 10.0 and conducted at 25°C for three hours. The reaction products were isolated and quantitatively analysed by GC (Figure 3.27).

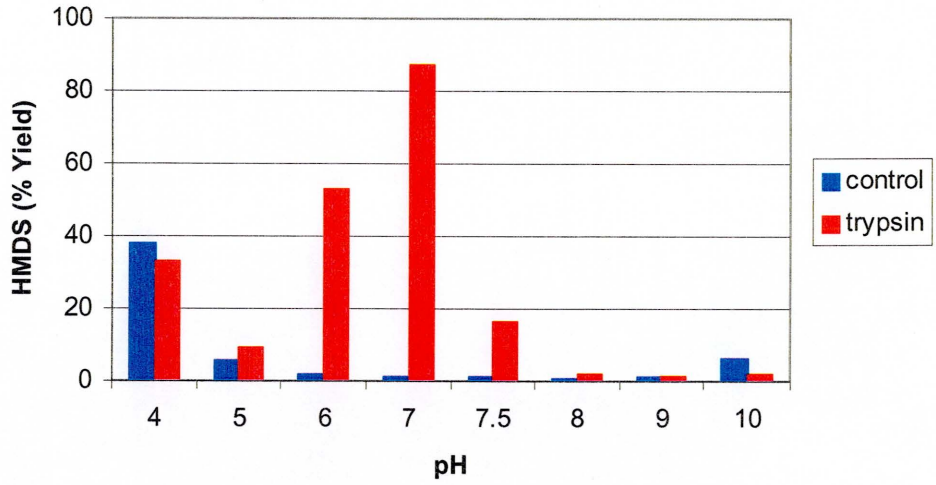

Figure 3.27: The effect of pH on the trypsin-catalysed condensation of trimethylsilanol at 25°C.

[1] Refer to Experimental section 7.2.2 and Table 7.25.

Based on the chromatographic data, the enzyme-catalysed condensation reaction was dependent on the pH. The silanol condensation reaction was optimum at pH 7.0. Comparatively, acid- and base-catalysed [29] silanol condensation (Scheme 2.2) was observed in the negative control reactions; primarily, at pH values less than 4 and greater than 10 (Figure 3.27). Given the natural hydrolytic activity profiles measured with BAEE (Figure 3.26), which show activity above pH 7, the decreased yields at pH values > 7.0 were further investigated.

As measured by the rate of hydrolysis of BAEE, the activities of bovine pancreatic trypsin were analysed at the beginning (t = 5 minutes) and end (t = 3 hours) of condensation reactions conducted with trimethylsilanol in aqueous media buffered from pH 7.0 to pH 9.0. The spectrophotometric activity data is illustrated in Figure 3.28.

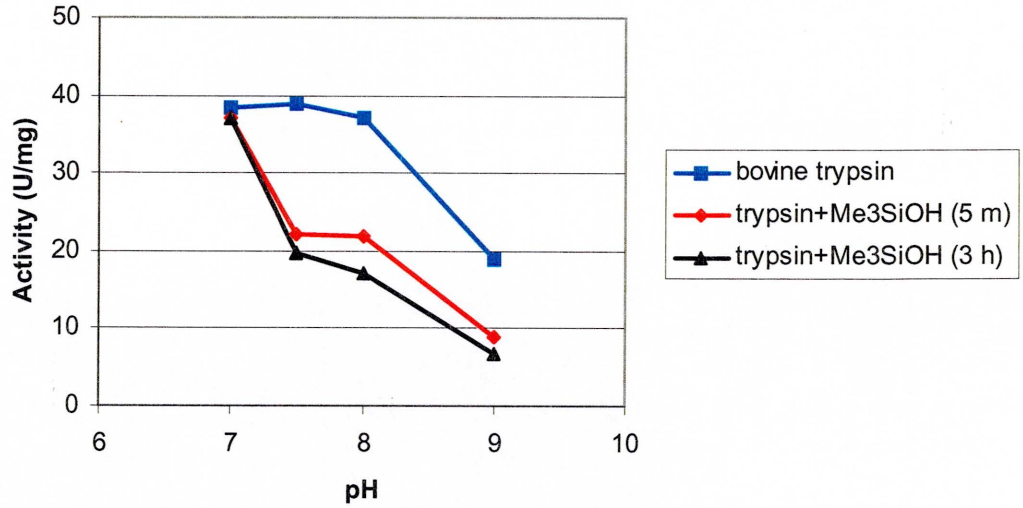

Figure 3.28: The effect of trimethylsilanol and pH on trypsin activity.[1]

[1] Refer to Experimental section 7.3.7 and Table 7.44.

In comparison to the natural pH activity profile (bovine trypsin, Figure 3.28), trimethylsilanol partially inhibited (> 50%) trypsin nearly immediately in basic buffered water (pH 7.5 to pH 9.0). Although trimethylsilanol did not inhibit trypsin in a neutral medium (pH 7.0), reactant inhibition increased by 50-65% with the basicity of the aqueous solution. Since trypsin was not denatured in the presence of trimethylsilanol, the inhibition of the hydrolysis (BAEE, Figure 3.28) and condensation (trimethylsilanol, Figure 3.27) reactions in basic media was hypothesised to be due to the silylation of other hydroxy-functional residues in the catalytic region. This would directly or indirectly reduce access to the active site and the activity of trypsin. As the pH decreases, these species would be prone to hydrolysis (acid catalysis), which would enable the active site to participate in the catalytic function of trypsin. Conversely, at high pH values, the longer lifetime of the silylated enzyme would inhibit both the hydrolysis of BAEE and the condensation of trimethylsilanol. Comparatively, a trimethylsilyl-functional steroid was documented to silylate and irreversibly inhibit cytochrome P-450_{scc} in the biosynthesis of hormones (Scheme 3.6) [30].

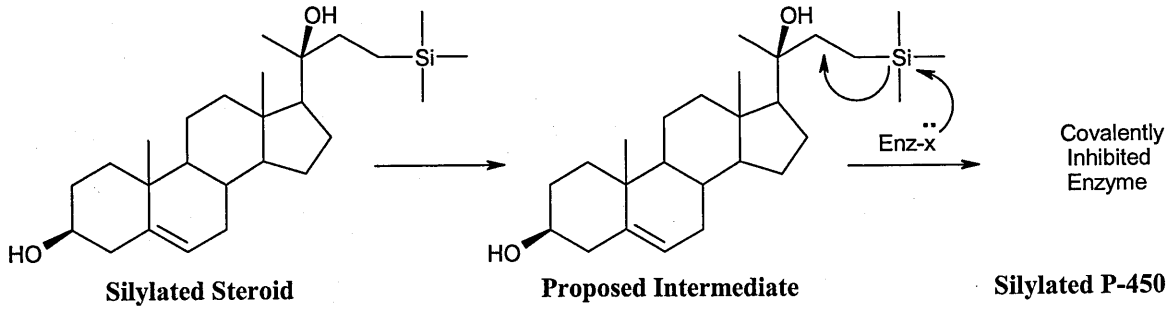

Scheme 3.6: Proposed inhibition of cytochrome P-450_{scc}.

These results further support the role of the active site of trypsin as a catalyst in the *in vitro* condensation of trimethylsilanol.

3.7 Summary

Bos taurus or bovine pancreatic trypsin (i.e. a serine-protease) was chosen to investigate the role of the enzymatic active site in the condensation of trimethylsilanol under mild conditions. Trypsin was inhibited with two distinctly different natural polypeptide inhibitors from soybean: Bowman-Birk (BBI) [5] and Popcorn (PCI) [6, 7] inhibitors. The proteinaceous inhibitors completely inhibited the trypsin-catalysed condensation reactions. Although trypsin appeared to be catalytically active over a broad temperature range, the rates of the trypsin-catalysed condensation reactions decreased due to the degree of thermal denaturation. Based on a standard enzymatic activity assay [10], the relative decrease in the rate of silanol condensation correlated with the enhanced stability of trypsin at higher protein concentrations. Consequently, it appears that the tertiary structure, functionality of the active site, and catalytic triad of trypsin are directly involved in the *in vitro* condensation of trimethylsilanol.

Furthermore, the trypsin-catalysed condensation of trimethylsilanol was nearly complete after three hours at 25°C. Based on a hydrolysis study with hexamethyldisiloxane, trypsin was not observed to catalyse the hydrolysis of a siloxane

bond in a neutral medium or organic solvent. Reactant and product inhibition were not observed in a neutral medium. Given the ability to self-associate, the autolysis of trypsin was insignificant at higher protein concentrations. This observation complements the enhanced thermal stability of trypsin at increased concentrations. Further verification came from the determination that trypsin could be recycled to catalyse a replicate three-hour condensation reaction with trimethylsilanol. The rate of condensation appears to be proportional to both the concentration of trimethylsilanol and trypsin. Although not definitive, the trypsin-catalysed condensation of non-saturated solutions of trimethylsilanol was estimated to fit the Michaelis-Menten kinetic model. In comparison to the maximum turnover numbers of other enzymes with their physiological substrates, the turnover number of the trypsin-catalysed condensation of trimethylsilanol was several orders of magnitude (i.e. 10-10,000,000) slower than the cited values. Based on the rate equation as well as the large relative K_m and slow V_{max} values, the formation of the trypsin-silanol intermediate appears to be the rate-limiting step. This is consistent with the fact that organosilicon molecules are larger than analogous hydrocarbon tryptic substrates. Since trypsin was not saturated with trimethylsilanol in aqueous media, the rate of condensation or hydrolysis of the trypsin-silanol intermediate must be faster than the formation of the enzymatic intermediate. Given this information, the trypsin-catalysed condensation of trimethylsilanol was hypothesised to have a reaction mechanism similar to the proteolytic hydrolysis of amide and ester bonds.

The trypsin-catalysed condensation reaction was also dependent on pH. The silanol condensation reaction was optimum at pH 7.0. Comparatively, acid- and base-catalysed [29] silanol condensation was observed in the negative control reactions. In comparison to the pH activity profile, trimethylsilanol partially inhibited trypsin (>50%) almost immediately in basic buffered water (pH 7.5 to pH 9.0). Although trimethylsilanol

did not inhibit trypsin in a neutral medium (pH 7.0), reactant inhibition increased by 50-65% with the basicity of the aqueous solution. Since trypsin was not denatured in the presence of trimethylsilanol, the inhibition of the hydrolysis (BAEE) and condensation (trimethylsilanol) reactions in basic media was hypothesised to be due to the silylation of other hydroxy-functional residues in the catalytic region. This would directly or indirectly reduce access to the active site and the activity of trypsin. As the pH decreases, these species would be prone to hydrolysis (acid catalysis), which would enable the active site to participate in the catalytic function of trypsin. Conversely, at high pH values, the longer lifetime of the silylated enzyme would inhibit both the hydrolysis of BAEE and the condensation of trimethylsilanol. These results further support the role of the active site of trypsin as a catalyst in the *in vitro* condensation of trimethylsilanol.

3.8 References

1. A. J. Barrett, N. D. Rawlings, and J. F. Woessner, (eds.), "*Handbook of proteolytic enzymes*." Academic Press, San Diego, 1998.

2. B. Keil, *in* "*Hydrolysis: Peptide bonds*," (eds. P. D. Boyer), Vol. 3, Academic Press, New York, 1971.

3. W. Bode, H. Fehlhammer, and R. Huber, *J. Mol. Biol.*, **111**, 415, (1977).

4. ExPASy Peptide Mass, Swiss Institute of Bioinformatics, http://us.expasy.org/cgi-bin/peptide-mass.pl, 2003.

5. Y. Birk, *Int. J. Peptide Protein Res.*, **25**, 113, (1985).

6. B. Kassell, *in* "*Proteolytic enzymes*,", Vol. 19, Academic Press, New York, 1970.

7. Y. Birk, *in* "*Proteolytic enzymes*,", Vol. 45, Academic Press, New York, 1976.

8. M. H. Werner and D. E. Wemmer, *Biochemistry*, **31**, 999, (1992).

9. H. K. Song and S. W. Suh, *J. Mol. Biol.*, **275**, 347, (1998).

10. G. W. Schwert and Y. Takenaka, *Biochimica et Biophysica Acta*, **16**, 570, (1955).

11. J. Koepke, U. Ermler, E. Warkentin, G. Wenzl, and P. Flecker, *J. Mol. Biol.*, **298**, 477, (2000).

12. L. Stryer, *in* "*Biochemistry*," W. H. Freeman and Company, New York, (1988).

13. R. A. Gross and H. N. Cheng, (eds.), "*Biocatalysis in polymer science*." American Chemical Society, Washington, D.C., 2003.

14. A. M. Klibanov, *Chemtech*, 354, (1986).

15. T. J. Ahern and A. M. Klibanov, *Science*, **228**, 1280, (1985).

16. M. L. Simon, K. Laszlo, M. Kotorman, and B. Szajani, *Acta Biologica Szegediensis*, **45(1-4)**, 43, (2001).

17. EPI Suite Software version 3.11, Environmental Protection Agency, http://www.epa.gov/opptintr/exposure/docs/episuite.htm, 2000.

18. U. T. Bornscheuer and R. J. Kazlauskas, *in* "*Hydrolases in organic synthesis*," Wiley-VCH, Weinheim, (1999).

19. B. G. Segal, *in* "*Chemistry experiment and theory*," John Wiley & Sons, New York, (1985).

20. M. Mortimer and P. G. Taylor, (eds.), "*Chemical kinetics and mechanism*." Royal Society of Chemistry, Cambridge, 2002.

21. G. Dodson and A. Wlodawer, *TIBS*, 347, (1998).

22. C. Eaborn, "*Organosilicon compounds*," Butterworths Scientific Publications, London, (1960).

23. A. R. Bassindale, S. J. Glynn, and P. G. Taylor, *in* "*The chemistry of organic silicon compounds*," (eds. Z. Rappoport and Y. Apeloig), John Wiley & Sons Ltd., Chichester, 1998.

24. A. R. Bassindale and P. G. Taylor, *in* "*The chemistry of organic silicon compounds*," (eds. S. Patai and Z. Rappoport), John Wiley & Sons, Chichester, 1989.

25. R. C. Weast, (ed.), "*CRC handbook of chemistry and physics*." CRC Press, Boca Raton, 1988.

26. M. A. Brook, "*Silicon in organic, organometallic, and polymer chemistry*," John Wiley & Sons, New York, (2000).

27. J. Y. Corey, *in* "*The chemistry of organic silicon compounds*," (eds. S. Patai and Z. Rappoport), John Wiley & Sons, Chichester, 1989.

28. T. Sipos and J. R. Merkel, *Biochemistry*, **9(14)**, 2766, (1970).

29. R. K. Iler, "*The chemistry of silica: Solubility, polymerization, colloid and surface properties, and biochemistry*," John Wiley & Sons, New York, (1979).

30. A. Nagahisa and W. H. Orme-Johnson, *J. Am. Chem. Soc.*, **106**, 1166, (1984).

Chapter Four

Trypsin-Catalysed Hydrolysis and Condensation of Alkoxysilanes

4.0 Introduction

The study of the hydrolysis and condensation reactions during biosilification is complicated due to the use of silicic acid analogues. Previously, silicatein was determined [1, 2] to catalyse the polycondensation of tetraethoxysilane during the formation of particulate silica (Figure 4.1).

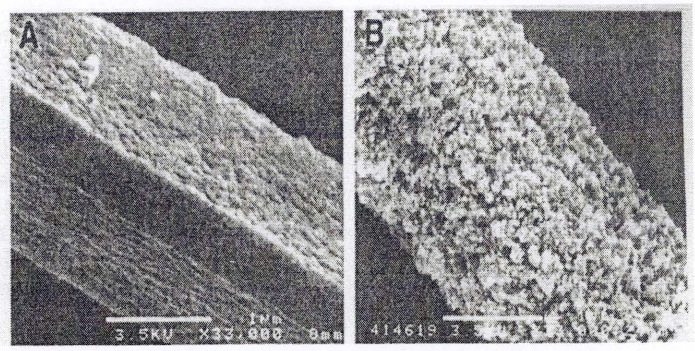

(A) (B)

Figure 4.1: Scanning electron micrographs of a silicatein filament before (A) and after (B) reaction with tetraethoxysilane (bars are 1 μm) [1].

Despite fractional yields (< 0.005%) and insignificant conversions (Chapter 2.1), the study focused on the analysis of the solid polycondensation products as opposed to a complete mass balance. Given the limitations of the product and the resultant analysis, the study was not able to differentiate between the role of silicatein in the hydrolysis and condensation reactions during biosilicification. Regardless, a general acid/base reaction mechanism was proposed to catalyse the hydrolysis reaction or "rate-limiting step [1]" during polycondensation (Scheme 1.2). Specifically, the nucleophilic oxygen atom of serine was hypothesised to attack the alkoxy-functional silane, while the unprotonated histidine nitrogen atom coordinated with the hydroxy hydrogen atom. Subsequently, the release of an alcohol and the formation of a histidine-stabilised pentacoordinate silylether-enzyme were proposed to create a reactive intermediate. In the presence of water, the process was repeated to form a silanol and recover the enzyme. Finally, the silanol

molecule was condensed with an alkoxy-functional silicone to form a siloxane bond and an alcohol. Complete hydrolysis and condensation of the multi-functional alkoxysilane resulted in the formation of biosilica. However, it should be noted that tetraalkoxysilanes are easily hydrolysed and silanols are condensed during the formation of particulate silica due to their enhanced sensitivity to pH, concentration, and temperature [3].

Consequently, model substrates were chosen to investigate the ability of trypsin to selectively catalyse the *in vitro* hydrolysis and condensation of organo-functional alkoxysilanes under mild conditions (Scheme 4.1).

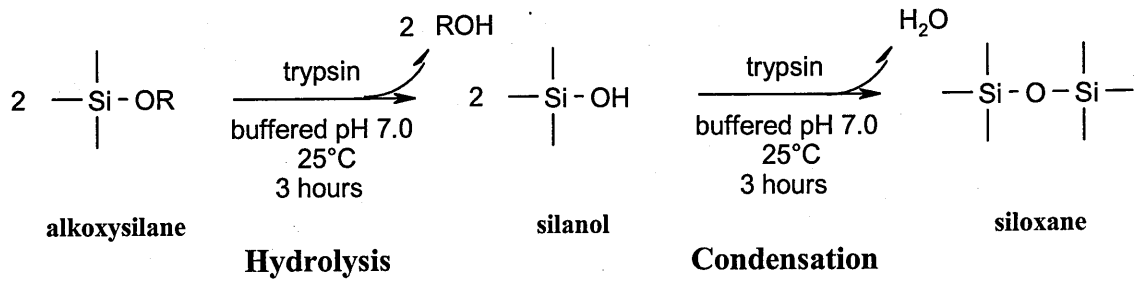

Scheme 4.1: Trypsin-catalysed hydrolysis and condensation of alkoxysilanes.

4.1 Trypsin-Catalysed Hydrolysis and Condensation of Trimethylethoxysilane

The role of trypsin in the formation of molecules with a single siloxane bond was studied during the *in vitro* hydrolysis and condensation of a model alkoxysilane, trimethylethoxysilane. Prior to reaction, the alkoxysilane was pre-treated with sodium hydrogencarbonate due to the potential presence of residual chloro-functional silanes (Experimental section 7.2.3). Alkoxysilanes are typically synthesised from chlorosilanes [4]. Since hydrochloric acid will catalyse the reactions of interest [4], the treatment was performed to prevent the formation of hydrochloric acid due to the rapid hydrolysis of inadvertent chlorosilane contaminates in an aqueous system. The reactions were formulated with a 4:1 trimethylethoxysilane to protein weight ratio (~1000:1 alkoxysilane

to trypsin mole ratio) in neutral media (pH 7.0) and conducted at 25°C for three hours. Based on the estimated solubility of trimethylethoxysilane in water (1 mg/mL) [5], the concentration of trimethylethoxysilane (~160 mg/mL) saturated the aqueous media and created two-phase reaction mixtures. The reaction products were isolated and quantitatively analysed by GC (Figure 4.2).

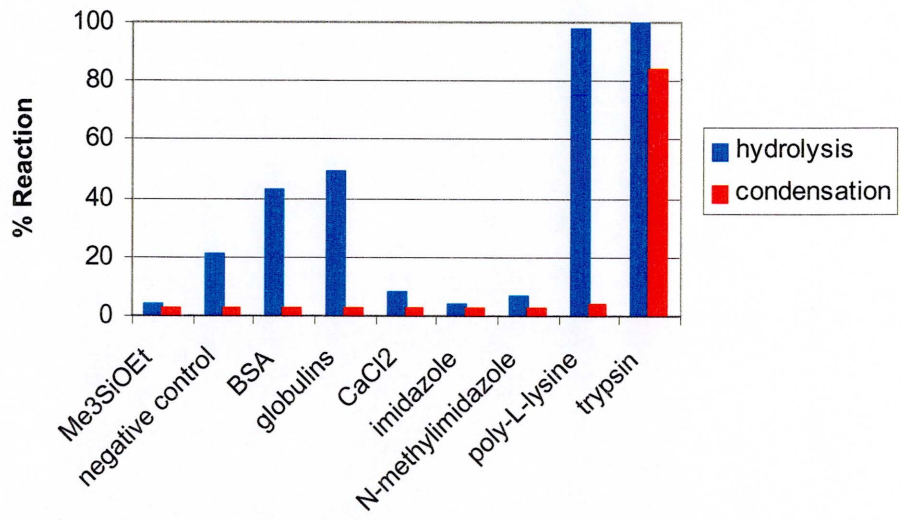

Figure 4.2: Hydrolysis and condensation control reactions of trimethylethoxysilane after three hours at 25°C.[1]

[1] Refer to Experimental section 7.2.3 and Table 7.26.

Although various rates of hydrolysis were observed, substantial condensation of trimethylethoxysilane was not observed in the negative control, non-specific protein (i.e. BSA, γ-globulins), small molecule (i.e. $CaCl_2$, imidazole, N-methylimidazole), and polypeptide (i.e. poly-L-lysine) reactions in comparison to the raw material. Although BSA (Chapter 2.1) [1] and poly-L-lysine (Table 1.1) [6] were not observed to catalyse the condensation of tetraethoxysilane or trimethylethoxysilane (Figure 4.2), BSA and poly-L-lysine promoted the hydrolysis of trimethylethoxysilane and formation of trimethylsilanol at different rates in a neutral medium (pH 7.0). In review, the trimethylsilanol (Figure

2.12) and trimethylethoxysilane (Figure 4.2) control reactions were comparable and highlighted the definitive scope of the model systems.

In the presence of trypsin, trimethylethoxysilane was hydrolysed (100%) and condensed (84%) during the formation of hexamethyldisiloxane in a neutral medium (pH 7.0) at 25°C over three hours (Figure 4.2). Since the relative rate of condensation decreased at temperatures < 25°C (Figure 3.9), a time study of the trimethylethoxysilane reaction was conducted at 10°C for defined periods of time over three hours. The reaction products were isolated and quantitatively analysed by GC (Figure 4.3).

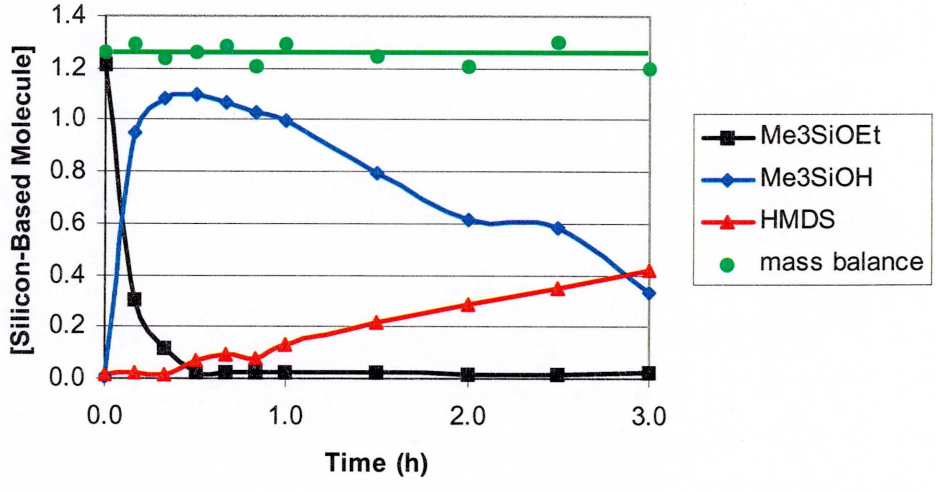

Figure 4.3: Trypsin-catalysed hydrolysis and condensation of trimethylethoxysilane at 10°C.[1]

[1] Refer to Experimental section 7.2.3 and Table 7.27.

Based on the stoichiometry of the hydrolysis and condensation reactions (Scheme 4.1), two moles of trimethylethoxysilane were consumed in the formation of two moles of trimethylsilanol, which produced one mole of hexamethyldisiloxane (mass balance, Figure 4.3). The chromatographic data set acquired during the time study was analysed in order

to study the kinetics of the hydrolysis and condensation reactions catalysed by trypsin at 10°C.

Comparatively, trimethylethoxysilane was readily hydrolysed within the initial 30 minutes and, subsequently, condensed during the formation of hexamethyldisiloxane. The partial orders of the reactions with respect to reactants as well as the turnover numbers (k_{cat}) in the hydrolysis and condensation reactions were calculated. As derived in Equations 3.4-3.6, the concentrations of the reactants were plotted versus time in order to experimentally assess the partial order of reaction with respect to trimethylethoxysilane (hydrolysis) and trimethylsilanol (condensation).

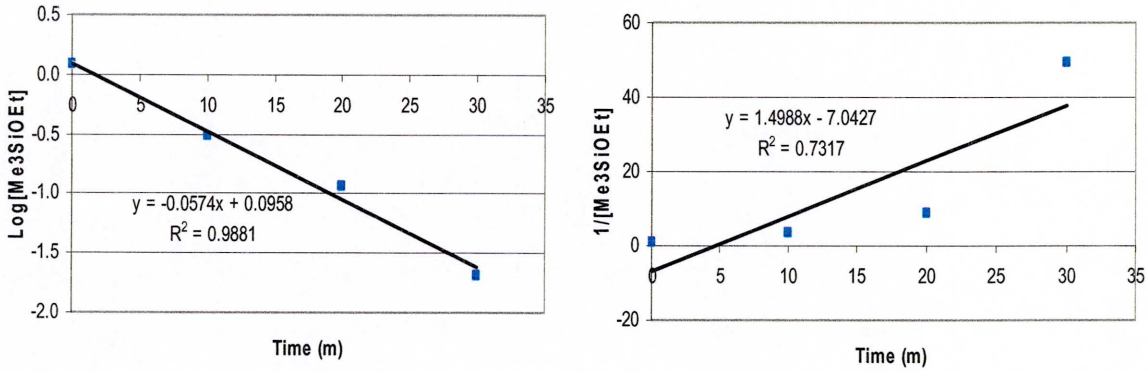

(A) **(B)**

Figure 4.4: First- (A) and second- (B) order evaluation of the hydrolysis of trimethylethoxysilane at 10°C.[1]

[1] Refer to Table 7.27.

After reviewing the correlation coefficients (R^2) of the first- and second-order plots for hydrolysis (Figure 4.4), the order of reaction with respect to trimethylethoxysilane appears to be first-order. Therefore, the rate of hydrolysis would be directly proportional to the concentration of trimethylethoxysilane (Equation 4.1).

$$V = k_R[Me_3SiOEt]^1[trypsin]^{\beta} \quad \textbf{(4.1)}$$

Since most enzymatic reactions are directly proportional to the concentration of enzyme ($\beta = 1$, Equation 4.1) with the exception of those that exhibit allostery (e.g. hemoglobin) [7], the rate equation (Equation 4.1) was hypothesized to be proportional to both the concentration of trimethylethoxysilane and trypsin. Based on the concentration of trypsin (i.e. $[E_t]$ = [trypsin] = 1.7 mM) and the initial rate of hydrolysis (i.e. $V_o = -\delta[Me_3SiOEt]/\delta t = 0.0549$ M/m ~ $\delta[Me_3SiOH]/\delta t = 0.0536$ M/m, Figure 4.5), a relative value of the turnover number (k_{cat}) was calculated to be 31.6 m^{-1} or 0.53 s^{-1} at 10°C (Equation 3.7).

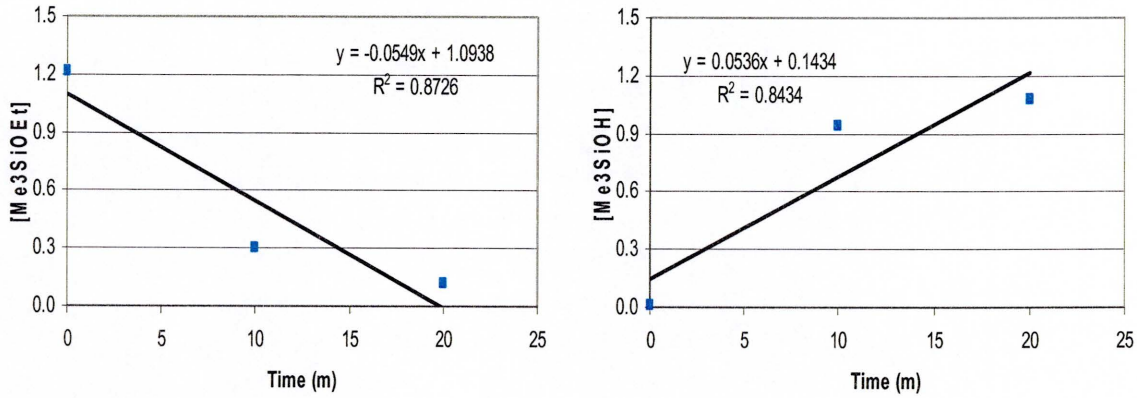

Figure 4.5: The rate of the trypsin-catalysed hydrolysis of trimethylethoxysilane at 10°C.[1]

[1] Refer to Table 7.27.

Since trypsin may not be saturated due to the limited solubility of trimethylethoxysilane in water, the turnover number was treated as a relative value. Given a relative turnover number equal to 0.53 s^{-1}, the time between each hydrolysis reaction catalysed by trypsin was calculated to be approximately 2 s or 30 reactions per minute at 10°C. Although this is comparable with the maximum turnover number of lysozyme, the turnover number of the trypsin-catalysed hydrolysis of trimethylethoxysilane at 10°C was approximately 200 times slower than a chymotrypsin-catalysed hydrolysis reaction (Table 3.2). Following the hydrolysis reaction, 2 moles of trimethylsilanol were condensed to form one mole of

hexamethyldisiloxane (Figure 4.3). Following the completion of the hydrolysis reaction (30 m), the concentrations of the reactants were plotted versus time (Equations 3.5-3.6) in order to experimentally assess the partial order of reaction with respect to trimethylsilanol (Figures 4.6-4.7).

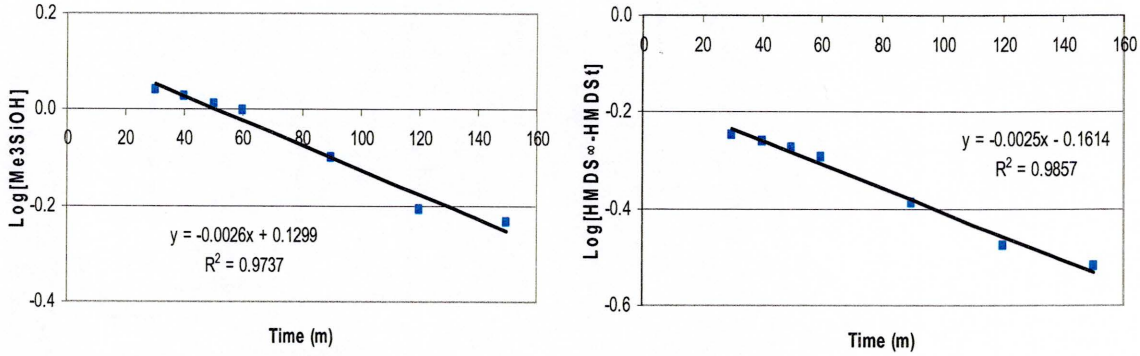

Figure 4.6: First-order evaluation of the condensation of trimethylsilanol at 10°C.[1]
[1] Refer to Table 7.27.

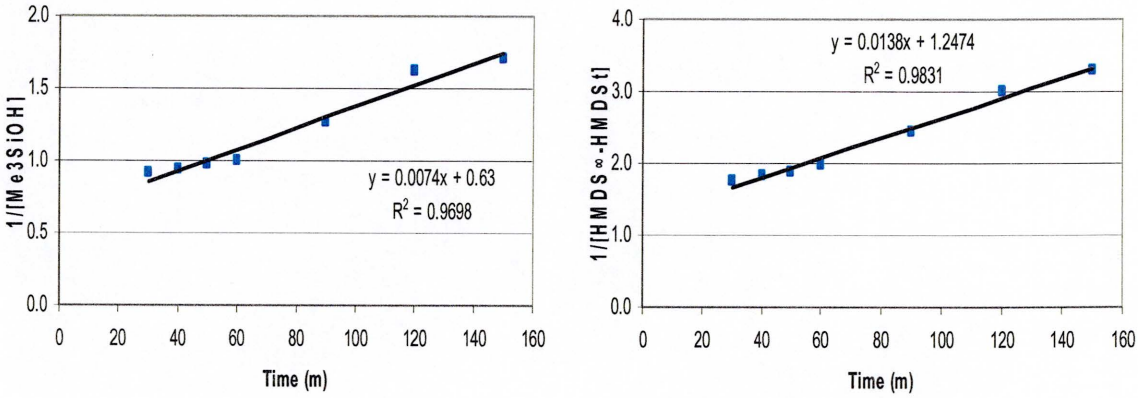

Figure 4.7: Second-order evaluation of the condensation of trimethylsilanol at 10°C.[1]
[1] Refer to Table 7.27.

Whether defined by the concentration of trimethylsilanol or the extent of reaction (i.e. $[HMDS]_\infty$ - $[HMDS]_t$), the rate constants (k_R', Table 4.1) were comparable for either the first- or second-order plots (Figures 4.6-4.7).

Table 4.1: Condensation rate constants (k_R') of trimethylsilanol at 10°C.[1]

	k_R'[2]	
Partial order of reaction with respect to Me_3SiOH[3]	$[Me_3SiOH]$[3]	$2*([HMDS]_\infty - [HMDS]t)$[4]
first-order	0.0030 s^{-1}	0.0029 s^{-1}
second-order	0.0037 $Lmol^{-1}s^{-1}$	0.0035 $Lmol^{-1}s^{-1}$

1 Refer to Equations 3.5-3.6 and Figures 4.6-4.7.
2 k_R' = rate constant = $k_R[trypsin]^\beta$. Refer to Equation 3.3.
3 Me_3SiOH = trimethylsilanol.
4 $2*([HMDS]_\infty - [HMDS]_t) = [Me_3SiOH]$ = extent of reaction, where HMDS = hexamethyldisiloxane.

However, after reviewing the correlation coefficients (R^2) of the first- and second-order plots, the order of reaction with respect to trimethylsilanol was ill defined. The inability to differentiate the order of reaction with respect to trimethylsilanol during condensation may be due to the analysis of an insufficient extent of reaction (% yield = 54, Table 7.27) over 2.5 hours at 10°C. Comparatively, the extent of the hydrolysis reaction was nearly complete (% yield = 91, Table 7.27) over 20 minutes at 10°C. Typically, the extent of reaction should be greater than 75% in order to differentiate between first- and second-order reactions with respect to a reactant [8]. Based on the concentration of trypsin (i.e. $[E_t] = [trypsin] = 1.7$ mM) and the rate of condensation (i.e. $V = -\delta[Me_3SiOH]/\delta t = 0.0048$ M/m ~ $\delta[HMDS]/\delta t = 0.0050$ M/m, Figure 4.8), a relative value of the turnover number (k_{cat}) was calculated to be 2.9 m^{-1} or 0.048 s^{-1} at 10°C (Equation 3.7). Again, this calculation was performed with the postulate that the rate equation was proportional to the concentration of trypsin ($\beta = 1$, Equation 3.10). Since trypsin may not be saturated due to the limited solubility of trimethylsilanol in water, the turnover number was treated as a relative value. Given a relative turnover number equal to 0.048 s^{-1}, the time period between a condensation reaction catalysed by trypsin was calculated to be approximately 20 s or 3 reactions per minute at 10°C.

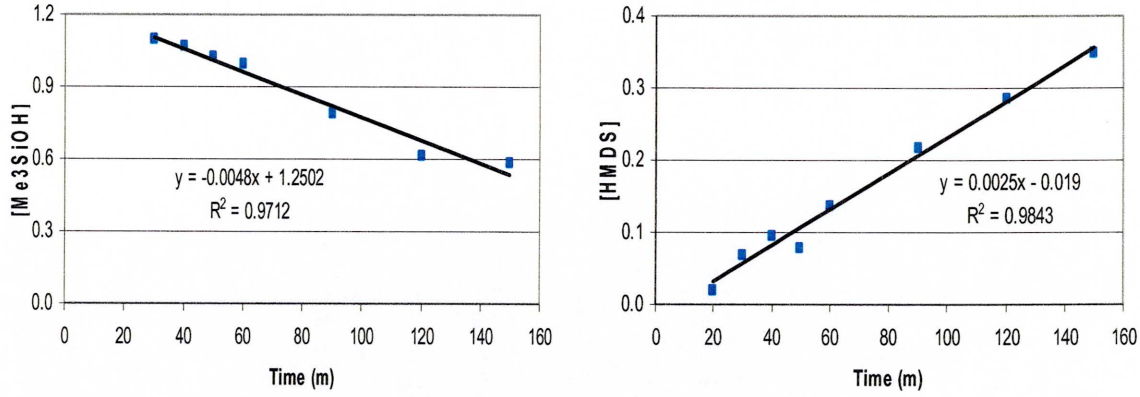

Figure 4.8: The rate of the trypsin-catalysed condensation of trimethylsilanol at 10°C.[1]

[1] Refer to Table 7.27.

Based on the relative turnover numbers, the rate of the trypsin-catalysed hydrolysis of trimethylethoxysilane (0.53 s^{-1}) was one order of magnitude (ten times) faster than the condensation of trimethylsilanol (0.048 s^{-1}) at 10°C (Figure 4.9). Comparatively, the rate of the trypsin-catalysed condensation of trimethylsilanol (k_{cat} = 0.066 s^{-1}) at 25°C was approximately 38% faster than the reaction conducted at 10°C.

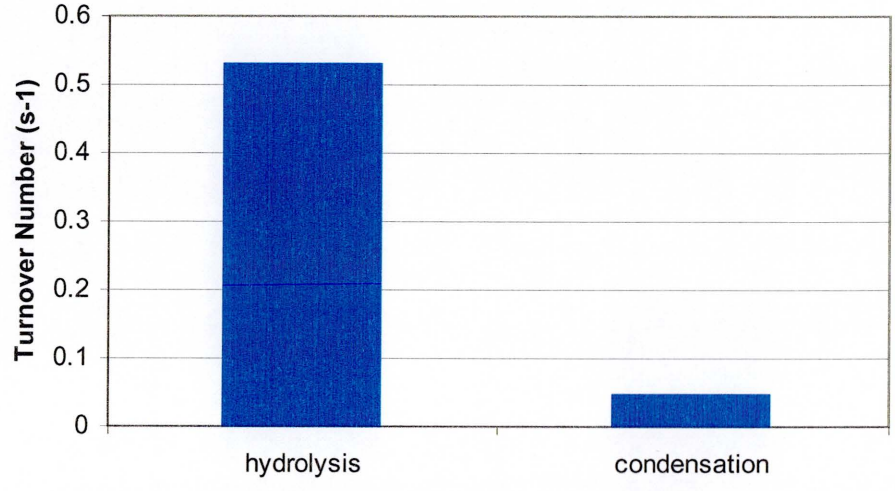

Figure 4.9: Turnover numbers of the trypsin-catalysed hydrolysis of trimethylethoxysilane and condensation of trimethylsilanol at 10°C.[1]

[1] Refer to Table 7.27.

4.2 Alkoxysilane Study

Since trypsin catalysed the formation of siloxane bonds, alternate mono-functional alkoxysilanes were chosen as substrates to investigate the ability of trypsin to selectively catalyse the *in vitro* hydrolysis and condensation of organo-functional alkoxysilanes under mild conditions. Initially, two additional trimethylalkoxysilanes (Figure 4.10) were selected with comparatively polar (i.e. tetraethylene glycol monomethyl ether) and non-polar (i.e. hexanol) substituents to study the activity of trypsin as a function of the solubility of the reactant in a neutral medium (pH 7.0). The syntheses of these trimethylalkoxysilanes are detailed Experimental section 7.1.5 (Scheme 4.2).

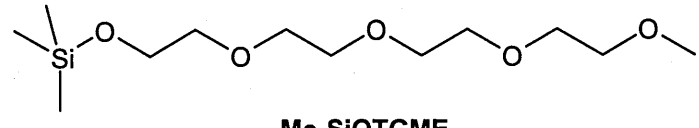

$Me_3SiOTGME$

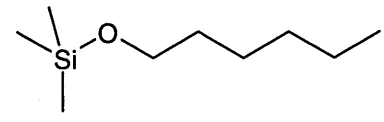

$Me_3SiOC_6H_{13}$

Figure 4.10: Trimethylsilylated tetraethylene glycol monomethyl ether ($Me_3SiOTGME$) and hexanol ($Me_3SiOC_6H_{13}$).[1]

[1] Refer to Experimental section 7.1.5.

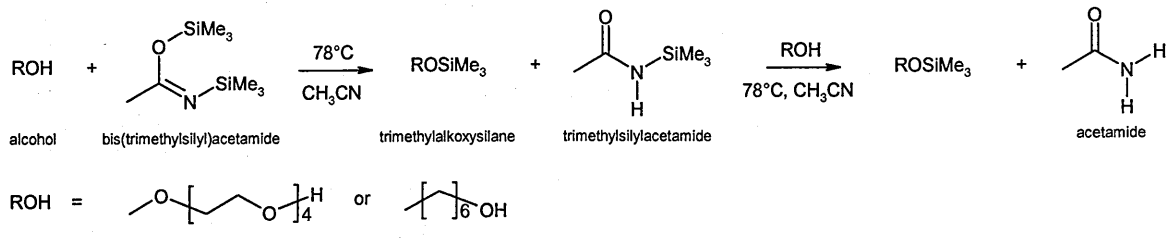

Scheme 4.2: Synthesis of trimethylsilylated tetraethylene glycol monomethyl ether ($Me_3SiOTGME$) and hexanol ($Me_3SiOC_6H_{13}$).[1]

[1] Refer to Experimental section 7.1.5.

The two-phase reactions were formulated with a 4:1 monomer to enzyme weight ratio (> 400:1 alkoxysilane to trypsin mole ratio) and conducted at 25°C for three hours. The reaction products were isolated and quantitatively analysed by GC (Figure 4.11).

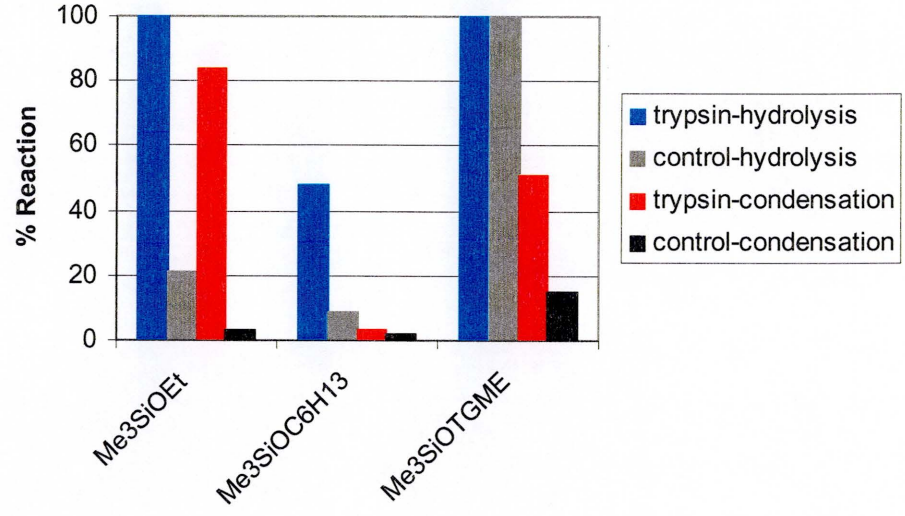

Figure 4.11: Trypsin-catalysed hydrolysis and condensation of trimethylalkoxysilanes at 25°C.[1]

[1] Refer to Experimental section 7.2.3 and Table 7.28.
TGME = tetraethylene glycol monomethyl ether.

Comparatively, the glycol-functional silane appeared to be more miscible than trimethylhexoxysilane in water. Based on the chromatographic results, trypsin catalysed the partial hydrolysis of trimethylhexoxysilane without condensation. Although the role of trypsin in the hydrolysis of the glycol-functional silane was not definitive, trypsin catalysed the condensation of the product, trimethylsilanol. The relative rates of the different hydrolysis and condensation reactions during the three-hour reactions were unknown.

Subsequently, four organo-functional alkoxysilanes (Figure 4.12) were selected to study how the activity of trypsin varied as a result of different steric and electronic interactions with the substrate.

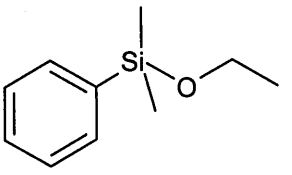

$PhMe_2SiOEt$

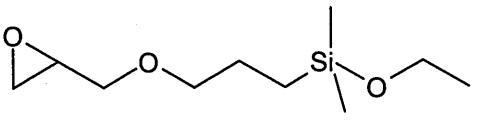

$(epoxy)Me_2SiOEt$

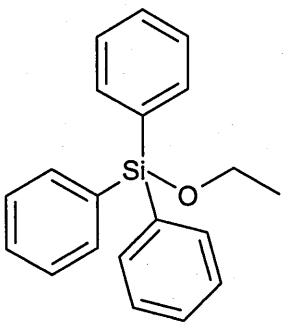

Ph_3SiOEt

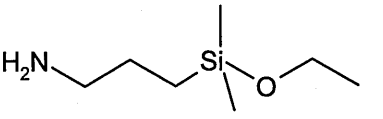

$(H_2N(CH_2)_3)Me_2SiOEt$

Figure 4.12: Phenyldimethylethoxysilane ($PhMe_2SiOEt$), triphenylethoxysilane (Ph_3SiOEt), 3-glycidoxypropyldimethylethoxysilane ($(epoxy)Me_2SiOEt$), and aminopropyldimethylethoxysilane ($(H_2N(CH_2)_3)Me_2SiOEt$).

The two-phase reactions were formulated with a 4:1 monomer to enzyme weight ratio (> 300:1 alkoxysilane to trypsin mole ratio) and conducted at 25°C for three hours. The reaction products were isolated and quantitatively analysed by GC (Figure 4.13). Based on the chromatographic results, trypsin was observed to preferentially catalyse the hydrolysis and condensation of trimethylethoxysilane and 3-glycidoxypropyldimethylethoxysilane. Comparatively, phenyldimethylethoxysilane was hydrolysed but not condensed, while triphenylethoxysilane was neither hydrolysed nor condensed in the presence of trypsin. Given the documented traits of the binding domain within the catalytic region of trypsin [7, 9], the decrease in enzymatic activity appeared to be due to the increased hydrophobicity and steric bulk of the phenyl-functional substrates. Despite trypsin's affinity for basic residues, aminopropyldimethylethoxysilane was fully hydrolysed and condensed in the presence and absence of trypsin. The basic amino-functional

alkoxysilane catalysed the formation of the disiloxane product, which was stabilised by an extra-coordinate intermediate with the primary amine (Scheme 4.3).

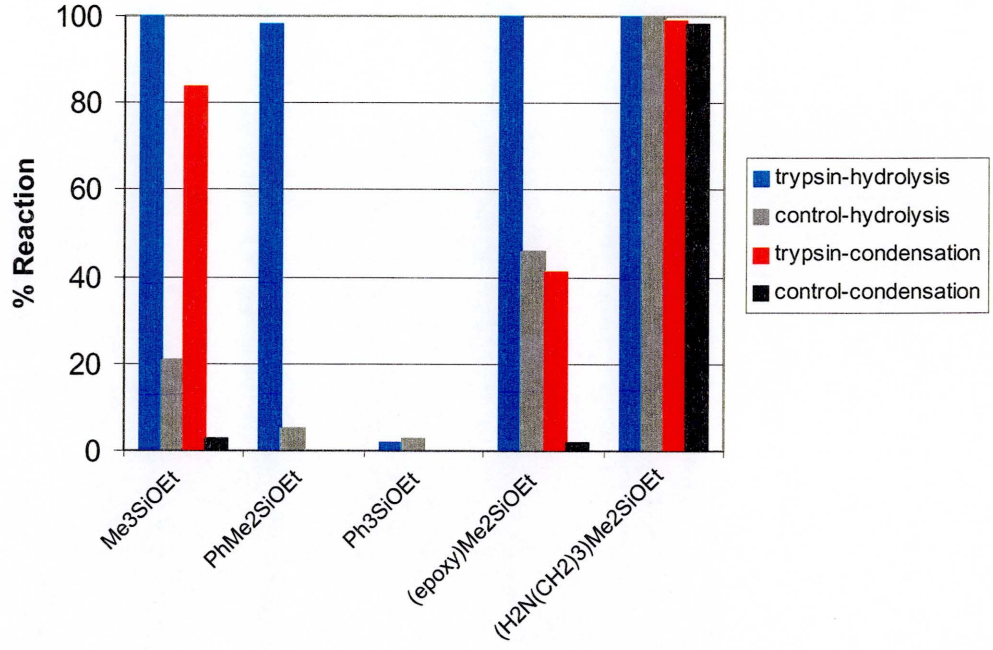

Figure 4.13: Trypsin-catalysed hydrolysis and condensation of ethoxysilanes at 25°C.[1]
[1] Refer to Experimental section 7.2.3 and Table 7.29.
epoxy = 3-glycidoxypropyl.

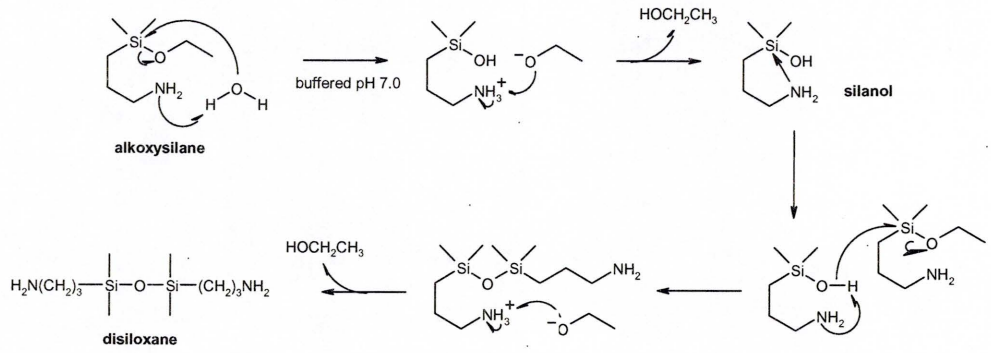

Scheme 4.3: Base-catalysed hydrolysis and condensation of aminopropyldimethylethoxysilane.

Alternatively, two silicon-functional molecules with cyclic architectures were chosen to further investigate the ability of trypsin to catalyse the cleavage and formation of Si-O bonds. The two-phase reactions were formulated with a 4:1 monomer to enzyme

weight ratio and conducted at 25°C for three hours (Scheme 4.4-4.5). The reaction products were isolated and quantitatively analysed by GC (Figure 4.14).

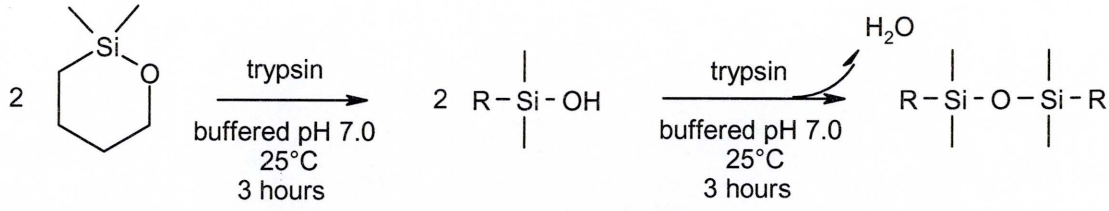

Scheme 4.4: Trypsin-catalysed hydrolysis and condensation of 1,1-dimethyl-1-sila-2-oxacyclohexane.
R = carbinol (i.e. $(CH_2)_4OH$).

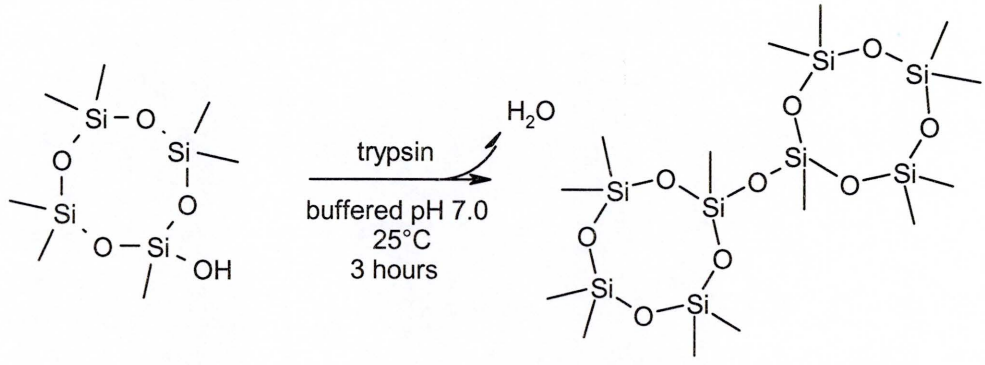

Scheme 4.5: Trypsin-catalysed condensation of heptamethylhydroxytetracyclosiloxane.

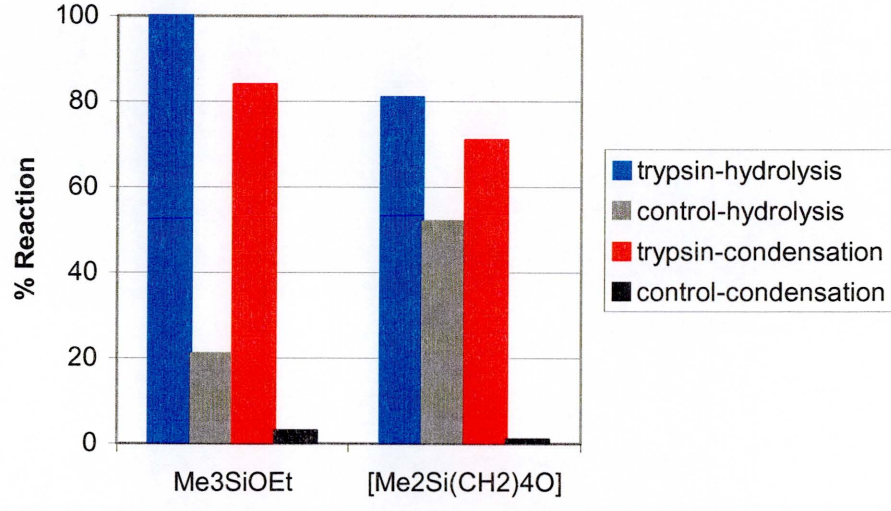

Figure 4.14: Trypsin-catalysed hydrolysis and condensation of 1,1-dimethyl-1-sila-2-oxacyclohexane at 25°C.[1]

[1] Refer to Experimental section 7.2.3 and Table 7.30.

Based on the chromatographic results, trypsin catalysed the ring-opening hydrolysis of 1,1-dimethyl-1-sila-2-oxacyclohexane and condensation of hydroxybutyldimethylsilanol during the formation of the carbinol-functional disiloxane (Scheme 4.4). Trypsin did not catalyse the condensation of heptamethylhydroxytetracyclosiloxane. Despite their cyclic architectures, these organosilicon molecules and the resultant intermediates and products were different. Comparatively, the cyclic siloxane is sterically larger than the cyclic alkoxysilane. Analogous to basic residues (Scheme 4.6), the carbinol-functional silanol intermediate was hypothesised to be an acceptable substrate due to its ability to hydrogen bond with the aspartic acid residue within the binding domain [7] of the catalytic region of trypsin.

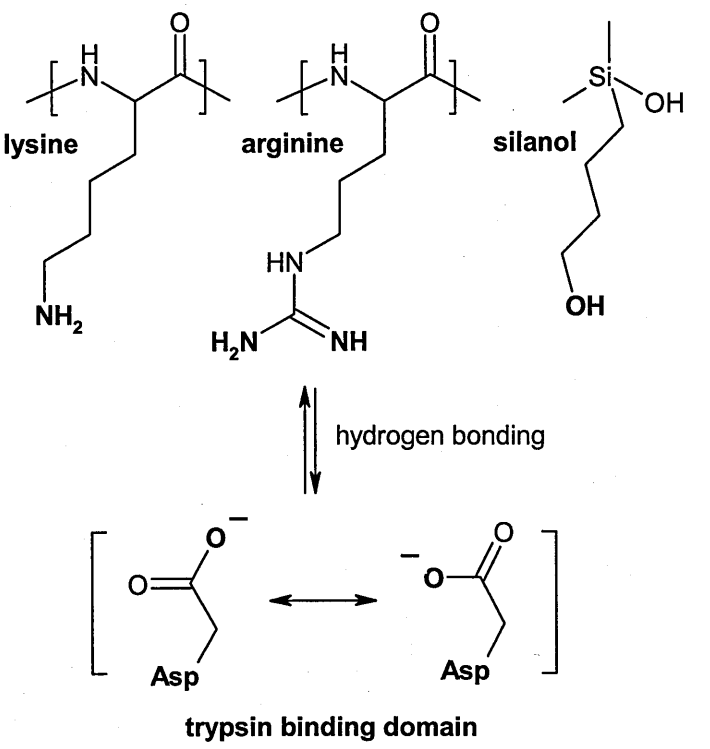

Scheme 4.6: Established (lysine and arginine) and proposed (silanol) hydrogen-bonding within the binding domain of trypsin.

In comparison to a control reaction, trypsin reportedly did not catalyse the polycondensation of a silicic acid precursor, tetraethoxysilane, in an aqueous medium at

pH 6.8 [1]. In this study, no reaction products were observed in a replicate reaction formulated with a 4:1 monomer to enzyme weight ratio and conducted at 25°C for three hours. Specifically, trypsin did not hydrolyse or condense tetraethoxysilane during the three-hour reaction (Table 7.30).

In review, trypsin was observed to selectively catalyse the hydrolysis and condensation of some organo-functional alkoxysilanes under mild conditions.

4.3 Proteinaceous Inhibition Study

A proteinaceous inhibition study was conducted to investigate the role of the enzymatic active site in the hydrolysis and condensation of trimethylethoxysilane (Scheme 4.1). Prior to reaction, trypsin was independently inhibited with an excess amount of the Bowman-Birk inhibitor [10] (4:1 BBI to trypsin mole ratio) and the Popcorn inhibitor [11, 12] (2:1 PCI to trypsin mole ratio) in stirred neutral media (pH 7.0) for two hours. Based on standard enzymatic activity assays [13], trypsin was fully inhibited by the BBI (98%) and PCI (91%) (Table 7.38). The reactions were formulated with a 4:1 monomer to enzyme weight ratio (~1000:1 trimethylethoxysilane to trypsin mole ratio) and conducted at 25°C for three hours. The reaction products were isolated and quantitatively analysed by GC (Figure 4.15). Although the treated enzymes were observed to catalyse the hydrolysis of trimethylethoxysilane, the condensation of trimethylsilanol was completely inhibited in comparison to the control reactions. Notably, the percent hydrolysis decreased in the presence of the BBI- (24%) and PCI- (6%) inhibited trypsin. Following thermal denaturation (Table 7.31), the activity of trypsin was comparable to the proteinaceous inhibition and previous denaturation experiments (Table 7.14). Consequently, it appeared that non-specific interactions with trypsin, including the active site, promoted the

hydrolysis of trimethylethoxysilane. However, the active site of trypsin was determined to selectively catalyse the *in vitro* condensation of trimethylsilanol under mild conditions.

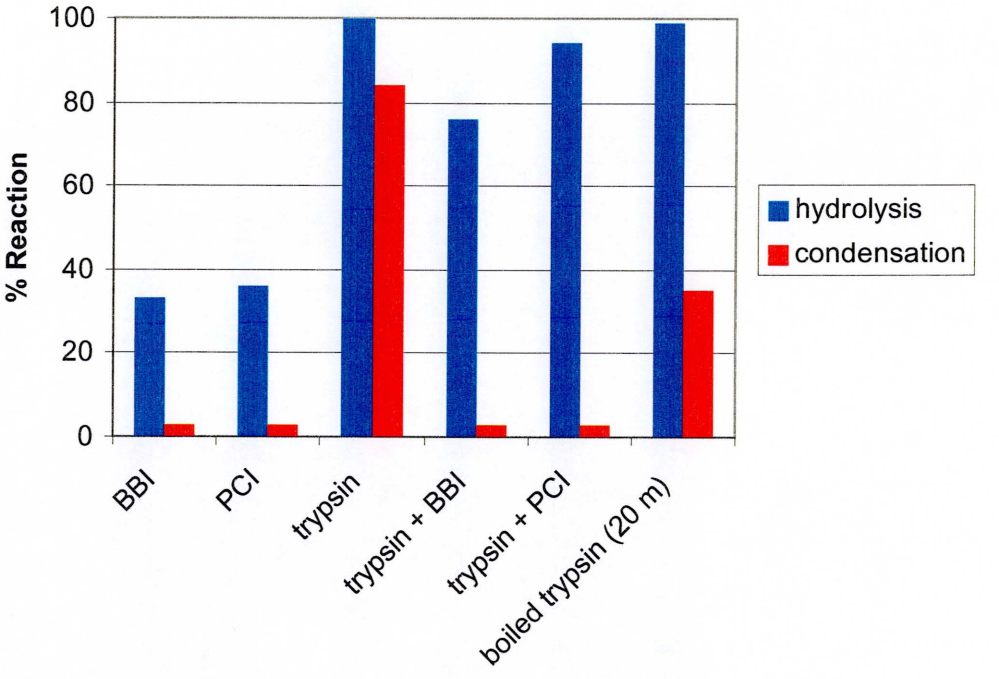

Figure 4.15: Proteinaceous inhibition of trypsin in the hydrolysis and condensation of trimethylethoxysilane at 25°C.[1]

[1] Refer to Experimental section 7.2.3 and Table 7.31.

4.4 Hydrolysis and Condensation of Trimethylethoxysilane with Different Sources of Trypsin

Although various sources (e.g. mammalian, fish) of trypsin are similar (e.g. tertiary structure), their selectivity and activity may be different [9]. Consequently, the ability of porcine pancreas, *Gadus morhua* (i.e. Atlantic cod), and recombinant bovine trypsin to catalyse the hydrolysis of trimethylethoxysilane and condensation of trimethylsilanol was evaluated in neutral media (pH 7.0) at 25°C. Although the pH may not have been optimal for these different sources of trypsin, a neutral pH was used to minimise acid- and base-catalysed hydrolysis and condensation [3]. The reaction products were isolated and quantitatively analysed by GC (Figure 4.16).

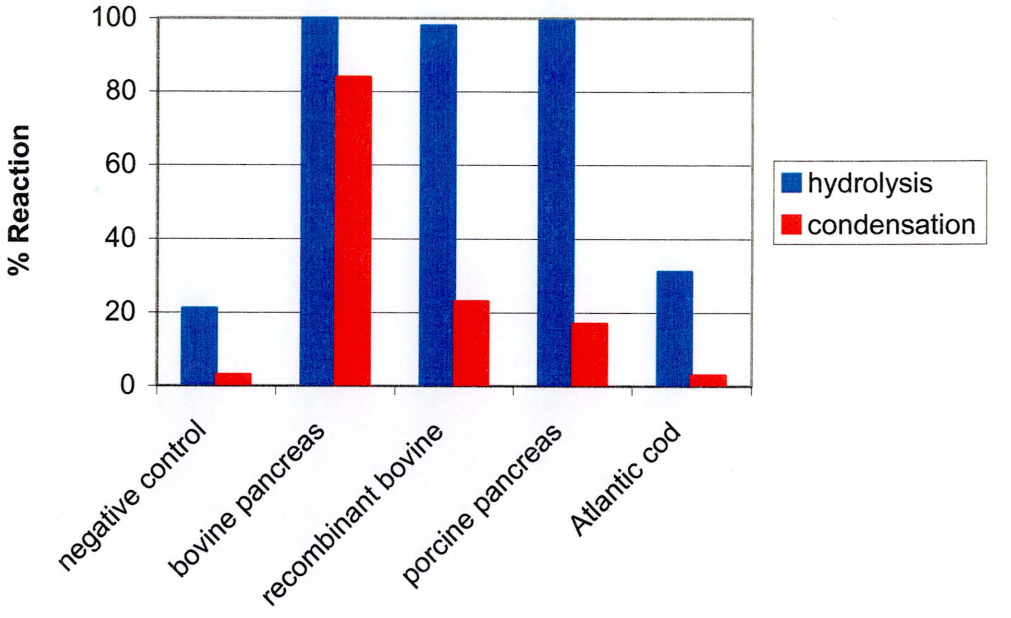

Figure 4.16: The hydrolysis and condensation of trimethylethoxysilane by different sources of trypsin at 25°C.[1]

[1] Refer to Experimental section 7.2.3 and Table 7.32.

Based on the chromatographic results, trypsin from porcine pancreas (i.e. mammalian) as opposed to Atlantic cod (i.e. fish) was observed to catalyse the hydrolysis and condensation reactions. Similar to the pH profiles measured with a natural substrate (Figure 3.26), the activity of trypsin from bovine pancreas was greater than the alternate sources of trypsin including the recombinant enzyme in a neutral medium (pH 7.0). The inactivity of trypsin from the Atlantic cod appeared to be due to pH (Figure 3.26). Since calcium was required to achieve the maximum activity and stability of trypsin [9], these observations may have been due to different optimum pH ranges and/or levels of calcium.

Calcium activation of trypsin induces changes in the tertiary structure of the enzyme [14]. Since the activity of trypsin is optimal in the presence of > 10 mM calcium [14], the ability of trypsin to catalyse the condensation of trimethylsilanol was studied in a neutral medium (pH 7.0) containing 20 mM $CaCl_2$. The reactions were formulated with a 4:1 monomer to enzyme weight ratio (~1000:1 silanol to trypsin mole ratio) and conducted

at 25°C for three hours. The reaction products were isolated and quantitatively analysed by GC (Figure 4.17).

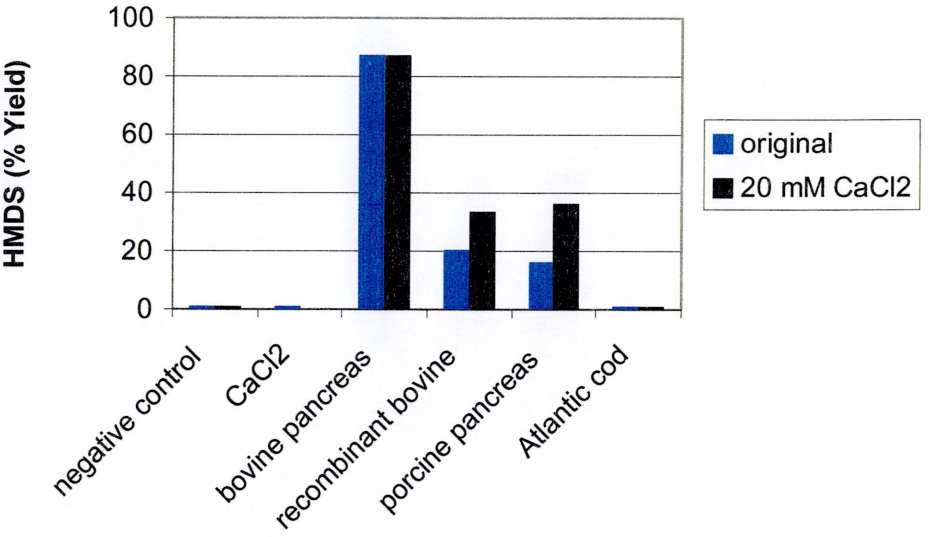

Figure 4.17: The effect of calcium on the trypsin-catalysed condensation of trimethylsilanol at 25°C.[1]

[1] Refer to Experimental section 7.2.2 and Table 7.33.

In comparison to the original sources of trypsin, the activities as measured by the yield of the recombinant bovine and porcine pancreas trypsin-catalysed reactions increased 65% and 125%, respectively. Comparatively, the yield of the bovine pancreas and Atlantic cod trypsin-catalysed reactions did not change. In review, the results correlated with the amount of calcium present in the commercial sources of trypsin (Table 3.7). In the absence of calcium chloride (Figure 4.16), porcine pancreas and recombinant bovine trypsin catalysed the complete hydrolysis of trimethylethoxysilane during the formation of trimethylsilanol. In the presence of calcium chloride, the increased activity of the porcine pancreas and recombinant bovine trypsin provided indirect evidence that the tertiary structure of the catalytic region was directly involved in the *in vitro* condensation of trimethylsilanol. Based on the yields of the hydrolysis and condensation reactions, the commercial source of bovine pancreatic trypsin (i.e. 886 ppm Ca) appeared to be optimal

in a neutral medium (pH 7.0). Comparatively, the potential effect of 20 mM calcium chloride was negligible in the presence of 2.1% calcium in the commercial source of Atlantic cod trypsin. As cited [9], the substrate selectivity and activity of the tryptic sources appeared to be different despite similar tertiary structures.

4.5 Summary

Model substrates were chosen to investigate the ability of trypsin to selectively catalyse the *in vitro* hydrolysis and condensation of organo-functional alkoxysilanes under mild conditions.

In the presence of trypsin, a model alkoxysilane, trimethylethoxysilane, was hydrolysed (100%) and condensed (84%) during the formation of hexamethyldisiloxane in a neutral medium (pH 7.0) at 25°C over three hours. Additional trimethylalkoxysilanes were selected with comparatively polar and non-polar substituents to study the activity of trypsin as a function of the solubility of the reactant in a neutral medium. Trypsin catalysed the partial hydrolysis of trimethylhexoxysilane without condensation. Although the role of trypsin in the hydrolysis of the glycol-functional (i.e. tetraethylene glycol monomethyl ether) silane was not definitive, trypsin catalysed the condensation of the product, trimethylsilanol. The relative rates of the different hydrolysis and condensation reactions during the three-hour reactions were unknown.

Alternatively, trypsin was observed to catalyse the hydrolysis and condensation of 3-glycidoxypropyldimethylethoxysilane, as well as the ring-opening hydrolysis of 1,1-dimethyl-1-sila-2-oxacyclohexane and condensation of hydroxybutyldimethylsilanol during the formation of the carbinol-functional disiloxane. Analogous to basic residues, the carbinol-functional silanol intermediate was hypothesised to be an acceptable substrate

due to its ability to hydrogen bond with the aspartic acid residue within the binding domain [7] of the catalytic region of trypsin.

Comparatively, phenyldimethylethoxysilane was hydrolysed but not condensed, while triphenylethoxysilane was neither hydrolysed nor condensed in the presence of trypsin. Similarly, trypsin did not catalyse the condensation of heptamethylhydroxytetracyclosiloxane. Given the documented traits of the binding domain within the catalytic region of trypsin [7, 9], the enzymatic selection appeared to be due to the increased hydrophobicity and steric bulk of the phenyl-functional substrates as well as the cyclic siloxane. Despite trypsin's affinity for basic residues, aminopropyldimethylethoxysilane was fully hydrolysed and condensed both in the presence and absence of trypsin. The basic amino-functional alkoxysilane catalysed the formation of the disiloxane product, which was stabilised by an extra-coordinate intermediate with the primary amine. Similar to a previously cited [1] polycondensation study, trypsin did not hydrolyse or condense tetraethoxysilane during a three-hour reaction. In review, trypsin was observed to selectively catalyse the hydrolysis and condensation of some organo-functional alkoxysilanes under mild conditions.

A proteinaceous inhibition study was conducted to study the role of the enzymatic active site in the hydrolysis and condensation of trimethylethoxysilane. Although the treated enzymes were observed to catalyse the hydrolysis of trimethylethoxysilane, the condensation of trimethylsilanol was completely inhibited when compared to the control reactions. Consequently, it appeared that non-specific interactions with trypsin, including the active site, promoted the hydrolysis of trimethylethoxysilane. However, the active site of trypsin was determined to selectively catalyse the *in vitro* condensation of trimethylsilanol under mild conditions. Based on the relative turnover numbers, the rate of

the trypsin-catalysed hydrolysis of trimethylethoxysilane was one order of magnitude (ten times) faster than the condensation of trimethylsilanol at 10°C.

The ability of porcine pancreas, *Gadus morhua* (i.e. Atlantic cod), and recombinant bovine trypsin to catalyse the hydrolysis of trimethylethoxysilane and condensation of trimethylsilanol was evaluated in neutral media at 25°C. Although the pH may not have been optimal for these different sources of trypsin, a neutral pH was used to minimise acid- and base-catalysed hydrolysis and condensation [3]. Trypsin from porcine pancreas as opposed to Atlantic cod was observed to catalyse the hydrolysis and condensation reactions. Similar to the pH profiles measured with a natural substrate, the activity of trypsin from bovine pancreas was greater than the alternate sources of trypsin including the recombinant enzyme in a neutral medium (pH 7.0). The inactivity of trypsin from the Atlantic cod appears to be due to pH. Since calcium is required to achieve the maximum activity and stability of trypsin [9], these observations were postulated to be due to different optimum pH ranges and/or levels of calcium. In the absence of calcium chloride, porcine pancreas and recombinant bovine trypsin catalysed the complete hydrolysis of trimethylethoxysilane during the formation of trimethylsilanol. In the presence of calcium chloride, the increased activity of the porcine pancreas and recombinant bovine trypsin provided indirect evidence that the tertiary structure of the catalytic region was directly involved in the *in vitro* condensation of trimethylsilanol. The commercial source of bovine pancreatic trypsin appeared to be optimal in a neutral medium. Comparatively, the potential effect of 20 mM calcium chloride was negligible in the presence of 2.1% calcium in the commercial source of Atlantic cod trypsin. As cited [9], the substrate selectivity and activity of the tryptic sources appeared to be different despite similar tertiary structures.

4.6 References

1. J. N. Cha, K. Shimizu, Y. Zhou, S. C. Christiansen, B. F. Chmelka, G. D. Stucky, and D. E. Morse, *Proc. Natl. Acad. Sci. USA*, **96**, 361, (1999).

2. Y. Zhou, K. Shimizu, J. N. Cha, G. D. Stucky, and D. E. Morse, *Angew. Chem. Int. Ed.*, **38(6)**, 780, (1999).

3. R. K. Iler, "*The chemistry of silica: Solubility, polymerization, colloid and surface properties, and biochemistry*," John Wiley & Sons, New York, (1979).

4. C. Eaborn, "*Organosilicon compounds*," Butterworths Scientific Publications, London, (1960).

5. EPI Suite Software version 3.11, Environmental Protection Agency, http://www.epa.gov/opptintr/exposure/docs/episuite.htm, 2000.

6. J. N. Cha, G. D. Stucky, D. E. Morse, and T. J. Deming, *Nature*, **403**, 289, (2000).

7. L. Stryer, "*Biochemistry*," W. H. Freeman and Company, New York, (1988).

8. M. Mortimer and P. G. Taylor, (eds.), "*Chemical kinetics and mechanism.*" Royal Society of Chemistry, Cambridge, 2002.

9. A. J. Barrett, N. D. Rawlings, and J. F. Woessner, (eds.), "*Handbook of proteolytic enzymes.*" Academic Press, San Diego, 1998.

10. Y. Birk, *Int. J. Peptide Protein Res.*, **25**, 113, (1985).

11. B. Kassell, *in* "*Proteolytic enzymes*,", Vol. 19, Academic Press, New York, 1970.

12. Y. Birk, *in* "*Proteolytic enzymes*,", Vol. 45, Academic Press, New York, 1976.

13. G. W. Schwert and Y. Takenaka, *Biochimica et Biophysica Acta*, **16**, 570, (1955).

14. T. Sipos and J. R. Merkel, *Biochemistry*, **9(14)**, 2766, (1970).

Chapter Five

Enzyme-Catalysed Polycondensation and Ring-Opening Polymerization of Silicon-Based Monomers

5.0 Introduction

The ability of trypsin to catalyze the formation of siloxane bonds during the *in vitro* polycondensation and ring opening polymerization of silicon-based monomers was explored under mild conditions.

5.1 Trypsin-Catalysed Polycondensation of Methyltriethoxysilane

As illustrated (Figure 4.1), silicatein was documented [1, 2] to catalyze the *in vitro* polycondensation of tetraethoxysilane as well as phenyl- and methyl-triethoxysilanes during the formation of siloxane precipitates. However, the study focused solely on the analysis of the solid polycondensation products despite fractional yields and insignificant conversions. Given the catalytic role of trypsin in the model siloxane condensation reactions, these experimental observations were extended to further explore the use of trypsin as a catalyst in the polycondensation of a trifunctional alkoxysilane, methyltriethoxysilane, under mild conditions. The reaction was formulated with a 4:1 methyltriethoxysilane (0.091 g, 511 μmol, 3.25 mmol Si) to trypsin (0.022 g, 0.9 μmol) weight ratio (~550 monomer to enzyme mole ratio) in a neutral medium (pH 7.0) and conducted at 25°C for seven days (Scheme 5.1).

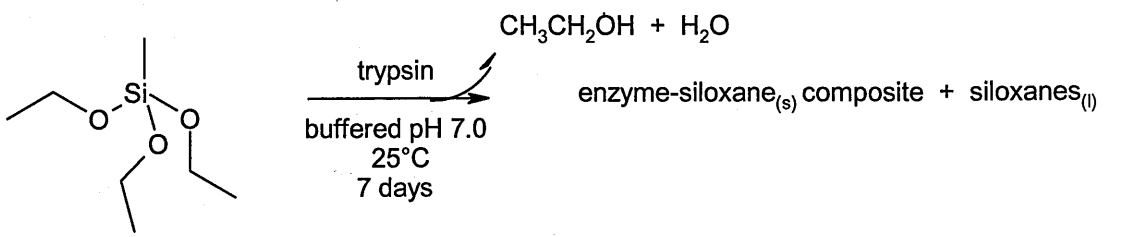

Scheme 5.1: Trypsin-catalyzed polycondensation of methyltriethoxysilane.[1]

1 Refer to Experimental section 7.2.3.

The solid and liquid reaction products were isolated and selectively characterized by infrared spectroscopy, microscopy, and mass spectrometry techniques.

Based on the diffuse reflectance infrared Fourier transform spectra of trypsin and the solid reaction product (Figures 5.1-5.2), the isolated solid was determined to be a composite material containing a mixture of methylsilsesquioxane resin and trypsin. Comparatively, the spectral peaks of a methylsilsesquioxane resin were observed in the presence of a control spectrum acquired with trypsin. Specifically, the symmetric methyl deformation ($MeSiO_{3/2}$, near 1270 cm^{-1}), siloxane asymmetric stretch (SiOSi, near 1000-1130 cm^{-1}), as well as the asymmetric methyl rock and silicon-carbon stretch ($MeSiO_{3/2}$, near 778 cm^{-1}) were observed in the presence of the spectral peaks associated with trypsin. As illustrated in the scanning electron microscopy (SEM) images (Figure 5.3), the solid was observed to contain thick agglomerates ranging in size from approximately 200 μm to 1.5 mm. The rough surfaces of the agglomerate particles were composed of submicron round particles. Based on an energy dispersive spectroscopy (SEM-EDS) analysis, the surfaces of the particles were determined to contain silicon, oxygen, carbon, and sulfur (Figure 5.4). These elements are consistent with the functionality of methylsilsesquioxane and trypsin. The surface also contained sodium and chloride due to the use of a salt (NaCl) in the extraction procedure detailed in Experimental section 7.2.3. Based on the silicon (Si) stoichiometry of the polycondensation reaction, the trypsin-catalyzed polycondensation reaction yielded 12% solid (0.011 g, 0.39 mmol Si). However, the yield value is an upper limit due to the presence of trypsin in the composite material. Comparatively, a solid precipitate was not observed in the negative control reaction.

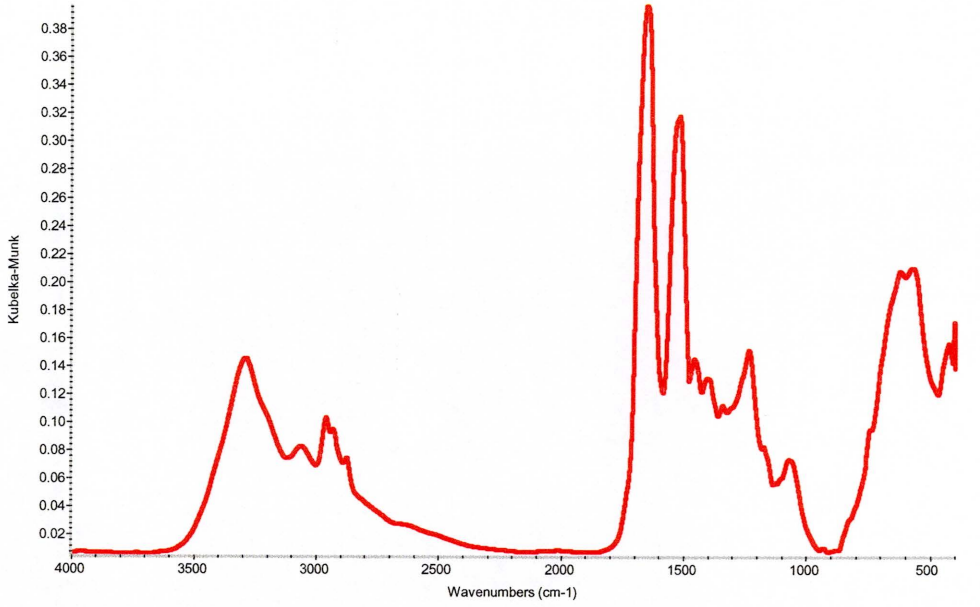

Figure 5.1: Diffuse reflectance infrared Fourier transform spectrum of trypsin (TPCK).[1]

[1] Refer to Experimental section 7.3.5.

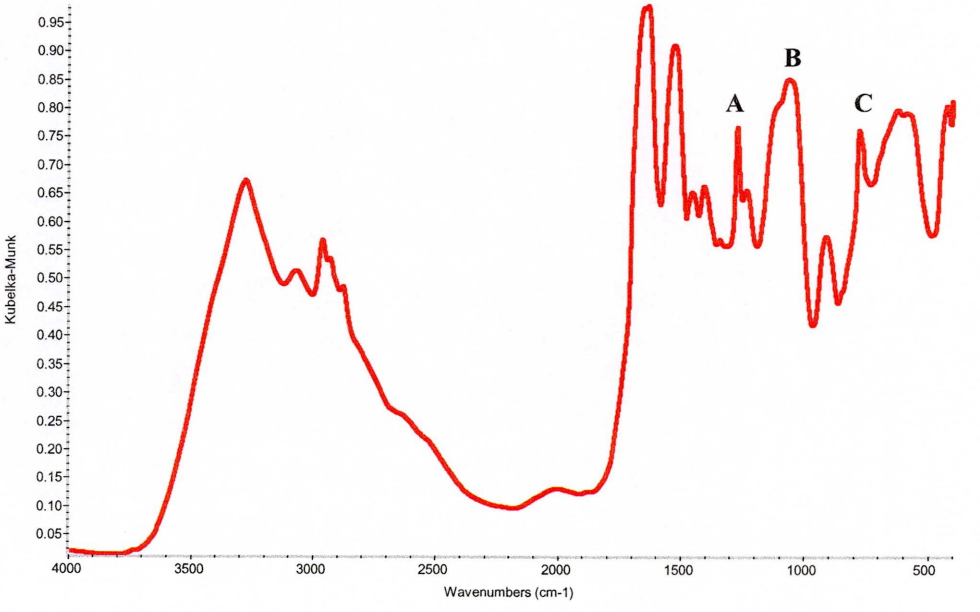

Figure 5.2: Diffuse reflectance infrared Fourier transform spectrum of a methylsilsesquioxane-trypsin (TPCK) composite material.[1]

[1] Refer to Experimental section 7.3.5.

A $MeSiO_{3/2}$, symmetric methyl deformation near 1270 cm^{-1}.

B SiOSi, siloxane asymmetric stretch near 1000-1130 cm^{-1}.

C $MeSiO_{3/2}$, assymetric methyl rock and SiC stretch near 778 cm^{-1}.

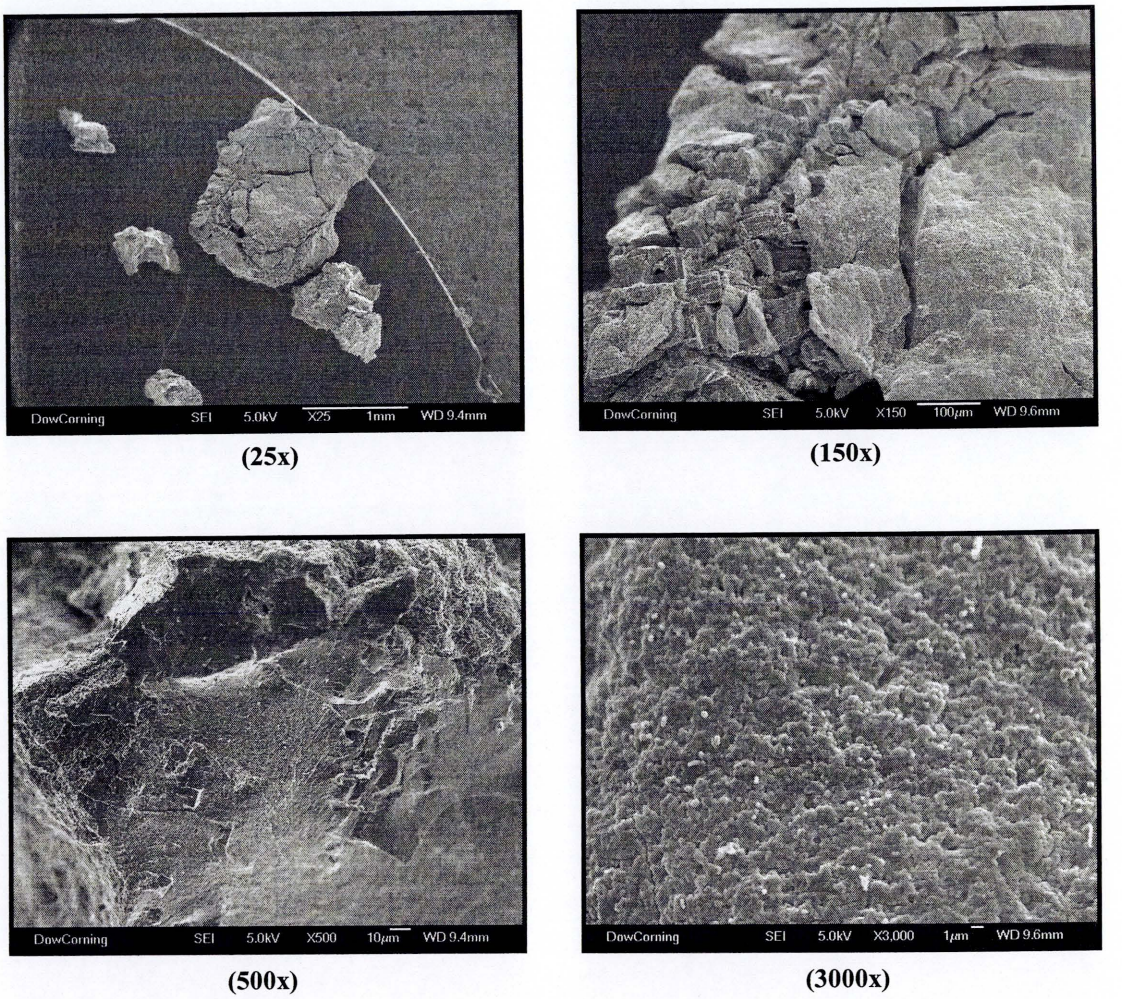

Figure 5.3: Scanning electron microscope images of a methylsilsesquioxane-trypsin composite material.[1]

[1] Refer to Experimental section 7.3.8.

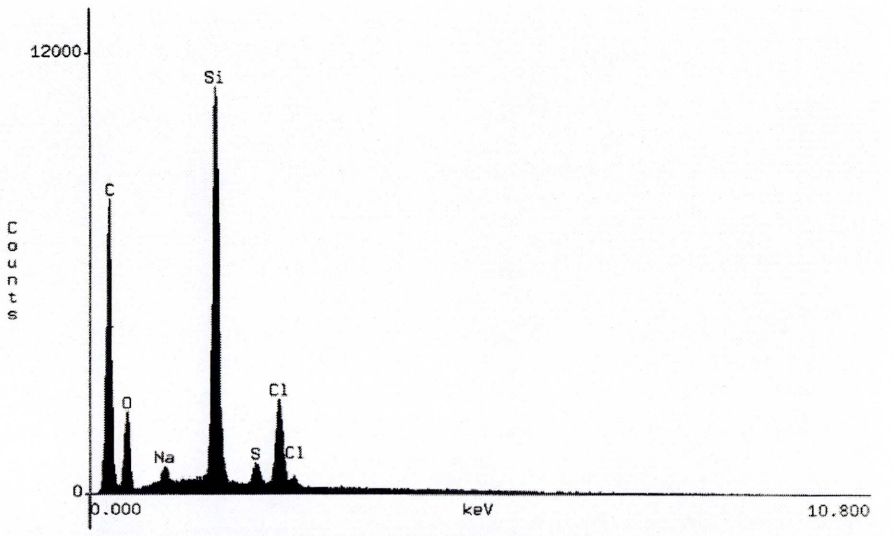

Figure 5.4: Scanning electron microscopy-energy dispersive spectroscopy surface analysis of a methylsilsesquioxane-trypsin (TPCK) composite material.[1]

[1] Refer to Experimental section 7.3.8.

The liquid reaction products were isolated and characterized by electrospray ionisation mass spectrometry (ESI MS). Although methyltriethoxysilane was not observed in the spectral results, substantial hydrolysis and condensation of methyltriethoxysilane was not observed in the absence of trypsin (Figure 5.5). Primarily, ethoxy-functional low molecular weight oligomers (e.g. dimers, trimers, tetramers) and cyclic siloxanes were observed in the ESI MS spectrum. In comparison to the negative control reaction, trypsin promoted the complete hydrolysis and, subsequent, polycondensation of methyltriethoxysilane (Figure 5.6). The distributions of linear, cyclic, and branched siloxane molecules were fully hydroxylated. Although trypsin promoted the hydrolysis of the alkoxy-functional silicon-based molecules, the role of the active site of trypsin in the polycondensation of these molecules was not defined in this study. In other words, the study did not differentiate between chemical- versus enzyme-catalysed condensation.

Although the ESI MS results are qualitative, the reaction products in the solid and liquid phases fully detail the polycondensation reactions. Prior to the precipitation of agglomerated silsesquioxanes in the presence of trypsin, the formation of linear, cyclic, and branched oligomers during the polycondensation of methyltriethoxysilane was analogous to the polymerization behavior of silica (Figure 2.3) [3]. Comparatively, the silicatein-catalysed biosilicification reactions [1, 2] focused solely on the analysis of the solid polycondensation products despite fractional yields and insignificant conversions. Specifically, silicatein was documented [1] to catalyse the formation of 0.005% particulate silica during the polycondensation of tetraethoxysilane. Unfortunately, the balance of the reaction was lost as 99.995% of the reaction (present in the liquid phase) went to waste in the process of washing and isolating the solid product. Consequently, the resultant siloxane molecules from the polycondensation reaction were unknown.

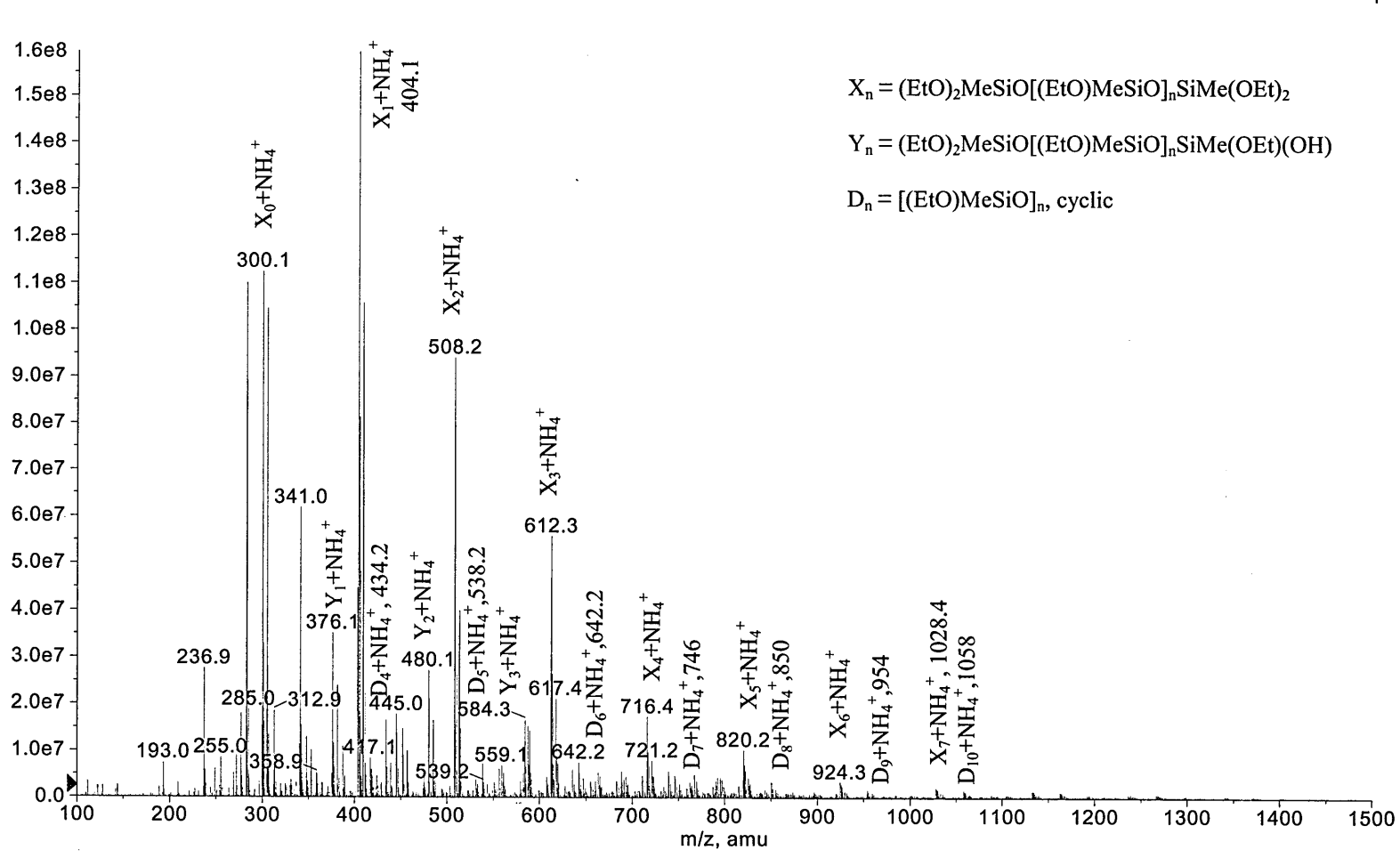

Figure 5.5: Electrospray mass spectrum of the liquid phase after the polycondensation of methyltriethoxysilane in the absence of trypsin.[1]

[1] Refer to Experimental section 7.3.1.

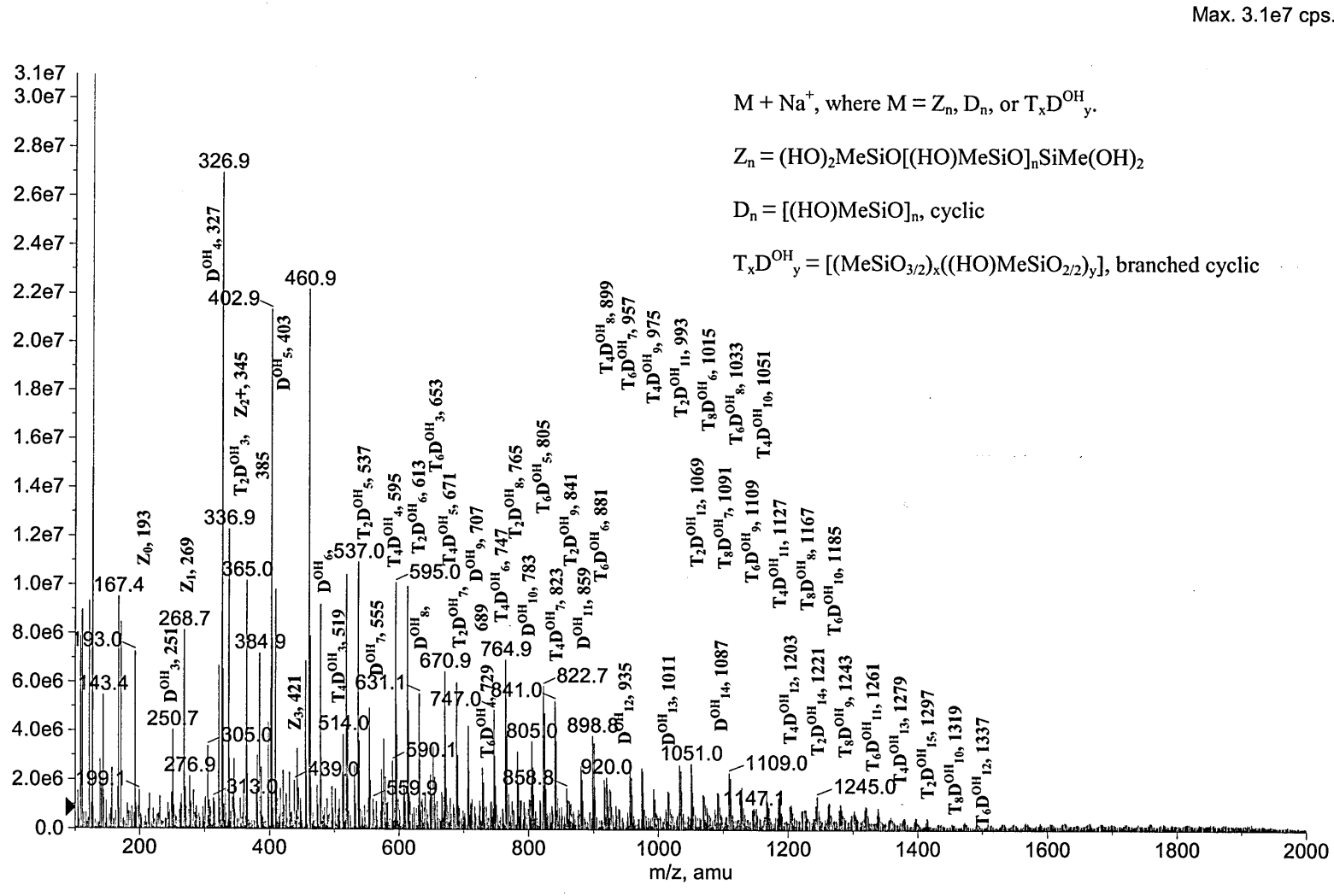

Figure 5.6: Electrospray mass spectrum of the liquid phase after the trypsin-catalyzed polycondensation of methyltriethoxysilane.[1]

[1] Refer to Experimental section 7.3.1.

5.2 Trypsin-Catalysed Ring-Opening Polymerisation of Cyclic Siloxanes

The ability of trypsin to catalyse the cleavage and formation of Si-O bonds during the ring opening polymerization of cyclic siloxanes was explored under mild conditions. Specifically, five cyclic siloxanes (Figure 5.7) were selected to study how the activity of trypsin varied as a result of different steric and electronic interactions with the substrate.

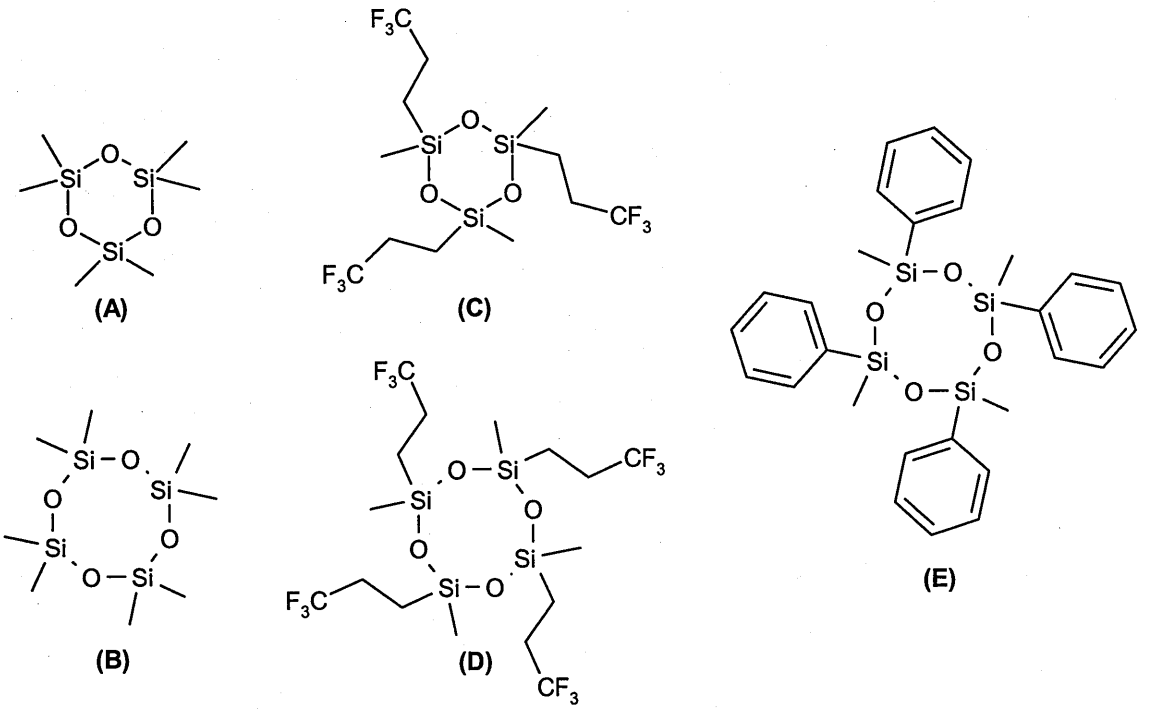

Figure 5.7: Hexamethylcyclotrisiloxane (A), octamethylcyclotetrasiloxane (B), trimethyltri(trifluoropropyl)cyclotrisiloxane (C), tetramethyltetra(trifluoropropyl)cyclotetrasiloxane (D), and tetramethyltetraphenylcyclotetrasiloxane (E).

The two-phase reactions were formulated with a 4:1 monomer to enzyme weight ratio and conducted at 25°C in neutral media (pH 7.0) for 8 days. The reaction products were isolated and qualitatively analysed by GC (Table 5.1).

Table 5.1: Trypsin-catalysed ring opening polymerization of cyclic siloxanes at 25°C.[1]

	Cyclic Area Percent[2]					
	Trimer (x = 3)		Tetramer (x = 4)		Pentamer (x = 5)	
Cyclic Siloxane[3]	Control[1]	Trypsin[1]	Control[1]	Trypsin[1]	Control[1]	Trypsin[1]
A, $[Me_2SiO]_3$	(100)	(100)				
B, $[Me_2SiO]_4$	(0.2)	(0.2)	(99.8)	(99.8)		
C, $[Me(CF_3CH_2CH_2)SiO]_3$	(97.5)	(97.1)	(1.7)	(1.9)	(0.8)	(1.0)
D, $[Me(CF_3CH_2CH_2)SiO]_4$	(0.2)	(0)	(96.3)	(94.9)	(3.4)	(5.1)
E, $[Me(Ph)SiO]_4$			(100)	(100)		

1 Refer to Experimental section 7.2.3 and Table 7.3. The control and trypsin reactions were conducted in the absence and presence of trypsin, respectively.
2 The GC cyclic area percent values are qualitative.
3 Refer to Figure 5.7.

Based on the chromatographic data, trypsin was not observed to catalyse the hydrolysis of the cyclic siloxane bonds. As previously reported (Chapter 3.3), trypsin was unable to hydrolyse hexamethyldisiloxane in a neutral medium (pH 7.0) at 25°C. Since proteases will only interact with water-soluble substrates [4], the hydrolysis reactions would be severely hindered due to the immiscibility of the cyclic siloxanes in the aqueous phase. Although trypsin would theoretically catalyse of the hydrolysis of a siloxane bond due to the law of microscopic reversibility, the reverse reaction was not favored.

5.3 Summary

The ability of trypsin to catalyze the formation of siloxane bonds during the *in vitro* polycondensation and ring opening polymerization of silicon-based monomers was explored under mild conditions.

Given the catalytic role of trypsin in the model siloxane condensation reactions, these experimental observations were extended to further explore the use of trypsin as a catalyst in the polycondensation of a trifunctional alkoxysilane, methyltriethoxysilane.

The solid and liquid reaction products were isolated and characterized. The reaction products in the solid and liquid phases fully detail the polycondensation reaction. Prior to the precipitation of agglomerated silsesquioxanes in the presence of trypsin, the formation of linear, cyclic, and branched oligomers during the polycondensation of methyltriethoxysilane was analogous to the polymerization behavior of silica [3]. Trypsin promoted the complete hydrolysis and, subsequent, polycondensation of methyltriethoxysilane. The distributions of linear, cyclic, and branched siloxane molecules were fully hydroxylated. Although trypsin promoted the hydrolysis of the alkoxy-functional silicon-based molecules, the role of the active site of trypsin in the polycondensation of these molecules was not defined in this study. In other words, the study did not differentiate between chemical- versus enzyme-catalysed condensation.

Comparatively, the silicatein-catalysed biosilicification reactions [1, 2] focused solely on the analysis of the solid polycondensation products despite fractional yields and insignificant conversions. Specifically, silicatein was documented [1] to catalyse the formation of 0.005% particulate silica during the polycondensation of tetraethoxysilane. Unfortunately, the balance of the reaction was lost as 99.995% of the reaction (present in the liquid phase) went to waste in the process of washing and isolating the solid product. Consequently, the resultant siloxane molecules from the polycondensation reaction were unknown.

The ability of trypsin to catalyse the cleavage and formation of Si-O bonds during the ring opening polymerization of cyclic siloxanes was explored under mild conditions. Five cyclic siloxanes were selected to study how the activity of trypsin varied as a result of different steric and electronic interactions with the substrate. Based on the chromatographic data, trypsin was not observed to catalyse the hydrolysis of the cyclic

siloxane bonds. As previously reported (Chapter 3.3), trypsin was unable to hydrolyse hexamethyldisiloxane in a neutral medium (pH 7.0) at 25°C. Since proteases will only interact with water-soluble substrates [4], the hydrolysis reactions would be severely hindered due to the immiscibility of the cyclic siloxanes in the aqueous phase. Although trypsin would theoretically catalyse of the hydrolysis of a siloxane bond due to the law of microscopic reversibility, the reverse reaction was not favored.

5.4 References

1. J. N. Cha, K. Shimizu, Y. Zhou, S. C. Christiansen, B. F. Chmelka, G. D. Stucky, and D. E. Morse, *Proc. Natl. Acad. Sci. USA*, **96**, 361, (1999).

2. Y. Zhou, K. Shimizu, J. N. Cha, G. D. Stucky, and D. E. Morse, *Angew. Chem. Int. Ed.*, **38(6)**, 780, (1999).

3. R. K. Iler, "*The chemistry of silica: Solubility, polymerization, colloid and surface properties, and biochemistry*," John Wiley & Sons, New York, (1979).

4. U. T. Bornscheuer and R. J. Kazlauskas, "*Hydrolases in organic synthesis*," Wiley-VCH, Weinheim, (1999).

Chapter Six

Conclusion

and

Future Endeavour

6.0 Conclusion

6.1 Enzyme-Catalysed Condensation of Silanols

Although silicon is essential for growth and biological function in a variety of plant, animal, and microbial systems [1, 2], the molecular mechanisms of these interactions are effectively unknown [3]. The *in vitro* studies [4-10] of natural systems within the area of silica biosynthesis are complicated. Early mechanistic queries including biomimetic approaches [11, 12] often failed to recognise the chemistry of silicic acid and its analogues [1]. Based on established enzymatic and microbial catalysed transformations [13, 14], organosilicon molecules were determined to be acceptable substrates in comparison to organic materials [15-17]. In order to better understand the role of various proteins in the biosilicification process, a carefully chosen model study was performed to test the ability of homologous enzymes to catalyse the formation of siloxane bonds.

The study of the hydrolysis and condensation reactions during biosilicification is complicated due to the sensitivity of silica, silicates, and silicic acid to pH, concentration, and temperature [1]. As a silicic acid precursor, tetraalkoxysilanes are easily hydrolysed and the resulting silanols are condensed during the formation of particulate silica. Given these complications, a series of homologous enzymes were screened with a simple model compound, trimethylsilanol. Trimethylsilanol was chosen to focus on the formation of a molecule, hexamethyldisiloxane, with a *single* siloxane bond during condensation. The data suggests that homologous lipases and proteases catalyse the formation of siloxane bonds under mild conditions. Since the exceptional activity of trypsin and α-chymotrypsin observed in the enzyme-catalysed condensation study was solely due to a tryptic impurity, trypsin preferentially catalysed the condensation of trimethylsilanol. Although trimethylsilanol appears to be an acceptable substrate, the activities of the enzymes are dependent on the functionality of the non-natural organosilicon substrates.

6.2 Trypsin-Catalysed Condensation of Silanols

Bos taurus or bovine pancreatic trypsin (i.e. a serine-protease) was chosen to investigate the role of the enzymatic active site in the condensation of trimethylsilanol under mild conditions. Trypsin was inhibited with two distinctly different natural polypeptide inhibitors from soybean: Bowman-Birk (BBI) [18] and Popcorn (PCI) [19, 20] inhibitors. The proteinaceous inhibitors completely inhibited the trypsin-catalysed condensation reactions. Although trypsin appeared to be catalytically active over a broad temperature range, the rates of the trypsin-catalysed condensation reactions decreased due to the degree of thermal denaturation. Based on a standard enzymatic activity assay [21], the relative decrease in the rate of silanol condensation correlated with the enhanced stability of trypsin at higher protein concentrations. Consequently, it appears that the tertiary structure, functionality of the active site, and catalytic triad of trypsin are directly involved in the *in vitro* condensation of trimethylsilanol.

Furthermore, the trypsin-catalysed condensation of trimethylsilanol was nearly complete after three hours at 25°C. Based on a hydrolysis study with hexamethyldisiloxane, trypsin was not observed to catalyse the hydrolysis of a siloxane bond in a neutral medium or organic solvent. Reactant and product inhibition were not observed in a neutral medium. Given the ability to self-associate, the autolysis of trypsin was insignificant at higher protein concentrations. This observation complements the enhanced thermal stability of trypsin at increased concentrations. Further verification came from the determination that trypsin could be recycled to catalyse a replicate three-hour condensation reaction with trimethylsilanol. The rate of condensation appears to be proportional to both the concentration of trimethylsilanol and trypsin. Although not definitive, the trypsin-catalysed condensation of non-saturated solutions of trimethylsilanol was estimated to fit the Michaelis-Menten kinetic model. In comparison to the maximum

turnover numbers of other enzymes with their physiological substrates, the turnover number of the trypsin-catalysed condensation of trimethylsilanol was several orders of magnitude (i.e. 10-10,000,000) slower than the cited values. Based on the rate equation as well as the large relative K_m and slow V_{max} values, the formation of the trypsin-silanol intermediate appears to be the rate-limiting step. This is consistent with the fact that organosilicon molecules are larger than analogous hydrocarbon tryptic substrates. Since trypsin was not saturated with trimethylsilanol in aqueous media, the rate of condensation or hydrolysis of the trypsin-silanol intermediate must be faster than the formation of the enzymatic intermediate. Given this information, the trypsin-catalysed condensation of trimethylsilanol was hypothesised to have a reaction mechanism similar to the proteolytic hydrolysis of amide and ester bonds.

The trypsin-catalysed condensation reaction was also dependent on pH. The silanol condensation reaction was optimum at pH 7.0. Comparatively, acid- and base-catalysed [1] silanol condensation was observed in the negative control reactions. In comparison to the pH activity profile, trimethylsilanol partially inhibited trypsin (>50%) almost immediately in basic buffered water (pH 7.5 to pH 9.0). Although trimethylsilanol did not inhibit trypsin in a neutral medium (pH 7.0), reactant inhibition increased by 50-65% with the basicity of the aqueous solution. Since trypsin was not denatured in the presence of trimethylsilanol, the inhibition of the hydrolysis (BAEE) and condensation (trimethylsilanol) reactions in basic media was hypothesised to be due to the silylation of other hydroxy-functional residues in the catalytic region. This would directly or indirectly reduce access to the active site and the activity of trypsin. As the pH decreases, these species would be prone to hydrolysis (acid catalysis), which would enable the active site to participate in the catalytic function of trypsin. Conversely, at high pH values, the longer lifetime of the silylated enzyme would inhibit both the hydrolysis of BAEE and the

condensation of trimethylsilanol. These results further support the role of the active site of trypsin as a catalyst in the *in vitro* condensation of trimethylsilanol.

6.3 Trypsin-Catalysed Hydrolysis and Condensation of Alkoxysilanes

Model substrates were chosen to investigate the ability of trypsin to selectively catalyse the *in vitro* hydrolysis and condensation of organo-functional alkoxysilanes under mild conditions.

In the presence of trypsin, a model alkoxysilane, trimethylethoxysilane, was hydrolysed (100%) and condensed (84%) during the formation of hexamethyldisiloxane in a neutral medium (pH 7.0) at 25°C over three hours. Additional trimethylalkoxysilanes were selected with comparatively polar and non-polar substituents to study the activity of trypsin as a function of the solubility of the reactant in a neutral medium. Trypsin catalysed the partial hydrolysis of trimethylhexoxysilane without condensation. Although the role of trypsin in the hydrolysis of the glycol-functional (i.e. tetraethylene glycol monomethyl ether) silane was not definitive, trypsin catalysed the condensation of the product, trimethylsilanol. The relative rates of the different hydrolysis and condensation reactions during the three-hour reactions were unknown.

Alternatively, trypsin was observed to catalyse the hydrolysis and condensation of 3-glycidoxypropyldimethylethoxysilane, as well as the ring-opening hydrolysis of 1,1-dimethyl-1-sila-2-oxacyclohexane and condensation of hydroxybutyldimethylsilanol during the formation of the carbinol-functional disiloxane. Analogous to basic residues, the carbinol-functional silanol intermediate was hypothesised to be an acceptable substrate due to its ability to hydrogen bond with the aspartic acid residue within the binding domain [22] of the catalytic region of trypsin.

Comparatively, phenyldimethylethoxysilane was hydrolysed but not condensed, while triphenylethoxysilane was neither hydrolysed nor condensed in the presence of trypsin. Similarly, trypsin did not catalyse the condensation of heptamethylhydroxytetracyclosiloxane. Given the documented traits of the binding domain within the catalytic region of trypsin [22, 23], the loss of enzymatic activity appeared to be due to the increased hydrophobicity and steric bulk of the phenyl-functional substrates as well as the cyclic siloxane. Despite trypsin's affinity for basic residues, aminopropyldimethylethoxysilane was fully hydrolysed and condensed both in the presence and absence of trypsin. The basic amino-functional alkoxysilane catalysed the formation of the disiloxane product, which was stabilised by an extra-coordinate intermediate with the primary amine. Similar to a previously cited [5] polycondensation study, trypsin did not hydrolyse or condense tetraethoxysilane during a three-hour reaction. In review, trypsin was observed to selectively catalyse the hydrolysis and condensation of some organo-functional alkoxysilanes under mild conditions.

A proteinaceous inhibition study was conducted to study the role of the enzymatic active site in the hydrolysis and condensation of trimethylethoxysilane. Although the treated enzymes were observed to catalyse the hydrolysis of trimethylethoxysilane, the condensation of trimethylsilanol was completely inhibited when compared to the control reactions. Consequently, it appears that non-specific interactions with trypsin, including the active site, promoted the hydrolysis of trimethylethoxysilane. However, the active site of trypsin was determined to selectively catalyse the *in vitro* condensation of trimethylsilanol under mild conditions. Based on the relative turnover numbers, the rate of the trypsin-catalysed hydrolysis of trimethylethoxysilane was one order of magnitude (ten times) faster than the condensation of trimethylsilanol at 10°C.

The ability of porcine pancreas, *Gadus morhua* (i.e. Atlantic cod), and recombinant bovine trypsin to catalyse the hydrolysis of trimethylethoxysilane and condensation of trimethylsilanol was evaluated in neutral media at 25°C. Although the pH may not have been optimal for these different sources of trypsin, a neutral pH was used to minimise acid- and base-catalysed hydrolysis and condensation [1]. Trypsin from porcine pancreas as opposed to Atlantic cod was observed to catalyse the hydrolysis and condensation reactions. Similar to the pH profiles measured with a natural substrate, the activity of trypsin from bovine pancreas was greater than the alternate sources of trypsin including the recombinant enzyme in a neutral medium (pH 7.0). The inactivity of trypsin from the Atlantic cod appears to be due to pH. Since calcium is required to achieve the maximum activity and stability of trypsin [23], these observations were postulated to be due to different optimum pH ranges and/or levels of calcium. In the absence of calcium chloride, porcine pancreas and recombinant bovine trypsin catalysed the complete hydrolysis of trimethylethoxysilane during the formation of trimethylsilanol. In the presence of calcium chloride, the increased activity of the porcine pancreas and recombinant bovine trypsin provided indirect evidence that the tertiary structure of the catalytic region was directly involved in the *in vitro* condensation of trimethylsilanol. The commercial source of bovine pancreatic trypsin appeared to be optimal in a neutral medium. Comparatively, the potential effect of 20 mM calcium chloride was negligible in the presence of 2.1% calcium in the commercial source of Atlantic cod trypsin. As cited [23], the substrate selectivity and activity of the tryptic sources appeared to be different despite similar tertiary structures.

Given the catalytic role of trypsin in the model siloxane condensation reactions, these experimental observations were extended to further explore the use of trypsin as a catalyst in the polycondensation of a trifunctional alkoxysilane, methyltriethoxysilane.

The solid and liquid reaction products were isolated and characterized. The reaction products in the solid and liquid phases fully detail the polycondensation reaction. Prior to the precipitation of agglomerated silsesquioxanes in the presence of trypsin, the formation of linear, cyclic, and branched oligomers during the polycondensation of methyltriethoxysilane was analogous to the polymerization behavior of silica [1]. Trypsin promoted the complete hydrolysis and, subsequent, polycondensation of methyltriethoxysilane. The distributions of linear, cyclic, and branched siloxane molecules were fully hydroxylated. Although trypsin promoted the hydrolysis of the alkoxy-functional silicon-based molecules, the role of the active site of trypsin in the polycondensation of these molecules was not defined in this study. In other words, the study did not differentiate between chemical- versus enzyme-catalysed condensation.

Comparatively, the silicatein-catalysed biosilicification reactions [5, 24] focused solely on the analysis of the solid polycondensation products despite fractional yields and insignificant conversions. Specifically, silicatein was documented [5] to catalyse the formation of 0.005% particulate silica during the polycondensation of tetraethoxysilane. Unfortunately, the balance of the reaction was lost as 99.995% of the reaction (present in the liquid phase) went to waste in the process of washing and isolating the solid product. Consequently, the resultant siloxane molecules from the polycondensation reaction were unknown.

The ability of trypsin to catalyse the cleavage and formation of Si-O bonds during the ring opening polymerization of cyclic siloxanes was explored under mild conditions. Five cyclic siloxanes were selected to study how the activity of trypsin varied as a result of different steric and electronic interactions with the substrate. Based on the chromatographic data, trypsin was not observed to catalyse the hydrolysis of the cyclic

siloxane bonds. As previously reported, trypsin was unable to hydrolyse hexamethyldisiloxane in a neutral medium (pH 7.0) at 25°C. Since proteases will only interact with water-soluble substrates [25], the hydrolysis reactions would be severely hindered due to the immiscibility of the cyclic siloxanes in the aqueous phase. Although trypsin would theoretically catalyse of the hydrolysis of a siloxane bond due to the law of microscopic reversibility, the reverse reaction was not favored.

6.4 Future Endeavor

Historically, conventional condensation catalysts and reaction conditions have limited the ability to control the structure of organosilicone materials [26]. Given the selectivity and mild reaction conditions of trypsin, the ability to control the molecular architecture [27] could lead to the development of novel materials. In comparison to the biomimetic analogues [6, 7, 11, 12], the role of the protein as a catalyst versus a template and the types of interactions produced are essentially unknown. Given the similarity of the organo-biosilica composites [4, 6, 8, 10], further understanding of the biotransformation strategy in the design and synthesis of structurally complex materials (e.g. stereoregular, chiral, or, possibly, organic hybrid materials) would be beneficial. The opportunity to strategically use biocatalysts to synthesise novel hybrid materials with structural control and spatial order is promising.

6.5 References

1. R. K. Iler, "*The chemistry of silica: Solubility, polymerization, colloid and surface properties, and biochemistry*," John Wiley & Sons, New York, (1979).

2. M. G. Voronkov, *in* "*Silicon in living systems*," Ellis Horwood Limited, Chichester, (1987).

3. D. E. Morse, *in* "*The chemistry of organic silicon compounds*," (eds. Z. Rappoport and Y. Apeloig), Vol. 3, John Wiley & Sons, New York, 2001.

4. K. Shimizu, J. Cha, G. D. Stucky, and D. E. Morse, *Proc. Natl. Acad. Sci. USA*, **95**, 6234, (1998).

5. J. N. Cha, K. Shimizu, Y. Zhou, S. C. Christiansen, B. F. Chmelka, G. D. Stucky, and D. E. Morse, *Proc. Natl. Acad. Sci. USA*, **96**, 361, (1999).

6. N. Kroger, R. Deutzmann, and M. Sumper, *Science*, **286**, 1129, (1999).

7. N. Kroger, R. Deutzmann, C. Bergsdorf, and M. Sumper, *Proc. Natl. Acad. Sci. USA*, **97(26)**, 14133, (2000).

8. N. Kroger, R. Deutzmann, and M. Sumper, *J. Biol. Chem.*, **276(28)**, 26066, (2001).

9. N. Kroger, S. Lorenz, E. Brunner, and M. Sumper, *Science*, **298**, 584, (2002).

10. C. C. Perry and T. Keeling-Tucker, *J. Chem. Soc. Chem. Commun.*, 2587, (1998).

11. J. N. Cha, G. D. Stucky, D. E. Morse, and T. J. Deming, *Nature*, **403**, 289, (2000).

12. R. R. Naik, L. L. Brott, S. J. Clarson, and M. O. Stone, *J. Nanosci. Nanotech.*, **2(1)**, 95, (2002).

13. K. Faber, "*Biotransformations in organic chemistry*," Springer-Verlag, New York, (2000).

14. J. B. Jones, *Tetrahedron*, **42**, 3351, (1986).

15. R. Tacke and S. A. Wagner, *in* "*The chemistry of organic silicon compounds*," (eds. Z. Rappoport and Y. Apeloig), Vol. 2(3), John Wiley & Sons, West Sussex, England, 1998.

16. T. Kawamoto and A. Tanaka, *in* "*Enzymes in nonaqueous solvents: Methods and protocols*," (eds. E. N. Vulfson, P. J. Halling, and H. L. Holland), Vol. 15, Humana Press, Inc., Totowa, NJ, 2001.

17. A. Tanaka, *Nippon Oyo Koso Kyokaishi*, **28**, 10, (1994).

18. Y. Birk, *Int. J. Peptide Protein Res.*, **25**, 113, (1985).

19. B. Kassell, *in* "*Proteolytic enzymes*,", Vol. 19, Academic Press, New York, 1970.

20. Y. Birk, *in* "*Proteolytic enzymes*,", Vol. 45, Academic Press, New York, 1976.

21. G. W. Schwert and Y. Takenaka, *Biochimica et Biophysica Acta*, **16**, 570, (1955).

22. L. Stryer, "*Biochemistry*," W. H. Freeman and Company, New York, (1988).

23. A. J. Barrett, N. D. Rawlings, and J. F. Woessner, (eds.), "*Handbook of proteolytic enzymes*." Academic Press, San Diego, 1998.

24. Y. Zhou, K. Shimizu, J. N. Cha, G. D. Stucky, and D. E. Morse, *Angew. Chem. Int. Ed.*, **38(6)**, 780, (1999).

25. U. T. Bornscheuer and R. J. Kazlauskas, "*Hydrolases in organic synthesis*," Wiley-VCH, Weinheim, (1999).

26. D. E. Morse, *TIBTECH*, **17(6)**, 230, (1999).

27. S. Mann, *Nature*, **365**, 499, (1993).

Chapter Seven

Experimental

7.1 Materials

7.1.1 Protein and Peptides

Aspergillus niger lipase (Amano lipase A, #53,478-1), N-α-benzoyl-L-arginine ethyl ester (BAEE, #B4500), N-benzoyl-L-tyrosine ethyl ester (BTEE, #B6125), bovine pancreatic α-chymotrypsin (#C-4129), bovine pancreatic α-chymotrypsin treated with TLCK (#C3142), bovine pancreatic phospholipase A2 (P-8913), bovine pancreatic trypsin (#T4665), bovine pancreatic trypsin treated with TPCK (#T1426), bovine serum albumin (BSA, #B4287), *Candida antarctica* lipase (#62299), *Candida lipolytica* lipase (#62303), *Gadus morhua* trypsin (#T9906), hog stomach pepsin (#P7012), *Mucor javanicus* lipase (#62304), Novozyme 435® (immobilized *Candida antarctica* lipase B, ~1% protein [1], #53,732-2), papaya latex papain (#P4762), *Penicillium roqueforti* lipase (#62308), porcine γ-globulins (#G2512), porcine pancreatic carboxypeptidase B (#C9584), porcine pancreatic elastase (#E0258), porcine pancreatic lipase (#L-3126), porcine pancreatic trypsin (#T0303), protease (subtilisin Carlsberg, #P8038), *Pseudomonas cepacia* lipase (Amano lipase PS, #53,464-1), *Pseudomonas fluorescens* lipase (#62321), *Rhizomucor miehei* lipase (#62291), trypsin inhibitor from Glycine max (Popcorn inhibitor from soybean, #T9128), trypsin-chymotrypsin inhibitor from soybean (Bowman-Birk inhibitor, #T9777), N-α-p-tosyl-L-lysine chloromethyl ketone hydrochloride (TLCK, #T7254), N-tosyl-L-phenylalanine chloromethyl ketone (TPCK, #T4376), wheat germ lipase (#62306) were purchased from Sigma-Aldrich (St. Louis, MO). Bovine kidney cathepsin L (#219418), human liver cathepsin L (#219402), and *Paramecium tetraurelia* cathepsin L (#219412) were purchased from Calbiochem®, EMD Biosciences (San Diego, CA). Recombinant bovine trypsin expressed in maize (#TRY, CAS #9002-07-7) was purchased from ProdiGene (College Station, TX).

7.1.2 Water

Ultra pure water was obtained from a Milli-Q system at the Dow Corning Corporation (Midland, MI). Trizma® pre-set crystals pH 7.0 (Tris-HCl, #T3503), pH 7.5 (Tris-HCl, #T4128), pH 7.8 (Tris-HCl, #T4503), pH 8.0 (Tris-HCl, #T4753), and pH 9.0 (Tris-HCl, #T6003) were purchased from Sigma-Aldrich. Buffer solutions pH 4.00 (potassium biphthalate, #SB101), pH 5 (sodium hydroxide-citric acid, #A015860101), pH 6.00 (monobasic potassium phosphate-sodium hydroxide, #SB104), and pH 10.00 (potassium carbonate-potassium borate-potassium hydroxide, #SB115) were purchased at Fisher Scientific (Pittsburgh, PA).

7.1.3 Organic Molecules

Acetonitrile (#A996-4), acetone (#A929-4), phosphorous pentoxide (#A244), 2-propanol (#A451-4), tetrahydrofuran (#T427-1), and toluene (#T291-4) were purchased from Fisher Scientific. Acetic acid (#A6283), calcium chloride (#C3881), dodecane (#44010), ethanol (#45,984-4), hexanol (#H13303), hydrochloric acid (#33,925-3), lithium aluminum hydride (#19,987-7), sodium chloride (#20,443-9), and sodium hydrogencarbonate (#34,094-4) were purchased from Sigma-Aldrich. Tetraethylene glycol monomethyl ether (#T1372) was purchased from TCI America (Portland, OR). HPLC grade organic solvents were used throughout the project.

7.1.4 Silicon-Based Molecules

Trimethylsilanol (CAS #1066-40-6, #12848-72), heptamethylhydroxytetracyclosiloxane (#11050-134B), hexamethylcyclotrisiloxane (#E-459-80, cut #3), octamethylcyclotetrasiloxane (#E-1927-93-2, lot #2), 1,3,5-trimethyl-1,3,5-tri(3,3,3-trifluoropropyl)cyclotrisiloxane (LS Trimer), 1,3,5,7-tetramethyl-1,3,5,7-tetra(3,3,3-trifluoropropyl)cyclotetrasiloxane (#H-1387-145), and 2,4,6,8-trimethyl-

2,4,6,8-tetraphenyl-cyclotetrasiloxane (#1923-44A) were obtained at the Dow Corning Corporation. 3-Aminopropyldimethylethoxysilane (#SIA0603.0), bis(trimethylsilyl)acetamide (#SIB1846.0), 1,1-dimethyl-1-sila-2-oxacyclohexane (#SID4234.0), 3-glycidoxypropyldimethylethoxysilane (#SIG5825), hexamethyldisiloxane (#SIH6115.0), trimethylethoxysilane (#SIT8515.0), and triphenylethoxysilane (#SIT8652.0) were purchased at Gelest, Inc. (Tullytown, PA). Hexamethyldisilazane (#37921-2) and tetraethoxysilane (#23620-9) were purchased at Sigma-Aldrich. Phenyldimethylethoxysilane (#P0161) was purchased from United Chemical Technologies, Inc. (Bristol, PA). Methyltriethoxysilane (#M9050) was purchased from Huls America, Inc. (Bristol, PA).

7.1.5 Trimethylalkoxysilane Syntheses

Two trimethylalkoxysilanes were synthesized with polar and non-polar substituents. Tetraethylene glycol monomethyl ether (TGME) and hexanol were silylated with bis(trimethylsilyl)acetamide to obtain the target polar ($Me_3SiO(CH_2CH_2O)_4CH_3$) and non-polar ($Me_3SiOC_6H_{13}$) silanes, respectively [2, 3]. Although bis(trimethylsilyl)acetamide is a bi-functional molecule, this reactive silylating agent was treated as a mono-functional molecule due to the potential presence of other protic molecules (e.g. water). The reaction is illustrated in Scheme 7.1.

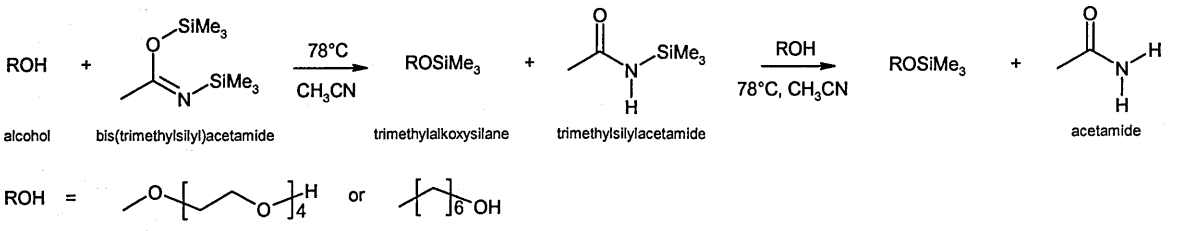

Scheme 7.1: Synthesis of trimethylsilylated tetraethylene glycol monomethyl ether and hexanol.

Prior to the experiments, the glassware was cleaned, dried in an oven, and cooled in a desiccator over Drierite® (W.A. Hammond Drierite Company, Xenia, Ohio). Due to the potential side reaction with water, the solvent (acetonitrile) was dried/distilled over phosphorus pentoxide (P_2O_5) at 81°C (head temperature) for 1 hour. The alcohol (4 g (19 mmol) TGME, 3 g (29 mmol) hexanol) and acetonitrile (16.59 g TGME reaction, 18.54 g hexanol reaction) were introduced into a 50 mL three-neck round-bottom flask equipped with a water-cooled condenser and a dry tube filled with Drierite® in an inert (nitrogen purged) glove bag. The bis(trimethylsilyl)acetamide (4.29 g (21 mmol) TGME reaction, 6.27 g (31 mmol) hexanol reaction) was added to the reaction mixtures by syringe through a rubber septum. The reaction mixtures were refluxed at 78°C for approximately 6 hours in a silicone oil bath controlled by a Therm-O-Watch® controller. Finally, the reaction mixtures were distilled under heat/vacuum to isolate the trimethylalkoxysilane products.

The TGME refluxed reaction mixture was distilled at 120°C/760 mmHg to primarily remove the solvent (acetonitrile) as well as 150°C/35 mmHg (head temperature = 95°C) and 110°C/4 mmHg (head temperature = 60°C) to remove residual trimethylsilylacetamide (MSA). Since MSA is a solid (BP = 105-107°C/35 mmHg) at room temperature [2], the water was removed from the condenser while using a heat gun to flush the distilling white solid into the dry ice/isopropanol cooled receiving flask. This step was necessary to avoid the formation of a solid plug in the heated/pressurized experimental apparatus. The solid distillate was isolated and characterized by GC-MS as a reference material of MSA. Following the vacuum distillation, the flask was cooled to room temperature and the vacuum was removed. Under a stream of nitrogen, a dark amber coloured liquid was recovered from the pot, characterized by gas chromatography- and electrospray ionisation-mass spectrometry (GC-MS and ESI MS, respectively) (Figures 7.1-7.2), and determined to be the trimethylsilylated TGME product.

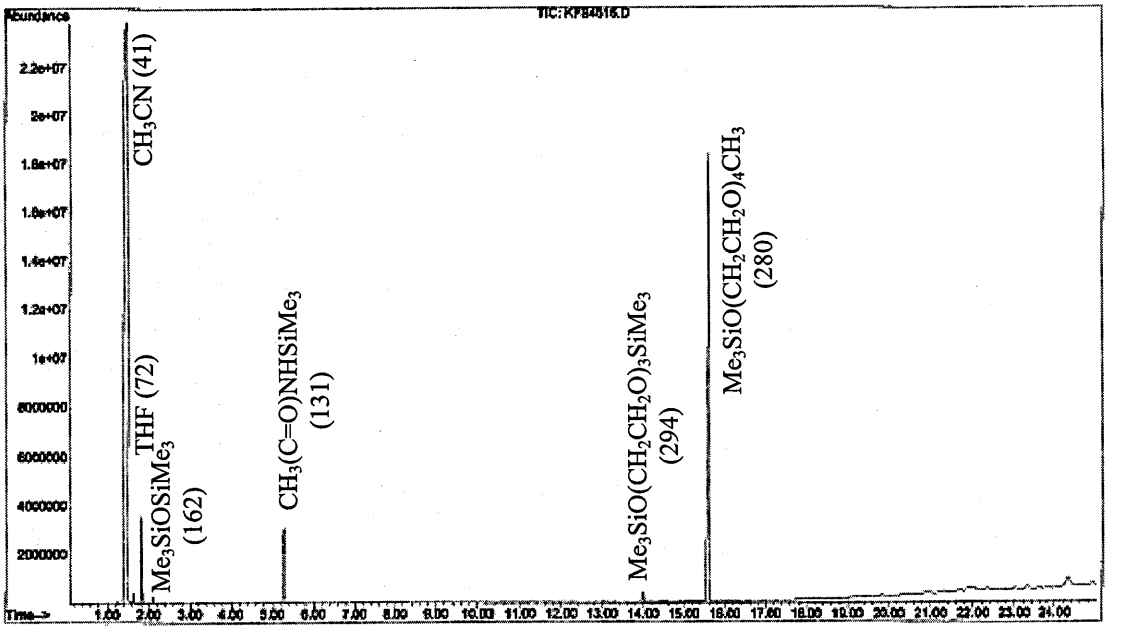

Figure 7.1: Gas chromatography-mass spectrum of trimethylsilylated tetraethylene glycol monomethyl ether.[1]

[1] Refer to Experimental section 7.3.3.

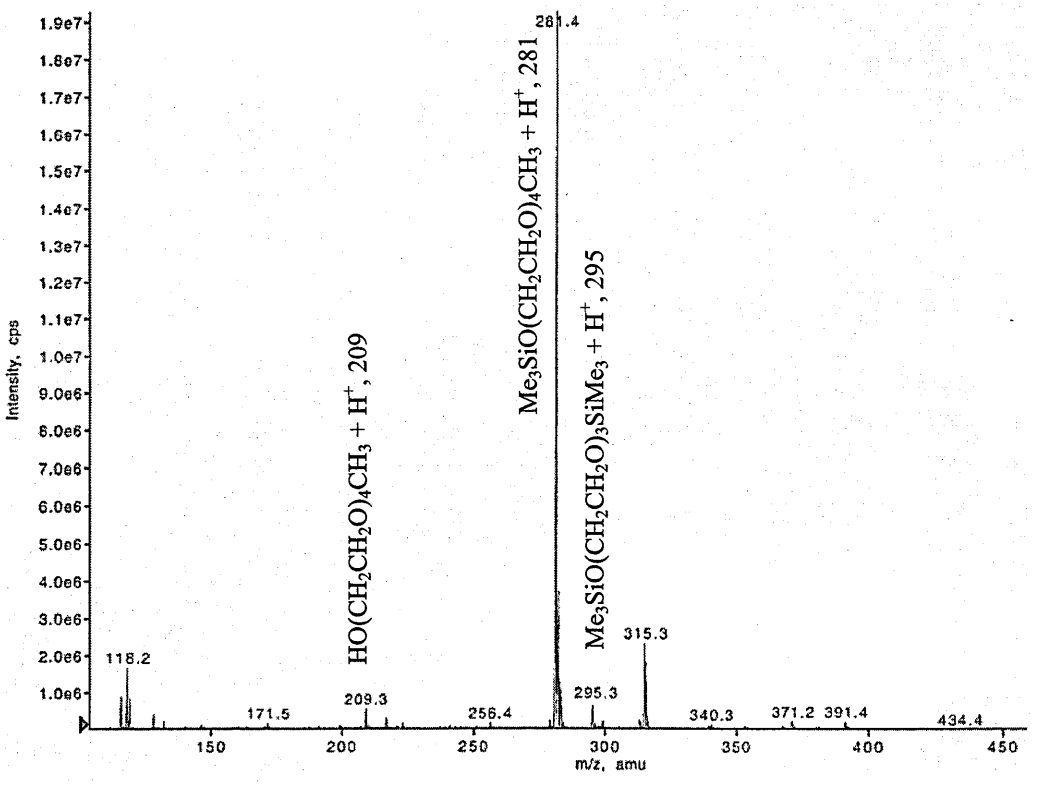

Figure 7.2: Electrospray ionisation mass spectrum of trimethylsilylated tetraethylene glycol monomethyl ether.[1]

[1] Refer to Experimental section 7.3.1.

Based on the chromatographic (GC-FID) results, the product was determined to be approximately 95% pure ($Me_3SiO(CH_2CH_2O)_4CH_3$). Trimethylsilylated tetraethylene glycol monomethyl ether is a new compound. The material also contained approximately 3-4% residual MSA and 1% disilylated tetraethylene glycol ($Me_3SiO(CH_2CH_2O)_4SiMe_3$). A trace amount of TGME was observed in the product.

Comparatively, the hexanol reaction mixture was observed to reflux with the exothermic addition of bis(trimethylsilyl)acetamide. After refluxing for approximately 6 hours at 78°C, the mixture was flash distilled at 50°C/20 mmHg to remove the solvent and 110°C/2 mmHg (head temperature = 60°C) to remove residual MSA. Following the distillation of MSA, a tan solid was isolated as the 'product' in the pot under a stream of nitrogen. After analyzing the distillation samples by GC-MS, it was determined that the trimethylsilylated hexanol product ($Me_3SiOC_6H_{13}$) co-distillated with acetonitrile during the flash distillation (50°C/20 mmHg) as well as the subsequent distillation (110°C/2 mmHg). In fact, the tan solid 'product' was MSA. Since the residual MSA was purified during the vacuum distillation, the tan solid was isolated as an additional reference source of MSA. Given the presence of residual Me_3SiOH, $Me_3SiOSiMe_3$, and hexanol in the 50°C/20 mmHg distillate, the 110°C/2 mmHg distillate fraction was isolated as the reaction product. Based on the chromatographic results (Figure 7.3), the product was determined to be approximately 95% pure ($Me_3SiOC_6H_{13}$). Trimethylhexoxysilane is a known compound. The material also contained approximately 4% residual MSA. No residual hexanol was observed in the product. A complete characterization was not performed.

Lastly, based on the GC-MS spectral results throughout the two 6-hour reactions, the trimethylalkoxysilane reflux reactions were determined to be complete within minutes (~10 minutes).

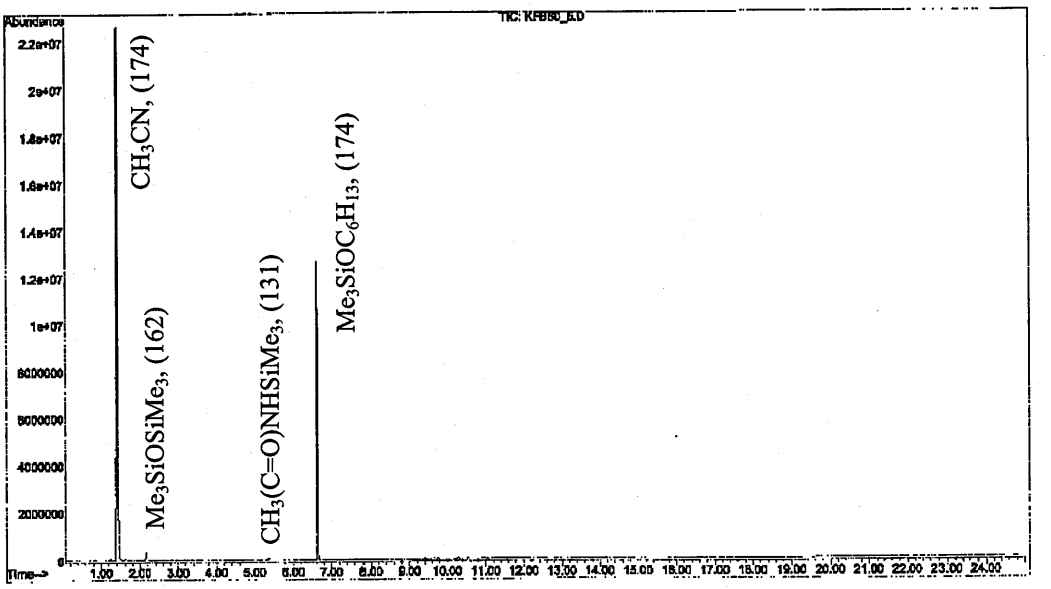

Figure 7.3: Gas chromatography-mass spectrum of trimethylsilylated hexanol.[1]

[1] Refer to Experimental section 7.3.3.

7.2 Biocatalysis Study

7.2.1 Enzyme-Catalysed Condensation Study

Prior to reaction, the glass vials were rinsed with acetone (x2) and ethanol (x2), dried, and silylated with hexamethyldisilazane (1 mmol) in the presence of acetic acid (0.2 mmol) for 30 m at 25°C. Subsequently, the vials were rinsed with ethanol (x2) and dried in an oven at 110°C. The silylated glass vials were confirmed not to contaminate the reactions with trimethylsilanol or hexamethyldisiloxane (Table 7.4). The reactions were formulated with a 5:1 trimethylsilanol (225 mg) to protein (45 mg lipase, protease, or BSA) weight ratio in 1.3 mL toluene or 1.1 mL water. Toluene was dried over lithium aluminum hydride ('dry toluene', 11 ppm water) and hydrated with Milli-Q water ('wet toluene', 467 ppm water). Karl Fischer titrations were performed on an Aquatest IV titrator (Photovolt Corporation, New York, NY) to measure the water content in toluene. Milli-Q water ('water') was buffered with 50 mM Tris-HCl buffer, pH 7.0 ('buffered pH 7'). The estimated solubility of trimethylsilanol in water is 4.2% (i.e. 42.56 mg/mL) [4].

Based on the formulation, the two-phase reactions conducted in water were saturated with trimethylsilanol (~200 mg/mL). The closed (screw capped) reactions were conducted in inert glass vials at 25°C with magnetic stirring for 6 days. The reaction products were isolated and quantitatively analysed by GC. Prior to analysis, the aqueous reactions were extracted (x2) with THF [5] in the presence of NaCl and filtered through a Whatman Autovial® 5 0.45 μm Teflon® filter (#AV115NPUORG). The toluene reactions were filtered and analysed directly by GC.

7.2.2 Protease-Catalysed Silanol Reactions

Prior to reaction, the glass vials were silylated as documented in Experimental section 7.2.1. The reactions were formulated with a 4:1 trimethylsilanol (80 mg) to protein (20 mg protease, BSA, or γ-globulins) weight ratio (~1000:1 silanol to protease mole ratio) in 0.5 mL of 50 mM Tris-HCl buffered Milli-Q water, pH 7.0. In the monomer to enzyme mole ratio study, the mole ratios were formulated with a constant amount of trimethylsilanol and a variable amount of trypsin (1-100 mg) in 0.5 mL of 50 mM Tris-HCl buffered Milli-Q water, pH 7.0. In the pH study, the condensation reaction was conducted in 50 mM buffered media from pH 4 to 10. In the soybean-inhibited (Bowman-Birk, BBI and Popcorn, PCI) reactions, excess inhibitor (i.e. > 1:1 (w/w) or 4:1 BBI to protease and 2:1 PCI to protease mole ratios, respectively) was added to the stirred protease solutions 2 hours before the addition of trimethylsilanol. During the temperature studies, the aqueous solutions of trypsin were stirred and equilibrated at set temperatures in a thermostatted water bath (+/- 0.1°C) for 20 minutes prior to reaction. In the thermal denaturation experiments, trypsin was boiled in 50 mM Tris-HCl buffered Milli-Q water (pH 7.0) for defined periods of time before the addition of trimethylsilanol. Based on the estimated solubility of trimethylsilanol in water (42.56 mg/mL), the concentration of trimethylsilanol (~160 mg/mL) saturated the aqueous media and created two-phase

reaction mixtures. Reactions formulated with less than 40 mg/mL trimethylsilanol in water were visually homogeneous. The closed (screw capped) reactions were conducted in inert glass vials at the documented temperatures with magnetic stirring for 3 hours. The time studies of the trypsin-catalysed condensation of trimethylsilanol were conducted for defined periods of time over 24 hours. The reaction products were isolated and quantitatively analysed by GC. Prior to analysis, the aqueous reactions were extracted (x2) with THF [5] in the presence of NaCl and filtered through a Whatman Autovial® 5 0.45 μm Teflon® filter.

7.2.3 Trypsin-Catalysed Alkoxysilane Reactions

Prior to reaction, the glass vials were silylated as documented in Experimental section 7.2.1. The alkoxysilanes (10 mL) were pre-treated with sodium hydrogencarbonate (1 g, 12 mmol) due to the potential presence of residual chloro-functional silanes (Scheme 7.2). Alkoxysilanes are typically synthesized from chlorosilanes [6].

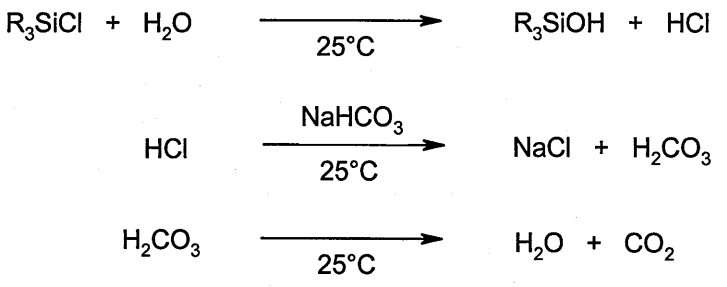

Scheme 7.2: Sodium hydrogencarbonate neutralization of chlorosilanes.

The treatment was performed to prevent the formation of hydrochloric acid due to the rapid hydrolysis of inadvertent chlorosilane contaminates in an aqueous system. Even trace quantities of hydrochloric acid will catalyse the reactions of interest [6]. The reactions were formulated with a 4:1 alkoxysilane (80 mg) to protein (20 mg trypsin, BSA, or γ-globulins) weight ratio in 0.5 mL of 50 mM Tris-HCl buffered Milli-Q water, pH 7.0.

In the soybean-inhibited (Bowman-Birk, BBI and Popcorn, PCI) reactions, excess inhibitor (i.e. > 1:1 (w/w) or 4:1 BBI to protease and 2:1 PCI to protease mole ratios, respectively) was added to the stirred protease solutions 2 hours before the addition of trimethylethoxysilane. In the thermal denaturation experiment, trypsin was boiled for 20 minutes in 50 mM Tris-HCl buffered Milli-Q water (pH 7.0) before the addition of trimethylethoxysilane. The closed (screw capped) two-phase reactions were conducted in inert glass vials at 25°C with magnetic stirring for 3 hours. The time study of the trypsin-catalysed hydrolysis and condensation of trimethylethoxysilane was conducted at 10°C for defined periods of time over 3 hours. The reaction products were isolated and quantitatively analysed by GC. Prior to analysis, the aqueous reactions were extracted (x2) with THF [5] in the presence of NaCl and filtered through a Whatman Autovial® 5 0.45 μm Teflon® filter.

7.2.4 Control Reactions

In this study, control reactions are defined as non-enzymatic reactions. Specifically, experiments conducted in the absence of a protein are defined as negative control reactions. Proteinaceous molecules such as bovine serum albumin and porcine γ-globulins were used to study non-specific protein catalysis.

7.3 Analytical

7.3.1 Electrospray Ionisation Mass Spectrometry

The electrospray MS (ESI MS) spectral data was acquired on a PE Sciex triple quadrupole API 350 mass spectrometer. The instrument has unit (1 Dalton) resolution throughout the mass range (30-4500 Daltons). The samples were prepared at 50 ppm (v/v) solutions in acetonitrile containing 1 mM ammonium acetate (NH_4OAc). The NH_4OAc salt is necessary to form stable and detectable ion-neutral complexes, $[M+ NH_4]^+$. A Harvard Apparatus model 22 syringe pump was used to directly infuse the samples into the electrospray ion source at a constant flow rate of 20 μL/min. The acetonitrile solutions were sprayed at ambient temperature and pressure from a needle biased at 5.5 kV. During the acquisition of the ESI spectra, approximately 20 scans were signal averaged at a rate of 29.7 sec/scan (dwell time = 1 ms, step size=0.1 Da). The gain setting of the electron multiplier detector was approximately 10^5. Since ESI MS is a 'soft' ionization technique, intact pseudomolecular ions, $[M+ NH_4]^+$, are used to determine the structural assignments necessary to characterize the molecules present in a material.

7.3.2 Gas Chromatography–Flame Ionisation Detection

The gas chromatography (GC) analysis was performed with a Hewlett-Packard 6890 Series injector on an HP 6890 plus gas chromatograph with a flame ionisation detector (FID). The system was configured as detailed in Table 7.1. A representative chromatogram is illustrated in Figure 2.8. The chromatographic retention times of the analytes are detailed in Tables 7.2-7.3.

Table 7.1: GC-FID experimental parameters.

Parameter	Setting
Carrier gas	99.9999% (99.9995% high purity helium + Valco Getter)
Detector	Flame ionisation detector at 275 ^{0}C, H_2 = 40 mL/min, Air = 450 mL/min, Make up He = 45 mL/min
GC inlet, split	250 ^{0}C, split ratio = 100:1, constant flow (rate = 1.0 mL/min)
GC column	HP-5MS crosslinked 5% phenyl methyl siloxane film (30m x 0.25mm, 0.25um film)
GC temperature program	50(2) → 250(5) @10^{0}C/min, 30 minute total run time
Internal standard	~1% (w/w) dodecane in THF
data system	Agilent Technologies ChemStation

Dodecane was used as an internal standard to gravimetrically quantify the chromatographic analyses. The samples were prepared at approximately 1% (w/w) product in a THF solution containing 1% (w/w) dodecane. Based on triplicate measurements, the response factors [7] for the analytes were calculated (Equation 7.1) and determined to be linear as a function of concentration over three orders of magnitude (i.e. 0.1-10% (w/w), Table 7.2).

$$RF_{analyte} = ([analyte]/Area_{analyte}) \times (Area_{IS}/[IS]) \times RF_{IS} \qquad \textbf{(7.1)}$$

For example, the linearity of a set of response factors is illustrated in Figure 7.4.

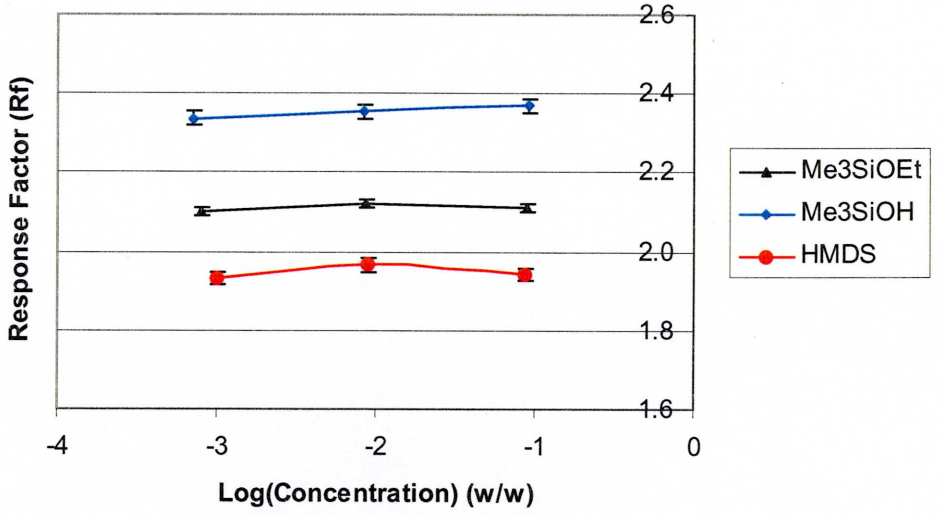

Figure 7.4: Evaluation of the experimental measurement of a response factor versus the concentration of an analyte over three orders of magnitude.[1]

[1] Refer to Table 7.2.

The terms in Equation 7.1 are defined as follows: $RF_{analyte}$ = response factor for the analyte, [analyte] = concentration of the analyte, $Area_{analyte}$ = peak area of the analyte, $Area_{IS}$ = peak area of the internal standard, [IS] = concentration of the internal standard, RF_{IS} = response factor for the internal standard = 1. Subsequently, Equation 7.1 was solved to quantitatively calculate the concentration of an analyte in the presence of an internal standard (Equation 7.2).

$$[analyte] = (Rf_{analyte} \times Area_{analyte}) \times ([IS]/Area_{IS}) \qquad \textbf{(7.2)}$$

Encompassing experimental and instrumental errors, the relative standard deviation of the measurements range between 0.3-10% depending on the concentration and, correspondingly, the yield of the analyte (Table 7.4). Throughout the study, reaction products were isolated and quantitatively analysed by GC. The chromatographic results are detailed in Tables 7.5-7.33.

Table 7.2: GC-FID analyte retention times and response factors.

Analyte[1]	Retention Time (m)	Response Factor (Rf) Average	Standard Deviation	RSD[2]
Me_3SiOEt	2.970	2.110	0.011	0.5%
$Me_3SiOTGME$	16.273	2.584	0.168	6.5%
$Me_3SiOC_6H_{13}$	8.130	1.479	0.0004	0.03%
Me_3SiOH	2.902	2.353	0.016	0.7%
HMDS	3.449	1.947	0.016	0.8%
(epoxy)Me_2SiOEt	13.891	1.982	0.004	0.2%
(epoxy)Me_2SiOH	13.229	---	---	---
epoxy disiloxane	22.159	---	---	---
$[Me_2Si(CH_2)_4O]$	5.434	---	---	---
(carbinol)Me_2SiOH	10.260	---	---	---
Carbinol disiloxane	17.882	---	---	---
$PhMe_2SiOEt$	10.585	1.352	0.003	0.2%
$PhMe_2SiOH$	10.202	---	---	---
phenyl disiloxane	17.746	---	---	---
Ph_3SiOEt	22.461	1.037	0.041	4.0%
(amine)Me_2SiOEt	9.017	2.089	0.132	6.3%
amine disiloxane	15.355	4.603	0.049	1.1%
cyclic siloxane	10.009	2.562	0.022	0.9%
TEOS	8.097	2.063	0.004	0.2%
dodecane	11.422	1.000	---	---

[1] Me_3SiOEt = trimethylethoxysilane, $Me_3SiOTGME$ = trimethylsilylated tetraethylene glycol monomethyl ether, $Me_3SiOC_6H_{13}$ = trimethylsilylated hexanol, Me_3SiOH = trimethylsilanol, HMDS = hexamethyldisiloxane, (epoxy)Me_2SiOEt = 3-glycidoxypropyldimethylethoxysilane, (epoxy)Me_2SiOH = 3-glycidoxypropyldimethylsilanol, epoxy disiloxane = diglycidoxypropyltetramethyldisiloxane, $[Me_2Si(CH_2)_4O]$ = 1,1-dimethyl-1-sila-2-oxacyclohexane, (carbinol)Me_2SiOH = hydroxybutyldimethylsilanol, carbinol disiloxane = dihydroxybutyltetramethyldisiloxane, $PhMe_2SiOEt$ = phenyldimethylethoxysilane, $PhMe_2SiOH$ = phenyldimethylsilanol, phenyl disiloxane = diphenyltetramethyldisiloxane, Ph_3SiOEt = triphenylethoxysilane, (amine)Me_2SiOEt = aminopropyldimethylethoxysilane, amine disiloxane = diaminopropyltetramethyldisiloxane, cyclic siloxane = heptamethylhydroxytetracyclosiloxane, TEOS = tetraethoxysilane, dodecane = internal standard.

[2] RSD = relative standard deviation (i.e. standard deviation/average).

Table 7.3: GC-FID cyclic siloxane retention times.

	Retention Time (m)		
Cyclic Siloxane	Cyclic Trimer	Cyclic Tetramer	Cyclic Pentamer
Dimethyl: $[D]_3$[1], $[D]_4$[2]	5.275	8.199	
trifluoropropylmethyl: $[D(TFP)]_3$[3], $[D(TFP)]_4$[4]	11.646, 11.717	14.660, 14.755	17.040, 17.133
phenylmethyl: $[D(Ph)]_4$[5]		29.168, 29.521, 29.879	

1 $[D]_3$ = hexamethylcyclotrisiloxane = dimethyl cyclic trimer.
2 $[D]_4$ = octamethylcyclotetrasiloxane = dimethyl cyclic tetramer.
3 $[D(TFP)]_3$ = 1,3,5-trimethyl-1,3,5-tri(3,3,3-trifluoropropyl)cyclotrisiloxane = trifluoropropylmethyl cyclic trimer.
4 $[D(TFP)]_4$ = 1,3,5,7-tetramethyl-1,3,5,7-tetra(3,3,3-trifluoropropyl)cyclotetrasiloxane = trifluoropropylmethyl cyclic tetramer.
5 $[D(Ph)]_4$ = 2,4,6,8-tetramethyl-2,4,6,8-tetraphenyl-cyclotetrasiloxane = phenylmethyl cyclic tetramer.

Table 7.4: Relative standard deviation of an analyte in a gas chromatogram.

	Reactant (μmol)	Outcome (μmol)		% Yield	
Replicate Reaction[1]	Me_3SiOH[2]	Me_3SiOH[2]	HMDS[3]	Me_3SiOH[2]	HMDS[3]
negative control	944	932	3.8	98.7	0.8
negative control	911	900	3.3	98.8	0.7
negative control	900	890	4.0	98.9	0.9
negative control	944	934	4.3	98.9	0.9
negative control	911	893	3.7	98.1	0.8
			Average =	98.7	0.8
			Standard Deviation =	0.3	0.08
			Relative Standard Deviation[4] =	0.3%	10%

1 Refer to Experimental section 7.2.2.
2 Me_3SiOH = trimethylsilanol.
3 HMDS = hexamethyldisiloxane.
4 Relative Standard Deviation = standard deviation/average.

Table 7.5: Study of the extraction efficiency of trimethylsilanol and hexamethyldisiloxane with different organic solvents.[1]

	Reactant (μmol)	Outcome (μmol)		% Yield		% Extraction
Extraction	Me_3SiOH[2]	Me_3SiOH[2]	HMDS[3]	Me_3SiOH[2]	HMDS[3]	Efficiency
diethylether, extraction #1	903	816	4	90	1	91
diethylether, extraction #2	903	122	< 1	14	< 1	14
					Total =	**105**
tetrahydrofuran, extraction #1	900	864	4	96	1	97
tetrahydrofuran, extraction #2	900	26	0	3	0	3
					Total =	**100**
methylene chloride, extraction #1	903	528	3	58	1	59
methylene chloride, extraction #2	903	195	1	22	< 1	22
					Total =	**81**
toluene, extraction #1	903	378	2	42	< 1	42
toluene, extraction #2	903	88	< 1	10	< 1	10
					Total =	**52**

[1] Refer to Experimental sections 7.2.2. Prior to extraction, the reactions were conducted in the absence of a protein (i.e. negative control reactions).
[2] Me_3SiOH = trimethylsilanol.
[3] HMDS = hexamethyldisiloxane.

Table 7.6: Enzyme-catalysed condensation study of trimethylsilanol after six days in dry toluene.[1]

	Reactant (μmol)	Outcome (μmol)		% Yield		Normalized Yield[2]	
Reaction	Me_3SiOH[3]	Me_3SiOH[3]	HMDS[4]	Me_3SiOH[3]	HMDS[4]	Me_3SiOH[3]	HMDS[4]
Me_3SiOH, raw material						(99.8)	(0.2)
negative control	2030	1690	4	83	< 1	99.5	0.5
bovine serum albumin	903	619	23	69	5	93	7
α-chymotrypsin	944	548	114	68	7	71	29
trypsin[5]	967	571	75	59	15	79	21
porcine pancreatic lipase	2030	1640	45	81	4	95	5
Candida antarctica lipase B[6]	2030	1710	45	84	4	95	5
Rhizomucor miehei lipase	2030	1680	28	83	3	97	3
wheat germ lipase	2030	1580	15	78	2	98	2
Candida antarctica lipase	2030	1750	15	86	2	98	2
Mucor javanicus lipase	2030	1830	11	90	1	99	1
Aspergillus niger lipase	2030	1660	8	82	1	99	1
phospholipase A2	2030	1890	5	93	1	99	1
Pseudomonas fluorescens lipase	2030	1550	5	76	1	99	1
Penicillium roqueforti lipase	2030	1600	4	79	< 1	99	1
Pseudomonas cepacia lipase	2030	1810	4	89	< 1	99	< 1
Candida lipolytica lipase	2030	1710	3	84	< 1	99	< 1

1 Refer to Experimental sections 7.2.1.
2 Normalized Yield = the normalized quantitative and qualitative (i.e. area percent) yield values are outside and inside of the parenthesis, respectively.
3 Me_3SiOH = trimethylsilanol.
4 HMDS = hexamethyldisiloxane.
5 trypsin treated with N-tosyl-L-phenylalanine chloromethyl ketone (TPCK).
6 *Candida antarctica* lipase B was immobilized on acrylic resin beads (Novozym® 435).

Table 7.7: Enzyme-catalysed condensation study of trimethylsilanol after six days in wet toluene.[1]

	Reactant (μmol)	Outcome (μmol)		% Yield		Normalized Yield[2]	
Reaction	Me_3SiOH[3]	Me_3SiOH[3]	HMDS[4]	Me_3SiOH[3]	HMDS[4]	Me_3SiOH[3]	HMDS[4]
Me_3SiOH, raw material						(99.8)	(0.2)
negative control	2030	1270	2	62	< 1	99.7	0.3
bovine serum albumin	903	530	21	59	5	93	7
α-chymotrypsin	903	489	87	54	19	74	26
trypsin[5]	922	569	93	62	20	75	25
wheat germ lipase	2030	945	155	47	15	75	25
Candida antarctica lipase	2030	744	52	37	5	88	12
Rhizomucor miehei lipase	2030	1660	48	82	5	94	6
Candida antarctica lipase B[6]	2030	1350	8	66	1	99	1
Mucor javanicus lipase	2030	1390	8	69	1	99	1
Aspergillus niger lipase	2030	1970	7	97	1	99	1
porcine pancreatic lipase	2030	345	2	17	< 1	99	1
Penicillium roqueforti lipase	2030	1440	3	71	< 1	99	< 1
Pseudomonas fluorescens lipase	2030	1610	3	79	< 1	99	< 1
Candida lipolytica lipase	2030	1740	3	86	< 1	99	< 1
Pseudomonas cepacia lipase	2030	1130	2	55	< 1	99	< 1

1 Refer to Experimental sections 7.2.1.
2 Normalized Yield = the normalized quantitative and qualitative (i.e. area percent) yield values are outside and inside of the parenthesis, respectively.
3 Me_3SiOH = trimethylsilanol.
4 HMDS = hexamethyldisiloxane.
5 trypsin treated with N-tosyl-L-phenylalanine chloromethyl ketone (TPCK).
6 *Candida antarctica* lipase B was immobilized on acrylic resin beads (Novozym® 435).

Table 7.8: Enzyme-catalysed condensation study of trimethylsilanol after six days in water.[1]

	Reactant (μmol)	Outcome (μmol)		% Yield		Normalized Yield[2]	
Reaction	Me_3SiOH[3]	Me_3SiOH[3]	HMDS[4]	Me_3SiOH[3]	HMDS[4]	Me_3SiOH[3]	HMDS[4]
Me_3SiOH, raw material						(99.8)	(0.2)
negative control	2030	635	8	31	1	97	3
bovine serum albumin	903	514	12	57	3	96	4
trypsin[5]	944	6	442	1	94	1	99
α-chymotrypsin	2030	2	122	< 1	12	1	99
Rhizomucor miehei lipase	2030	22	626	1	62	2	98
Candida antarctica lipase B[6]	2030	9	103	< 1	10	4	96
Candida antarctica lipase	2030	123	128	6	13	32	68
wheat germ lipase	2030	249	63	12	6	66	34
phospholipase A2	2030	700	89	34	9	80	20
porcine pancreatic lipase	2030	1280	68	63	7	90	10
Candida lipolytica lipase	2030	781	31	38	3	93	7
Mucor javanicus lipase	2030	1220	38	60	4	94	6
Pseudomonas fluorescens lipase	2030	401	10	20	1	95	5
Pseudomonas cepacia lipase	2030	1260	17	62	2	97	3
Aspergillus niger lipase	2030	1060	14	52	1	97	3
Penicillium roqueforti lipase	2030	963	7	47	1	98	2

1 Refer to Experimental sections 7.2.1.
2 Normalized Yield = the normalized quantitative and qualitative (i.e. area percent) yield values are outside and inside of the parenthesis, respectively.
3 Me_3SiOH = trimethylsilanol.
4 HMDS = hexamethyldisiloxane.
5 trypsin treated with N-tosyl-L-phenylalanine chloromethyl ketone (TPCK).
6 *Candida antarctica* lipase B was immobilized on acrylic resin beads (Novozym® 435).

Table 7.9: Enzyme-catalysed condensation study of trimethylsilanol after six days in buffered pH 7.[1]

	Reactant (μmol)	Outcome (μmol)		% Yield		Normalized Yield[2]	
Reaction	Me_3SiOH[3]	Me_3SiOH[3]	HMDS[4]	Me_3SiOH[3]	HMDS[4]	Me_3SiOH[3]	HMDS[4]
Me_3SiOH, raw material	89	87	0.3	98	1	99	1
negative control	856	801	19	94	5	96	4
bovine serum albumin	903	514	12	57	3	95	5
trypsin[4]	922	6	425	1	92	1	99
α-chymotrypsin	967	6	454	1	94	1	99
Candida antarctica lipase	903	294	64	33	14	70	30
Candida antarctica lipase B[5]	944	570	36	60	8	89	11
Rhizomucor miehei lipase	903	406	23	45	5	90	10
wheat germ lipase	903	343	18	38	4	90	10
phospholipase A2	878	707	29	81	7	93	7
porcine pancreatic lipase	903	425	16	47	4	93	7

1 Refer to Experimental sections 7.2.1.
2 Me_3SiOH = trimethylsilanol.
3 HMDS = hexamethyldisiloxane.
4 trypsin treated with N-tosyl-L-phenylalanine chloromethyl ketone (TPCK).
5 *Candida antarctica* lipase B was immobilized on acrylic resin beads (Novozym® 435).

Table 7.10: Protease-catalysed condensation study of trimethylsilanol after three hours.[1]

	Reactant (μmol)	Outcome (μmol)		% Yield	
Reaction	Me_3SiOH[2]	Me_3SiOH[2]	HMDS[3]	Me_3SiOH[2]	HMDS[3]
trypsin, bovine pancreas	811	94	354	12	87
α-chymotrypsin, bovine pancreas	1210	366	371	30	61
elastase, porcine pancreas	911	879	4	97	1
subtilisin, *B. licheniformis*	933	873	4	94	1
papain, papaya latex	944	865	14	92	3
cathepsin L, bovine kidney	267	259	1	97	1
cathepsin L, human liver	244	241	1	99	1
cathepsin L, *Paramecium tetraurelia*	211	205	1	97	1
pepsin, hog stomach	956	911	19	95	4
carboxypeptidase B, porcine pancreas	567	524	2	92	1

1 Refer to Experimental sections 7.2.2.
2 Me_3SiOH = trimethylsilanol.
3 HMDS = hexamethyldisiloxane.

Table 7.11: Condensation control reactions with trimethylsilanol after three hours.[1]

	Reactant (μmol)	Outcome (μmol)		% Yield	
Reaction	Me_3SiOH[2]	Me_3SiOH[2]	HMDS[3]	Me_3SiOH[2]	HMDS[3]
Me_3SiOH, raw material	89	87	0.3	98	1
negative control	900	890	4	99	1
bovine serum albumin	889	845	3	95	1
γ-globulins	911	843	4	93	1
calcium chloride, $CaCl_2$	933	921	4	99	1
imidazole	911	847	5	93	1
N-methylimidazole	911	841	3	92	1
poly-L-lysine	878	829	6	94	1
α-chymotrypsin, bovine pancreas	1210	366	371	30	61
trypsin, bovine pancreas	811	94	354	12	87

1 Refer to Experimental sections 7.2.2.
2 Me_3SiOH = trimethylsilanol.
3 HMDS = hexamethyldisiloxane.

Table 7.12: The use of N-α-*p*-tosyl-L-lysine chloromethyl ketone hydrochloride (TLCK) and N-tosyl-L-phenylalanine chloromethyl ketone (TPCK) to assess the proteolytic impurity of α-chymotrypsin and trypsin during the condensation of trimethylsilanol.[1]

	Reactant (μmol)	Outcome (μmol)		% Yield	
Reaction	Me_3SiOH[2]	Me_3SiOH[2]	HMDS[3]	Me_3SiOH[2]	HMDS[3]
α-chymotrypsin, bovine pancreas	1210	366	371	30	61
α-chymotrypsin, treated with TLCK	933	786	74	84	16
TLCK[4]	889	720	77	81	17
trypsin, bovine pancreas	811	94	354	12	87
trypsin, treated with TPCK	922	116	402	13	87
TPCK[5]	933	926	4	99	1

1 Refer to Experimental sections 7.2.2.
2 Me_3SiOH = trimethylsilanol.
3 HMDS = hexamethyldisiloxane.
4 TLCK = N-α-p-tosyl-L-lysine chloromethyl ketone hydrochloride.
5 TPCK = N-tosyl-L-phenylalanine chloromethyl ketone.

Table 7.13: Proteinaceous inhibition of the condensation of trimethylsilanol.[1]

	Reactant (μmol)	Outcome (μmol)		% Yield	
Reaction	Me_3SiOH[2]	Me_3SiOH[2]	HMDS[3]	Me_3SiOH[2]	HMDS[3]
Bowman-Birk inhibitor (BBI)	956	917	4	96	1
Popcorn inhibitor (PCI)	911	902	4	99	1
α-chymotrypsin, bovine pancreas	1210	366	371	30	61
α-chymotrypsin + BBI	933	821	11	88	2
α-chymotrypsin + PCI	922	916	5	99	1
trypsin, treated with TPCK	922	116	402	13	87
trypsin (TPCK)[4] + BBI	933	903	9	97	2
trypsin (TPCK)[4] + PCI	933	918	5	98	1

1 Refer to Experimental sections 7.2.2.
2 Me_3SiOH = trimethylsilanol.
3 HMDS = hexamethyldisiloxane.
4 trypsin (TPCK) = TPCK treated trypsin.

Table 7.14: The effect of temperature on the trypsin-catalysed condensation of trimethylsilanol.[1]

	Reactant (μmol)	Outcome (μmol)		% Yield	
Reaction	Me_3SiOH[2]	Me_3SiOH[2]	HMDS[3]	Me_3SiOH[2]	HMDS[3]
10°C, trypsin (TPCK)[4]	867	297	278	34	64
10°C, control	911	905	4	99	1
25°C, trypsin (TPCK)[4]	922	116	402	13	87
25°C, control	900	890	4	99	1
25°C, boiled trypsin (TPCK)[4], 20 m	944	644	131	68	28
25°C, boiled trypsin (TPCK)[4], 3 h	922	874	13	95	3
35°C, trypsin (TPCK)[4]	867	140	361	16	83
35°C, control	1040	1020	5	98	1
50°C, trypsin (TPCK)[4]	911	178	360	20	79
50°C, control	967	944	6	98	1

1 Refer to Experimental sections 7.2.2.
2 Me_3SiOH = trimethylsilanol.
3 HMDS = hexamethyldisiloxane.
4 trypsin (TPCK) = TPCK treated trypsin.

Table 7.15: Trypsin-catalysed condensation of trimethylsilanol at 25°C.[1]

	Reactant (μmol)	Outcome (μmol)		% Yield	
Time (h)	Me_3SiOH[2]	Me_3SiOH[2]	HMDS[3]	Me_3SiOH[2]	HMDS[3]
0.08	856	819	17	96	4
0.25	922	827	39	90	8
0.50	944	811	66	86	14
0.75	933	704	90	75	19
1.00	956	721	114	75	24
2.00	922	469	230	50	50
3.00	922	116	402	13	87
9.00	911	35	428	4	94
22.00	933	13	447	1	96

1 Refer to Experimental sections 7.2.2.
2 Me_3SiOH = trimethylsilanol.
3 HMDS = hexamethyldisiloxane.

Table 7.16: Trypsin-catalysed hydrolysis of hexamethyldisiloxane at 25°C.[1]

	Reactant (μmol)	Outcome (μmol)		% Yield	
Reaction	HMDS[2]	Me_3SiOH[3]	HMDS[2]	Me_3SiOH[3]	HMDS[2]
negative control[1], buffered pH = 7.0	469	0	468	0	100
trypsin (TPCK)[4], buffered pH = 7.0	457	0	457	0	100
negative control[1], toluene	469	0	470	0	100
trypsin (TPCK)[4], toluene	475	0	462	0	97

1 Refer to Experimental sections 7.2.2. The negative control reactions were performed in the absence of trypsin. The organic reactions were conducted in 0.5 mL of toluene.
2 HMDS = hexamethyldisiloxane.
3 Me_3SiOH = trimethylsilanol.
4 trypsin (TPCK) = TPCK treated trypsin.

Table 7.17: Recycled trypsin-catalysed condensation of trimethylsilanol at 25°C.[1]

	Reactant (μmol)[2]	Outcome (μmol)		% Yield	
Reaction	Me_3SiOH[3]	Me_3SiOH[3]	HMDS[4]	Me_3SiOH[3]	HMDS[4]
negative control	1831 = 888 + 943	1810	11	99	1
recycled trypsin (TPCK)	1880 = 923 + 957	433	719	23	76

1 Refer to Experimental sections 7.2.2. Following the completion of the first three-hour reaction with trimethylsilanol, another 80 mg aliquot of reactant was added to the two-phase reaction mixture for an additional three-hour reaction.
2 The total amount of reactant (μmol) is equal to the sum of the two aliquots of Me_3SiOH in the recycled trypsin-catalysed condensation of trimethylsilanol study.
3 Me_3SiOH = trimethylsilanol.
4 HMDS = hexamethyldisiloxane.

Table 7.18: Study of the condensation of a saturated-solution of trimethylsilanol as a function of the amount of trypsin at 25°C.[1]

M:E[2] (mol/mol)	M:E[2] (w/w)	Trypsin[3] (mg/mL)	Reactant (μmol) Me_3SiOH[4]	Outcome (μmol) Me_3SiOH[4]	Outcome (μmol) HMDS[5]	% Yield Me_3SiOH[4]	% Yield HMDS[5]
222	1:1	198	944	18	451	2	96
411	2:1	102	900	53	408	6	91
1023	5:1	38	922	116	402	13	87
2199	10:1	20	944	863	42	91	9
4295	20:1	10	922	878	6	95	1
7245	40:1	6	933	904	5	97	1
22253	100:1	2	956	934	5	98	1

1 Refer to Experimental sections 7.2.2.
2 M:E = monomer to enzyme ratio.
3 Trypsin = TPCK treated trypsin.
4 Me_3SiOH = trimethylsilanol.
5 HMDS = hexamethyldisiloxane.

Table 7.19: Trypsin-catalysed condensation of non-saturated solutions of trimethylsilanol at 25°C.[1]

		Reactant (μmol)	Outcome (μmol)		% Yield	
Me_3SiOH[2]	Time (m)	Me_3SiOH[2]	Me_3SiOH[2]	HMDS[3]	Me_3SiOH[2]	HMDS[3]
~40 mg/mL	15	246	161	42	66	34
	30	208	100	53	48	51
	45	216	84	66	39	61
	60	218	75	71	34	65
~37 mg/mL	15	197	76	59	39	60
	30	219	55	81	25	74
	45	177	41	67	23	76
	60	222	40	91	18	82
~31 mg/mL	15	167	69	48	42	58
	30	179	52	63	29	71
	45	168	41	63	25	75
	60	184	34	75	18	82
~20 mg/mL	15	129	95	17	74	26
	30	112	70	21	62	37
	45	116	56	29	48	51
	60	123	49	37	39	60
~10 mg/mL	15	52	44	4	84	16
	30	60	42	8	71	28
	45	64	44	10	68	31
	60	58	39	9	67	33

[1] Refer to Experimental section 7.2.2. The amount of trimethylsilanol (~10-40 mg/mL) was adjusted to create homogeneous solutions in 40-mg/mL neutral (pH 7.0) solutions of trypsin.

[2] Me_3SiOH = trimethylsilanol.

[3] HMDS = hexamethyldisiloxane.

Table 7.20: Trypsin-catalysed condensation of non-saturated solutions of trimethylsilanol at 15°C.[1]

		Reactant (μmol)	Outcome (μmol)		% Yield	
Me_3SiOH[2]	Time (m)	Me_3SiOH[2]	Me_3SiOH[2]	HMDS[3]	Me_3SiOH[2]	HMDS[3]
~29 mg/mL	15	169	103	33	61	39
	30	156	70	42	45	54
	45	158	63	47	40	60
	60	166	55	55	33	66
~26 mg/mL	15	148	92	28	63	37
	30	136	61	37	45	54
	45	140	65	37	46	53
	60	149	56	46	38	62
~20 mg/mL	15	122	81	21	66	34
	30	114	63	25	55	44
	45	108	53	28	49	51
	60	102	47	28	46	54
~15 mg/mL	15	72	57	8	79	21
	30	67	45	11	68	32
	45	84	42	21	50	49
	60	114	50	32	44	55

1 Refer to Experimental section 7.2.2. The amount of trimethylsilanol (~15-29 mg/mL) was adjusted to create homogeneous solutions in 40-mg/mL neutral (pH 7.0) solutions of trypsin.

2 Me_3SiOH = trimethylsilanol.

3 HMDS = hexamethyldisiloxane.

Table 7.21: Rates of the trypsin-catalysed condensation of non-saturated solutions of trimethylsilanol at 25°C.[1]

Me_3SiOH[2]	Reactant average [Me_3SiOH]	Rate of Condensation V = M/m
~40 mg/mL	0.44	0.0032
~37 mg/mL	0.41	0.0022
~31 mg/mL	0.35	0.0024
~20 mg/mL	0.24	0.0018
~10 mg/mL	0.12	0.0008

1 Refer to Experimental section 7.2.2. The amount of trimethylsilanol (~10-40 mg/mL) was adjusted to create homogeneous solutions in 40-mg/mL neutral (pH 7.0) solutions of trypsin.
2 Me_3SiOH = trimethylsilanol.

Table 7.22: Rates of the trypsin-catalysed condensation of non-saturated solutions of trimethylsilanol at 15°C.[1]

Me_3SiOH[2]	Reactant average [Me_3SiOH]	Rate of Condensation V = M/m
~29 mg/mL	0.32	0.0020
~26 mg/mL	0.29	0.0016
~20 mg/mL	0.22	0.0013
~15 mg/mL	0.17	0.0010

1 Refer to Experimental section 7.2.2. The amount of trimethylsilanol (~15-29 mg/mL) was adjusted to create homogeneous solutions in 40-mg/mL neutral (pH 7.0) solutions of trypsin.
2 Me_3SiOH = trimethylsilanol.

Table 7.23: Trypsin-catalysed condensation of non-saturated solutions of trimethylsilanol between 6-25°C.[1]

		Reactant (μmol)	Outcome (μmol)		% Yield	
Temperature	Time (m)	Me_3SiOH[2]	Me_3SiOH[2]	HMDS[3]	Me_3SiOH[2]	HMDS[3]
25°C	15	167	69	48	42	58
	30	179	52	63	29	71
	45	168	41	63	25	75
	60	184	34	75	18	82
20°C	15	171	70	50	41	59
	30	174	40	67	23	77
	45	182	39	72	21	79
	60	182	23	80	13	87
15°C	15	169	103	33	61	39
	30	156	70	42	45	54
	45	158	63	47	40	60
	60	166	55	55	33	66
10°C	15	190	111	39	58	41
	30	179	74	52	41	58
	45	193	67	63	34	65
	60	182	46	68	25	74
6°C	15	176	121	27	69	30
	30	177	92	42	52	48
	45	174	93	40	53	46
	60	173	64	55	37	63

1 Refer to Experimental section 7.2.2. The amount of trimethylsilanol (~30 mg/mL) was adjusted to create homogeneous solutions in 40-mg/mL neutral (pH 7.0) solutions of trypsin.

2 Me_3SiOH = trimethylsilanol.

3 HMDS = hexamethyldisiloxane.

Table 7.24: Rates of the trypsin-catalysed condensation of non-saturated solutions of trimethylsilanol between 6-25°C.[1]

Temperature (°C)	Average [Me_3SiOH]	Rate (V = M/m)	Rate Constant ($k_R = s^{-1}$)
25	0.35	0.0024	0.023
20	0.35	0.0021	0.020
15	0.32	0.0020	0.019
10	0.37	0.0026	0.025
6	0.35	0.0022	0.021

[1] Refer to Experimental section 7.2.2. The amount of trimethylsilanol (~30 mg/mL) was adjusted to create homogeneous solutions in 40-mg/mL neutral (pH 7.0) solutions of trypsin.

Table 7.25: The effect of pH on the trypsin-catalysed condensation of trimethylsilanol at 25°C.[1]

	Reactant (μmol)	Outcome (μmol)		% Yield	
Reaction	Me_3SiOH[2]	Me_3SiOH[2]	HMDS[3]	Me_3SiOH[2]	HMDS[3]
pH 4, control	922	541	173	59	38
pH 4, trypsin (TPCK)[4]	778	475	128	61	33
pH 5, control	933	866	26	93	6
pH 5, trypsin (TPCK)[4]	956	870	42	91	9
pH 6, control	922	910	6	99	1
pH 6, trypsin (TPCK)[4]	956	454	252	48	53
pH 7, control	900	890	4	99	1
pH 7, trypsin (TPCK)[4]	922	116	402	13	87
pH 7.5, control	922	907	3	97	1
pH 7.5, trypsin (TPCK)[4]	944	790	74	84	16
pH 8, control	933	925	4	99	1
pH 8, trypsin (TPCK)[4]	889	857	4	96	1
pH 9, control	900	885	5	98	1
pH 9, trypsin (TPCK)[4]	922	909	4	99	1
pH 10, control	933	824	28	88	6
pH 10, trypsin (TPCK)[4]	933	896	8	96	2

[1] Refer to Experimental sections 7.2.2.
[2] Me_3SiOH = trimethylsilanol.
[3] HMDS = hexamethyldisiloxane.
[4] trypsin (TPCK) = TPCK treated trypsin.

Table 7.26: Hydrolysis and condensation control reactions of trimethylethoxysilane after three hours at 25°C.[1]

	Reactant (μmol)	Outcome (μmol)			% Yield		
Reaction	Me_3SiOEt[2]	Me_3SiOEt[2]	Me_3SiOH[3]	HMDS[4]	Me_3SiOEt[2]	Me_3SiOH[3]	HMDS[4]
Me_3SiOEt, raw material	68	65	0.5	1	96	1	3
negative control	669	529	118	10	79	18	3
bovine serum albumin	593	341	208	8	57	35	3
γ-globulins	627	317	250	9	51	40	3
calcium chloride, $CaCl_2$	644	590	1	10	92	< 1	3
imidazole	678	654	1	11	96	< 1	3
N-methylimidazole	661	614	1	10	93	< 1	3
poly-L-lysine	669	16	613	13	2	92	4
trypsin, bovine pancreas	627	0	86	268	0	14	86
TPCK[5]	653	455	168	9	70	26	3
Trypsin[6], treated with TPCK	627	0	52	262	0	8	84

1 Refer to Experimental sections 7.2.3.
2 Me_3SiOEt = trimethylethoxysilane.
3 Me_3SiOH = trimethylsilanol.
4 HMDS = hexamethyldisiloxane.
5 TPCK = N-tosyl-L-phenylalanine chloromethyl ketone
6 plotted in Figure 4.2.

Table 7.27: Trypsin-catalysed hydrolysis and condensation of trimethylethoxysilane at 10°C.[1]

	Reactant (μmol)	Outcome (μmol)			% Yield		
Time (h)	Me_3SiOEt[2]	Me_3SiOEt[2]	Me_3SiOH[3]	HMDS[4]	Me_3SiOEt[2]	Me_3SiOH[3]	HMDS[4]
0.00	632	608	5	9	96	1	3
0.17	644	151	473	10	24	73	3
0.33	627	58	541	10	9	86	3
0.50	636	10	549	35	2	86	11
0.67	644	13	533	48	2	83	15
0.83	610	12	512	39	2	84	13
1.00	644	11	497	68	2	77	21
1.50	627	11	396	108	2	63	35
2.00	619	6	309	143	1	50	46
2.50	653	7	292	175	1	45	54
3.00	619	11	167	209	2	27	68
24.00	627	4	17	301	1	3	96

1 Refer to Experimental sections 7.2.3.
2 Me_3SiOEt = trimethylethoxysilane.
3 Me_3SiOH = trimethylsilanol.
4 HMDS = hexamethyldisiloxane.

Table 7.28: Trypsin-catalysed hydrolysis and condensation of trimethylalkoxysilanes at 25°C.[1]

	Reactant (μmol)	Outcome (μmol)			% Yield		
Reaction	Me_3SiOR[2]	Me_3SiOR[2]	Me_3SiOH[3]	HMDS[4]	Me_3SiOR[2]	Me_3SiOH[3]	HMDS[4]
Me_3SiOEt, control	669	529	118	10	79	18	3
Me_3SiOEt, trypsin-reaction	627	0	52	262	0	8	84
$Me_3SiOC_6H_{13}$, control	471	427	13	5	91	3	2
$Me_3SiOC_6H_{13}$, trypsin-reaction	437	227	174	5	52	40	3
$Me_3SiOTGME$, control	343	0	284	26	0	83	15
$Me_3SiOTGME$, trypsin-reaction	350	0	168	90	0	48	51

1 Refer to Experimental sections 7.2.3.
2 Me_3SiOR = trimethylalkoxysilane, where R = ethyl (Et), hexyl (C_6H_{13}), or TGME = $(CH_2CH_2O)_4CH_3$.
3 Me_3SiOH = trimethylsilanol.
4 HMDS = hexamethyldisiloxane.

Table 7.29: Trypsin-catalysed hydrolysis and condensation of ethoxysilanes at 25°C.[1]

	Reactant (μmol)	Outcome (μmol)			% Yield[2]		
Reaction	R_3SiOEt[3]	R_3SiOEt[3]	R_3SiOH[4]	$R_3SiOSiR_3$[5]	R_3SiOEt[3]	R_3SiOH[4]	$R_3SiOSiR_3$[5]
Me_3SiOEt, control	669	529	118	10	79	18	3
Me_3SiOEt, trypsin-reaction	627	0	52	262	0	8	84
$PhMe_2SiOEt$, control	483	461			95 (98)	(1)	(1)
$PhMe_2SiOEt$, trypsin-reaction	528	12			2 (2)	(96)	(2)
Ph_3SiOEt, control	322	312			97 (100)	(0)	(0)
Ph_3SiOEt, trypsin-reaction	322	318			99 (100)	(0)	(0)
$(CH_2OCHCH_2O(CH_2)_3)Me_2SiOEt$, control	343	185			54 (54)	(44)	(2)
$(CH_2OCHCH_2O(CH_2)_3)Me_2SiOEt$, trypsin-reaction	343	1			< 1 (< 1)	(58)	(41)
$(H_2NCH_2CH_2CH_2)Me_2SiOEt$, control	509	< 1		250	< 1 (< 1)	(0)	98 (99)
$(H_2NCH_2CH_2CH_2)Me_2SiOEt$, trypsin-reaction	516	< 1		256	< 1 (< 1)	(0)	99 (99)

1 Refer to Experimental sections 7.2.3.
2 % Yield = = the quantitative and qualitative (i.e. area percent) values are outside and inside of the parenthesis, respectively.
3 R_3SiOEt = ethoxysilane.
4 R_3SiOH = silanol.
5 $R_3SiOSiR_3$ = disiloxane.

Table 7.30: Trypsin-catalysed hydrolysis and condensation of alternate organosilicon molecules at 25°C.[1]

		Outcome (μmol)			% Yield[2]		
Reaction	Reactant (μmol)	Reactant	Silanol	Product	Reactant	Silanol	Product
Me_3SiOEt, control	669	529	118	10	79	18	3
Me_3SiOEt, trypsin-reaction	627	0	52	262	0	8	84
$[Me_2Si(CH_2)_4O]$[2], control	707				(48)	(51)	(1)
$[Me_2Si(CH_2)_4O]$[2], trypsin-reaction	685				(19)	(10)	(71)
$[(Me_2SiO)_3(Me(HO)SiO)_1]$[3], control	322	N/A	314		N/A	98	(0)
$[(Me_2SiO)_3(Me(HO)SiO)_1]$[3], trypsin-reaction	403	N/A	399		N/A	99	(0)
tetraethoxysilane, control	447	446			100		
tetraethoxysilane, trypsin-reaction	452	446			99		

1 Refer to Experimental sections 7.2.3.
2 % Yield = the quantitative and qualitative (i.e. area percent) values are outside and inside of the parenthesis, respectively.
3 $[Me_2Si(CH_2)_4O]$ = 1,1-dimethyl-1-sila-2-oxacyclohexane.
4 $[(Me_2SiO)_3(Me(HO)SiO)_1]$ = heptamethylhydroxytetracyclosiloxane.
N/A = not applicable.

Table 7.31: Proteinaceous inhibition of trypsin in the hydrolysis and condensation of trimethylethoxysilane at 25°C.[1]

	Reactant (μmol)	Outcome (μmol)			% Yield		
Reaction	Me_3SiOEt[2]	Me_3SiOEt[2]	Me_3SiOH[3]	HMDS[4]	Me_3SiOEt[2]	Me_3SiOH[3]	HMDS[4]
Bowman-Birk inhibitor (BBI)	610	409	164	9	67	27	3
Popcorn inhibitor (PCI)	644	409	195	9	64	30	3
trypsin, treated with TPCK	627	0	52	262	0	8	84
trypsin (TPCK)[5] + BBI	636	151	469	10	24	74	3
trypsin (TPCK)[5] + PCI	636	38	548	9	6	86	3
boiled trypsin (TPCK)[5], 20 m	610	5	387	106	1	64	35

1 Refer to Experimental sections 7.2.3.
2 Me_3SiOEt = trimethylethoxysilane.
3 Me_3SiOH = trimethylsilanol.
4 HMDS = hexamethyldisiloxane.
5 trypsin (TPCK) = trypsin treated with TPCK.

Table 7.32: The hydrolysis and condensation of trimethylethoxysilane by different sources of trypsin at 25°C.[1]

	Reactant (μmol)	Outcome (μmol)			% Yield		
Reaction	Me_3SiOEt[2]	Me_3SiOEt[2]	Me_3SiOH[3]	HMDS[4]	Me_3SiOEt[2]	Me_3SiOH[3]	HMDS[4]
negative control	669	529	118	10	79	18	3
trypsin (TPCK)[5], bovine pancreas	627	0	52	262	0	8	84
trypsin, recombinant bovine	627	12	459	73	2	73	23
trypsin, porcine pancreas	636	3	490	53	1	77	17
trypsin, *Gadus morhua* (Atlantic cod)	644	444	163	9	69	25	3

1 Refer to Experimental sections 7.2.3.
2 Me_3SiOEt = trimethylethoxysilane.
3 Me_3SiOH = trimethylsilanol.
4 HMDS = hexamethyldisiloxane.
5 trypsin (TPCK) = trypsin treated with TPCK.

Table 7.33: The effect of calcium on the trypsin-catalysed condensation of trimethylsilanol at 25°C.[1]

Reaction	Reactant (μmol)	Outcome (μmol)		% Yield	
	Me_3SiOH[2]	Me_3SiOH[2]	HMDS[3]	Me_3SiOH[2]	HMDS[3]
negative control	900	890	4	99	1
negative control, 20 mM $CaCl_2$	944	934	5	99	1
calcium chloride ($CaCl_2$)	933	921	4	99	1
bovine trypsin[4]	922	116	402	13	87
bovine trypsin[4], 20 mM $CaCl_2$	942	98	411	10	87
recombinant trypsin[5]	922	738	91	80	20
recombinant trypsin[5], 20 mM $CaCl_2$	911	613	149	67	33
porcine trypsin[6]	967	799	79	83	16
porcine trypsin[6], 20 mM $CaCl_2$	916	565	166	62	36
cod trypsin[7]	911	851	4	93	1
cod trypsin[7], 20 mM $CaCl_2$	980	964	7	98	1

1 Refer to Experimental sections 7.2.3.
2 Me_3SiOH = trimethylsilanol.
3 HMDS = hexamethyldisiloxane.
4 bovine trypsin = bovine pancreas trypsin treated with TPCK.
5 recombinant trypsin = recombinant bovine trypsin from maize.
6 porcine trypsin = porcine pancreatic trypsin.
7 cod trypsin = *Gadus morhua* (Atlantic cod) trypsin.

7.3.3 Gas Chromatography – Mass Spectrometry

The gas chromatography – mass spectrometry (GC-MS) analysis was performed with an HP 6890 Series injector on an HP 6890 plus GC with a 5973 MS detector. The MS detector was tuned with perfluorotributylamine (PFTBA) prior to analysis. The system was configured as detailed in Table 7.34.

Table 7.34: GC-MS experimental parameters.

Parameter	Setting
Carrier gas	99.999% high purity helium
GC inlet	250 ^{0}C, split ratio = 100:1, constant flow (rate = 1.0 mL/min)
GC column	HP-5MS crosslinked 5% phenyl methyl siloxane film (30m x 0.25mm, 0.25um film)
GC temperature program	50(2) → 250(3) @10^{0}C/min, 25 minute total run time
GC-MS transfer line temperature	280 ^{0}C
MS ionization	electron impact
MS full scanning mass range	15 – 550 amu, 1 scan/sec
Data system	Agilent Technologies ChemStation

7.3.4 Inductively Coupled Plasma-Atomic Emission Spectroscopy

The inductively coupled plasma-atomic emission spectroscopy (ICP-AES) analysis was performed on a Perkin-Elmer Optima 3000DV spectrometer. The instrumental parameters are as follows: argon plasma = 14 L/min, auxillary argon = 0.5 L/min, nebulizer argon = 0.65 L/min, RF power = 1400 W, pump flow rate = 1.00 mL/min. The system was calibrated with a multi-element (i.e. Ag, Al, B, Ca, Co, Cr, Cu, Fe, K, Mg, Mn, Na, Ni, P, Pb, Si, Sn, Ti, V, Zn) standard solution (0-2 ppm) in 5% nitric acid. The samples (approximately 0.02 g) were prepared in quartz crucibles and digested with sulfuric acid, nitric acid, and hydrogen peroxide. Subsequently, the samples were concentrated to near dryness and brought to a final volume of 10 mL with approximately 5% nitric acid. Scandium (1 ppm) was used as an internal standard. Calcium was

analyzed with the following emission lines: 317.933, 396.847, 422.673 nm. The detection limit of calcium was 50 ppm. Given the increased level of calcium in Atlantic cod trypsin, the detection limit of calcium was 500 ppm due to a 10:1 dilution.

7.3.5 Infrared Spectroscopy

The Fourier transform infrared (FTIR) analysis was conducted on a Thermo Nicolet Magna 750 FTIR spectrometer. The samples were mixed with spectroscopic grade potassium bromide, added to a micro sampling cup, and analyzed by diffuse reflectance infrared Fourier transform spectroscopy (DRIFTS). Prior to analysis, the sample compartment was purged with nitrogen and a background spectrum of potassium bromide was collected in a micro sampling cup. The FTIR experimental parameters are detailed in Table 7.35.

Table 7.35: FTIR experimental parameters.

Parameter	Setting
Number of scans	256
Resolution	8
Apodization	Happ-Genzel
Zero-filling	None
Final Format	Kubelka-Munk
Correction	None
Sample gain	8.0
Mirror velocity	0.6329
Aperture	150
Detector	DTGS KBr
Beamsplitter	KBr
Source	IR

7.3.6 Matrix-Assisted Laser Desorption/Ionisation Time-of-Flight Mass Spectrometry

The experiments were performed using a Bruker Biflex III matrix-assisted laser desorption/ionisation time-of-flight mass spectrometry (MALDI-TOF MS) instrument. A pulsed nitrogen laser producing a wavelength of 337 nm was used for MALDI. The laser system also includes an attenuator which allows fine adjustment of the laser fluence, beam splitters to direct a fraction of the laser light to a photodiode starting the time-of-flight measurement, a lens system to focus the laser beam and a mirror system to direct the beam into ion source on a scout 386 probe which was used to spot the sample/matrix solutions.

All measurements were performed either in the linear mode or the reflectron mode. A patented two-stage gridless reflector was used in the reflectron mode, yielding a higher resolving power than a single stage reflector. Instrumental parameters in the linear mode are: IS1 = 19.00 kV, IS2 = 17.42 kV, Lens = 9.6 kV, detector = 1.65 kV. In the reflectron mode, the instrumental parameters are: IS1 = 19.00 kV, IS2 = 15.73 kV, Refl = 20 kV, Lens = 9.4 kV, detector = 1.65 kV.

The matrices are typically made with dithranol and 2,5-dihydroxybenzoic acid. The sample is prepared with either chloroform or acetone. Silver trifluoroacetate (AgTFA) is normally added to facilitate the ionisation. The experimental error of the mass calibration was 0.5%.

7.3.7 Spectrophotometric Analysis: Enzyme Activity Assay

Natural substrates, N-α-benzoyl-L-arginine ethyl ester (BAEE) and N-benzoyl-L-tyrosine ethyl ester (BTEE), were used to study the enzymatic activity of trypsin and chymotrypsin, respectively (Figure 7.5) [8].

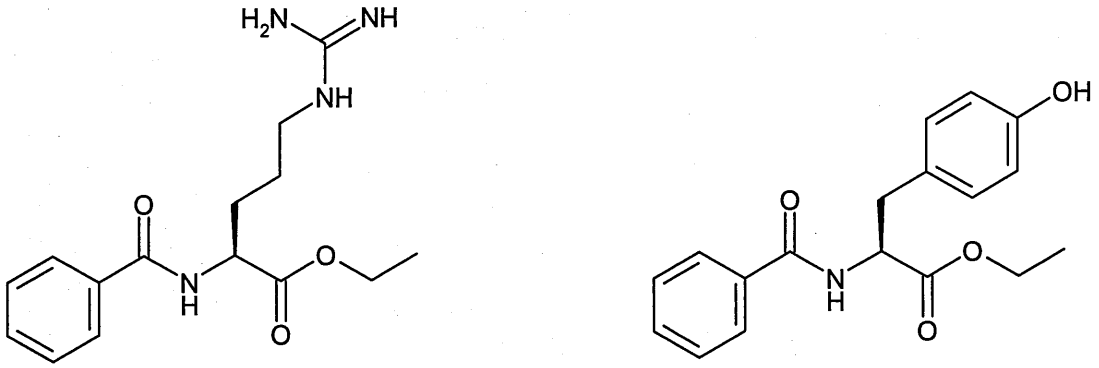

BAEE **BTEE**

Figure 7.5: N-α-benzoyl-L-arginine ethyl ester (BAEE) and N-benzoyl-L-tyrosine ethyl ester (BTEE).

The measurement of enzymatic activity is defined as a unit. Based on the spectrophotometric analyses, one unit of trypsin will hydrolyse 1.0 μmole of BAEE per minute per mg protein at pH 7.0 at 25°C in the presence of 20 mM $CaCl_2$. One unit of chymotrypsin will hydrolyze 1.0 μmole of BTEE per minute per mg protein at pH 7.8 at 25°C in the presence of 53 mM $CaCl_2$. As detailed in Table 7.36, the assays were formulated by transferring the reagents with the exception of the protease solutions (i.e. trypsin assay reagent C, chymotrypsin assay reagent E) into a quartz cuvette. After mixing the contents, background spectra were acquired at 253 (trypsin assay) and 256 (chymotrypsin assay) nm on an Agilent 8453 ultraviolet-visible spectrophotometer. Subsequently, the protease solutions were added to the cuvettes, mixed, and analyzed.

Table 7.36: Spectrophotometric enzymatic activity assays.

Trypsin Assay			Chymotrypsin Assay		
Reagent		Volume	Reagent		Volume
A	50 mM Tris-HCl buffer (pH 7.0) with 20 mM $CaCl_2$	0.87 mL	A	50 mM Tris-HCl buffer (pH 7.8)	0.71 mL
B	10 mM BAEE[1] in reagent A	0.10 mL	B	1.18 mM BTEE[2] in 3:2 (v/v) methanol/DI water	0.70 mL
C	Trypsin solution in reagent A (~2 μg/μL)	~5 μL	C	2 M $CaCl_2$ in DI[3] water	0.04 mL
			D	1 mM HCl in DI[3] water	0.05 mL
			E	Chymotrypsin solution in reagent D (~2-5 units/mL)	0.05 mL

1 BAEE = N-α-benzoyl-L-arginine ethyl ester.
2 BTEE = N-benzoyl-L-tyrosine ethyl ester.
3 DI = deionized (water).

Based on replicate analyses, the activities were measured by calculating the change in absorbance with time (ΔA/min) due to the formation of N-α-benzoyl-L-arginine (253 nm, Scheme 3.2) and N-benzyoyl-L-tyrosine (256 nm) at 25°C. The calculation is detailed in Equation 7.3.

$$\text{Units/mg protein} = \frac{(\Delta A/\text{min}) \times 1000 \times \text{dilution}}{\varepsilon \times (\text{mg protein})} \qquad \textbf{(7.3)}$$

$$\text{mg protein} = (\text{mg/mL protein}) \times \text{mL sample}$$

The extinction coefficient (ε) of BAEE is 808 M^{-1} cm^{-1} (pH 5-10) [9] and BTEE is 964 M^{-1} cm^{-1} [10]. Based on plots of absorbance vs. time (Figure 7.6), the rates of hydrolysis were measured as the linear slope (ΔA/min) during the first minute. Given a cycle time of 0.5 seconds, approximately 90 data points were acquired to calculate the slope over 45 seconds during the first minute of hydrolysis.

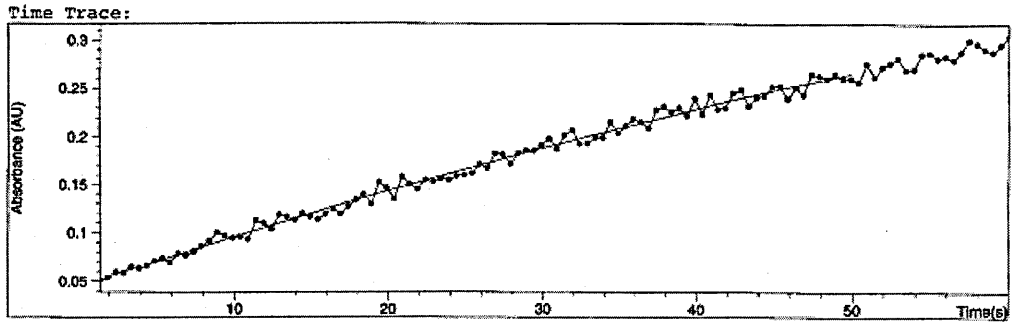

Figure 7.6: Trypsin-catalyzed hydrolysis of N-α-benzoyl-L-arginine ethyl ester (253 nm).

In application, BAEE was also used to study the activity of trypsin in different trimethylsilanol condensation reactions with time. Given the increased stability of trypsin at higher concentrations (e.g. 40 mg/mL), the tryptic reactions were diluted 20:1 in 50 mM Tris-HCl buffer (pH 7.0) with 20 mM $CaCl_2$. Subsequently, an aliquot (e.g. 5 μL) from the aqueous layer was sampled and the proteolytic activity due to trypsin (e.g. 10 μg) was measured. Encompassing experimental and instrumental errors, the relative standard deviation of the measurements was 4% (Table 7.37). The spectrophotometric results are detailed in Tables 7.38-7.44.

Table 7.37: Relative standard deviation of an enzymatic activity measurement.

Replicate Sample	Trypsin (μg)	Rate (ΔA_{253}/min)	Activity[1]
trypsin (TPCK)[2]	9.7	0.28122	35.9
trypsin (TPCK)[2]	9.7	0.30525	38.9
trypsin (TPCK)[2]	9.7	0.30165	38.5
trypsin (TPCK)[2]	9.7	0.30098	38.4
		Average =	37.9
		Standard Deviation =	1.4
		Relative Standard Deviation[3] =	4%

1 Activity = units/mg protein, one unit will hydrolyse 1.0 μmole of N-α-benzoyl-L-arginine ethyl ester (BAEE) per minute at pH 7.0 at 25°C in the presence of 20 mM $CaCl_2$.
2 trypsin (TPCK) = trypsin treated with TPCK.
3 Relative Standard Deviation = standard deviation/average.

Table 7.38: Proteinaceous inhibition study.[1]

Reaction	Activity[2,3]	% Inhibition
trypsin (TPCK)[4]	38.2	0
trypsin (TPCK)[4] + BBI[5]	0.8	98
trypsin (TPCK)[4] + PCI[6]	3.3	91
α-chymotrypsin	10.4	0
α-chymotrypsin + BBI[5]	3.9	63

1 Refer to Experimental sections 7.2.2.
2 Trypsin Activity = units/mg protein, one unit will hydrolyse 1.0 μmole of N-α-benzoyl-L-arginine ethyl ester (BAEE) per minute at pH 7.0 at 25°C in the presence of 20 mM $CaCl_2$.
3 Chymotrypsin Activity = units/mg protein, one unit will hydrolyse 1.0 μmole of N-benzoyl-L-tyrosine ethyl ester (BTEE) per minute at pH 7.8 at 25°C in the presence of 53 mM $CaCl_2$.
4 trypsin (TPCK) = TPCK treated trypsin.
5 BBI = Bowman-Birk inhibitor.
6 PCI = Popcorn inhibitor.

Table 7.39: Study of the thermal denaturation of trypsin in neutral media as a function of the concentration of trypsin.[1]

Trypsin Concentration[2]	Original Activity[3]	Denatured Activity[3]	% Inhibition
40 mg/mL	38.2	21.9	43
20 mg/mL	38.2	24.0	37
10 mg/mL	37.5	5.3	86
5 mg/mL	34.3	3.9	89
2 mg/mL	36.4	1.4	96

1 Solutions of trypsin treated with TPCK were prepared in 0.5 mL of 50 mM Tris-HCl buffered Milli-Q water (pH 7.0). The solutions were boiled for 20 minutes before measuring their enzymatic activity.
2 The standard protein concentration was 40 mg/mL in the model condensation study. Refer to Experimental section 7.2.2.
3 Activity = units/mg protein, one unit will hydrolyse 1.0 μmole of N-α-benzoyl-L-arginine ethyl ester (BAEE) per minute at pH 7.0 at 25°C in the presence of 20 mM $CaCl_2$.

Table 7.40: Autolysis of trypsin at 25°C.[1]

Trypsin Concentration[2]	Original Activity[3]	1-Day Activity[3]	% Inhibition
40 mg/mL	38.2	36.9	3
20 mg/mL	38.2	27.1	29
10 mg/mL	37.5	20.1	46
5 mg/mL	34.3	9.9	71
2 mg/mL	36.4	7.1	81
1 mg/mL	37.4	8.2	78

1 The autolysis of different concentrations of trypsin (treated with TPCK) in 50 mM Tris-HCl buffered Milli-Q water (pH 7.0) was studied over a one-day period. The original enzymatic activities were measured and compared with the activities measured after 1 day.

2 The standard protein concentration was 40 mg/mL in the model condensation study. Refer to Experimental section 7.2.2.

3 Activity = units/mg protein, one unit will hydrolyse 1.0 μmole of N-α-benzoyl-L-arginine ethyl ester (BAEE) per minute at pH 7.0 at 25°C in the presence of 20 mM $CaCl_2$.

Table 7.41: Autolysis of a 40-mg/mL solution of trypsin at 25°C.[1]

Time (d)	Activity[2]	% Inhibition
0	38.2	0
1	36.9	3
2	33.7	12
3	28.0	27
4	26.5	31

1 The enzymatic activity of a 40-mg/mL solution of trypsin (treated with TPCK) in 0.5 mL of 50 mM Tris-HCl buffered Milli-Q water (pH 7.0) was measured daily over a four-day period at 25°C. The standard protein concentration was 40 mg/mL in the model condensation study (Experimental section 7.2.2).

2 Activity = units/mg protein, one unit will hydrolyse 1.0 μmole of Nα-benzoyl-L-arginine ethyl ester (BAEE) per minute at pH 7.0 at 25°C in the presence of 20 mM $CaCl_2$.

Table 7.42: Reactant (trimethylsilanol) and product (hexamethyldisiloxane) inhibition study during the condensation of trimethylsilanol in a neutral medium (pH 7.0).[1]

Time (m)	Control Reaction Activity[2]	Condensation Reaction Activity[2]
0	34.4	37.0
30	35.7	33.0
60	39.2	39.8
91	37.1	32.9
123	36.1	33.1
150	38.3	34.3
182	37.8	37.2

[1] Refer to Experimental sections 7.2.2. The control reaction was conducted in the absence of trimethylsilanol. Throughout the three-hour condensation reaction, trypsin was exposed to trimethylsilanol and hexamethyldisiloxane.

[2] Activity = units/mg protein, one unit will hydrolyse 1.0 μmole of N-α-benzoyl-L-arginine ethyl ester (BAEE) per minute at pH 7.0 at 25°C in the presence of 20 mM $CaCl_2$.

Table 7.43: pH study of the activity of different tryptic species.[1]

	Activity[2]			
Trypsin	pH 7.0	pH 7.5	pH 8.0	pH 9.0
bovine[3]	38.2	38.9	37.0	19.0
recombinant bovine	29.6	29.6	30.7	5.4
porcine	31.8	31.0	31.4	24.8
Atlantic cod	27.2	20.3	14.9	14.0

[1] The activities of different sources of trypsin were studied as a function of pH. The enzymatic activities of 40-mg/mL solutions of trypsin in 0.5 mL of 50 mM Tris-HCl buffered Milli-Q water (pH 7.0-9.0) were measured at 25°C. The standard protein concentration was 40 mg/mL in the model condensation study (Experimental section 7.2.2).

[2] Activity = units/mg protein, one unit will hydrolyse 1.0 μmole of N-α-benzoyl-L-arginine ethyl ester (BAEE) per minute at pH 7.0 at 25°C in the presence of 20 mM $CaCl_2$.

[3] bovine = TPCK treated bovine pancreatic trypsin.

Table 7.44: The effect of trimethylsilanol and pH on trypsin activity.[1]

	Activity[2]			
Trypsin	pH 7.0	pH 7.5	pH 8.0	pH 9.0
trypsin[3], bovine pancreas	38.2	38.9	37.0	19.0
trypsin[3] + Me_3SiOH, 5 m	37.0	21.9	21.8	8.8
trypsin[3] + Me_3SiOH, 3 h	37.2	19.6	17.2	6.6
Inhibition	3%	50%	53%	65%

1 In comparison to control experiments performed in the absence of the reactant, the enzymatic activities of 40-mg/mL solutions of trypsin in 0.5 mL of 50 mM Tris-HCl buffered Milli-Q water (pH 7.0-9.0) were measured at the beginning (5 m) and end (3 h) of the trimethylsilanol condensation reaction at 25°C. The standard protein concentration was 40 mg/mL in the model condensation study (Experimental section 7.2.2).

2 Activity = units/mg protein, one unit will hydrolyse 1.0 μmole of Nα-benzoyl-L-arginine ethyl ester (BAEE) per minute at pH 7.0 at 25°C in the presence of 20 mM $CaCl_2$.

3 trypsin = TPCK treated bovine pancreatic trypsin.

7.3.8 Surface Analysis

Scanning electron microscopy (SEM) images were acquired on a JEOL JSM-6330 FESEM instrument. Images were acquired between 25x and 3000x magnification using 5 kV accelerating voltage. A Noran Vantage energy dispersive spectroscopy (EDS) system attached to a JOEL JSM-6100 SEM instrument was used to conduct the elemental analysis. EDS spectra were individually collected on various particles for 100 seconds with 15 kV accelerating voltage. Sample preparation consisted of mounting a small amount of sample on a carbon stub and evaporating a thin layer of carbon on the sample, in order to promote conductivity during contact with the electron beam in the microscope.

Optical images were obtained with a Nikon stereoscope at 40x magnification.

7.3.9 Thermal Analysis

The thermogravimetric analysis (TGA) was performed by heating approximately 1 mg of material in a Pt pan from room temperature to 300°C at 10°C/min under a He atmosphere in a TA Instruments 2950 Thermogravimetric Analyzer. The TGA was calibrated for weight using 100 mg and 1 g Class 1 weights. Temperature calibration was completed using Alumel and Nickel and following ASTM E1582, "Standard Practice for Calibration of Temperature Scale for Thermogravimetry".

The differential scanning calorimetry (DSC) analysis was conducted by encapsulating and heating approximately 1-3 mg of material in a crimp lid or hermetic lid Al pan from −100 to 175 C at 10°C/min under a He atmosphere in a TA Instruments 2920 Differential Scanning Calorimeter. The temperature of the DSC was calibrated using n-Pentane and Indium as documented in ASTM E967, "Standard Practice for Temperature Calibration of Differential Scanning Calorimeters and Differential Thermal Analyzers". Heat flow calibration was completed using Indium as reported in ASTM E968, "Standard Practice for Heat Flow Calibration of Differential Scanning Calorimeters".

7.4 References

1. K. Faber, "*Biotransformations in organic chemistry*," Springer-Verlag, New York, (2000).

2. J. F. Klebe, H. Finkbeiner, and D. M. White, *J. Am. Chem. Soc.*, **88:14**, 3390, (1966).

3. T. H. Lane and C. L. Frye, *Journal of Organic Chemistry*, **43**, 4890, (1978).

4. EPI Suite Software version 3.11, Environmental Protection Agency, http://www.epa.gov/opptintr/exposure/docs/episuite.htm, 2000.

5. S. Varaprath, K. L. Salyers, K. P. Plotzke, and S. Nanavati, *Analytical Biochemistry*, **256(1)**, 14, (1998).

6. C. Eaborn, "*Organosilicon compounds*," Butterworths Scientific Publications, London, (1960).

7. A. L. Smith, (ed.), "*The analytical chemistry of silicones*." John Wiley & Sons, Inc., New York, 1991.

8. G. W. Schwert and Y. Takenaka, *Biochimica et Biophysica Acta*, **16**, 570, (1955).

9. T. E. Barman, (ed.), "*Enzyme Handbook.*" Springer-Verlag, New York, 1969.

10. "Enzymatic assay of chymotrypsin," *Sigma Quality Control Test Procedure*, Sigma-Aldrich, August 1995.